

2-P (mix)

NASA CR-112126

PROGRAM FOR ESTABLISHING LONG-TIME FLIGHT SERVICE PERFORMANCE
OF COMPOSITE MATERIALS IN THE
CENTER WING STRUCTURE OF C-130 AIRCRAFT

PHASE I - ADVANCED DEVELOPMENT

By W. E. Harvill, A. O. Kays, E. C. Young, and W. M. McGee

(NASA-CR-112126) PROGRAM FOR ESTABLISHING
LONG-TIME FLIGHT SERVICE PERFORMANCE OF
COMPOSITE MATERIALS IN THE CENTER WING
W.E. Harvill, et al (Lockheed-Georgia
Co.) [1972] 192 p

N73-13011

Unclas

CSCL 01B

G3/02 49058

Prepared under Contract No. NAS1-11100 by
LOCKHEED-GEORGIA COMPANY
Marietta, Georgia

for

Langley Research Center
NATIONAL AERONAUTICS AND SPACE ADMINISTRATION

REPRODUCED BY
NATIONAL TECHNICAL
INFORMATION SERVICE
U. S. DEPARTMENT OF COMMERCE
SPRINGFIELD, VA. 22161

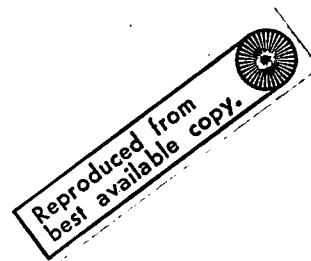
FOREWORD

This Phase I-Final Technical Report is submitted in fulfillment of the requirements of Contract NAS 1-11100 and reports contract effort from August 1971 through July 1972. Phase I consisted of advanced development activities necessary prior to the detailed design (Phase II) of a composite-reinforced C-130 center wing box. Subsequent program phases include fabrication of three C-130 center wing boxes, selectively reinforced with boron-epoxy composites, and ground/flight acceptance tests of these structures. Two of the wing boxes will be flown on C-130 aircraft for a period of up to five years to demonstrate the long-time capabilities of such composite utilization.

This contract is conducted under the sponsorship of the Materials Division, Materials Application Branch of the NASA Langley Research Center. Mr. H. Benson Dexter, Composites Section, is the NASA project monitor. Mr. W. E. Harvill is the Lockheed-Georgia Program Manager, and is assisted in these duties by Mr. A. C. Fehrle, Assistant Program Manager.

Major contribution to the work described herein and to this report were provided by the following Lockheed-Georgia personnel:

Design & Analysis:	R. W. Coleman D. C. Gibson M. G. Huff J. N. Dickson
Adhesives:	A. O. Kays
Materials & Processes:	G. E. Davis
Cost/Productibility	K. M. Barre'
Manufacturing:	E. C. Young
Structural Test:	W. M. McGee
Reliability:	J. J. Duhig
Quality Assurance:	J. B. Larsen



**Details of illustrations in
this document may be better
studied on microfiche**

ABSTRACT

One of the most advantageous structural uses of advanced filamentary composites has been shown, in previous studies, to be in areas where selective reinforcement of conventional metallic structure can improve static strength/fatigue endurance at lower weight than would be possible if metal reinforcement were used. These advantages are now being demonstrated by design, fabrication, and tests of three boron-epoxy reinforced C-130E center wing boxes. This structural component was previously redesigned using an aluminum build-up to meet increased severity of fatigue loadings. Direct comparisons of relative structural weights, manufacturing costs, and producibility can therefore be obtained, and the long-time flight service performance of the composite reinforced structure can be evaluated against the wide background of metal reinforced structure.

The first phase of a five-phased NASA program to demonstrate the long-time flight service performance of a selectively reinforced center wing box has been completed. During this phase of program activity, the advanced development work necessary to support detailed design of a composite reinforced C-130 center wing box was conducted. Activities included the development of a basis for structural design, selection and verifications of materials and processes, manufacturing and tooling development, and fabrication and test of full-scale portions of the center wing box.

CONTENTS

	Page
1.0 SUMMARY	1
2.0 INTRODUCTION	3
2.1 Joint Evaluation Specimens	5
2.2 Panel Fatigue Specimens	6
2.3 Panel Buckling Specimens	7
3.0 STRUCTURAL DESIGN	9
3.1 Structural Design Philosophy	9
3.2 Structural Analysis	9
3.2.1 Phase IA Analysis	10
3.2.2 Phase IB Analysis	15
3.2.3 Computer Program	22
3.2.4 Estimated Weight Saving	22
3.2.5 Wing Box Configuration	23
4.0 MATERIALS AND PROCESSES	31
4.1 Materials	31
4.1.1 Boron-Epoxy Preimpregnated Tape	31
4.1.2 Adhesives Selection and Evaluation	33
4.2 Processes	43
4.2.1 Laminate Preparation	43
4.2.2 Surface Preparation for Bonding	45
4.2.3 Other Surfaces	45
4.2.4 Bonding Boron-Epoxy Laminates to Aluminum Parts	46
4.2.5 Sealing and Painting	46
5.0 MANUFACTURING DEVELOPMENT	47
5.1 Bonding Techniques	47
5.1.1 Bonding without Restraint	47
5.1.2 Bonding with Restraint	47
5.1.3 Tooling Development	49
5.1.4 Warpage Study - Constant Thickness Aluminum	52
5.1.5 Cool Tool Approach	53
5.1.6 Warpage Study - Varying Thickness Aluminum	55
5.2 Generation of Holes in Boron-Epoxy Laminates Reinforced with Titanium	58
5.2.1 Drilling and Reaming	58
5.2.2 Punching and Reaming	58

CONTENTS (Continued)

	Page
6.0 COMPONENT FABRICATION	61
6.1 Metal Processing	61
6.2 Boron-Epoxy Processing	61
6.3 Assembly of Details	62
6.4 Assembly of Major Components	63
7.0 COST/PRODUCIBILITY DEVELOPMENT	65
7.1 Cost	65
7.2 Producibility	66
8.0 RELIABILITY AND QUALITY ASSURANCE	67
8.1 Reliability Program	67
8.1.1 Reliability Progress	67
8.1.2 Reliability Assessment	68
8.2 Quality Assurance Program	69
8.2.1 Procurement Controls	69
8.2.2 Fabrication Controls	70
8.2.3 In-Process Controls	70
8.2.4 Destructive Tests	70
8.2.5 Non-Destructive Inspection	72
8.2.6 Material Review Board Actions	72
9.0 COMPONENT DESCRIPTION AND TEST DATA	74
9.1 Fabrication Development Tests	74
9.1.1 Fabrication Development Specimen Description	75
9.1.2 Fabrication Development Specimens - Test & Evaluation	75
9.2 Joint Evaluation Components	87
9.2.1 130-JE-1 & 130-JE-4 Specimens	87
9.2.2 130-JE-2 Specimen	104
9.2.3 130-JE-3A Specimens	113
9.3 Panel Fatigue Components	119
9.3.1 130-PF-1 Specimen	120
9.3.2 130-PF-2 Specimen	123
9.3.3 130-PF-3 Specimen	130
9.4 Panel Buckling Components	134
9.4.1 130-PB-1 Specimen	136

CONTENTS (Continued)

	Page
9.4.2 130-PB-2 Specimen	138
9.4.3 130-PB-3-3 Specimen	142
APPENDIX A - RELATIONSHIP BETWEEN SI UNITS AND U.S. CUSTOMARY UNITS	149
APPENDIX B - ANALYSIS METHODS TO ESTABLISH PRELIMINARY THERMAL RESIDUAL STRESSES AND STRESSES DUE TO APPLIED AIRPLANE LOADS	151
APPENDIX C - ANALYSIS METHODS	161
APPENDIX D - TABULAR TEST DATA FROM ADHESIVE EVALUATIONS	169
APPENDIX E - PREPARATION OF ALUMINUM SURFACES	175

TABLES

No.		Page
I	Fatigue Endurance Summary	21
II	Room Temperature Mechanical Property Requirements	32
III	Boron-Epoxy Tape Requirement and Delivery Schedule	33
IV	Initial Cure Study of AF127-3 Adhesive	34
V	Tensile Shear and Bell Peel Tests of AF127-3	35
VI	Infrared Analysis of AF127-3 with Various Cures	39
VII	Adhesive Verification Test - AF127-3 Cured 4 Hrs. at 366°K (200°F)	40
VIII	Creep Studies on AF127-3 Adhesive	43
IX	Shear Strength of AF127-3 Cured 1 Hr. at 380°K (225°F) and 1.38 x 10 ⁵ N/m ² (20 psi)	44
X	Boron-Epoxy Acceptance Test Summary	71
XI	Material Review Actions	73
XII	Static Test Results for Fabrication Development Specimens 130-FD-1	79
XIII	Static Test Results for Fabrication Development Specimens 130-FD-2	80
XIV	Fatigue Test Results of Fabrication Development Specimens 130-FD-1	85
XV	Fatigue Test Results of Fabrication Development Specimens 130-FD-2	88
XVI	Block Loading Fatigue Spectrum for JE-1 & JE-4 Specimen	98
XVII	JE-3A Component Test Summary	115

FIGURES

No.		Page
1	Schedule	3
2	C-130 Center Wing Box	4
3	Composite Reinforcement Concept	5
4	Locations of Joint Evaluation Specimens	6
5	Locations of Panel Fatigue Specimens	7
6	Locations of Panel Buckling Specimens	8
7	Phase IA Aluminum Thermal Residual Stresses Due to Unrestrained Autoclave Bonding at Elevated Temperatures	12
8	Phase IA Analysis - Unrestrained Autoclave Cure: Fatigue Endurance Comparison of Aluminum and Boron-Epoxy Reinforced Aluminum Elements at High Cyclic Stress Levels	13
9	Phase IA Analysis - Unrestrained Autoclave Cure: Fatigue Endurance Comparison of Aluminum and Boron-Epoxy Reinforced Aluminum Elements at Low Cyclic Stress Levels	14
10	Phase IB - Restrained Autoclave Cure: Aluminum Residual Stress Due to Adhesive Cure at Elevated Temperature (Area of Steel Tool = $3A_a$)	17
11	Phase IB - Restrained Autoclave Cure: Upper Surface Fatigue Endurance Versus Weight Factor for Composite Reinforced Aluminum Elements	18
12	Phase IB - Restrained Autoclave Cure: Lower Surface Fatigue Endurance Versus Weight Factor for Composite Reinforced Aluminum Elements	19
13	Residual Stress Versus Temperature for "Cool Tool" Cure Process	20
14	Upper Surface Stringer Element Areas (Typical) (Includes Effective Skin Area)	24
15	Lower Surface Stringer Element Areas (Typical) (Includes Effective Skin Area)	25
16	C-130 Boron-Epoxy Reinforced Center Wing Structure	26
17	Typical Upper Surface Stringer Element	27
18	Typical Lower Surface Stringer Element	27
19	Typical Wing Station 220.00 Joint Design	29

FIGURES (Continued)

No.		Page
20	Typical Wing Plank and Laminate Run Out at Access Door	30
21	Tensile Shear Test Specimens	37
22	Peel Test Panel and Test Specimen	38
23	Shear and Peel Strength for AF 127-3 Adhesive	41
24	Tensile Shear Strength of Boron-to-Aluminum with Long Overlap	42
25	Boron-to-Aluminum Tensile Shear Strength After Environmental Exposure	42
26	Effects of Unrestrained Bonding of Aluminum to Steel at 400°K (260°F)	48
27	Effects of Restrained Bonding of Aluminum to Steel at 400°K (260°F)	50
28	Effects of Restrained Bonding of Aluminum to Steel at 366°K (200°F)	51
29	Steel Tool for Bonding Phase I Components	52
30	Autoclave-Bonded Boron-Epoxy-To-Aluminum Specimen Showing Hole Damage Caused by Stretching Boron	53
31	"Cool Tool" Restraining Device Concept	54
32	"Cool Tool" Process for Bonding Boron-Epoxy to Aluminum	56
33	Bonded Boron-Epoxy to Aluminum Specimen Shown on Steel Tool	57
34	Drilling the Boron-Epoxy Laminate with Diamond Core Drill	59
35	Drilling the Interleaved Titanium Shims With Standard Drill	59
36	Punching Holes in Uncured Boron-Epoxy Laminates	60
37	Uncured Boron-Epoxy Laminates With Punched Holes and Slot	60
38	Boron-Epoxy Strips on Tool Prior to Cure	62
39	Specimen PF-2 Skin After Bonding	63
40	Installation of Stringer on PF-1	64
41	Drilling and Reaming PF-2 for Taper-Lok Fasteners	64
42	Installation of Access Door Pad on PF-2	65
43	Fabrication Development Specimen (FD-1) From Boron-Epoxy Reinforcement Side	76
44	Fabrication Development Specimen (FD-2) Boron-Epoxy Reinforcement Side	76

FIGURES (Continued)

No.		Page
45	Typical Lateral Support Arrangement for 130-FD-1 Specimens	77
46	Missimers Environmental Chamber Installed in the Test Machine	78
47	Fabrication Development Specimen Installed in Missimers Environmental Chamber	78
48	Typical Static Test Failure of 130-FD-1 Specimen	81
49	Typical Room Temperature Static Test Failure for 130-FD-2 Specimen	81
50	Static Test Failure Specimen Number 2 of 130-FD-2	82
51	Typical -67°F Static Test Failure for 130-FD-2 Specimens	83
52	Static and Fatigue Tests 130-FD-1	86
53	Static and Fatigue Tests 130-FD-2	89
54	Typical Wing Station 220.00 Joint Design	90
55	Strain Gage Locations for JE-1 and JE-4 Specimens	92
56	Thermocouple Locations for JE-1 and JE-4 Specimens	93
57	JE-1 Partially Assembled in MTS Testing Machine	94
58	Environmental Control Arrangement for JE-1 and JE-4	95
59	Fatigue Test Arrangement for JE-1 and JE-4 Specimens	97
60	Typical Temperature Versus Time Cycle for JE-1 and JE-4	99
61	X-Ray of Specimen JE-1 After Eight Lifetimes of Fatigue Testing	100
62	Specimen JE-1 Disassembled for Inspection	100
63	Static Residual Strength Test Arrangement for JE-1	101
64	Static Residual Strength Failure for JE-1	102
65	JE-4 Failure	103
66	Actual Stress Versus Predicted Stress for JE-1	105
67	Actual Stress Versus Predicted Stress for JE-4	106
68	Predicted Failure Loads for Static Test JE-1	107
69	130-JE-2 Specimen Installed in Test Machine	108
70	130-JE-2 Test Support Arrangement	109
71	130-JE-2 Test Arrangement	110

FIGURES (Continued)

No.		Page
72	Compressive Failure of 130-JE-2	111
73	Failure of 130-JE-2 (Opposite Predominant End)	111
74	Failure of 130-JE-2 (Predominant End)	112
75	Laminate Side of JE 3A-1	114
76	Skin Side of JE 3A-1	114
77	Specimen JE 3A-5 Installed in Test Machine (Overall View)	116
78	Specimen JE 3A-5 Installed in Test Machine (Close-Up View)	116
79	Test Specimens JE 3A-1 and JE 3A-3 Failure	117
80	Test Specimens JE 3A-5 and JE 3A-7 Failure	118
81	PF-1 Installed in Test Machine	120
82	PF-1 Fatigue Damage	121
83	PF-1 Fatigue Damage Repair	122
84	Stress Versus Applied Load for PF-1	124
85	130-PF-2 Installed in the Test Machine	125
86	Fatigue Crack in PF-2	127
87	Damage to PF-2 Repair Strap at 6.11 Lifetimes	128
88	Applied Load Versus Stress Values for PF-2	129
89	130-PF-3 Installed in Test Machine	131
90	Residual Strength Failure of PF-3	132
91	Applied Load Versus Test Values for PF-3	133
92	Test Arrangement for Panel Buckling Specimens	135
93	Twisting Loads Reaction Mechanism for Panel Buckling Specimens	135
94	130-PB-1 Installed in Test Machine	137
95	Views of PB-1 Failure	139
96	PB-1 Failed Laminates	140
97	PB-2 Installed in Test Machine	141
98	PB-2 Failure	143
99	PB-3-3 Installed in Test Machine	145

FIGURES (Continued)

No.		Page
100	PB-3-3 Failure	146
101	PB-3-3 Strain Distribution Along Center Stringer Skin Panel Element	147

LIST OF SYMBOLS AND ABBREVIATIONS

<u>Symbol</u>	<u>Description</u>
A	Cross section area
Al	Aluminum
α	Coefficient of thermal expansion
b	Width
c	Column end fixity factor
\bar{C}	Centerline
cm	centimeter
δ	Deflection
Δ	Incremental change
ϵ	Strain
$^{\circ}\text{F}$	Temperature in degrees Fahrenheit
G	Shear modulus of elasticity
g	Gram
Hg	Mercury
Hz	Frequency
I	Moment of inertia
in.	Inch
$^{\circ}\text{K}$	Temperature in degrees Kelvin
kip	One thousand pounds force
ksi	One thousand pound force per square inch
K_t	Quality level

<u>Symbol</u>	<u>Description</u>
L	Length
lb.	Pound (mass or force)
L/t	Length to thickness ratio
m	Meter
N	Newton (force)
N/mw	Newtons per meter width
N/m ²	Newtons per square meter
N _x	Column load per inch width
η	Shear flow parameter
ν	Poisson's ratio
μ	Micro
P	Load (force)
piw	Pounds force per inch of width
psi	Pounds force per square inch
psig	Pounds force per square inch (gage)
R	Ratio of minimum stress to maximum stress
RT	Room temperature
σ	Stress
T	Temperature
t	Thickness
W	Weight
w	Deflection

<u>Symbol</u>	<u>Description</u>
W.S.	Wing station

Subscripts

A, a	Aluminum (also used as superscript)
B, b	Boron-epoxy (also used as superscript)
cr	Critical
i	i th element
j	j th element
m	Mean
o	Operating temperature
R	Restraint load
ST	Steel
v	Varying
1, 2	Normal to and in the plane of cross-section
12, 21	Refers to major and minor Poisson's ratio

PROGRAM FOR ESTABLISHING LONG-TIME FLIGHT SERVICE PERFORMANCE OF COMPOSITE MATERIALS IN THE CENTER WING STRUCTURE OF C-130 AIRCRAFT

PHASE I - ADVANCED DEVELOPMENT

By W. E. Harvill, A. O. Kays, E. C. Young, and W. M. McGee

1.0 SUMMARY

One of the most advantageous structural uses of advanced filamentary composites has been shown, in previous studies, to be in areas where selective reinforcement of conventional metallic structure can improve static strength/fatigue endurance at lower weight than would be possible if metal reinforcement were used. These advantages are now being demonstrated by design, fabrication, and tests of three boron-epoxy reinforced C-130E center wing boxes. This structural component was previously redesigned using an aluminum build-up to meet increased severity of fatigue loadings. Direct comparisons of relative structural weights, manufacturing costs, and producibility can therefore be obtained, and the long-time flight service performance of the composite reinforced structure can be evaluated against the wide background of metal reinforced structure.

The first phase of a five-phased NASA program to demonstrate the long-time flight service performance of a selectively reinforced center wing box has been completed. During this phase of program activity, the advanced development work necessary to support detailed design of a composite reinforced C-130 center wing box was conducted. Activities included the development of a basis for structural design, selection and verifications of materials and processes, manufacturing and tooling development, and fabrication and test of full-scale portions of the center wing box.

The baseline design philosophy was established to allow retention of full limit load capability without benefit of any composite reinforcement. Unidirectional boron-epoxy reinforcements were then bonded to the crown of the hat section stiffeners and to the wing skins beneath the stiffeners to provide ultimate strength and structural fatigue endurance to meet existing C-130 aircraft requirements. The composite reinforcement was added in an 80/20 area ratio of aluminum to boron-epoxy. This ratio was shown to provide a good trade-off between weight saved and fatigue endurance achieved. Analytical methods to represent the reinforced areas were developed, computerized, and used in the design of test components.

Extensive adhesive evaluations were conducted, including environmental exposures and variation in cure cycles, to enable selection of the optimum adhesive for bonding boron to aluminum in this particular application. These studies led to selection of AF 127-3 cured at $386 \pm 8^{\circ}\text{K}$ ($235 \pm 15^{\circ}\text{F}$) for 1.5 hours as the primary adhesive. Studies also showed that a

lower cure temperature was permissible if a longer cure time was used. Evaluations of room temperature curing adhesives were conducted but were discontinued when the tooling being developed appeared capable of providing low thermal stresses in the bondline for high-temperature bonds. Some of the room-temperature cured adhesive tests were encouraging, but results were somewhat erratic.

The boron-epoxy tape was acquired in the desired widths from two separate suppliers to gain service experience for use in later program phases. All tape was purchased to the requirements of an existing Lockheed specification, and updated to reflect currently attainable mechanical properties. Both suppliers provided adequate schedule and quality performance. Laminates for reinforcing the aluminum parts were laid up and cured in the usual manner. Tooling was developed for minimizing the warpage, due to residual thermal stress which results from bonding the boron-epoxy laminates to aluminum parts at elevated temperature. In the developed process, the aluminum was restrained to approximately its room temperature length by a steel fixture, insulated from the part to be bonded. The boron-epoxy reinforcing laminate was allowed to expand freely during the bond cycle. The bondline was heated with electrical heaters, monitored to maintain an even heat distribution. External pressure was used on the adherends to assure good adhesive flow and to minimize porosity. Although some work remains to be done to adapt this process to tooling for the full wing box, the principle has been demonstrated in fabrication of the test components.

Active reliability and quality assurance monitoring has been an integral part of the Phase I activity. At the program outset, an R & QA plan was published, summarizing policies for organization, implementation, and control of the total program in order to achieve stated objectives. This plan will continue in effect during subsequent program phases.

Tests of nine major components were conducted to verify static strength and fatigue endurance. The selected components were from the same wing box areas as components previously tested in the all-metal reinforcement. All component tests were satisfactorily concluded. Prior to these major tests, a sizeable number of smaller specimens were tested to provide design data and to assist in defining fabrication techniques.

The successful completion of advanced development work enabled initiation of a Detailed Design Phase of the program. This second phase is now being conducted.

2.0 INTRODUCTION

Preliminary application studies, conducted for NASA by Lockheed, have shown that boron-epoxy composite laminates bonded to the skin and stiffeners of the C-130 aircraft center wing box can significantly improve the overall fatigue endurance of the structure, at a significantly lower weight cost than would be possible if metal reinforcements were used to achieve the same endurance levels. These advantages will be demonstrated by design, fabrication, ground qualification tests, and flight tests of three boron-epoxy reinforced C-130E center wing boxes, in a five-phase program extending over four and one-half years. The program phases and associated schedules are illustrated in Figure 1. Phase I has been completed and Phase II is now being conducted.

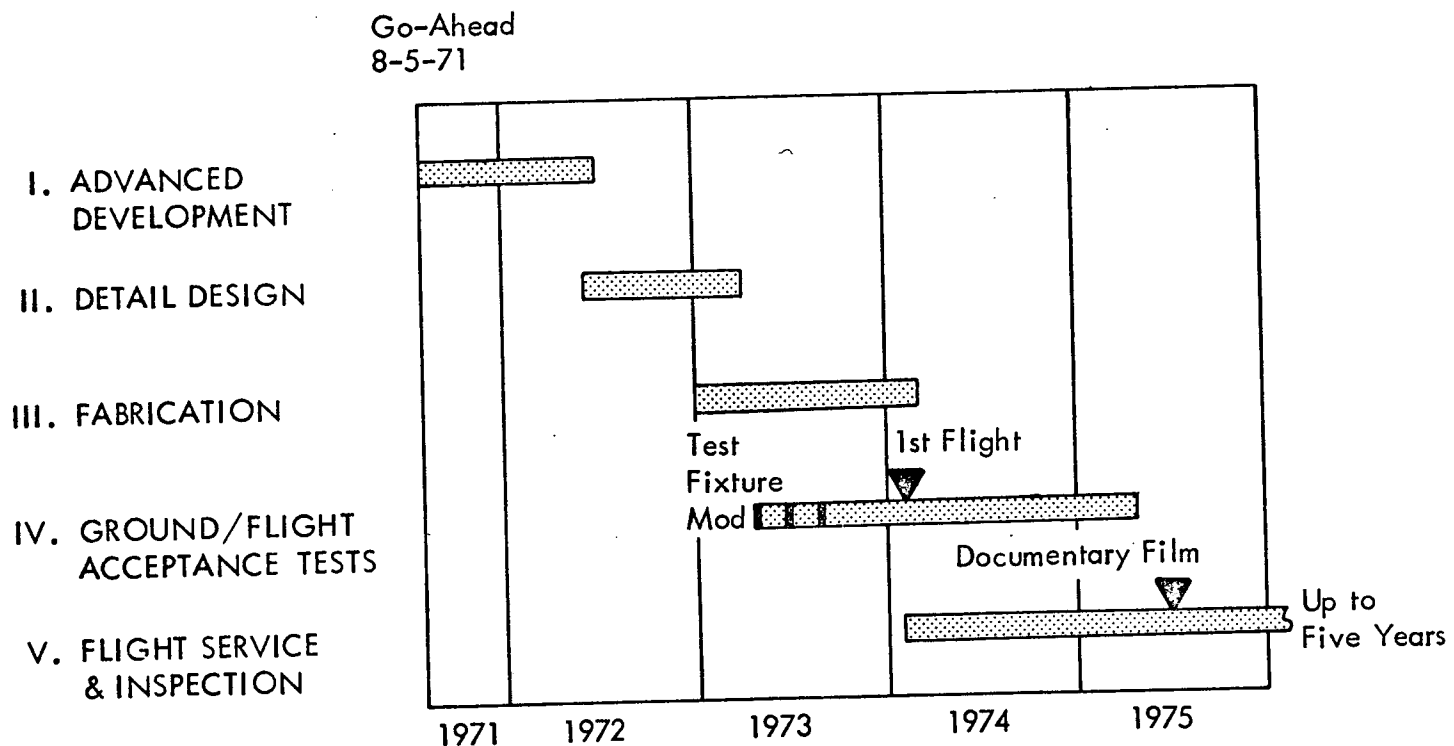


FIGURE 1.-SCHEDULE

The size and location of the center wing box are illustrated in Figure 2. The box is 11.2m (440 in.) long, 2.03m (80 in.) in chord, and - in the all-metal configurations - weighs about 2243 kg (4944 lb). Using boron-epoxy reinforcements as shown in Figure 3, equivalent static strength and fatigue endurance can be provided with a weight saving of about 274 kg (605 lb). This concept uses existing Model C-130 B/E components such as ribs, spars, fittings, and access panels.

NOTE: The terminology "C-130 B/E" or "B/E" refers to the existing metallic center wing box which is installed in Model C-130B and C-130E aircraft. This is the metal-reinforced center wing retrofitted to a sizeable part of the C-130 fleet, and is the wing box being used in current production aircraft. In this report, the "B/E" designation always refers to an aircraft model and never means boron-epoxy. Where boron-epoxy is discussed, the words are spelled out.

Upper and lower skin panel assemblies are redesigned using boron composite reinforcements bonded to aluminum skin planks and hat section stringers. The aluminum skins and stringers have a reduced thickness compared to those of the Model C-130 B/E; equivalent strength is provided by the unidirectional composite. The final design configuration will be structurally and functionally interchangeable with the production Model C-130 B/E wing box. Extensive reliability and quality assurance involvement throughout the program will provide intensive control over the development and production of the boron-reinforced wing boxes.

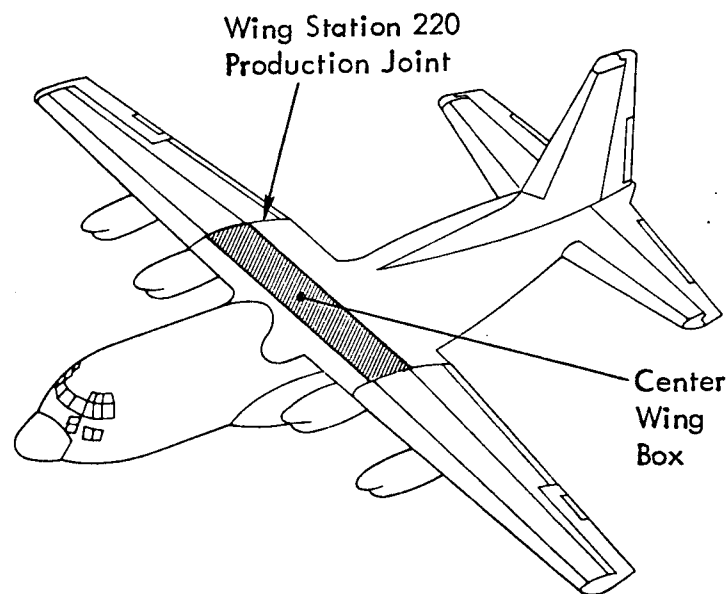


FIGURE 2.-C-130 CENTER WING BOX

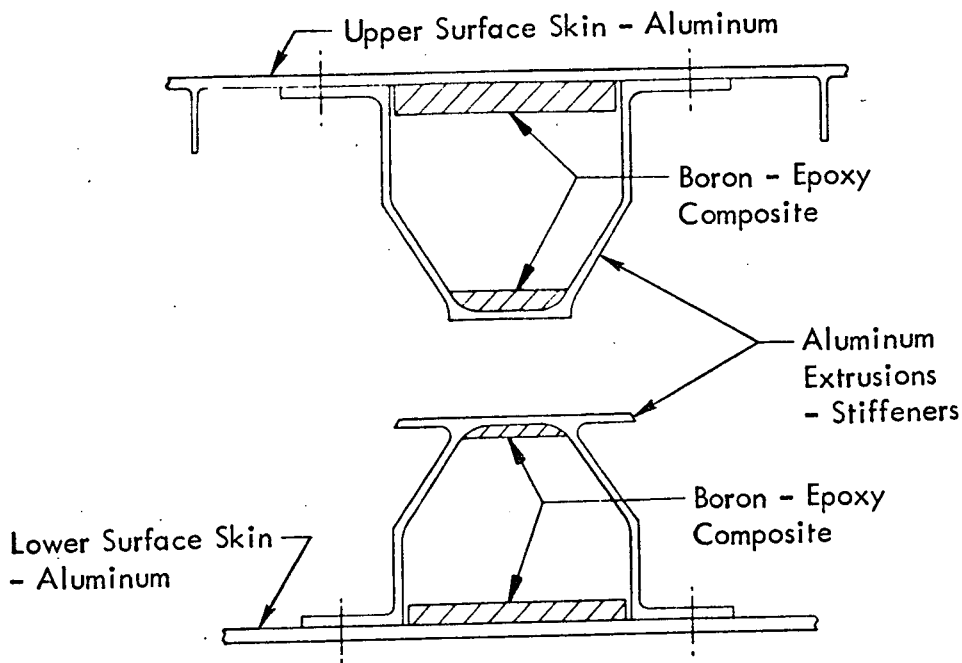


FIGURE 3.-COMPOSITE REINFORCEMENT CONCEPT

The first composite-reinforced wing box will be static-tested to limit load, followed by an endurance test to a fatigue spectrum representative of four aircraft lifetimes. Finally, this box will be tested statically to determine its residual strength. The other two wing boxes will be subjected to FACI (First Article Configuration Inspection) and then will be installed in two Air Force C-130E aircraft and the aircraft returned to operational service. Service experience will be monitored and documented. Detailed inspections of these two wing boxes, including the use of sophisticated non-destructive test techniques, are scheduled to coincide with regularly phased aircraft inspections.

During the advanced development phase of the program, nine major components have been designed, fabricated, and tested. The general size and location of these components is discussed below.

2.1 JOINT EVALUATION SPECIMENS

Three structural elements representative of high load introduction areas in the composite reinforced metal structure were designed, fabricated, and tested to verify design concepts from a static strength standpoint. These were representative of the Wing Station 220 upper and lower surface joints. They were designed to evaluate the load transfer at that location and were 31.5 x 104 cm (12.4 x 40.8 in.). The locations for these specimens are shown in Figure 4.

Design of the W.S. 220 joint specimens included fittings for the inboard and outboard ends to provide proper axial load introduction and allow adapting to a universal testing machine. The inboard fitting design was integrated with specimen design to ensure proper centroid loading and an adequate static strength margin over the test section. The W.S. 220 joint fitting was attached to the test specimen using production bolts, nuts, and installation torques to duplicate standard assembly stresses.

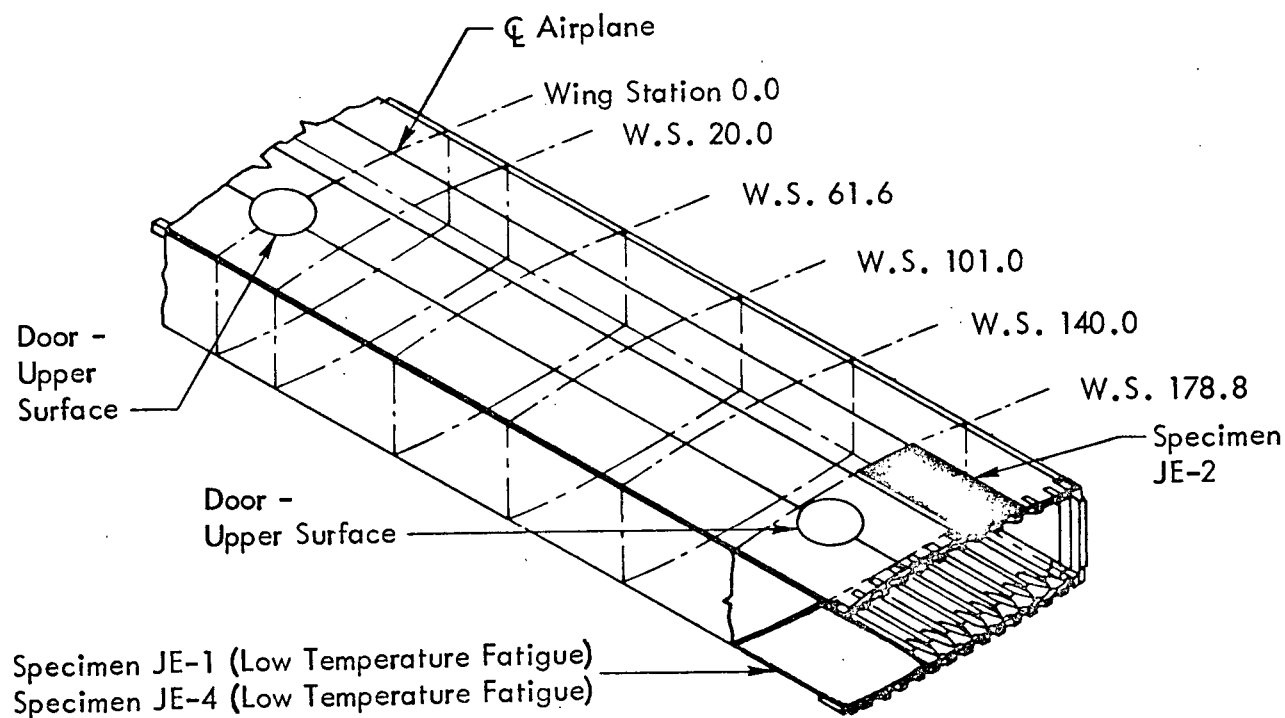


FIGURE 4.-LOCATIONS OF JOINT EVALUATION SPECIMENS

2.2 PANEL FATIGUE SPECIMENS

Three large specimens representative of three different center wing surface areas were designed and tested to verify fatigue endurance. One specimen was a combination of two upper surface panels, 102 x 366 cm (40 x 144 in.), containing the aircraft centerline access door. A second specimen, combining two upper surface panels, included the W.S. 220 joint and one access door. This specimen was 102 x 323 cm (40 x 127 in.). The third specimen was 61 x 156 cm (24 x 61.6 in.). It consisted of a single lower surface panel and included the W.S. 220 joint. The panel locations are illustrated in Figure 5.

Design of test specimens included end fittings to allow attachment to the fatigue testing machines. End fitting designs included bonded doublers combined with bolted attachments. This approach has provided an adequate end fitting fatigue margin on previous applications. Load introduction fittings, representative of outer wing structure, were designed for the

W.S. 220 joint specimens considering applicable outer wing fatigue requirements and centroid locations. Production bolts, nuts, and installation torques were used to attach the center and outer wing sections of joint specimens.

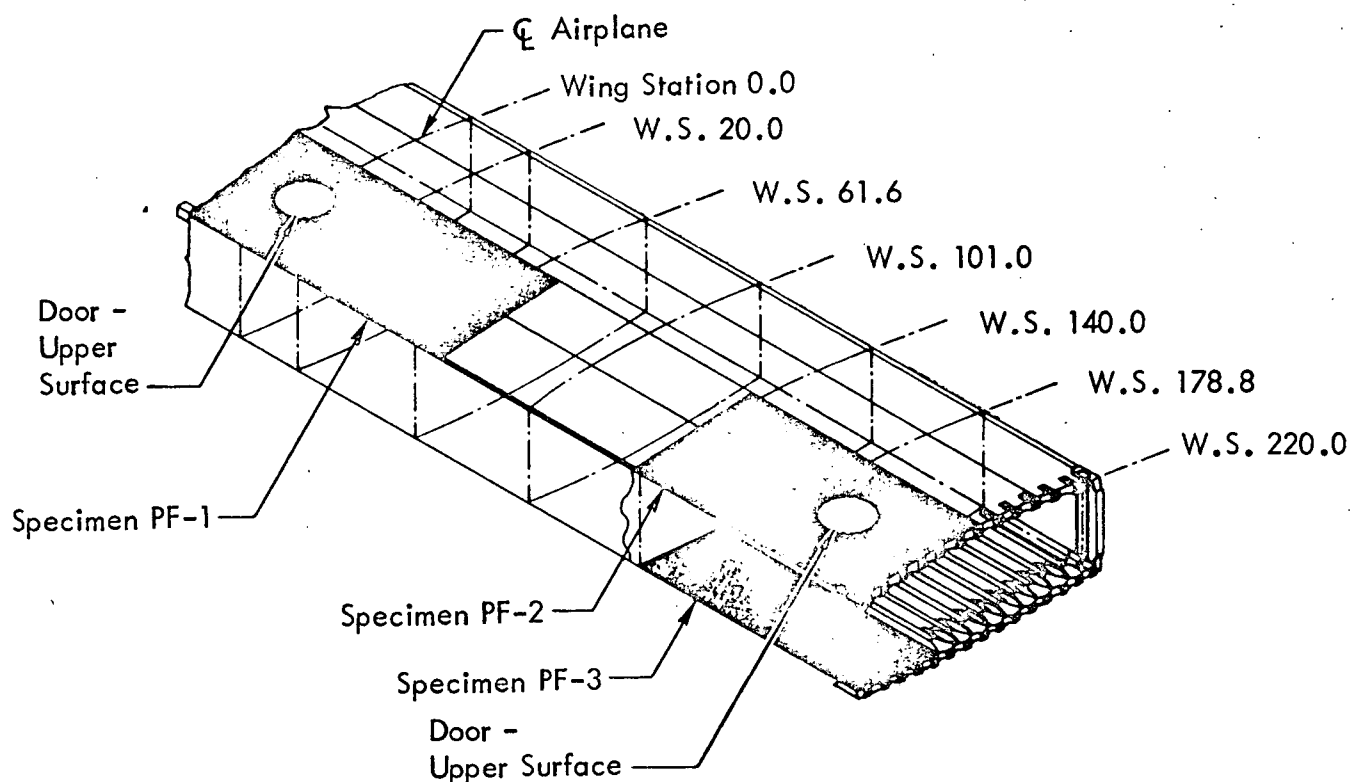


FIGURE 5.-LOCATIONS OF PANEL FATIGUE SPECIMENS

2.3 PANEL BUCKLING SPECIMENS

Panel buckling specimens in selected locations were designed. These specimens used the design configurations established for the fatigue panel test specimens. Three different compression panels representative of stiffened wing skin structure were included. Two of the panels were 51 x 191 cm (20 x 75 in.) and the third panel was 102 x 191 cm (40 x 75 in.). Two specimens represented the upper surface and one 51 x 191 cm (20 x 75 in.) specimen simulated the lower surface. The general location of these panels is in the area of the aircraft centerline, as illustrated in Figure 6. These tests were conducted to experimentally verify the analysis method for predicting buckling loads for laminated plates which have discrete stiffeners. The tests provided empirical design data, as well as substantiating the design concept. All of the panels were representative of a single bay between rib supports; consequently, lateral support was not required.

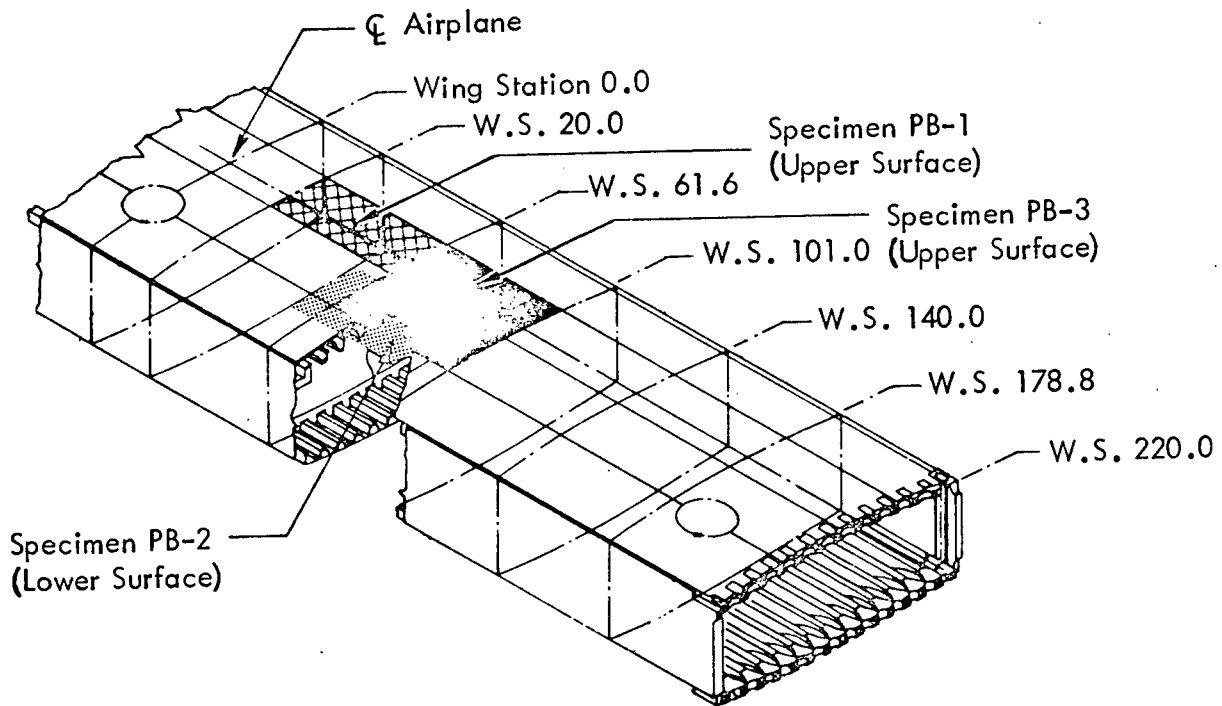


FIGURE 6.-LOCATIONS OF PANEL BUCKLING SPECIMENS

The Advanced Development Phase of this program has been successfully completed. Details of the design, development, and tests are included in the body of this report.

3.0 STRUCTURAL DESIGN

3.1 STRUCTURAL DESIGN PHILOSOPHY

The design philosophy established in Phase I retained the basic dimensions of the C-130E configuration and the material of the C-130 B/E wing box. This criteria allowed, as a minimum, the development of 100 percent of the design limit load requirement, without benefit of any composite reinforcement, and also provides a degree of fail-safe capability.

The basic aluminum center wing box was reinforced with unidirectional boron-epoxy laminates in the crown of the hat stiffeners and on the skin under the stiffeners. The laminates added were sufficient to allow the center wing box to develop the ultimate load requirements of the C-130E wing box and the fatigue life of the C-130 B/E wing box. Functional and selected structural configurations of the current C-130 B/E model were maintained in the areas of access cutouts, fuselage interface, and joint runouts. Residual thermal stresses induced by joining dissimilar materials were accounted for in the analysis for static and fatigue loading.

3.2 STRUCTURAL ANALYSIS

The selection of the aluminum/boron area distribution for the center wing box was predicted on a workable balance of four criteria: reduction in weight, equivalent ultimate strength, equivalent damage tolerance, and equivalent fatigue endurance of the C-130 B/E wing box. In addition, thermal residual stresses were found to have considerable effect on the fatigue loads and endurance of composite structure. Manufacturing methods were therefore developed to reduce residual stresses to a minimum and thereby preserve maximum weight savings by use of boron-epoxy reinforced structure.

Preliminary analyses to define the aluminum/boron area ratio requirements were performed in two phases. In Phase 1A, the effects of thermal residual stresses on the fatigue endurance of composite structure resulting from unrestrained autoclave adhesive cure methods were considered. In Phase 1B, these same effects were considered except that expansion restraints were used to reduce the expansion of aluminum to a lower apparent value. The proportions of aluminum and boron-epoxy used in both phases were such that the static strength of the basic C-130E box was maintained or exceeded at all times.

The comparison of the calculated fatigue endurance of the C-130 B/E and boron-epoxy reinforced wing boxes was based on the following assumptions:

- o The aluminum structure of the composite is fatigue-critical and the boron-epoxy is not.
- o The calculated fatigue endurance of the boron-epoxy reinforced wing box is based on the equivalent aluminum area of the composite.
- o When comparing the fatigue endurance of the C-130 B/E aluminum structure with boron-epoxy reinforced C-130E structure the quality level, K_t , is considered constant.¹

3.2.1 Phase IA Analysis

Preliminary analysis performed early in the program showed that, within the established design guidelines, static strength considerations were of secondary importance to the fatigue endurance requirements of the wing box. Simple fatigue analyses were conducted for various combinations of aluminum and boron-epoxy, using only those segments of the C-130 B/E fatigue spectrum which gave the majority of fatigue damage on the upper and lower surfaces. Residual thermal stresses in the structure resulting from bonding at elevated temperature (materials with different coefficients of expansion) were included in the fatigue analysis. The results of this preliminary analysis were later confirmed (Table I) by a complete fatigue analysis utilizing the full C-130 B/E spectrum.

¹ Practically, however, the quality level does vary. The quality level is defined as the numerical value of the stress concentration factor which yields a Miner's damage of unity. However, the effect of a number of uncontrolled variables are included in the calculation of the quality level of a specific area of a complex structure such as a wing box. These variables include:

- i Material inconsistencies such as: anisotropy; non-homogeneity; inelasticity; inclusions; voids; variations in physical properties; grain size.
- ii Manufacturing variables such as: tolerances causing variations in part size and thickness, surface finish; fastener size; hole size; joint friction; assembly errors.
- iii Other variables such as: non-linear slippage of joints; local plastic yielding at points of high stress concentration; complexity and redundancy of load paths; fretting of joints; fretting corrosion; design errors; irregularity of service usage and external loadings.

The following criteria were used to establish the mean thermal residual stresses for use in fatigue analysis:

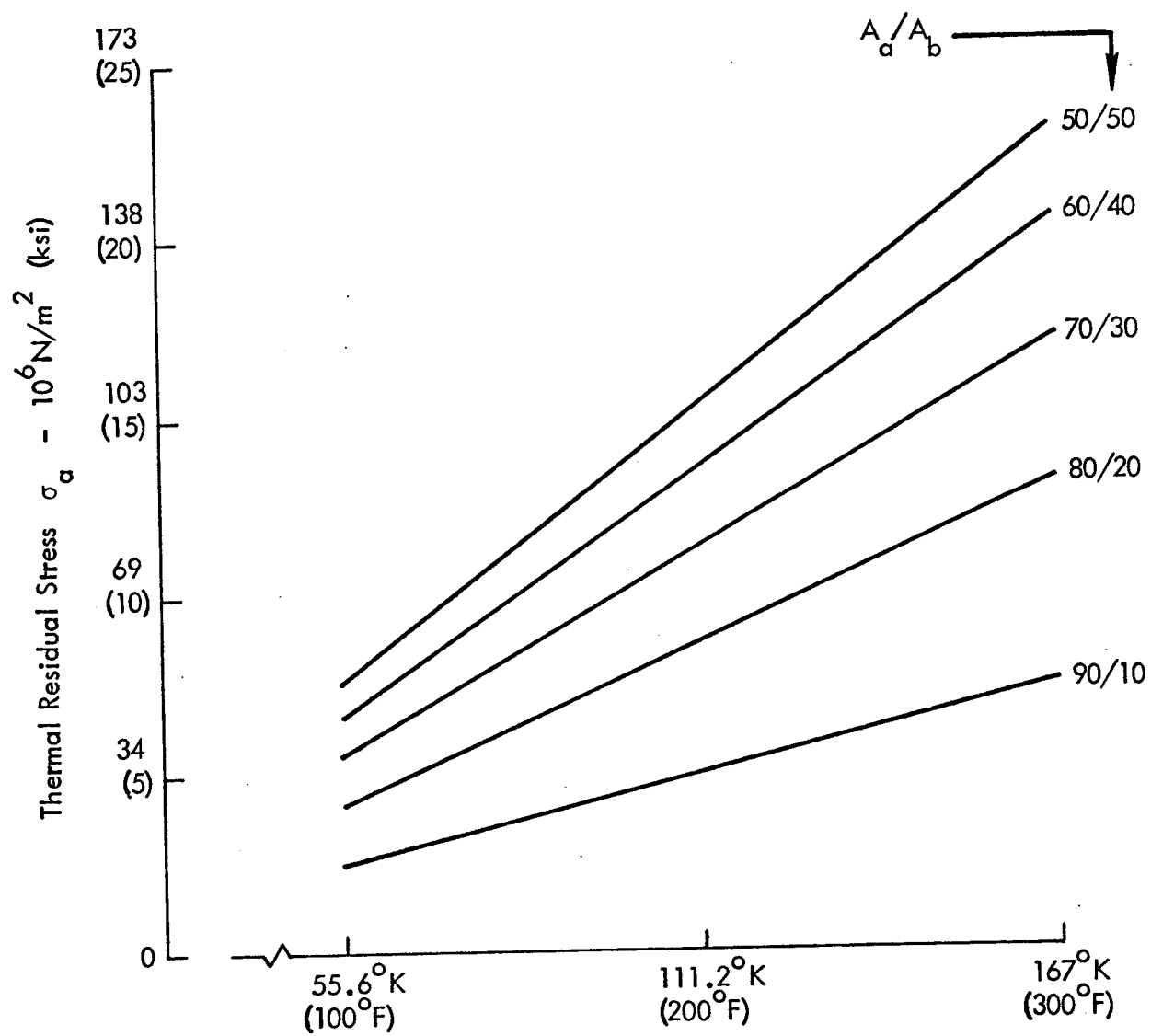
- o The adhesive was cured by placing the aluminum and boron-epoxy elements in an autoclave and heating to elevated temperature.
- o The aluminum and boron-epoxy structural elements were allowed to expand freely until effective adhesive cure temperature of 353°K (175°F) was reached.
- o A mean structural operating temperature of 255°K (0°F) was assumed for the lower surface. This temperature was selected on the basis of the majority of damage occurring at altitude.
- o A mean structural operating temperature of 297°K (75°F) was assumed for the upper surface. This temperature was selected on the basis of the majority of damage occurring at sea level during ground-air-ground cycles. (This temperature was later changed to 269°K (25°F) during Phase IB analysis.)

Using the above data and the analytical procedure outlined in Appendix B, mean thermal residual stresses for various combinations of aluminum/boron-epoxy cross-section areas were established. These are shown in Figure 7. Only the tensile residual stresses for the aluminum portions of the composite structure are shown since the corresponding stresses in the boron-epoxy laminates are compressive and therefore have a negligible effect on the fatigue endurance. In addition, the fatigue endurance of boron-epoxy laminates in a composite structure is less critical than the endurance of aluminum and is therefore not presented in this report.

Fatigue endurance comparisons, using the residual stresses of Figure 7, were made between typical elements of the C-130 B/E wing box and typically equivalent elements of the boron-epoxy reinforced structure. Curves of cycles-to-failure versus quality level (K_t) for a 70/30 distribution of aluminum to boron-epoxy are plotted in Figures 8 and 9 for specified conditions.

The conclusions drawn from the Phase IA analysis were as follows:

- o Bonding the boron-epoxy reinforcement to aluminum structure with an unrestrained autoclave cure does not necessarily produce an improvement of fatigue life or a weight savings when compared to the addition of aluminum reinforcement.
- o Improved fatigue life and corresponding weight savings may be obtained by the unrestrained autoclave adhesive cure technique when the thermally induced residual stresses are relatively low in comparison to the applied fatigue stresses. This conclusion is illustrated in Figure 8, where an improved fatigue life is shown for the boron reinforced structure when using a residual thermal stress of $48 \times 10^6 \text{ N/m}^2$ (6950 psi) compared to mean and variable stresses of $93.4 \times 10^6 \text{ N/m}^2$ (13,550 psi) for the all-aluminum structure.



Difference Between Bonding and Operating Temperatures

FIGURE 7. - PHASE 1A ALUMINUM THERMAL RESIDUAL STRESSES DUE TO UNRESTRAINED AUTOCLAVE BONDING AT ELEVATED TEMPERATURES

$$A_a/A_b = 70/30$$

C-130 B/E Aluminum Stresses: $\sigma_{(\text{mean})} = 93.4 \times 10^6 \text{ N/m}^2$ (13,550 psi)

$$\sigma_{(\text{variable})} = 93.4 \times 10^6 \text{ N/m}^2$$
 (13,550 psi)

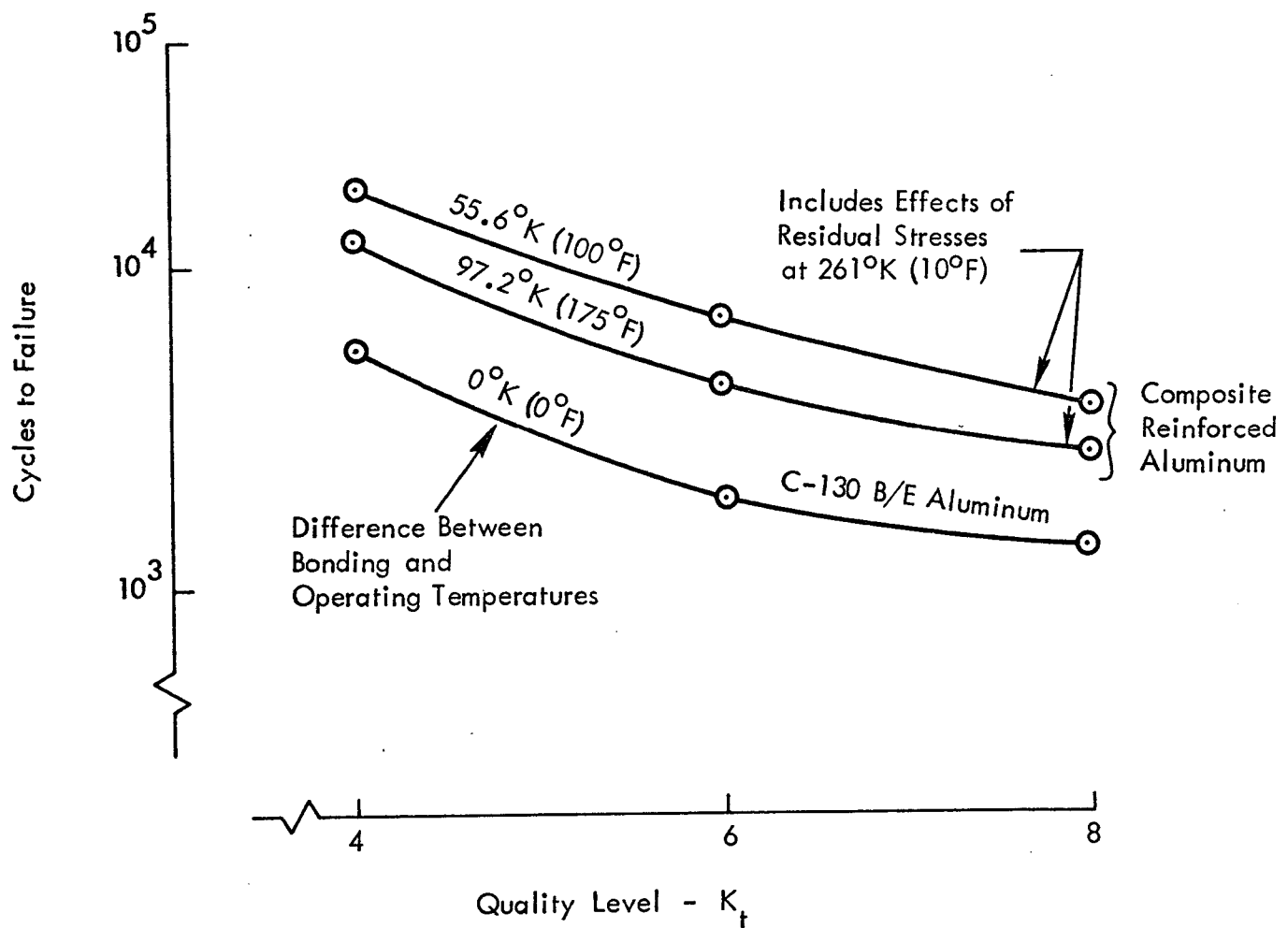


FIGURE 8. - PHASE 1A ANALYSIS - UNRESTRAINED AUTOCLAVE CURE: FATIGUE ENDURANCE COMPARISON OF ALUMINUM AND BORON-EPOXY REINFORCED ALUMINUM ELEMENTS AT HIGH CYCLIC STRESS LEVELS

$$A_a/A_b = 70/30$$

C-130 B/E Aluminum Stresses: $\sigma_{(\text{mean})} = 46.2 \times 10^6 \text{ N/m}^2$ (6700 psi)
 $\sigma_{(\text{variable})} = \pm 29.6 \times 10^6 \text{ N/m}^2$ (4300 psi)

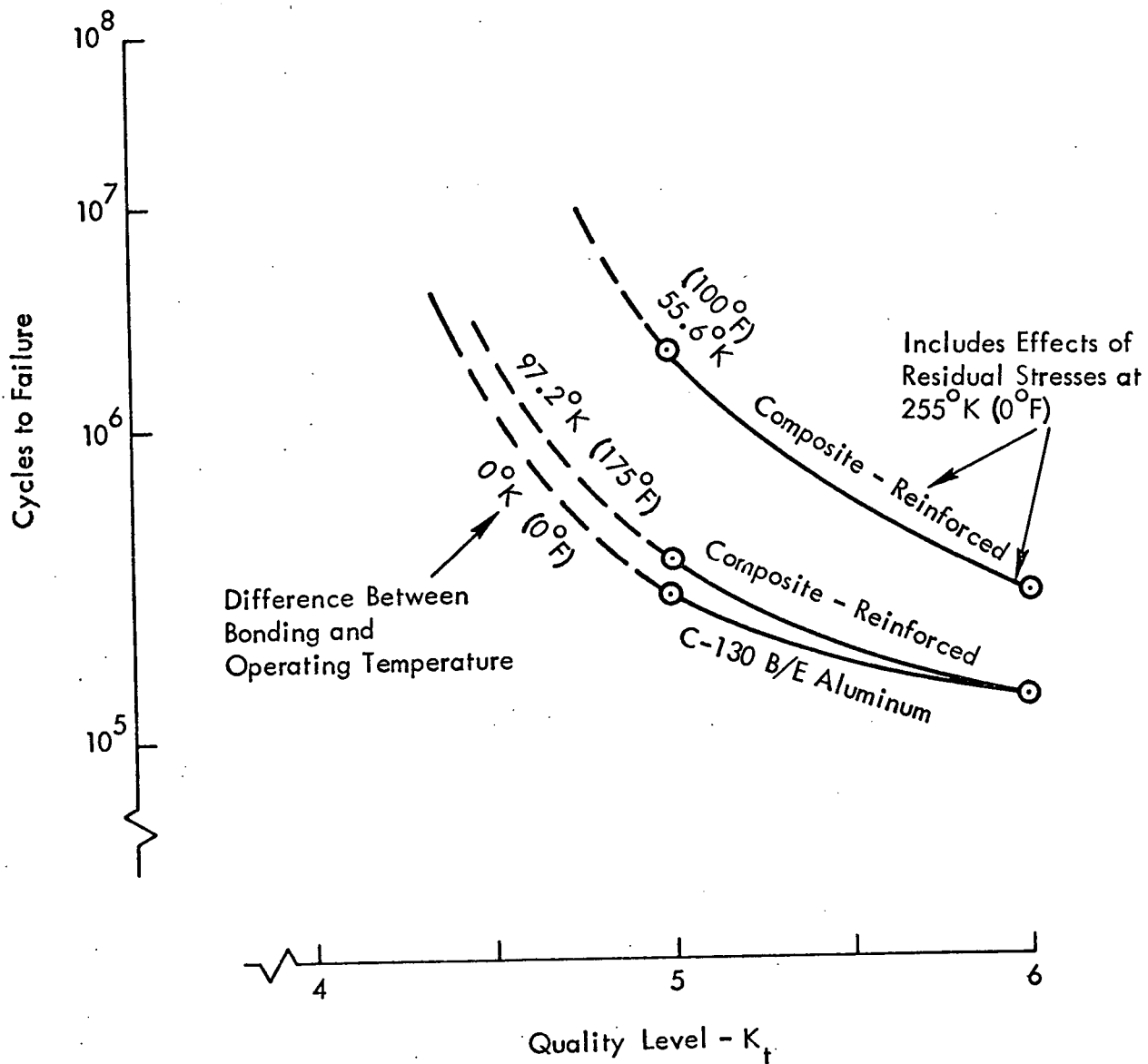


FIGURE 9. - PHASE 1A ANALYSIS - UNRESTRAINED AUTOCLAVE CURE: FATIGUE ENDURANCE COMPARISON OF ALUMINUM AND BORON-EPOXY REINFORCED ALUMINUM ELEMENTS AT LOW CYCLIC STRESS LEVELS

- o Improved fatigue life and corresponding weight savings are small when thermally induced residual stresses are relatively high compared to cyclic fatigue stresses. This conclusion is illustrated in Figure 9 where a residual thermal stress of $48 \times 10^6 \text{ N/m}^2$ (6950 psi) is included in the fatigue analysis of the boron reinforced wing compared to mean and variable stresses of $46.2 \times 10^6 \text{ N/m}^2$ (6700 psi) and $29.5 \times 10^6 \text{ N/m}^2$ (4300 psi) respectively, for the all aluminum structures. These mean and variable stresses are typical of major sources of damage in the C-130 B/E fatigue spectrum.

3.2.2 Phase IB Analysis

Phase IB analysis considered various methods of reducing the magnitude of thermal residual stress below that obtained with unrestrained autoclave adhesive cure techniques described in Phase IA. Two such methods were considered, employing basically the same techniques except that different methods of curing the adhesive were used.

3.2.2.1 Method 1 - Restrained Autoclave Cure

The principle of this concept is to provide constraint to the aluminum adherend as it is heated to bonding temperature, while allowing the boron-epoxy laminate to expand freely. This process requires that the aluminum be restrained by a steel tool fixture. This process effectively reduces the actual expansion of the aluminum to a lower "apparent" value and therefore reduces the induced thermal residual stresses. Residual stresses were calculated utilizing the above principle and the method of analysis described in Appendix C. These stresses are graphically illustrated for various aluminum : boron-epoxy cross-sectional area ratios on Figure 10. Simple fatigue analyses, using typical stresses from segments of the C-130 B/E spectrum and including the effects of induced thermal residual stresses, were conducted for typical elements of upper and lower wing box surfaces. The results of the analyses are shown on Figures 11 and 12 and show that an 80/20 distribution of aluminum : boron-epoxy area ratio gives maximum weight savings of 21 percent and 16 percent on upper and lower surfaces, respectively. The 80/20 distribution was later confirmed by full C-130 B/E fatigue spectrum analysis.

Residual stresses and fatigue endurance were established utilizing the following criteria:

- o 352°K (175°F) adhesive cure temperature.
- o Aluminum restrained by steel tool fixture with minimum steel : aluminum cross section area ratio of 3 : 1.
- o Boron-epoxy laminate expands freely during heating to cure temperature.
- o 255°K (0°F) mean operating temperature for lower surface structure.
- o 269°K (25°F) mean operating temperature for upper surface structure.

- o A constant area for aluminum equivalent to the C-130E wing elements was used in all composite combinations.
- o Loads equivalent to the C-130 B/E wing major source of damage were used to compute fatigue endurance.

3.2.2.2 Method 2 - "Cool Tool" Cure

This is basically a restrained non-autoclave cure technique which provides maximum constraint to the aluminum adherend as it is heated to bonding temperature while allowing the boron-epoxy laminate to expand freely. The process requires that the aluminum be restrained by the steel tool and that the steel tool be kept at room temperature with minimum expansion. Heating to cure temperature is accomplished by the use of heating blankets applied to the aluminum and boron-epoxy adherends. The temperature of the steel tool is maintained close to room temperature by the use of Maronite insulating material. This process reduces the expansion of the aluminum to approximately the same value as that of the freely expanding boron, and lower thermal residual stresses are obtained than from the restrained autoclave cure technique. Thermal residual stresses were calculated using the method of analysis described in Appendix C. An efficiency of 90 percent was used for the Maronite insulating material, i.e., the "cool tool" was assumed to increase in temperature by one-tenth of the increase experienced in the aluminum and boron-epoxy adherends. Thermal residual stresses due to the "cool tool" bonding technique are shown on Figure 13 for the selected 80/20 distribution of aluminum/boron. This technique not only permits a further improvement of fatigue endurance and/or weight saving, but substantially reduces the structural warpage experienced with other bonding methods.

A summary of fatigue endurances based on the criteria established in each phase of analysis is presented in Table I. Included in Table I is the fatigue endurance of the final 80/20 distribution employing the "cool tool" method of residual stress reduction. These calculations were derived from a computer program that is used in computing fatigue damages and endurances. Stored in this program is the fatigue spectrum applied to the C-130 B/E center wing box in the current fatigue test. By inserting into the program the reduction in mean and variable stresses due to addition of the boron-epoxy laminates to the basic aluminum structure and adding the subsequent thermal residual stress to the mean stress, the fatigue endurance of each composition listed in Table I may be compared to the C-130 B/E fatigue endurance. These calculations show that the 80/20 distribution of aluminum to boron-epoxy (Aa/Ab) on the upper and lower wing box have fatigue endurances equal to or exceeding the C-130 B/E wing when restraint techniques of the cool tool method are employed.

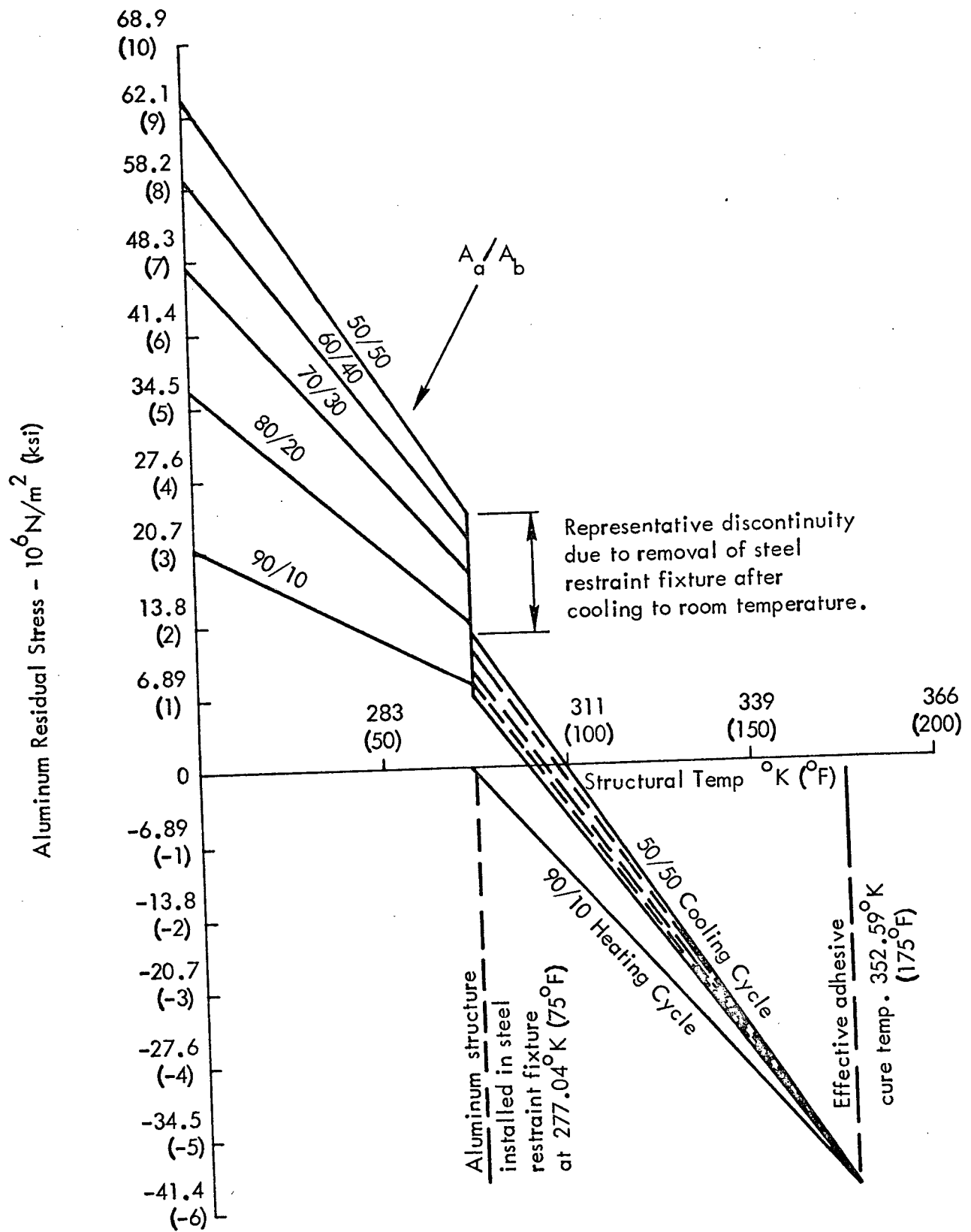
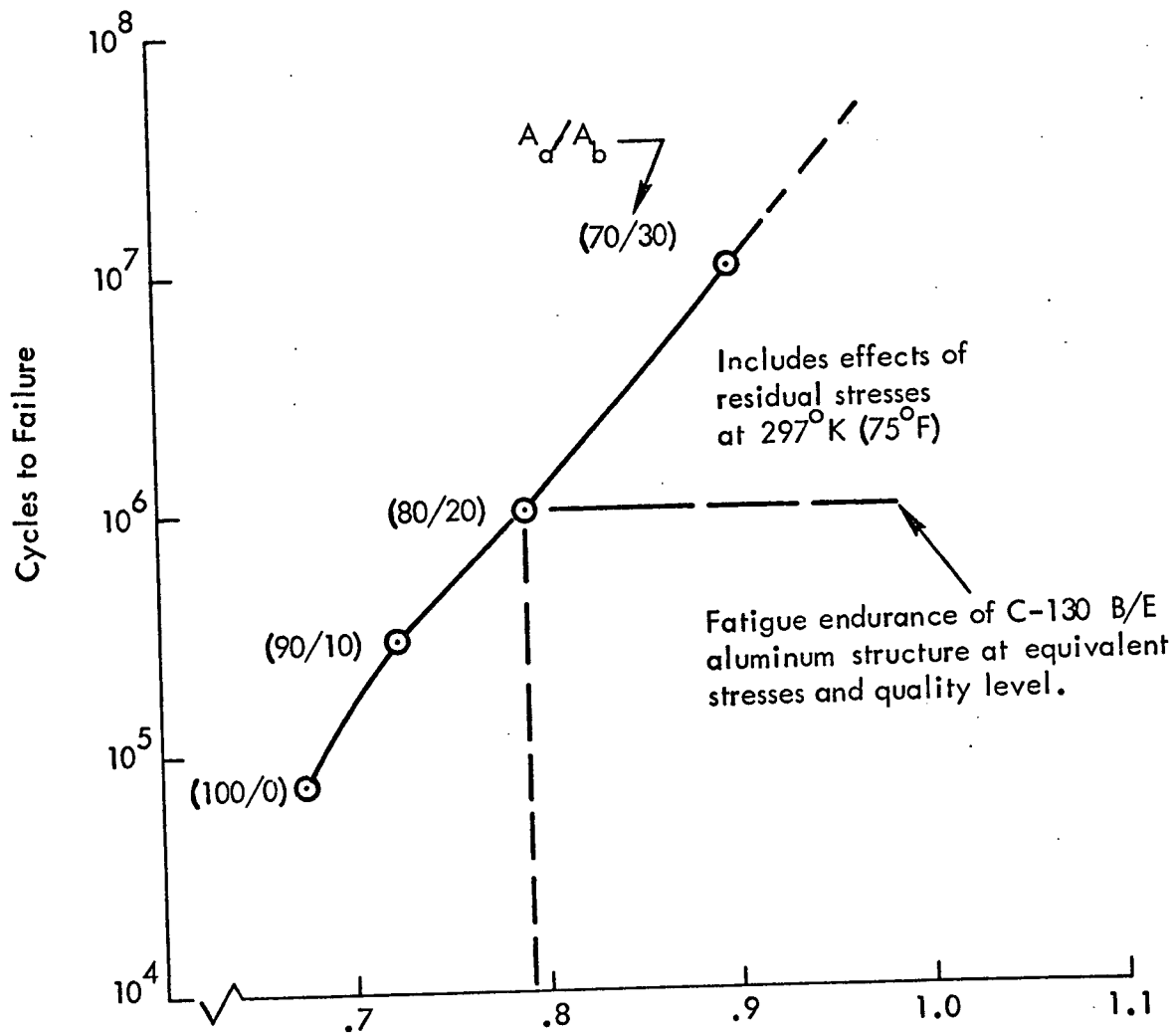


FIGURE 10. - PHASE 1B - RESTRAINED AUTOCLAVE CURE ;
ALUMINUM RESIDUAL STRESS DUE TO ADHESIVE CURE
AT ELEVATED TEMPERATURE (AREA OF STEEL TOOL = $3A_a$)

$$\sigma_m = 1.9 \times 10^6 \text{ N/m}^2 \text{ (282 psi)}$$

$$\sigma_v = \pm 38.7 \times 10^6 \text{ N/m}^2 \text{ (5614 psi)}$$

$$K_t = 6.0$$



$$\text{Weight Factor} = \frac{\text{Element weight for composite reinforced wing.}}{\text{Element weight for C-130 B/E wing.}}$$

FIGURE 11. - PHASE 1B - RESTRAINED AUTOCLAVE CURE:
UPPER SURFACE FATIGUE ENDURANCE VERSUS
WEIGHT FACTOR FOR COMPOSITE REINFORCED
ALUMINUM ELEMENTS

$$\sigma_m = 4.62 \times 10^6 \text{ N/m}^2 \text{ (6700 psi)}$$

$$\sigma_v = \pm 2.97 \times 10^6 \text{ N/m}^2 \text{ (4300 psi)}$$

$$K_T = 6.0$$

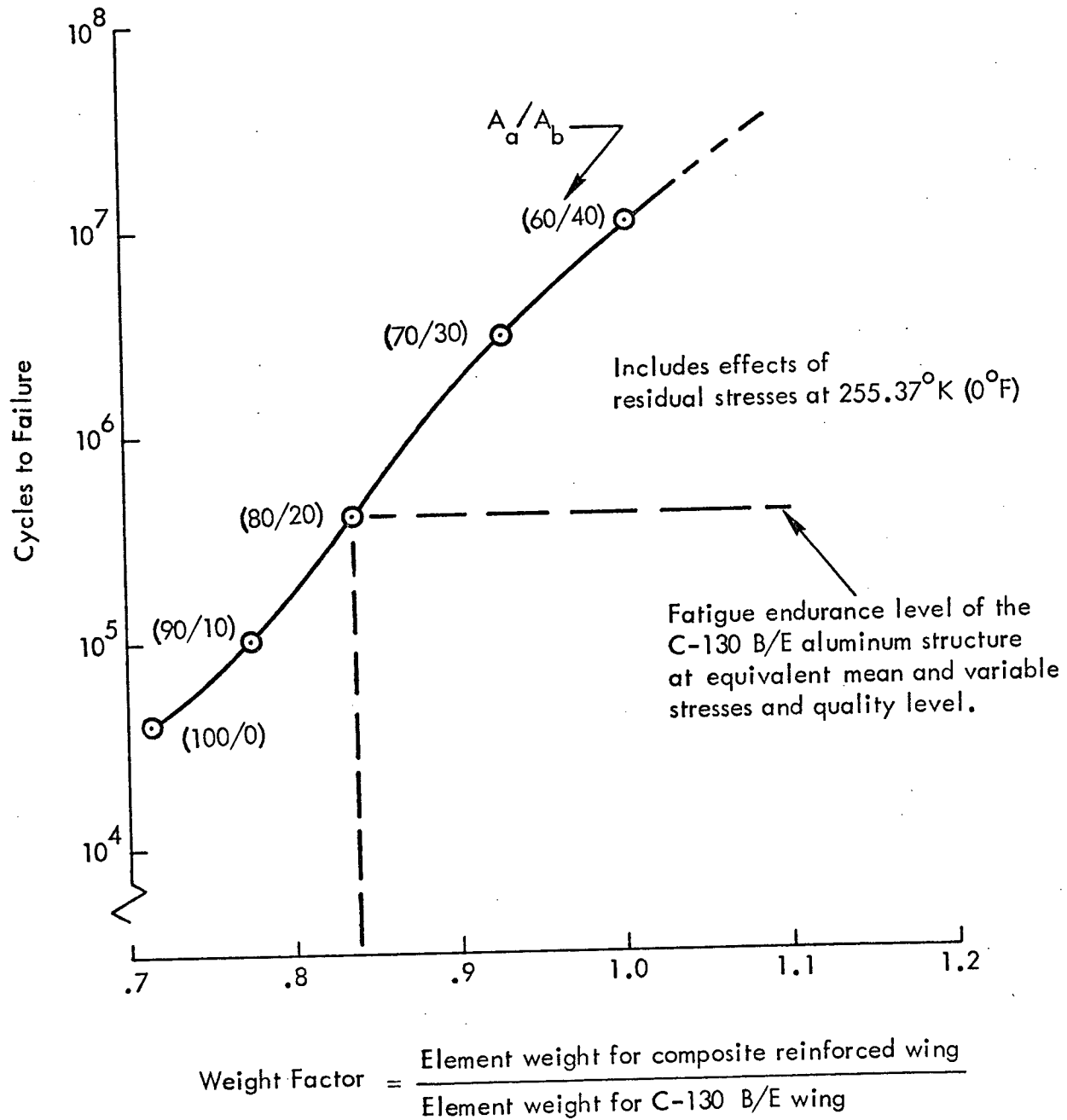


FIGURE 12. - PHASE 1B - RESTRAINED AUTOCLAVE CURE
LOWER SURFACE FATIGUE ENDURANCE VERSUS
WEIGHT FACTOR FOR COMPOSITE REINFORCED
ALUMINUM ELEMENTS

$$A_d/A_b = 80/20$$

Steel Tool : Aluminum Area Ratio = 3 : 1

Insulation Efficiency = 90%

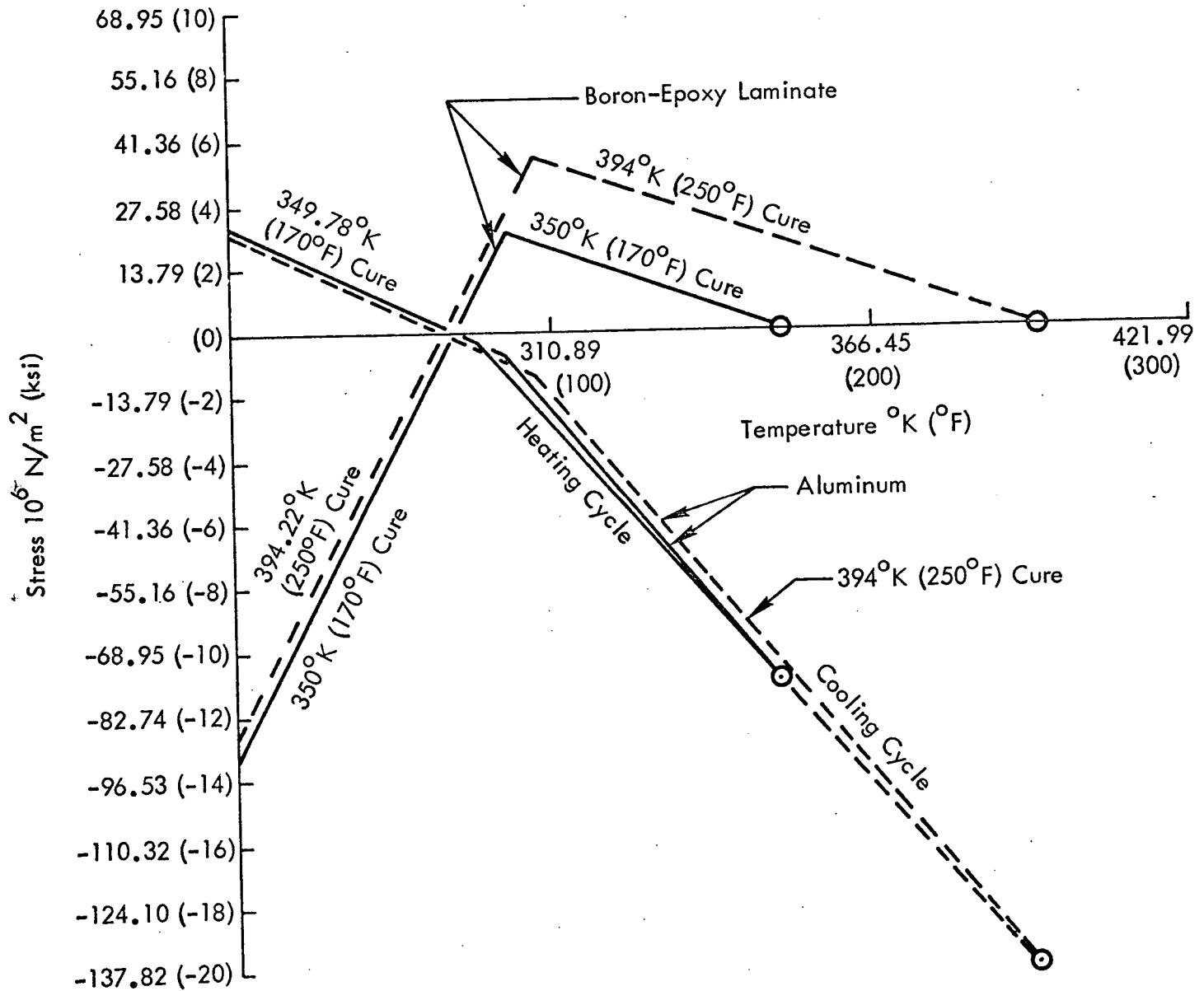


FIGURE 13. - RESIDUAL STRESS VERSUS TEMPERATURE FOR "COOL TOOL" CURE PROCESS

TABLE 1.- FATIGUE ENDURANCE SUMMARY

Surface (@ W.S. 142)	Analysis Phase	A _a /A _b	Maximum Potential Weight Savings (%)	Fatigue Endurance (Millions of Flight Hours)			Temperature			Residual Thermal Stress 10 ⁷ N/m ² (psi)
				K _t (Quality Level)			ΔT	T _{cure}	T _{operating}	
				4.0	6.0	12.0	°K (°F)	°K (°F)	°K (°F)	
Upper	C-130B/E	100/0	-	8.4	.55	.076	-	-	-	-
	Phase IA	70/30	9	1000.0	2.2	.19	55.6 (100)	352.6 (175)	297 (75)	3.86 (5600)
		70/30	9	16	.19	.035	111.1 (200)	352.6 (175)	241.5 (-25)	7.72 (11,200)
		70/30	9	1.9	.087	.019	134.4 (242)	352.6 (175)	218.2 (-67)	9.65 (14,000)
	Phase IB Method 1	80/20	21	74.	1.3	.14	55.6 (100)	352.6 (175)	297 (75)	1.38 (2,000)
		80/20	21	28.	.60	.080	80.5 (145)	352.6 (175)	272 (30)	2.69 (3,900)
		80/20	21	21.	.49	.068	86.1 (155)	352.6 (175)	266.5 (20)	3.03 (4,400)
		70/30	-	4900.	15.	.6	55.6 (100)	352.6 (175)	297 (75)	1.79 (2,600)
		60/40	-	380000.	540.	5.	55.6 (100)	352.6 (175)	297 (75)	2.14 (3,100)
	Phase IB Method 2	80/20	21	74.	1.3	.14	83.3 (150)	352.6 (175)	269.3 (25)	1.37 (2000)
Lower	C-130B/E	100/0	-	1.7	.086	.013	-	-	-	-
	Phase IA	70/30	9	130.	.36	.033	55.6 (100)	352.6 (175)	297 (75)	3.86 (5,600)
		70/30	9	1.5	.044	.0069	111.1 (200)	352.6 (175)	241.5 (-25)	7.72 (11,200)
		70/30	9	.22	.017	.0041	134.4 (242)	352.6 (175)	218.2 (-67)	9.65 (14,000)
	Phase IB Method 1	80/20	16	4.2	.086	.01	97.2 (175)	352.6 (175)	255.4 (0)	3.62 (5,250)
		70/30	-	130.	.29	.028	97.2 (175)	352.6 (175)	255.4 (0)	4.79 (6,950)
		60/40	-	12000.	1.5	.085	97.2 (175)	352.6 (175)	255.4 (0)	5.58 (8,100)
	Phase IB Method 2	80/20	16	12.	.2	.023	97.2 (175)	352.6 (175)	255.4 (0)	2.26 (3,200)

3.2.3 Computer Program

A computer program for the analysis of the composite reinforced aluminum structure in the hat section/skin areas has been completed and checked out. Thermal stresses, induced in the structure as a result of the difference in thermal expansion coefficients of boron-epoxy and aluminum, are calculated in two parts. The first part computes the stresses caused by bonding at elevated temperatures and subsequently cooling to the temperature at which the panels are assembled. This computer program includes the effects of bonding while the aluminum is externally restrained during cure. Because of different area ratios of boron-epoxy to aluminum, stresses are calculated separately for the skin and hat sections. The second part of the program determines the stresses caused by the aircraft operating at a temperature above or below that at which the structure was assembled. In this case the stiffened skin plus stringer assembly is assumed to expand or contract as a unit.

Program output data includes:

- o Stresses in the skin and stiffener elements resulting from the applied loading.
- o Residual thermal stresses caused by bonding at elevated temperatures and subsequent cooling to operating temperatures.
- o Wide column buckling allowable of stiffened skin panel.
- o Stiffness properties and centroid location of cross section.
- o Weight of compound composite configuration.
- o Stresses in an "all-aluminum" section of the same weight.

Stresses resulting from shear loading have been incorporated into the computer program. Details of the analysis procedure are included herein as Appendix C.

3.2.4 Estimated Weight Saving

An estimated weight savings of 274.4 kg (605 lb.) per airplane has been predicted using the selected 80/20 distribution of aluminum/boron-epoxy. This estimate is based on the typical element cross sectional areas shown on Figures 14 and 15 and on the following:

Upper Surface - 11 Total Stringer Elements¹

Density of aluminum = $2.8 \times 10^3 \text{ kg/m}^3$ (0.101 lb./in.³)

Density of Boron-Epoxy = $1.94 \times 10^3 \text{ kg/m}^3$ (0.07 lb./in.³)

Mean Aluminum weight removed = 2.16 kg/m/stringer (0.121 lb./in./stringer)

Mean Boron-Epoxy Weight Added = 0.56 kg/m/stringer (0.0315 lb./in./stringer)

Mean Weight Saved = 1.6 kg/m/stringer (0.0895 lb./in./stringer)

Assume effective stringer element length of 10.16 m (400 in.) to account for end fittings, etc.

Weight Saved = 178.7 kg (394 lb.)

Lower Surface - 13 Total Stringer Elements¹

Mean Aluminum weight saved = 1.225 kg/m/stringer (0.0686 lb./in./stringer)

Mean Boron-Epoxy weight added = 0.5 kg/m/stringer (0.028 lb./in./stringer)

Mean Weight Saved = 0.725 kg/m/stringer (0.0406 lb./in./stringer)

Assume again an effective stringer length of 10.16 m (400 in.)

Weight Saved = 95.7 kg (211 lb.)

3.2.5 Wing Box Configuration

The center wing box size and location is illustrated in Figure 16. The box is 11.2 m (440 in.) long, 2.03 m (80 in.) in chord, and weighs approximately 2243 kg (4944 lbs.) in the all-metal versions. Using boron-epoxy reinforcements as shown in Figures 17 and 18, equivalent static strength and fatigue endurance can be provided with a weight saving of 274 kg (605 lbs.). This concept uses existing C-130 B/E components such as ribs, spars, fittings, and access panels. Upper and lower skin panel assemblies are redesigned using boron-epoxy composite reinforcements bonded to aluminum skin planks and hat section stringers. The aluminum skins and stringers have reduced thicknesses compared to those of the model C-130 B/E aircraft; equivalent strength is provided by the unidirectional composite. The final design configuration will be structurally and functionally interchangeable with the production C-130 B/E wing box. Extensive reliability and quality assurance involvement throughout the program will provide intensive control over the development and production of the boron-reinforced wing boxes.

¹ A stringer element is defined as a hat section stiffener, the amount of wing skin surface which is associated with it, and the applicable boron-epoxy reinforcements.

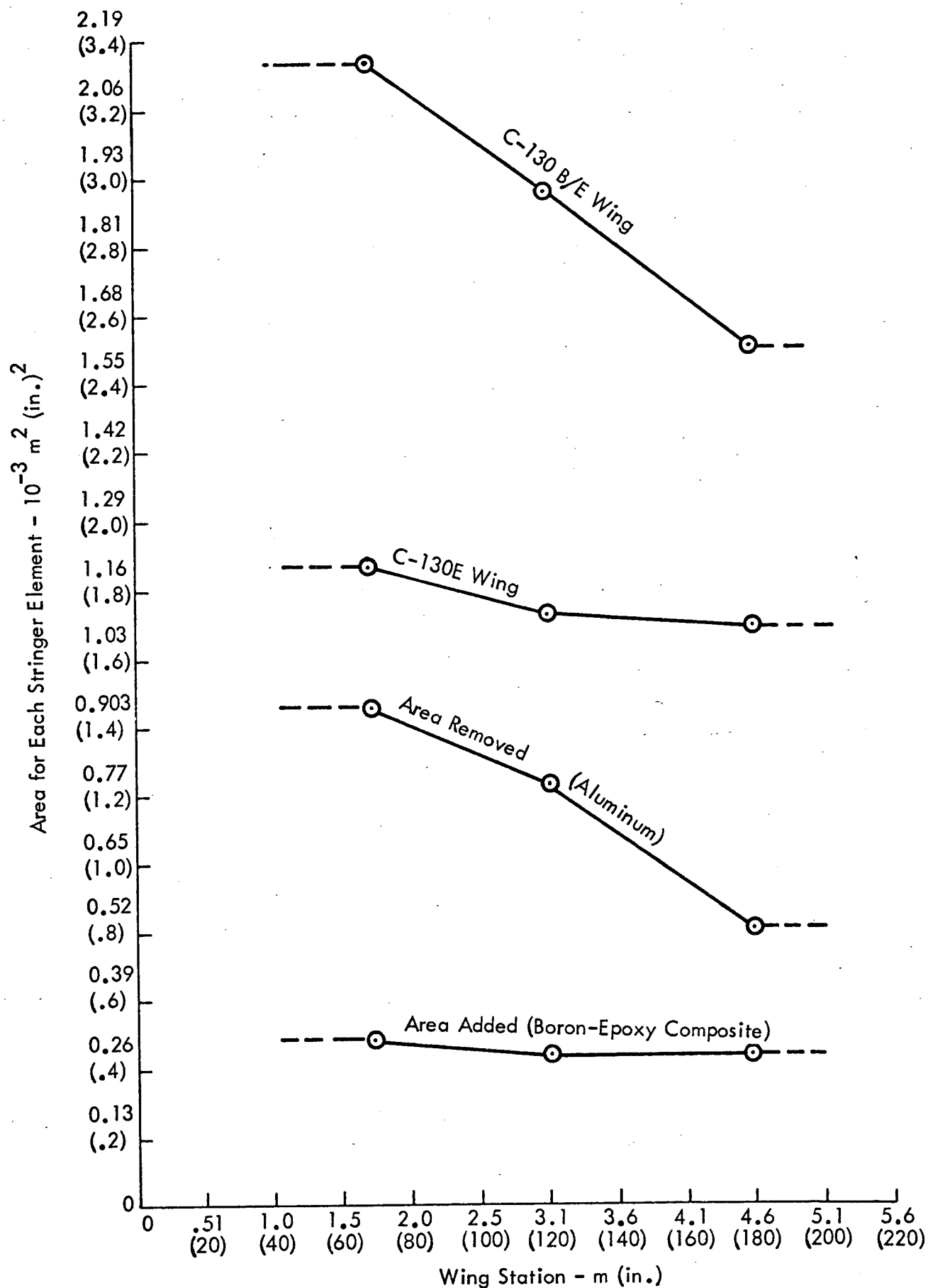


FIGURE 14. - UPPER SURFACE STRINGER ELEMENT AREAS (TYPICAL)
(INCLUDES EFFECTIVE SKIN AREA)

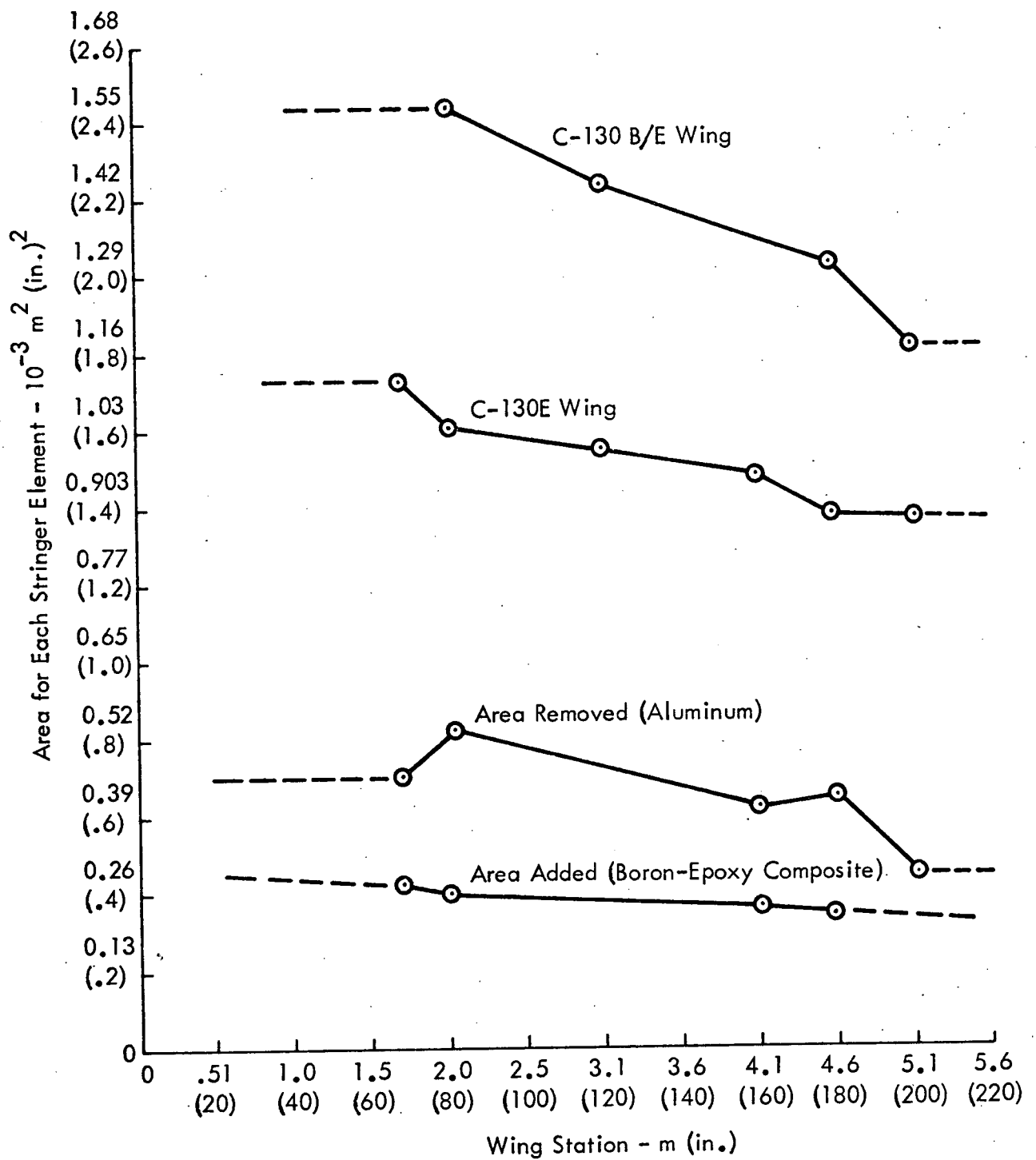


FIGURE 15. - LOWER SURFACE STRINGER ELEMENT AREAS (TYPICAL)
(INCLUDES EFFECTIVE SKIN AREA)

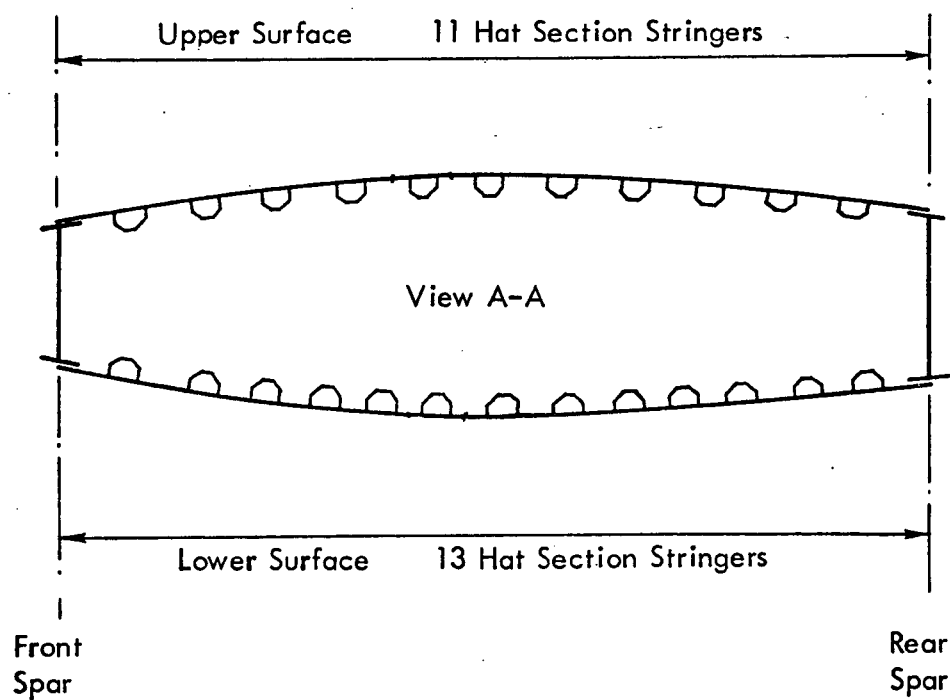
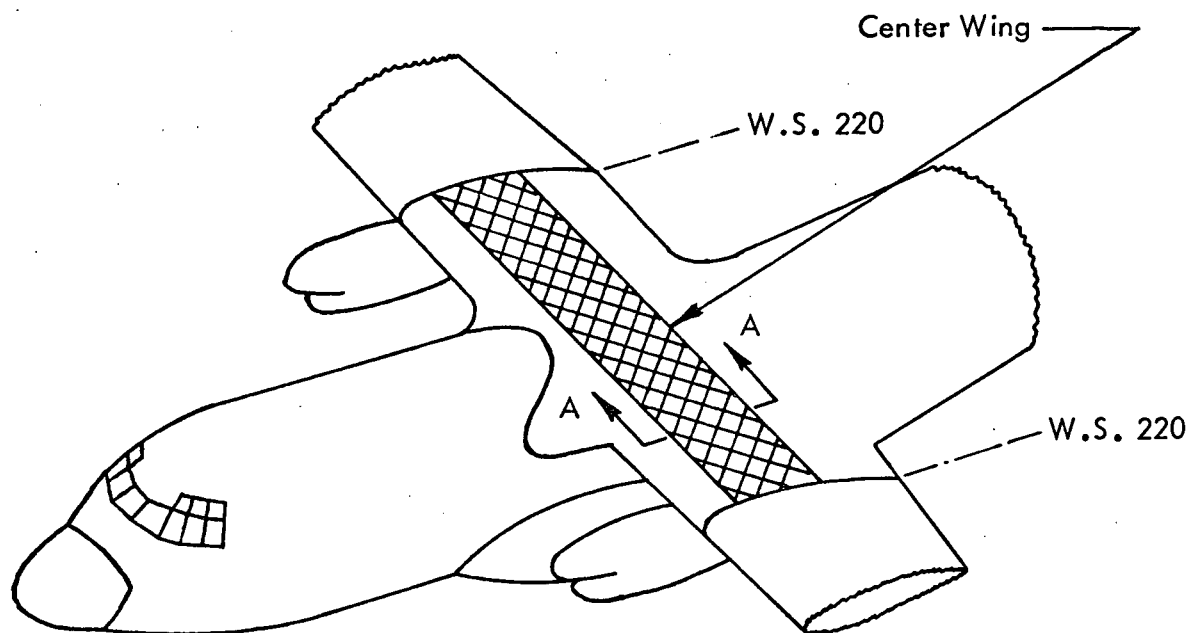


FIGURE 16.-C-130 BORON-EPOXY REINFORCED CENTER WING STRUCTURE

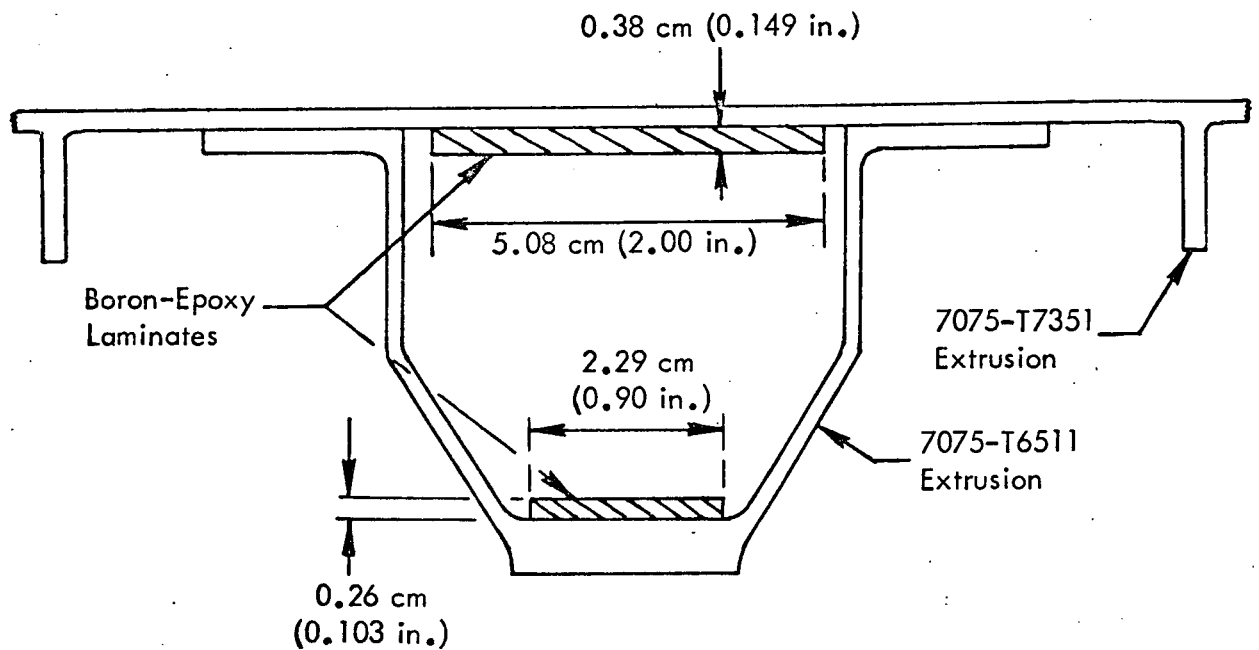


FIGURE 17. - TYPICAL UPPER SURFACE STRINGER ELEMENT

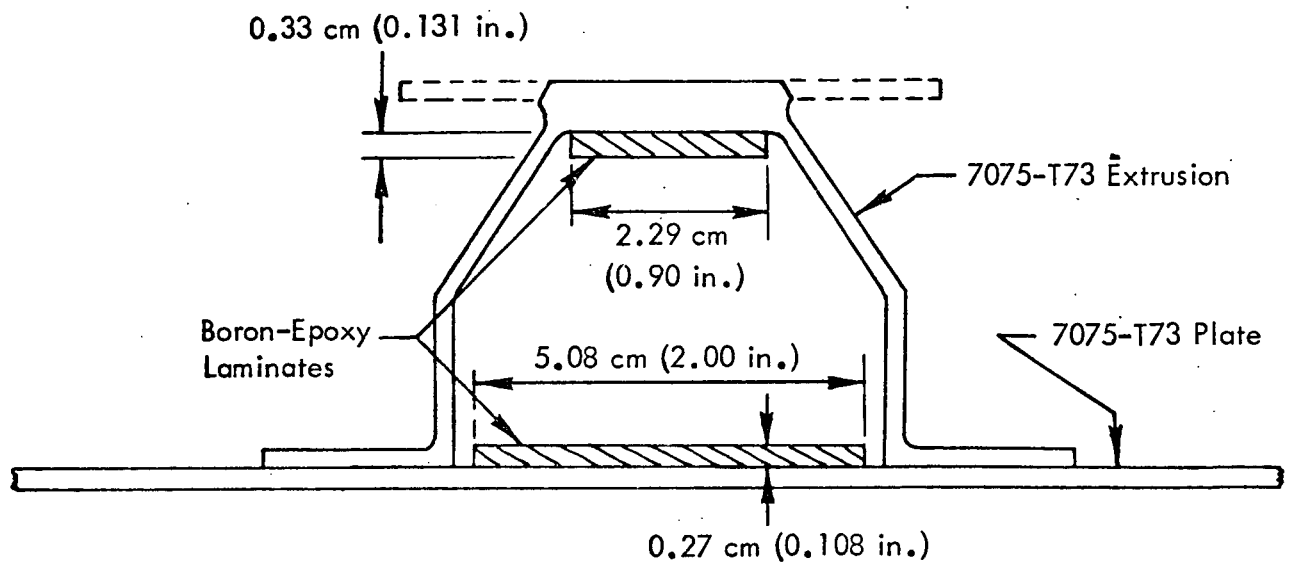


FIGURE 18. - TYPICAL LOWER SURFACE STRINGER ELEMENT

3.2.5.1 Rainbow Fittings

Special considerations were given to the transition area at the Wing Station 220.00 joint. Because of the complexity of the design in this area, several structural configurations were assessed; the final selected configuration is illustrated in Figure 19. In this configuration, the existing rainbow fittings and splice straps were maintained. The wing planks and hat section stiffeners were machined to the C-130 B/E configuration in the joint area and transitioned to the thinner C-130E configuration inboard of the joint. The laminates for both the wing planks and stiffeners are designed to taper out in this transition area, where the C-130E skin thickness tapers to the C-130 B/E skin thickness at the rainbow fitting. This results in an all-metal joint in the rainbow fitting area and a composite reinforced structure at the net section area of the wing plank.

3.2.5.2 Doors

In the area of the access doors the wing planks and hat section stiffeners are of the same configuration and cross sectional area as the C-130 B/E structure. Design of the transition areas is handled in a manner similar to that used for the rainbow fitting at the W.S. 220.0 joint. The material in the planks and stringers tapers from the thinner C-130E configuration to the thicker C-130 B/E configuration at the openings. The boron-epoxy laminates in these areas on the planks taper down at the openings as shown in Figure 20.

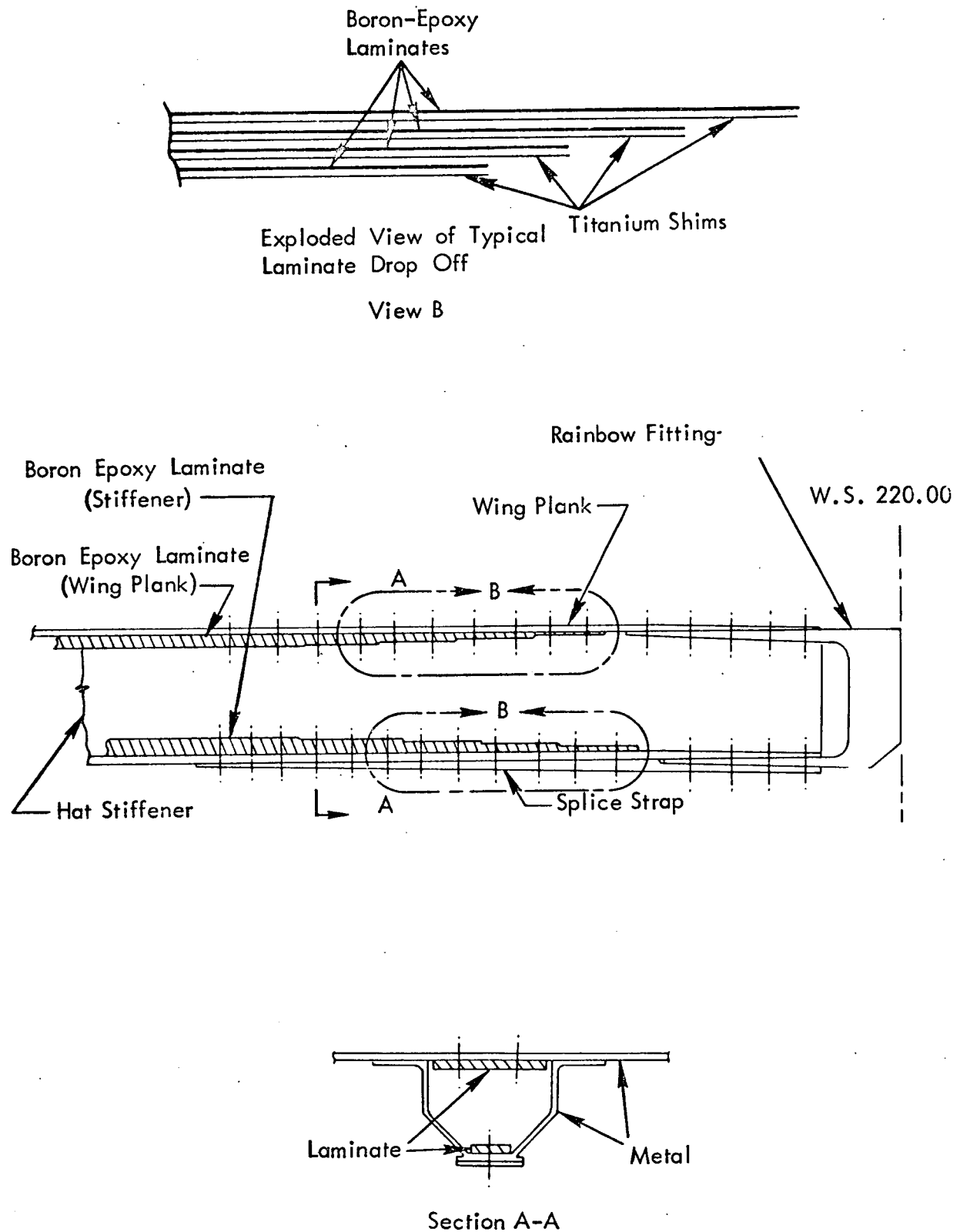


FIGURE 19.- TYPICAL WING STATION 220.00 JOINT DESIGN

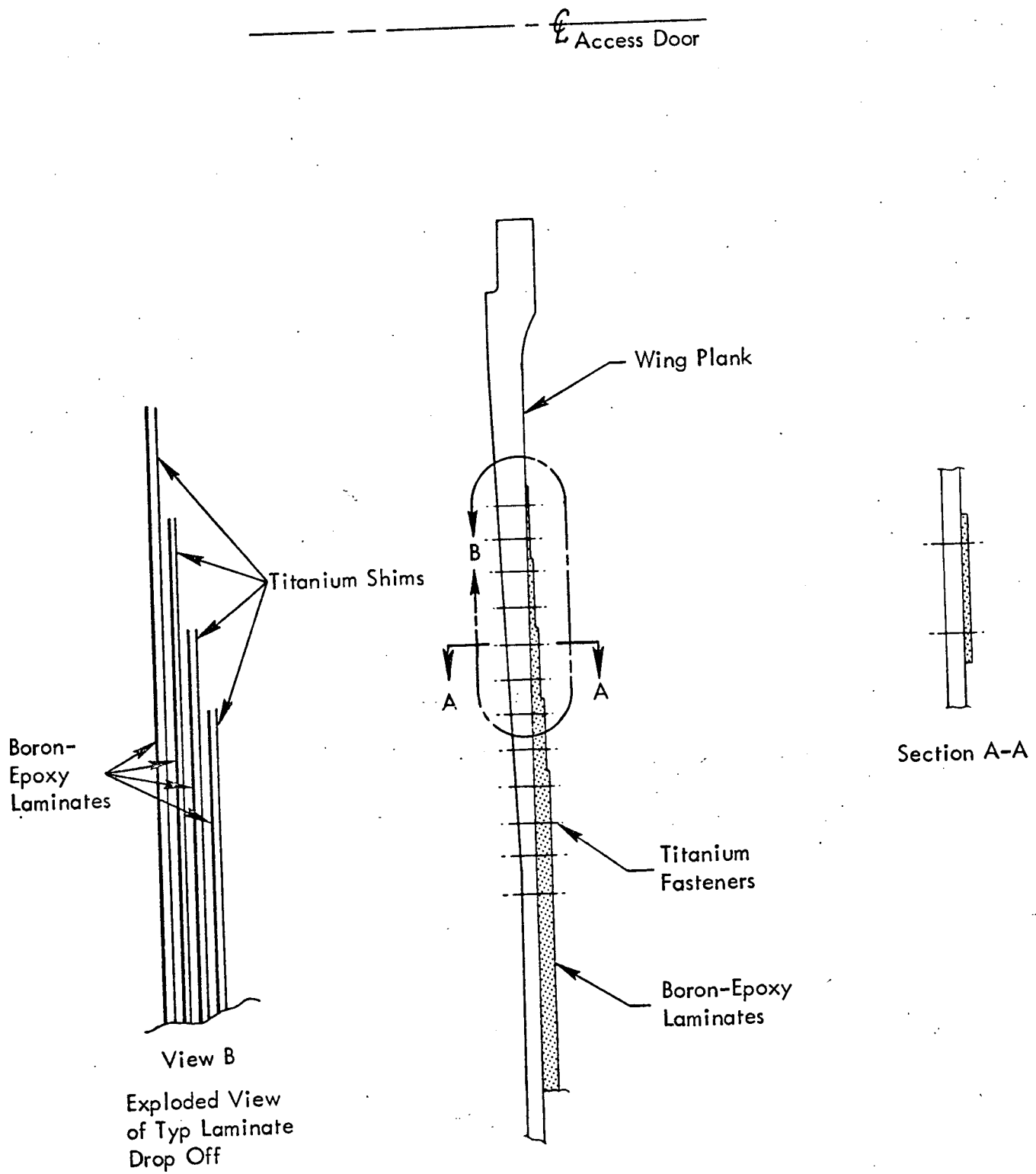


FIGURE 20.- TYPICAL WING PLANK AND LAMINATE RUN OUT AT ACCESS DOOR

4.0 MATERIALS AND PROCESSES

4.1 MATERIALS

New material development for this program was minimal and was limited to adhesives and their processing. This developmental work was directed toward providing a low-temperature curing adhesive system and related processing to effect its cure for bonding boron-epoxy laminate to aluminum. Other materials such as boron-epoxy preimpregnated tape, aluminum, sealants, finishes, titanium, and fasteners were procured and/or processed to the requirements of existing Lockheed specifications.

4.1.1 Boron-Epoxy Preimpregnated Tape

All Phase I material was procured to the requirements of Lockheed Material Specification STM22-450 which was revised to reflect specific program requirements and currently attainable mechanical properties. The Phase I material quantity requirement was released to previously qualified vendors for quotation purposes.

Since material for initial Phase I development work was required at the onset of the program, surplus material from Lockheed stores was checked for conformance to the receiving inspection mechanical property requirement. Conformance to receiving inspection requirements was verified and the material was issued for use. The remaining quantity requirement for Phase I boron-epoxy material production was shared by the two lowest bidders. One of the vendors supplied 2.54 cm (1 in.) wide tape and the other vendor supplied 5.08 cm (2 in.) wide tape. Dual sources were used in order to gain servicing experience from both suppliers, which will be an important consideration at the time of selecting the supplier for Phase III material.

4.1.1.1 Boron-Epoxy Tape Specification

Lockheed Material Specification STM22-450 was revised by Specification Revision Notice (SRN) Number 2 to reflect mechanical properties presently being realized by material suppliers. These properties are contained in Table II. Additionally, this document was revised to allow procurement of various widths of tape by specifying the width in the purchase order, to clarify the mechanical property test methods, to incorporate a standard cure cycle, and to clarify packaging requirements.

TABLE II. -ROOM TEMPERATURE MECHANICAL PROPERTY REQUIREMENTS

Property	Units	Required Average	Minimum Individual
0° Flexure Strength	10^9 N/m^2 (10^3 psi)	1.65 (240.0)	1.55 (225.0)
0° Flexure Modulus	10^{11} N/m^2 (10^6 psi)	2.07 (30.0)	1.93 (28.0)
90° Flexure Strength	10^7 N/m^2 (10^3 psi)	8.96 (13.0)	7.58 (11.0)
0° Horizontal Shear Strength	10^7 N/m^2 (10^3 psi)	8.96 (13.0)	7.58 (11.0)
0° Tensile Strength	10^9 N/m^2 (10^3 psi)	- -	1.24 (180.0)
0° Tensile Modulus	10^{11} N/m^2 (10^6 psi)	2.07 (30.0)	1.93 (28.0)
90° Tensile Strength	10^7 N/m^2 (10^3 psi)	7.58 (11.0)	6.21 (9.0)
90° Tensile Modulus	10^{10} N/m^2 (10^6 psi)	2.00 (2.9)	1.86 (2.7)
0° Tensile Strain	10^{-6} m/m (10^{-6} in./in.)	6000 (6000)	- -
90° Tensile Strain	10^{-6} m/m (10^{-6} in./in.)	4100 (4100)	4000 (4000)

4.1.1.2 Boron-Epoxy Tape Procurement

After the Phase I material requirements were established and quotations obtained from qualified suppliers, orders were released to the two lowest bidders. The need schedule (quantity and date) was established and released to each supplier and performance records maintained in accordance with this schedule. Table III reflects the performance of each supplier.

4.1.1.3 Boron-Epoxy Tape Inspection

All material procured for this program was checked by the supplier for all properties listed in Table II. In addition, the supplier verified the material's conformance to specification requirements for resin content, volatile content and resin flow. Upon receipt, the material was checked by Lockheed for conformance to specification requirements for resin content, volatile content, resin flow, longitudinal flexure strength, transverse flexure strength, and horizontal shear strength. Tests on the first lot of material received indicated low transverse flexure strength properties. Analysis of the data and visual examination of the failed test specimens showed that the indicated low transverse flexure strength was not a material deficiency but was due to the tape's physical dimension and the method of preparing the test specimens. Since the transverse flexure specimen length is 7.62 cm (3 in.), using tapes whose width is less than this dimension requires butt joining of each ply to achieve the proper specimen length. This results in butt joints in the reinforcing scrim and in turn results

TABLE III.-BORON-EPOXY TAPE REQUIREMENT AND DELIVERY SCHEDULE

Tape Width	Length of Tape Meters (Feet)		Receipt Date		Supplier Identification	
	Ordered	Received	Scheduled	Actual	Batch	Roll
5.08 cm (2 in.)	579 (1900)	579 (1900)	11/1/71	11/2/71	47	166, 167, 168 & 170
	884 (2900)	884 (2900)	12/6/71	12/10/71	46	21B, 22, 23, 24, 25, 27 & 29
	853 (2800)	895 (2935)	1/6/72	1/5/72	46	28, 30, 31, 32, 33, 34 & 35
	853 (2800)	866 (2840)	2/1/72	2/17/72	46	56, 57, 58, 59, 60, & 61
	165 (540)	152 (500)	3/1/72	3/1/72	46	62
2.54 cm (1 in.)	396 (1300)	396 (1300)	11/1/71	11/19/71	191	11
	610 (2000)	610 (2000)	12/6/71	12/10/71	183	4-1, 4-2, & 4-3
	579 (1900)	579 (1900)	1/6/72	1/12/72	183	5-1, 5-2, 5-3, & 5-4
	579 (1900)	689 (2260)	2/1/72	2/7/72	183	4, 5, & 7
	110 (360)	(*)	3/1/72	2/7/72	-	-

*Included in the 2/7/72 material shipment.

in low transverse flexure strength. Therefore, since this was not a deficiency in the material, but was a peculiarity of the tape dimension, the requirement for conducting this test as part of receiving inspection was deleted.

4.1.2 Adhesives Selection and Evaluation

AF 127-3 adhesive was selected as the primary adhesive for bonding the boron-epoxy laminates to the aluminum skins and hat stiffeners, and studies were conducted to determine the minimum cure temperature to obtain satisfactory strength values. As shown in Table IV the 218°K (-67°F) tensile shear strength was slightly low for both the 353°K (175°F) and 361°K (190°F) cure. To see if increased cure time would improve these low temperature strengths, both tensile shear and Bell peel specimens, using AF 127-3 adhesive cured six hours, were fabricated and tested. The actual cure temperature for these runs was 358°K (185°F) and 369°K (205°F), respectively, slightly higher than desired but within acceptable limits. Peel and shear strength of the 358°K (185°F) cure was low, but the 369°K (205°F) cure provided good shear and peel strengths as shown in Table V. These results, together with the analytical studies discussed later in this section, led to the adoption of a minimum cure cycle of four hours at $366 \pm 5.6^\circ\text{K}$ ($200^\circ \pm 10^\circ\text{F}$) for bonding boron-epoxy to aluminum with AF 127-3 adhesive.

TABLE IV.-INITIAL CURE STUDY OF AF 127-3 ADHESIVE

Cure Cycle				Tensile Shear Strength $\triangle 2$		
Temp $^{\circ}\text{K}$ ($^{\circ}\text{F}$)	Time (Hrs)	Pressure 10^5N/m^2 (psi)	Surface Condition $\triangle 1$	218.2 $^{\circ}\text{K}$ (-67 $^{\circ}\text{F}$) 10^7N/m^2 (psi)	RT 10^7N/m^2 (psi)	344.3 $^{\circ}\text{K}$ (160 $^{\circ}\text{F}$) 10^7N/m^2 (psi)
394.3 (250)	1	2.07 (30)	1	2.55 (3700)	3.24 (4700)	1.98 (2800)
394.3 (250)	1	2.07 (30)	2	4.07 (5900)	3.52 (5100)	2.34 (3400)
380.4 (225)	1	.517 (7.5)	1	3.09 (4400)	2.67 (3875)	1.34 (1950)
380.4 (225)	1	.517 (7.5)	2	3.86 (5600)	3.17 (4595)	2.07 (3000)
360.9 (190)	2	.517 (7.5)	1	2.28 (3300)	3.37 (4890)	2.17 (3150)
360.9 (190)	2	.517 (7.5)	2	2.55 (3700)	3.47 (5030)	2.21 (3200)
352.6 (175)	4-1/2	.517 (7.5)	1	1.45 (2100)	3.10 (4500)	2.00 (2900)
352.6 (175)	4-1/2	.517 (7.5)	2	2.07 (3000)	3.29 (4770)	2.03 (2950)

$\triangle 1$ 1 - Metal Bond Etch with Primer
2 - Metal Bond Etch without Primer

$\triangle 2$ Specimens used 1.6 mm
(0.063 in.) thick aluminum
adherends with 1.27 cm
(0.5 in.) overlap.

TABLE V.-TENSILE SHEAR AND BELL PEEL TESTS OF AF 127-3

Tensile Shear Tests	Cure Temp., °K (°F)	Test Temp. °K (°F)	Shear Strength 10 ⁷ N/m ² (psi)
	358.2 (185)	218.2 (-67)	1.72 (2500)
		RT	3.59 (5200)
		344.3 (160)	2.07 (3000)
369.3 (205)	218.2 (-67)	3.45 (5000)	
	RT	3.59 (5200)	
	344.3 (160)	2.48 (3600)	
Bell Peel Tests	Cure Temp., °K (°F)	Test Temp. °K (°F)	Peel Strength N/mw (piw)
	358.2 (185)	218.2 (-67)	1874 (10.7)
		RT	6637 (37.9)
		344.3 (160)	6988 (39.9)
369.3 (205)	218.2 (-67)	4431 (25.3)	
	RT	6585 (37.6)	
	344.3 (160)	6707 (38.3)	

- NOTES: 1. Cure time - 6 hours
2. Cure pressure - 2.07×10^5 N/m² (30 psi)
3. Adherends for tensile tests were aluminum and steel.
4. Adherends for peel tests were both aluminum.
5. All aluminum surfaces were primed with EC 3921 non-self-curing primer.

Work has been conducted on a room-temperature-curing adhesive, EA9309-1, as a backup to the AF 127-3 adhesive. This room-temperature-curing adhesive exhibited 218°K (-67°F) peel strength and 344°K (160°F) shear strength slightly lower than desired. These properties were improved by pre-coating adherends with cured AF 127-3. A peel ply was used on the bonding surface and was removed just prior to bonding. This method increased the 218°K (-67°F) peel strength from 1751 to 4378 Newtons per meter width (N/mw)(10 to 25 pounds per inch width (piw)).

The tensile shear and Bell peel test specimens for adhesive evaluation are shown in Figures 21 and 22, respectively. For the shear test specimens reported in Table V, steel was substituted for one of the aluminum adherends to determine the effects of different coefficients of thermal expansion of the two adherends on the shear strength. The shear test specimens were machined from standard finger panels and the peel specimens were machined from the panel illustrated in Figure 22.

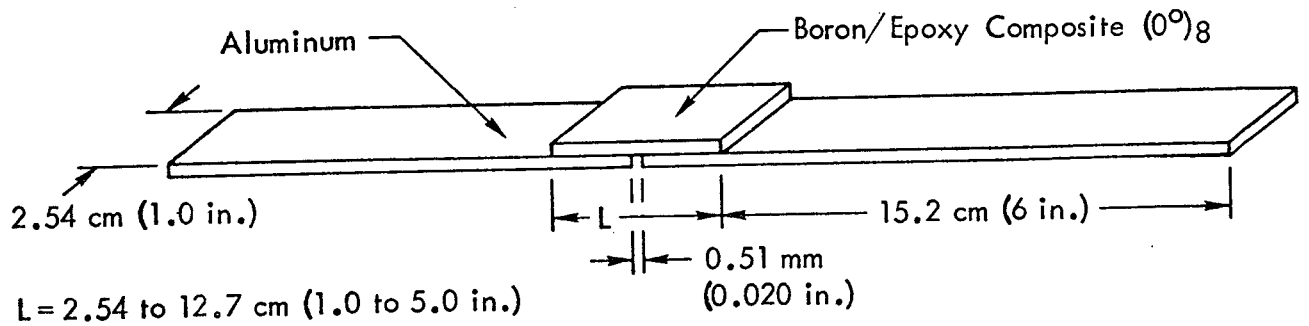
Surface preparations for the adhesive evaluations, reported above, were metal-bond etch for the aluminum and hand sanding and solvent wash for the steel adherends. The adherends were then either primed with EC 3921, a non-self-curing primer, or else the adhesive was applied directly to the cleaned metal. After adhesive application, the panels were cured at noted temperatures and times prior to machining and testing.

Shear tests were conducted at a loading rate between 8.27×10^6 and 9.65×10^6 N/m² (1200-1400 psi) per minute, with load being applied through spherically seated Templin grips. A low-temperature Missimer furnace was used for the environmental chamber for the 218°K (-67°F) and 344°K (160°F) tests. Shear tests were conducted using MMM-A-132* as a guide. Peel tests were conducted at a loading rate of 15.2 cm (6.0 in.) of peel per minute in the environmental chamber which was described for the shear tests. The peel tests were conducted using ASTM D-14 as a guide. All specimens were allowed to soak a minimum of ten minutes at the test temperature prior to testing.

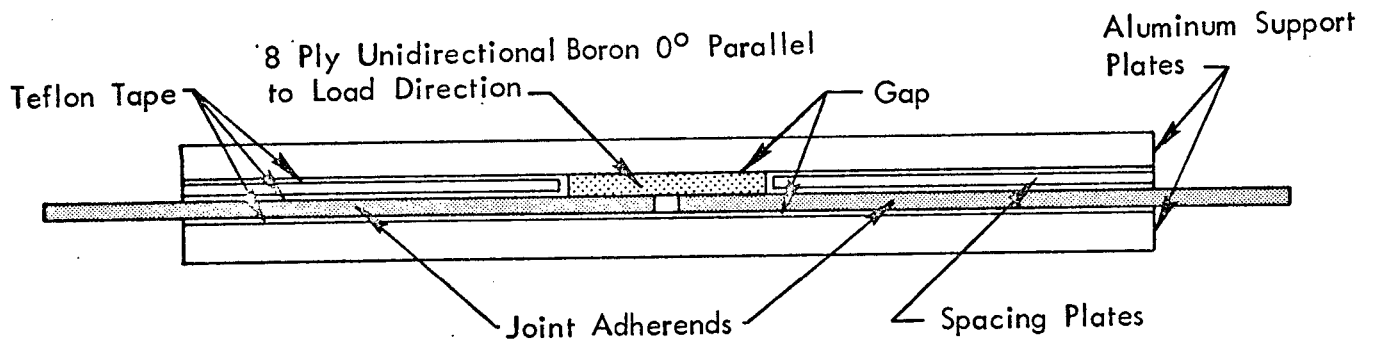
Analytical studies were conducted to determine the degree of cure of the adhesive using Infrared (IR), Differential Thermal Analysis (DTA), and Automated Dielectrometry (Audrey II). The IR analysis defines the ratio of the aromatic absorption peak at 6.6 micron and the epoxide absorption peak at 10.9 micron as an indication of the degree of cure. The ratio measured for several AF 127-3 adhesive cure cycles is shown in Table VI.

*MMM-A-132 is a military specification titled, "Adhesive, Heat Resistance, Airframe Structural Metal to Metal."

BORON-EPOXY TO ALUMINUM



(Test Fixture To Preclude Lateral Bending)



METAL TO METAL

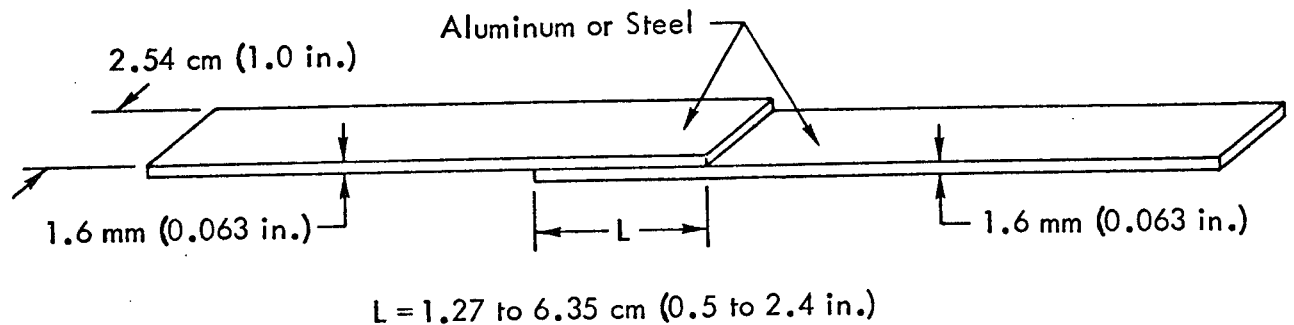


FIGURE 21.-TENSILE SHEAR TEST SPECIMENS AND TEST SUPPORT FIXTURE

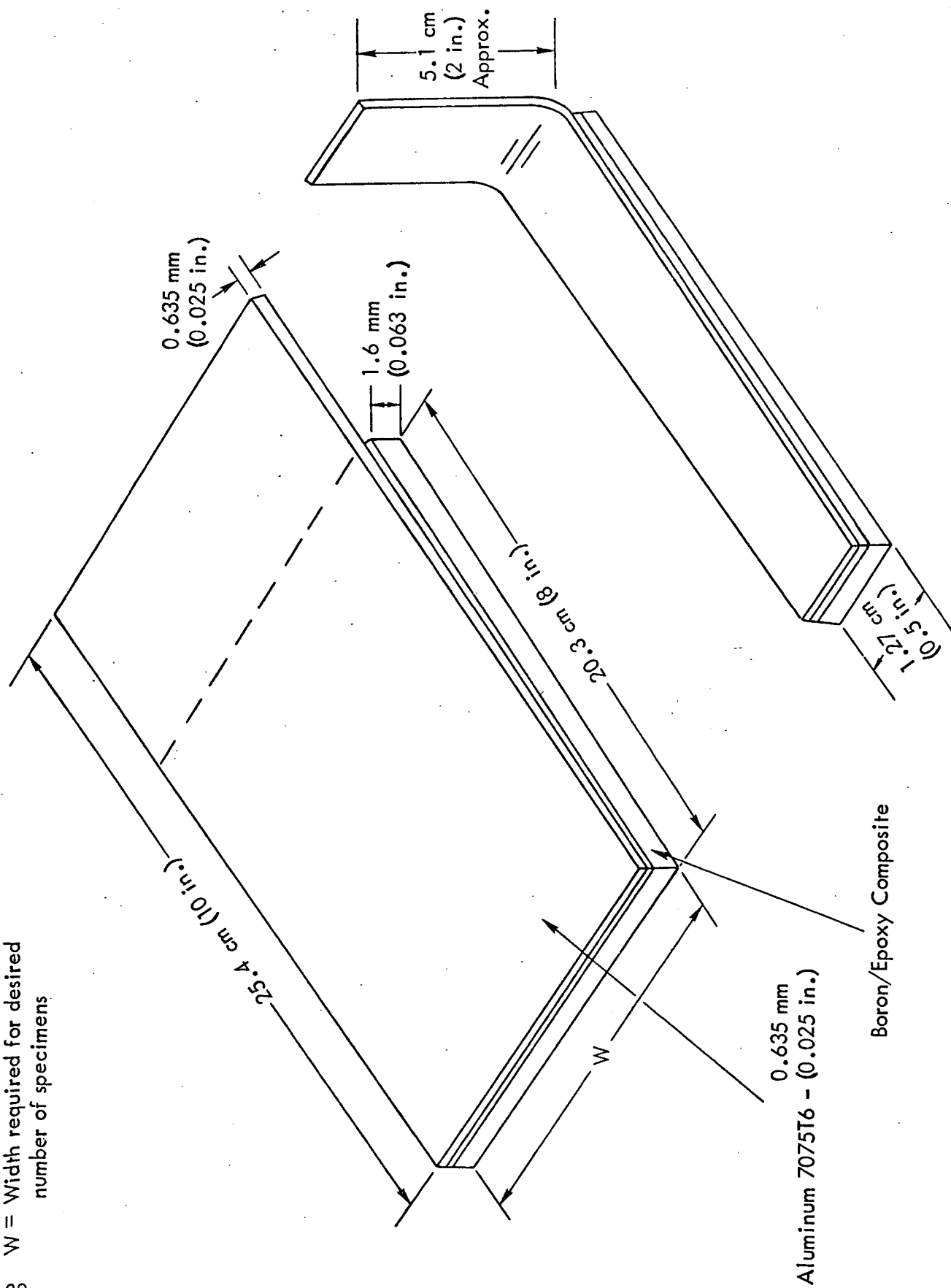


FIGURE 22.- PEEL TEST PANEL AND TEST SPECIMEN

TABLE VI. - INFRARED ANALYSIS OF AF127-3 WITH VARIOUS CURES

Cure Temp.		Time/Hours	Ratio
$^{\circ}\text{K}$	$(^{\circ}\text{F})$		
		Uncured	12
352.6	(175)	4-1/2	42
352.6	(175)	6	46
363.7	(195)	2	56
363.7	(195)	6	81
360.9	(190)	4	108
369.27	(205)	4	75
394.3	(250)	1/2	83
394.3	(250)	2	101

The cure of a polymer may be monitored by DTA which measures exotherm during cure. Several cures of AF 127-3 were subjected to DTA with the following results:

1. No exothermic reaction occurred with AF 127-3 adhesive below 355°K (180°F), but occurred in all cures between 355°K (180°F) and 361°K (190°F).
2. DTA indicated complete cure of AF 127-3 adhesive under the following conditions:
 - o 20 minutes at 394°K (250°F)
 - o 45 minutes at 361°K (190°F) plus 30 minutes at 366°K (200°F)
 - o 4 hours at 361°K (190°F)

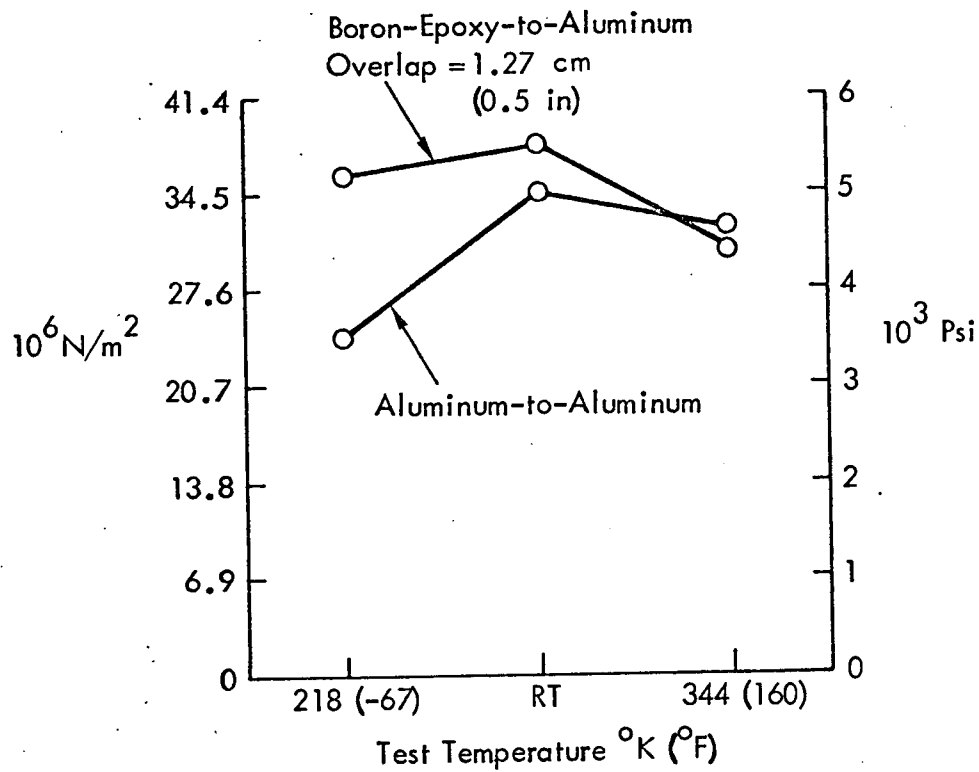
Results of the IR, DTA, and the mechanical properties, discussed previously, was the basis for establishing the minimum cure cycle of 4 hours at 366.5°K (200°F). The tests shown in Table VII were conducted to verify this selection for bonding boron-epoxy laminates to aluminum.

Aluminum adherend surfaces for these specimens were prepared for bonding by reduced chromic acid anodizing followed by EC 3921 primer. A fiberglass outer ply was incorporated in the composite adherend during layup and cure. This ply was stripped off just prior to bonding the laminate to the metal adherend.

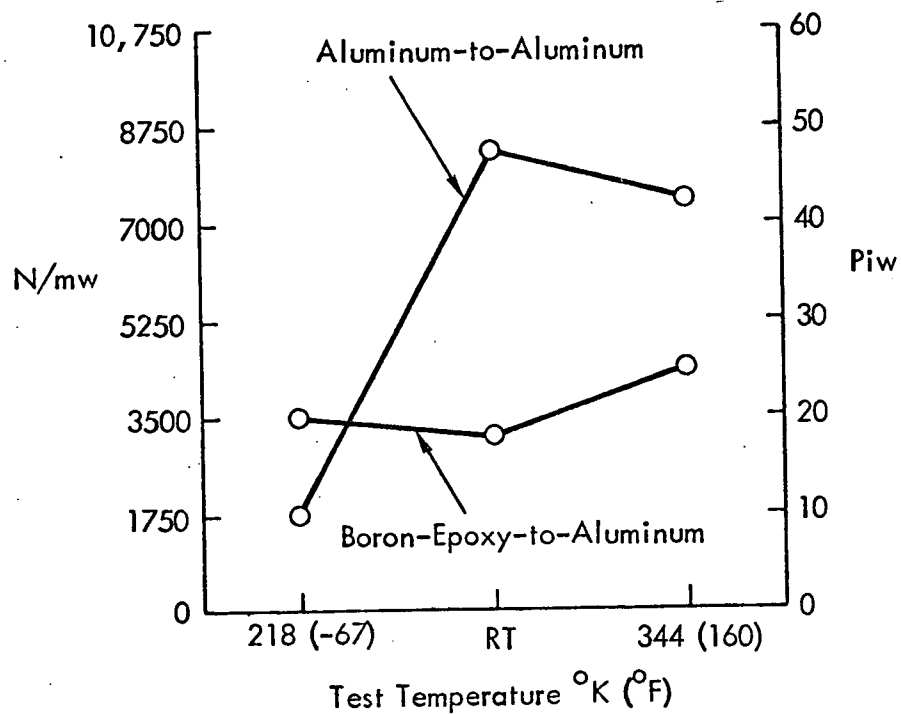
TABLE VII.-ADHESIVE VERIFICATION TEST -
AF127-3 CURED 4 HRS. AT 366°K (200°F)

Type of Test	Test Temp. °K (°F)	Adherends	Overlap cm (in.)	Prior Environmental Exposure
Tensile Shear	218.2 (-67) RT 344.3 (160)	Aluminum- to-Aluminum	1.27 (0.5)	None
Tensile Shear	218.2 (-67) RT 344.3 (160)	Boron-Epoxy- to-Aluminum	1.27 (0.5) 3.81 (1.5) 6.35 (2.5)	None
Bell Peel	218.2 (-67) RT 344.3 (160)	Aluminum- to-Aluminum and Boron- Epoxy-to- Aluminum	-	None
Tensile Shear	RT	Boron-Epoxy- to-Aluminum	1.27 (0.5)	JP-4 for 7 days Hi-humidity/ 30 days 5% Salt Spray/ 30 days Temp/Humidity Cycling (30 cycles)
Tensile Shear Creep	RT 344.3 (160)	Aluminum- to-Aluminum and Boron- Epoxy-to- Aluminum	1.27 (0.5)	None

Figures 23, 24, and 25 indicate the effects of test temperature, overlap length and/or environmental exposure on the adhesive in aluminum-to-aluminum and boron-epoxy-to-aluminum bond applications. Creep studies were conducted on both aluminum-to-aluminum and boron-epoxy-to-aluminum adherend systems and tested at room temperature and 344°K (160°F). Room temperature creep data was developed by exposing the specimens to a bond-line load of $11.0 \times 10^6 \text{ N/m}^2$ (1600 psi) for at least 192 hours. Elevated temperature data at 344°K (160°F) was generated by loading the specimen bondlines to $5.5 \times 10^6 \text{ N/m}^2$ (800 psi) for a minimum of 192 hours. Average creep deflection is shown in Table VIII.



(a) Tensile Shear Strength



(b) Bell Peel Strength

FIGURE 23.-SHEAR AND PEEL STRENGTH FOR AF 127-3 ADHESIVE

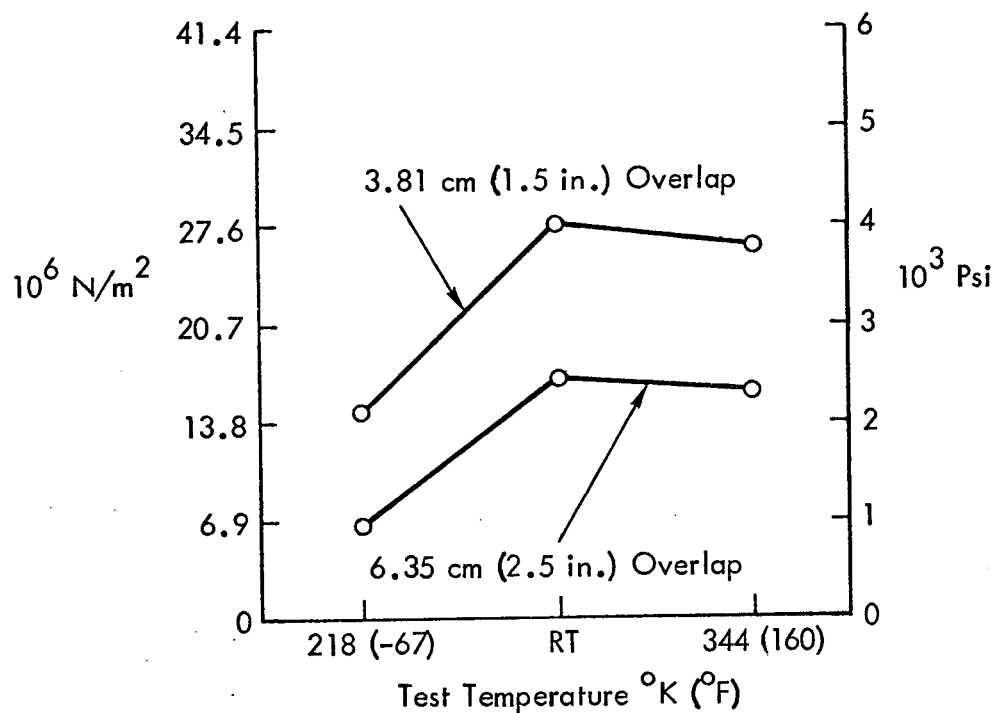


FIGURE 24.-TENSILE SHEAR STRENGTH OF BORON-TO-ALUMINUM WITH LONG OVERLAP

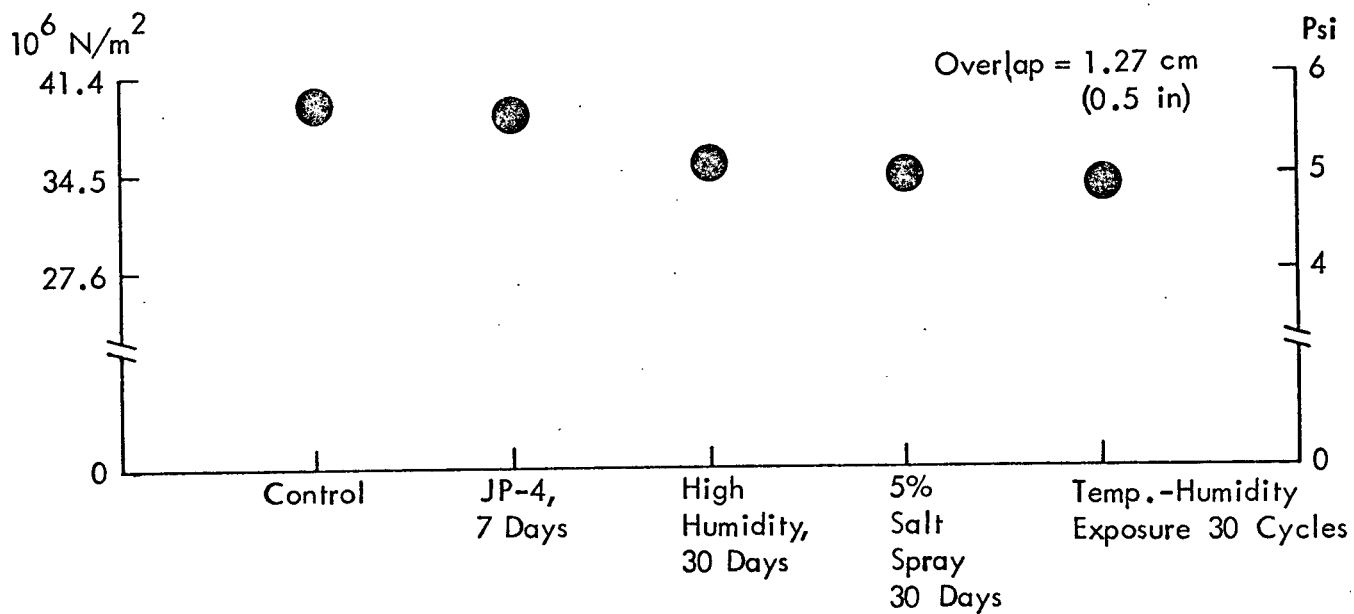


FIGURE 25.-BORON-TO-ALUMINUM TENSILE SHEAR STRENGTH AFTER ENVIRONMENTAL EXPOSURE

TABLE VIII.-CREEP STUDIES ON AF 127-3 ADHESIVE

Material Combination	Test Temp. °K (°F)	Hours at Load	Load 10^6N/m^2 (psi)	Creep Deflection 10^{-5}m (in)
Boron-Epoxy-to-Aluminum	RT	243.9	11.0 (1600)	2.54 (0.0010)
	344.3 (160)	211.8	5.5 (800)	2.54 (0.0010)
Aluminum-to-Aluminum	RT	223.0	11.0 (1600)	1.27 (0.0005)
	344.3 (160)	274.2	5.5 (800)	2.54 (0.0010)

The fairly extensive data obtained during the adhesive evaluation task, including individual tests, are tabulated in Appendix D.

New tooling development accomplished during Phase I allows a higher temperature cure for a shorter period of time to be used.

Testing to verify adequate properties of bonding boron-epoxy to aluminum using AF 127-3 adhesive cured for one hour at 380°K (225°F) and $1.35 \times 10^5\text{N/m}^2$ (20 psi) was conducted for comparison of this cure cycle with the cure cycle of four hours at 366°K (200°F) and $2.07 \times 10^5\text{N/m}^2$ (30 psi). The adherend surfaces were prepared for bonding as previously described. In addition, self-curing (EC3926) and non-self-curing (EC3921) primers were evaluated. Test results are shown in Table IX. The final bonding temperature was specified as $386 \pm 8^\circ\text{K}$ ($235 \pm 15^\circ\text{F}$).

4.2 PROCESSES

Boron-epoxy lamination, metal surface preparation and protection, and bonding were accomplished in accordance with the procedures outlined in this section.

4.2.1 Laminate Preparation

All boron-epoxy laminates were fabricated and prepared for bonding in accordance with Lockheed-Georgia Company Specification STP 60-202. The layup of the reinforcing boron-epoxy strips was accomplished on a flat tool with ply sequencing in accordance with the engineering drawings. Each laminate layup had a peel ply incorporated into the faying surface which, when removed prior to bonding, provided a good surface for bonding. A boundary support was placed around the periphery of each laminate to prevent fiber wash-out. The laminate was then bagged for autoclave curing. The cure cycle was $449.8 \pm 5.56^\circ\text{K}$ ($350 \pm 10^\circ\text{F}$) for 60 minutes minimum at a pressure of $5.86 \pm 0.345 \times 10^5\text{N/m}^2$ (85 ± 5 psi). Process controls included standard fifteen-ply laminate panels from which longitudinal flexural and horizontal shear specimens were prepared and tested.

TABLE IX.-SHEAR STRENGTH OF AF127-3 CURED 1 HR. AT 380°K (225°F)
AND $1.38 \times 10^5 \text{N/m}^2$ (20 psi)

EC3926			EC3921		
Specimen	Lap Shear 10^7N/m^2 (psi)	Failure Mode	Specimen	Lap Shear 10^7N/m^2 (psi)	Failure Mode
Tests at 218°K (-67°F)					
1-2	4.48 (6500)	90% AM/10% C	2-2	3.38 (4900)	95% AB/5% BP
1-5	5.31 (7700)	90% AM/10% C	2-5	3.79 (5500)	90% AB/10% BP
1-8	4.21 (6100)	80% AM/20% C	2-8	4.96 (7200)	60% C/20% AB/ 20% BP
Avg.	4.69 (6800)		Avg.	4.07 (5900)	
Room Temperature Tests					
1-1	3.65 (5300)	100% C	2-1	3.79 (5500)	100% C
1-4	3.72 (5400)	100% C	2-4	3.79 (5500)	100% C
1-7	3.86 (5600)	100% C	2-7	3.86 (5600)	100% C
Avg.	3.72 (5400)		Avg.	3.79 (5500)	
Tests at 344°K (160°F)					
1-3	2.69 (3900)	100% C	2-3	2.76 (4000)	100% C
1-6	2.62 (3800)	100% C	2-6	2.62 (3800)	100% C
1-9	2.83 (4100)	100% C	2-9	2.62 (3800)	100% C
Avg.	2.69 (3900)		Avg.	2.69 (3900)	

- NOTES: 1. All specimens have 1.27 cm (0.5 inch) overlap
2. C - Cohesive failure
3. AM - Adhesive to metal failure
4. AB - Adhesive to boron-epoxy failure
5. BP - Boron-epoxy peel

4.2.2 Surface Preparation for Bonding

All bonded interfaces were prepared in accordance with the procedures discussed below.

4.2.2.1 Aluminum

Aluminum details were protected against hostile and corrosive environments, and were prepared for bonding in accordance with standard Lockheed procedures. These procedures cover chromic acid anodizing and priming of bond surfaces.

Since a light chromic acid anodize provides a better bond surface than the sulfuric acid anodize, the sulfuric anodic film in the bond areas was replaced with chromic anodic film. This was accomplished by first masking the entire detail with chem mill maskant, removing the maskant from the bond areas, stripping the sulfuric acid anodize from the bond areas, and then applying a controlled thickness, non-sealed chromic acid anodize surface to the bond areas. The sulfuric acid strip and chromic acid anodize processes are outlined in Appendix E.

Within sixteen hours after chromic acid anodizing, the bond areas require priming. After priming, the parts may remain at room temperature for a period up to ninety days in a controlled environment before bonding. This provides, in addition to improved environmental resistance, a prolonged shelf life for the prepared metal details. Priming is conducted in accordance with the procedure shown in Appendix E.

4.2.2.2 Titanium

All titanium surfaces to be bonded were cleaned in accordance with the applicable portions of Lockheed-Georgia Standard Process Specification STP 57-004. The titanium cleaning procedure contained in this document is Lockheed proprietary information and is not available for publication.

4.2.2.3 Boron-Epoxy Laminate

During the lamination process, peel plies consisting of fiberglass impregnated with the same or compatible resin systems were placed over the laminate faying surface(s) and cured with the laminate. Prior to bonding, the peel plies were removed, providing clean roughened surfaces ready for bonding.

4.2.3 Other Surfaces

Laminate surfaces other than those to be bonded were coated with a standard sealant or sprayed with an epoxy overcoating. On some of the test specimens, no coating was

required. All other surfaces were aluminum and were sulfuric acid anodized to provide maximum corrosion protection.

4.2.4 Bonding Boron-Epoxy Laminates to Aluminum Parts

Processes for bonding boron-epoxy laminates to aluminum details were established during the development program and will be documented in a bonding process specification to be released later. The development work was directed to reduction of residual bondline stresses which were due to differences in coefficients of thermal expansion. Test components were fabricated with a standard adhesive film system cured with a special cure cycle. The cure cycle developed for the "cool tool" process (described in detail in other sections of this report) is 90 minutes minimum at $386 \pm 8.3^{\circ}\text{K}$ ($235 \pm 15^{\circ}\text{F}$) and 1.38 to $1.72 \times 10^5 \text{N/m}^2$ (20 to 25 psi), using a heat-up rate of 1.67 to 2.78°K (3 to 5°F) per minute.

4.2.5 Sealing and Painting

The next phase of operation consists of sealing and painting of details prior to assembly. The first operation was to overcoat all boron-epoxy laminates with STM40-111, Class A-2 (Productions Research Company, PR 1422G, A-2 or equivalent) fuel-resistant, high-adhesion, corrosion inhibiting sealing compound. The next operation consists of overcoating all details with MIL-C-27725 urethane. During assembly of the details, STM40-112, Class B12 (Products Research Company PR 1432G or equivalent) corrosion inhibiting, extended assembly time, faying surface sealing compound was applied to all faying surfaces. After assembly, squeeze-out of sealant along all faying surface edges was verified.

STM40-111 and STM40-112 sealants were selected over MIL-S-8802 sealants to obtain the corrosion inhibiting properties provided by the STM materials. STM40-111, Class A sealant was selected for sealing the boron-epoxy and bonds because its consistency made it applicable by brush coating. STM40-112, Class B sealants gave long assembly times as required for riveting the stiffener to skin joints.

5.0 MANUFACTURING DEVELOPMENT

5.1 BONDING TECHNIQUES

Difficulties in manufacturing a composite-reinforced metal structure are created by the differential thermal expansion of the two adherends during the bonding cycle. The aluminum adherend has a coefficient of thermal expansion five to six times that of the boron-epoxy laminate. This difference can cause high residual stresses at temperatures other than the bonding temperature. Development of bonding techniques to minimize this problem was a sizeable part of the Phase I activity, and culminated in the "cool tool" restraint process. Studies conducted included bonding with and without restraint, and even considered means to increase the extension of the boron at bonding temperature.

5.1.1 Bonding without Restraint

This study was undertaken to determine the resulting warp in panels developed due to variation of the areas of adherends of steel and aluminum. Steel was chosen as a substitute for boron for economic reasons. The area of the steel adherends was maintained constant and the area of the aluminum was varied. All bonding was done without restraint under similar bonding conditions. The adhesive system used was AF127-3, 0.293 kg/m^2 (0.06 psf), manufactured by the 3M Company. The steel was 4130 and the aluminum was 7075-T6.

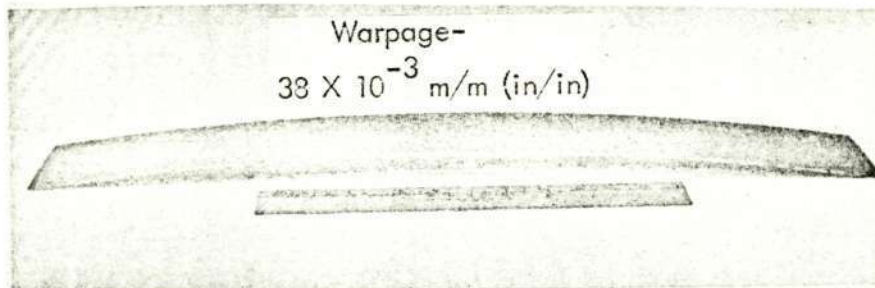
Three specimens were bonded without restraint. The steel adherends in all three were 1.02 mm (0.040 in.) thick, and the adhesive cure temperature was 400°K (260°F). Bonding pressure was supplied by using a vacuum bag. The aluminum adherend thickness was varied from 1.52 mm (0.060 in.) to 6.35 mm (0.250 in.). The resulting warpage of the three specimens is shown in Figure 26, and was computed by dividing the specimen deviation from flatness by its length.

Based on the relative areas of aluminum used and the resulting warpage, it was concluded that there would be combinations which could be bonded without restraint, but that within the area ratios being considered for the boron-epoxy laminate to aluminum bond, restraint would be required. The resulting studies are reported in the following section.

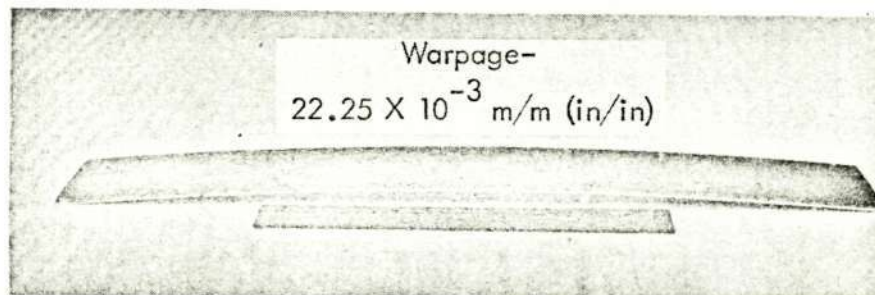
5.1.2 Bonding with Restraint

In this study, the material with the lower coefficient of expansion and higher modulus was stretched at elevated temperature and the material with the higher coefficient of expansion and lower modulus was compressed in a manner so that the loads were equivalent in each bonded element.

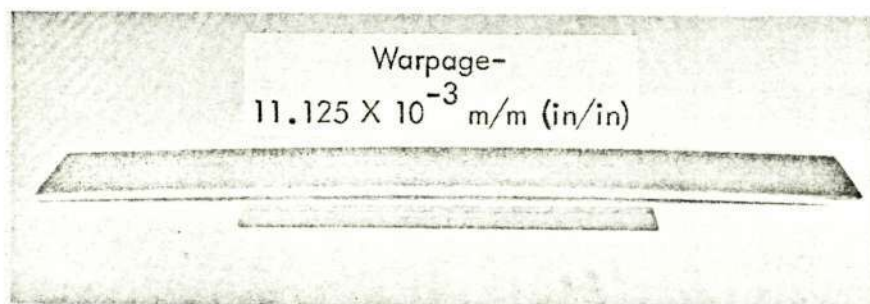
To minimize cost, steel was used in lieu of boron-epoxy laminates. Steel was chosen because its modulus of elasticity is comparable to boron-epoxy laminate and its thermal



(a) 1.02 mm (0.040 in) Steel Bonded To 1.52 mm (0.060 in) Aluminum



(b) 1.02 mm (0.040 in) Steel Bonded to 3.18 mm (0.125 in) Aluminum



(c) 1.02 mm (0.040 in) Steel Bonded to 6.35 mm (0.250 in) Aluminum

FIGURE 26.- EFFECTS OF UNRESTRAINED BONDING OF ALUMINUM TO STEEL AT 400°K (260°F)

Reproduced from
 best available copy.

expansion coefficient is approximately one-half that of aluminum whereas boron-epoxy is about one-sixth. The steel was stretched using an aluminum stretch plate pinned to the ends of the steel plate to be bonded. In all cases investigated, the steel plate was of the same cross-sectional area. The thickness of the aluminum plate was varied to determine its effect on warpage.

The aluminum was placed on a steel tool and was restrained by steel bars pinned to the tool at the ends of the aluminum. The aluminum was allowed to expand only to the length of the steel tool with the differential expansion between the steel and the aluminum imposing the compression force on the aluminum. This configuration was held constant for this study.

In the first specimen, 1.02 mm (0.040 in.) thick steel was tensioned with a 3.18 mm (0.125 in.) thick aluminum stretch plate. The aluminum to be bonded was 0.064 mm (0.0025 in.) thick and restrained in the steel tool. The assembly was bagged under full vacuum and cured at 400°K (260°F). The resulting bow was 19.39×10^{-3} m/m (in./in.) as shown in Figure 27a.

For the second specimen, Figure 27b, the same configuration was bonded using a 9.53 mm (0.375 in.) aluminum stretch plate. Again the bond temperature was 400°K (260°F), but the resulting bow was reduced to 5.46×10^{-3} m/m (in./in.).

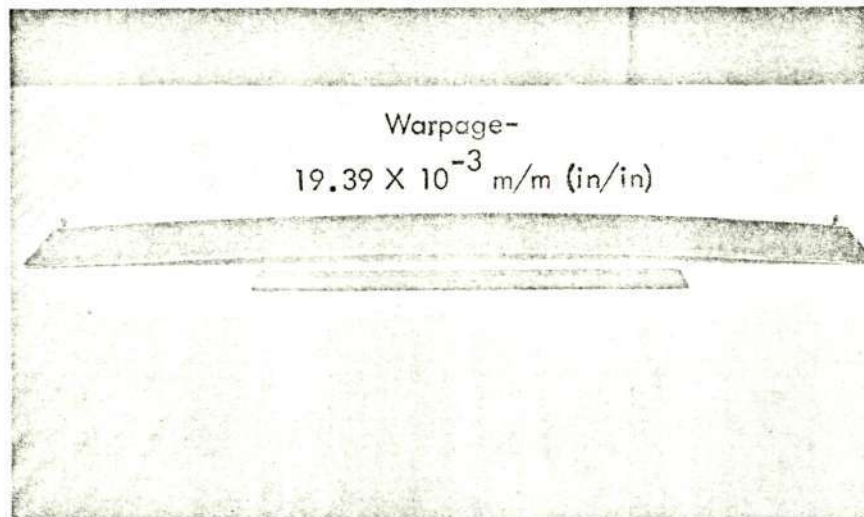
For the third specimen, the same configuration was used as for the second specimen, but the bond temperature was reduced to 366°K (200°F). For this case, the resulting bow was 5.58×10^{-3} m/m (in./in.). This indicated that the temperature at which the steel and aluminum were bonded was not greater than 366°K (200°F) since the bow was basically equal in both cases. This specimen is shown in Figure 28a.

The fourth specimen, Figure 28b, was bonded using a 12.7 mm (0.500 in.) aluminum stretch plate and cured at 366°K (200°F). The resulting bow for this specimen was 1.00×10^{-3} m/m (in./in.).

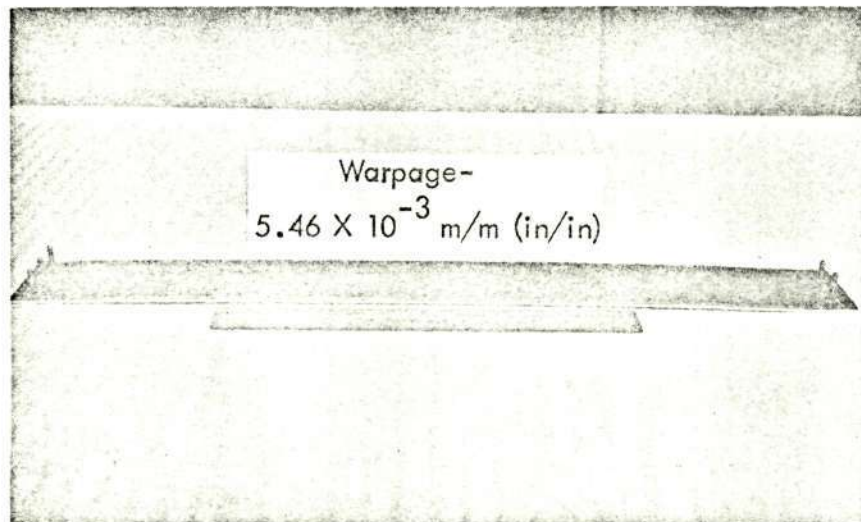
5.1.3 Tooling Development

Based on preliminary analysis and tests conducted, it was determined that a steel plate of 12.7 mm (0.50 in.) thickness was needed to restrain the aluminum thermal expansion by prestressing the part to be bonded to the differential thermal expansion between the steel and the aluminum. Low carbon steel, hot rolled plate was used for the tool face sheet. Structural I-beams were used for supporting the plate with four 15.2 cm (6 in.) I-beams used for longitudinal support and five 10.2 cm (4 in.) I-beams for transverse support. The plate and beams were welded together using tack welding techniques.

Some inherent waviness is typically found in the mill plate used for the tool face, requiring the upper surface of the tool to be machined to a flat condition. The surface finish was completed by grinding in the surface grinder shown in Figure 29. The tool was sandblasted and painted with a high temperature aluminum paint on all surfaces except for the top flat surface which was painted with a high temperature epoxy paint.

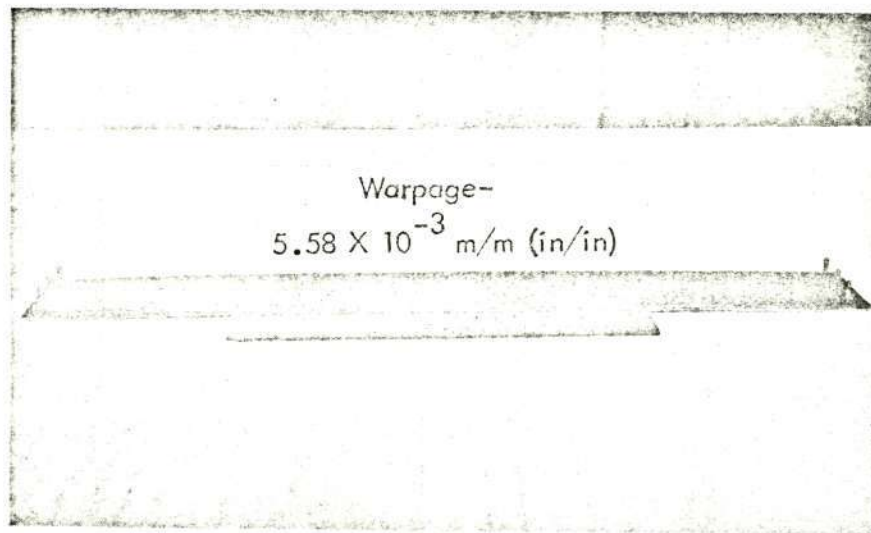


(a) 3.18 mm (0.125 in) Aluminum Stretch Plate

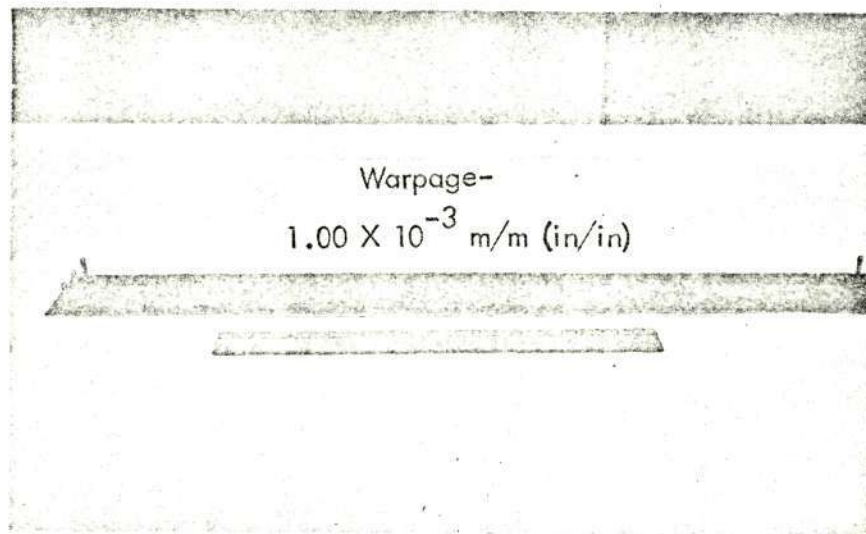


(b) 9.53 mm (0.375 in) Aluminum Stretch Plate

FIGURE 27. - EFFECTS OF RESTRAINED BONDING OF ALUMINUM TO STEEL AT 400°K (260°F)



(a) 9.53 mm (0.375 in) Aluminum Stretch Plate



(b) 12.7 mm (0.500 in) Aluminum Stretch Plate

FIGURE 28. - EFFECTS OF RESTRAINED BONDING OF ALUMINUM TO STEEL AT 366°K (200°F)

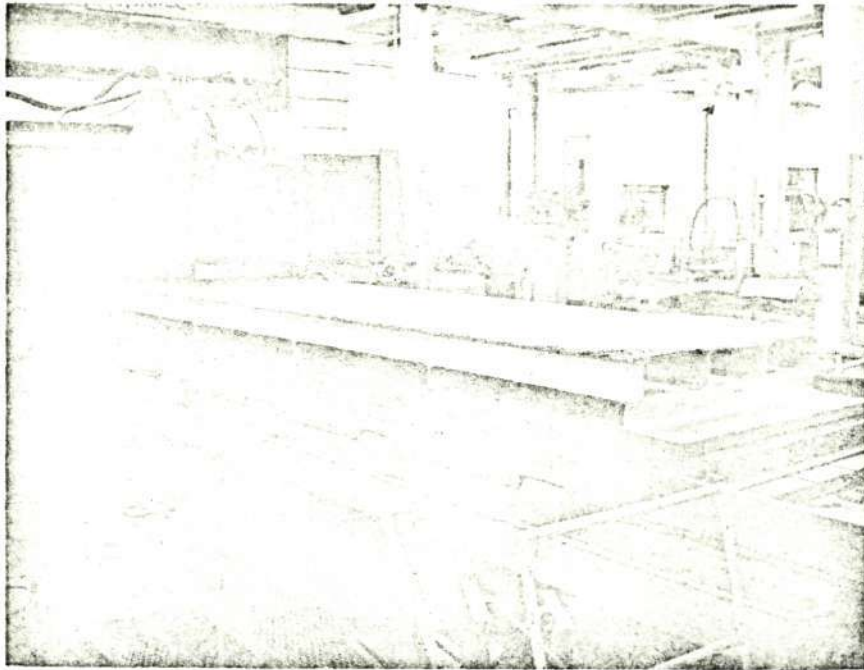


FIGURE 29.- STEEL TOOL FOR BONDING PHASE I COMPONENTS

Tooling aids were designed and fabricated, including a 76.2 cm (30 in.) long sliding parallel bar which was used for end adjustment to lock the aluminum parts to the same length as the steel. In production, a fixed bar will be installed at one end of the aluminum part and fixed to the tool. The adjustable parallel bar will have one-half fixed to the tool and the other half, which butts the aluminum, adjustable to assure a tight fit. Once the bar is adjusted, locking bolts will be tightened to clamp the adjustable half to the fixed half.

5.1.4 Warpage Study - Constant Thickness Aluminum

In the initial study on a 3.66 m (12 ft.) long specimen, a method was devised for bonding the laminate to the aluminum with minimum warpage using an autoclave cure and the restraining tool. This method required restraining the aluminum between the end bars secured to the steel tool and stretching the boron-epoxy laminate during the cure cycle. For the specimen fabricated, a 2.54 cm x 5.08 cm (1 in. x 2 in.) aluminum bar was used to stretch the laminate. The aluminum plate to be bonded was 2.54 mm (0.100 in.) thick x 15.2 cm (6 in.) wide x 366 cm (144 in.) long. The laminate was 21 plies thick and 5.08 cm (2 in.) wide x 361 cm (142 in.) long, with two 0.3 mm (0.012 in.) titanium doublers in each end. Five holes were drilled in the boron-epoxy laminate and match drilled in the aluminum stretch bar and, for this case, in the aluminum plate to be bonded. Steel pins were positioned in the holes after lay-up for bonding. The assembly was bagged and cured, producing

a panel which was flat with no measurable warpage. However, as can be seen in Figure 30, some delamination in the fiberglass scrim and bearing failure in the titanium was seen. Due to the problem involved with these holes as well as possible creep in the boron-epoxy under these conditions, this method was discontinued.

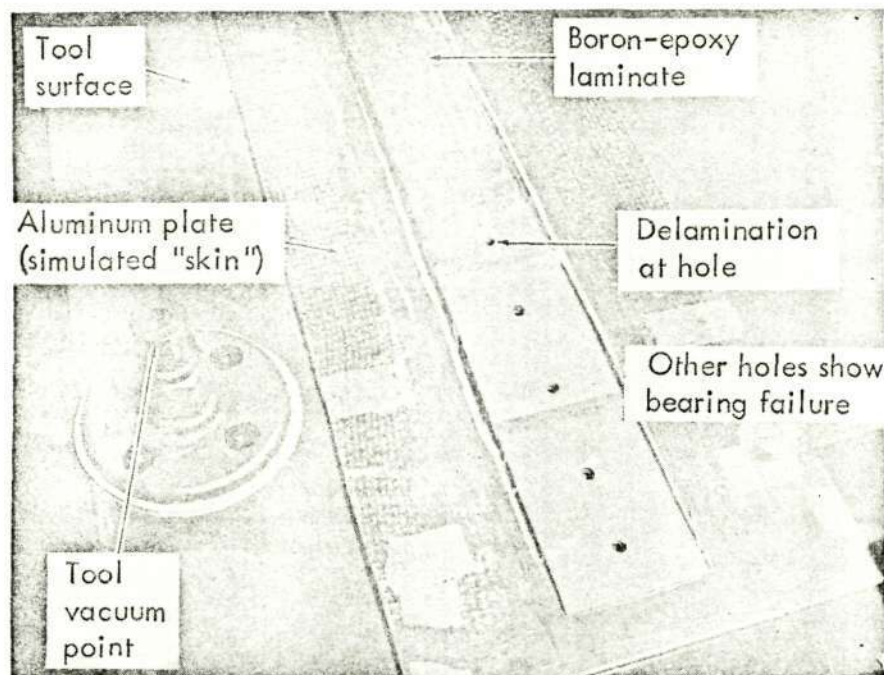
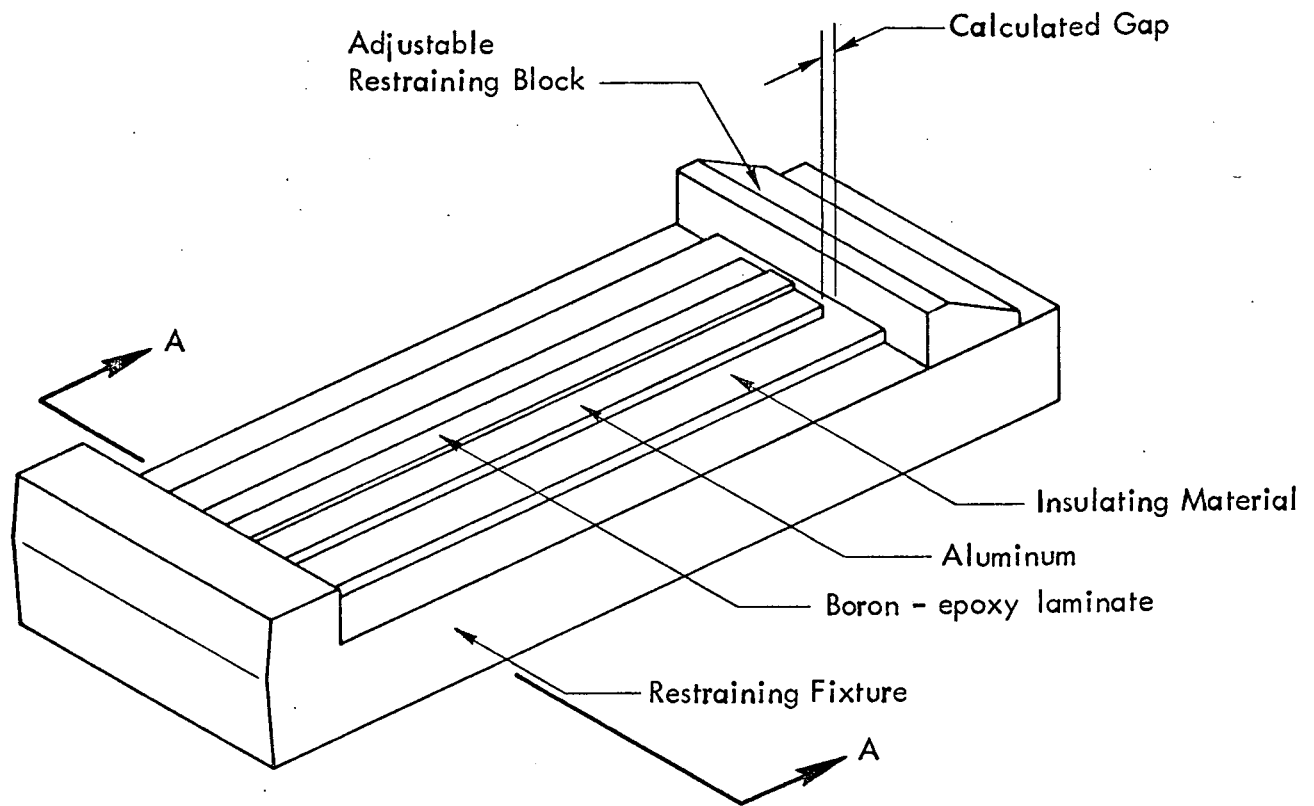


FIGURE 30.-AUTOCLAVE-BONDED BORON-EPOXY-TO-ALUMINUM SPECIMEN SHOWING HOLE DAMAGE CAUSED BY STRETCHING BORON

5.1.5 Cool Tool Approach

The principle of the "cool tool" concept was to provide constraint to the aluminum during thermal expansion, and to allow the boron-epoxy laminate to expand freely during the bonding process. The process required that the aluminum be restrained by the steel tool, that the steel tool be kept at room temperature with zero or minimum expansion, that the aluminum and boron-epoxy laminate be uniformly heated to the cure temperature, and that the laminate be allowed to expand freely. A sketch of the "cool tool" is shown in Figure 31.

The aluminum was restrained by end bars bolted and pinned to the steel tool. To assure intimate contact at room temperature, one of the end bars was made adjustable by sliding one-half along a wedge surface. This half was moved along the wedge until it was in contact with the aluminum and then locked in place.



A - A

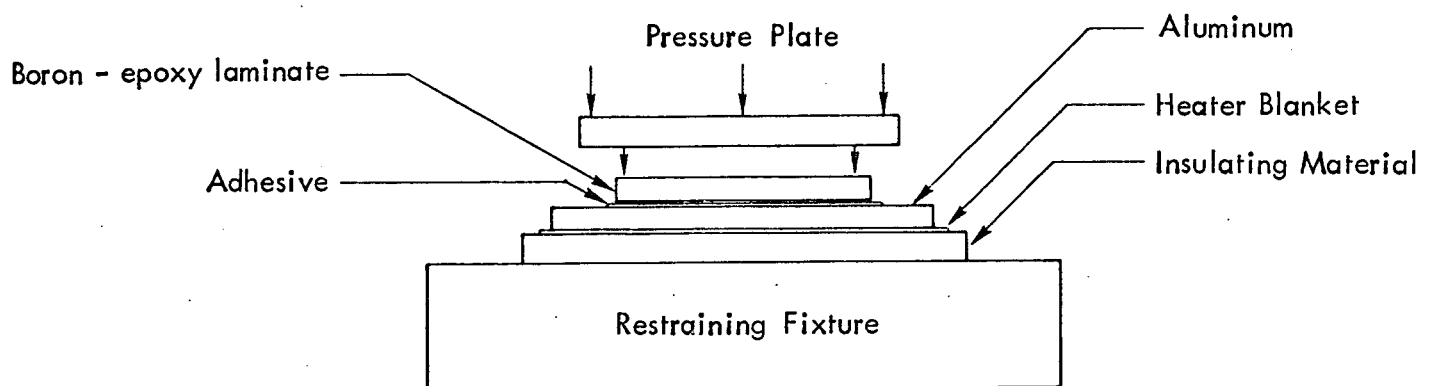


FIGURE 31.- "COOL TOOL"
RESTRAINING DEVICE CONCEPT

Heat was applied using a Briskeat-type heating blanket. The blanket was made in zones with individual controls for each zone. This enables the prevention of hot and cold spots on the specimen during cure. In order to assure that the steel tool remained cool, a 2.54 cm (1 in.) thick Maronite sheet was placed between the heating blanket and the tool. The aluminum to be bonded was positioned directly above the heating blanket.

The pressure application for the bond was accomplished by using rubber tubes restrained in channel sections as shown in Figure 32. The channels were held to the aluminum sheet by cross-bars bolted to the steel tool. Fiberglass insulation material was placed over the assembly to reduce heat losses. The tubes in contact with the boron-epoxy strips were inflated to $1.38 \times 10^5 \text{ N/m}^2$ (20 psig) to achieve the bonding pressure. A pressure regulator was used to maintain the pressure at $1.38 \times 10^5 \text{ N/m}^2$ (20 psig) and to bleed the air when pressure increases were generated due to the heating process.

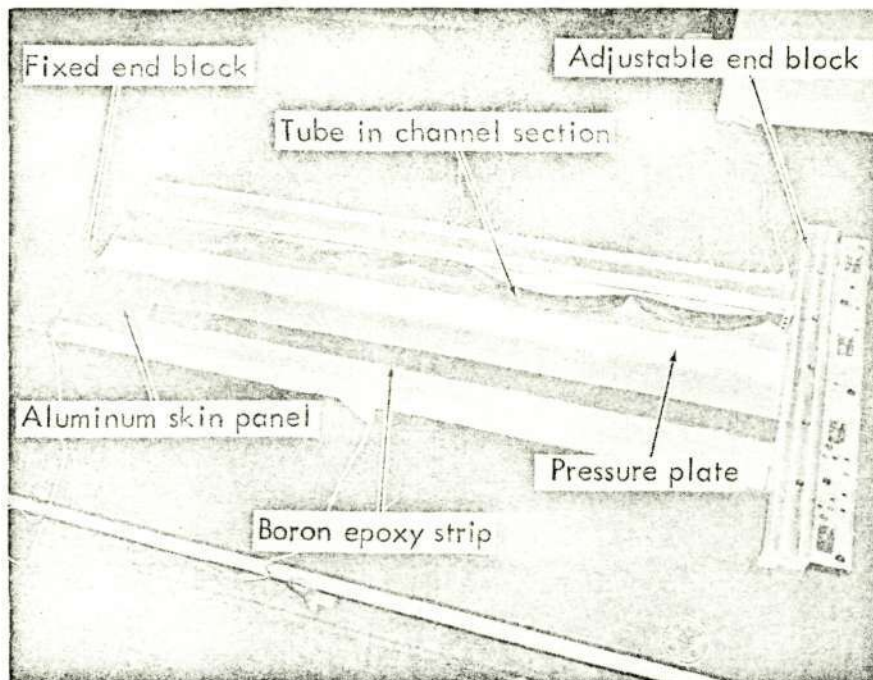
The "cool tool" approach was first tried on a constant-thickness aluminum plank. In the first attempt, calculations were made to control the expansion of the aluminum by allowing some expansion prior to contact with the end plates. This resulted in a 5.08 cm (2 in.) bow in the 3.05 m (120 in.) specimen after bonding. The next attempt was to fully restrain the aluminum prior to application of heat, which resulted in a bow of less than 2.54 cm (1 in.) in the 3.05 m (120 in.) bonded panel. Since this could be removed with hand pressure for assembly, it was decided that this approach would be used for building the Phase I specimens.

5.1.6 Warpage Study - Varying Thickness Aluminum

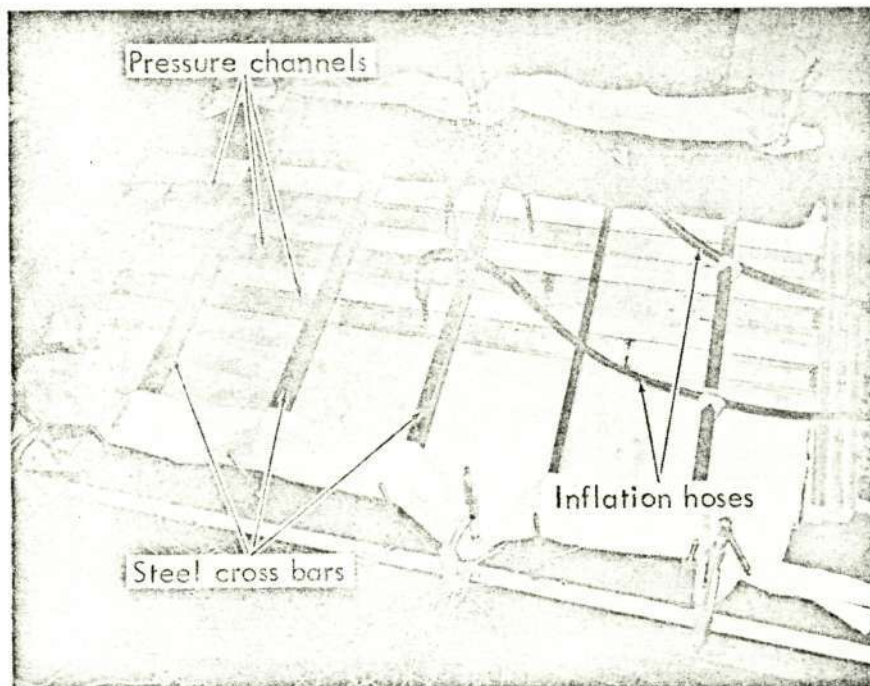
The aluminum section investigated was a scrapped plank which varied in thickness from that of the C-130 B/E box at an access door to the thickness of the C-130E box in the straight run of the plank. The aluminum was cut to a 15.2 cm (6 in.) width and was 366 cm (144 in.) long. The thickness variation was from 2.54 mm (0.100 in.) to 7.62 mm (0.300 in.).

In the first attempt the aluminum plate was not sufficiently supported in the "cool tool." The resulting warp from the bond occurred in the area where the aluminum was approximately 5.08 mm (0.2 in.) thick and could not be straightened using hand pressure.

In the second attempt, the aluminum was completely supported using glass cloth to build up a support under the thin area. In this case, the resulting warp from the bond occurred in the thin aluminum area. The remaining sections of the plank were flat. Figure 33 shows two views of the bonded assembly. The side view shows the extent of the warp in the thin section. Since this warp could be flattened with hand pressure, it was concluded that this process could produce bonded parts which would not be difficult to assemble and which would have a minimum of residual thermal stress.

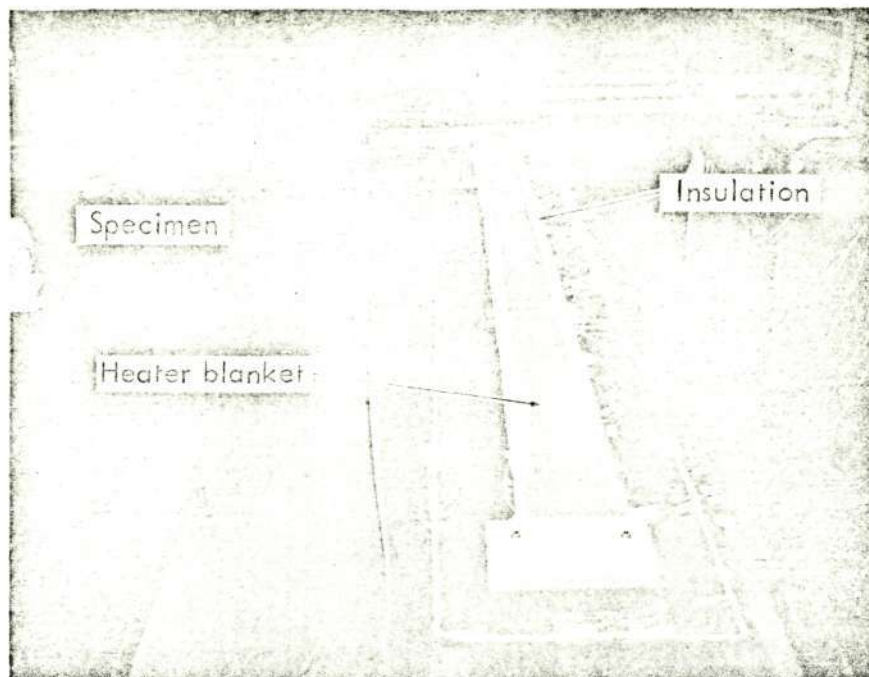


Bonding Pressure Devices Shown During Preparation of PF-3 Panel for Bonding

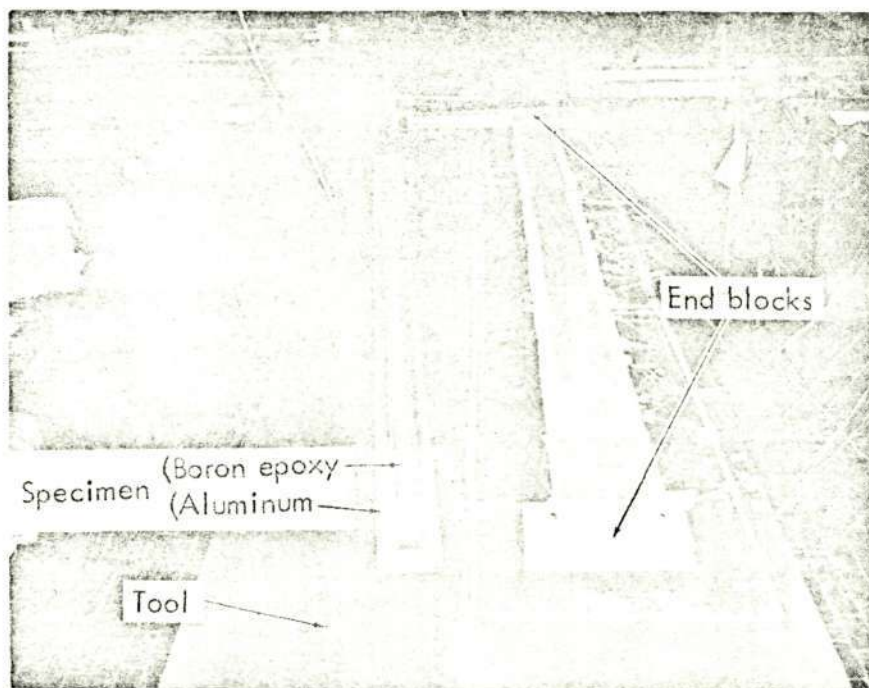


Bonding Pressure Devices Installed and Panel Ready for Cure

FIGURE 32.- "COOL TOOL" PROCESS FOR BONDING BORON EPOXY-TO-ALUMINUM



Side View



Top View

FIGURE 33.- BONDED BORON EPOXY-TO-ALUMINUM SPECIMEN SHOWN ON STEEL TOOL

5.2 GENERATION OF HOLES IN BORON-EPOXY LAMINATES REINFORCED WITH TITANIUM

5.2.1 Drilling and Reaming

For the JE-1 and PF-3 specimens, holes were generated in the boron-epoxy laminates reinforced with titanium using a diamond core drill for the boron-epoxy (Figure 34) and an end mill for the titanium (Figure 35). Although this method produced good holes in the laminate, it was time-consuming, and the development of a different technique was undertaken.

5.2.2 Punching and Reaming

The titanium doublers were stack drilled, using a drill template, prior to cleaning and processing for bonding. A punch template was made and the boron-epoxy plies were punched prior to curing the laminate. Pins were placed in the punched holes and the titanium doubler was positioned over the uncured laminate. This process was continued until the laminate lay-up was completed. Before bagging for cure, pins were placed in the holes to maintain alignment during cure. After cure, the laminate was checked for dimensional stability. It was found that over the full 50.8 cm (20 in.) of the test coupon the holes retained their dimensions and that the pins could be finger pressed through the laminate and into the holes in the punch template.

This approach was used for the fabrication of the balance of the Phase I specimens. Holes were punched one drill size under that required by the drawing and the holes were reamed to size during the drilling process for the aluminum. This method was established since its bearing characteristics would be comparable to holes previously generated and tested. Figure 36 shows the technician punching the holes in the laminate. In Figure 37, the laminate is shown after punching. The slot shown between the holes was also punched successfully, and several manhours were saved when the diamond routing process for this slot was eliminated.

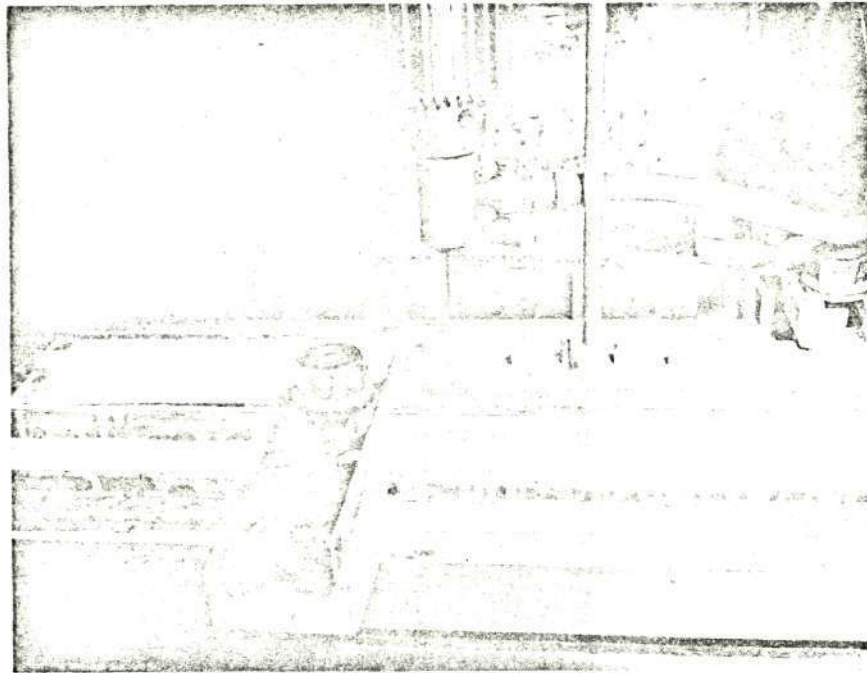


FIGURE 34.- DRILLING THE BORON-EPOXY LAMINATE WITH
DIAMOND CORE DRILL

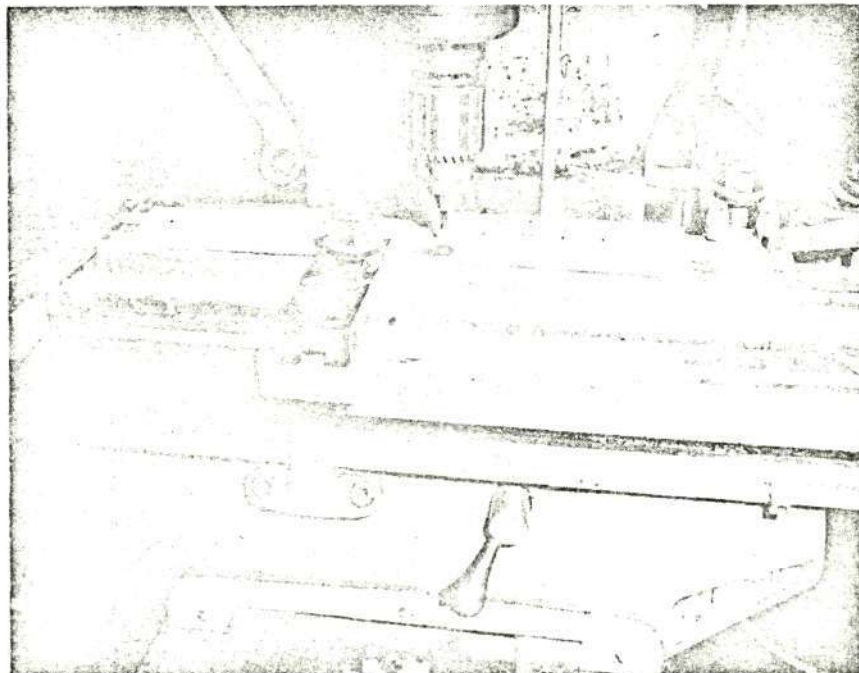


FIGURE 35.- DRILLING THE INTERLEAVED TITANIUM SHIMS
WITH STANDARD DRILL

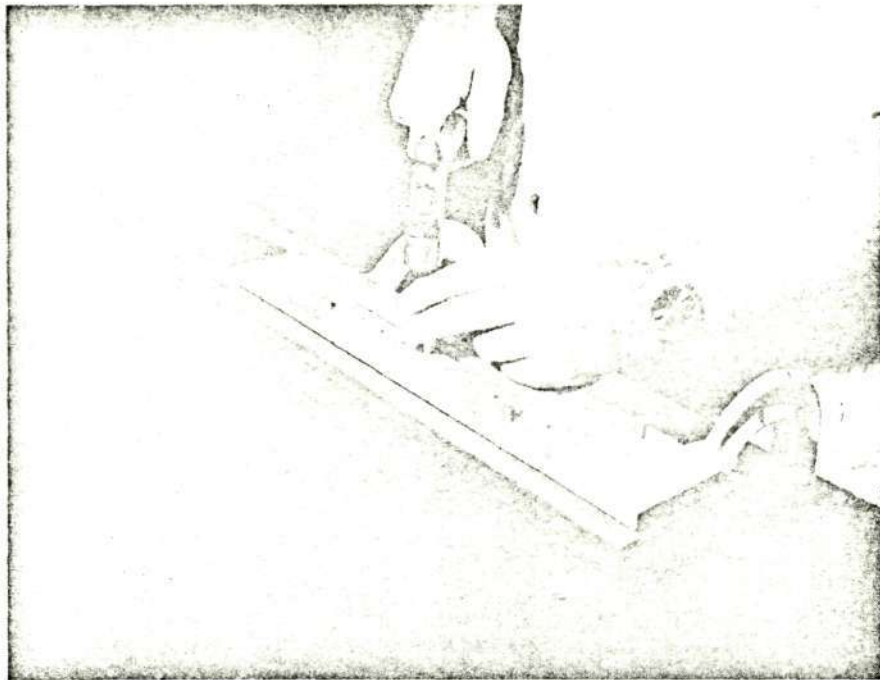


FIGURE 36.- PUNCHING HOLES IN UNCURED BORON-EPOXY LAMINATES

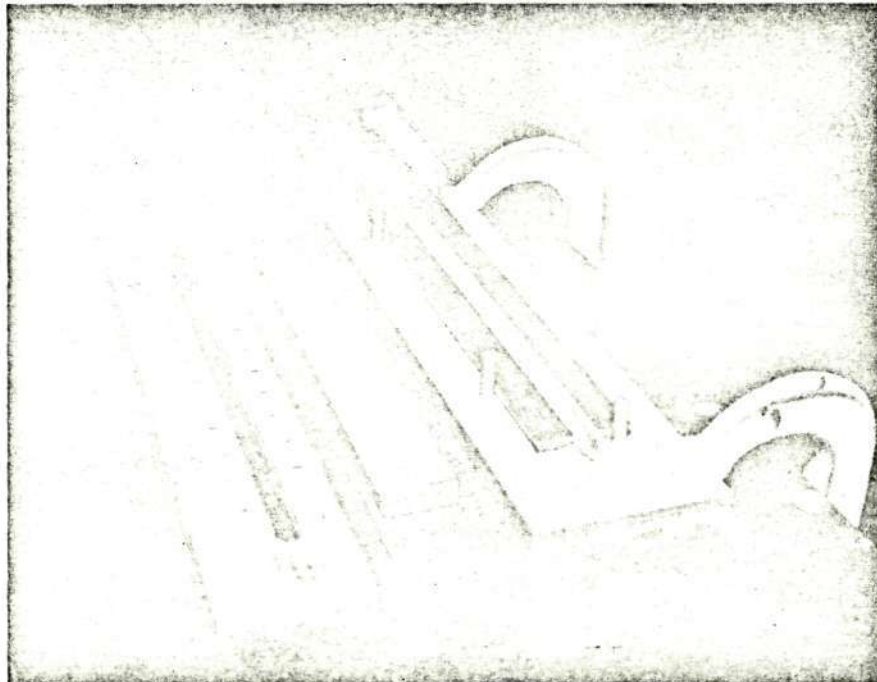


FIGURE 37.- UNCURED BORON-EPOXY LAMINATES WITH PUNCHED HOLES AND SLOT

6.0 COMPONENT FABRICATION

6.1 METAL PROCESSING

In the fabrication of specimens in Phase I of this program, the metallic details were fabricated using materials and processes identical to those used in the fabrication of the components which make up the C-130 center wing box. The machining of the detail parts for test specimens simulating C-130E and C-130B/E parts was accomplished with the machine tools and cutters used in production of their counterparts. After machining, these detail parts were shot peened as required by the drawings.

After shot peening, the details were processed for environmental protection. The specifications for the C-130 center wing box details required sulfuric acid anodizing. To provide improved bonding characteristics, the sulfuric acid anodize was stripped from the bonding surfaces and replaced with chromic acid anodize. To do this, the sulfuric anodized detail had to be chem-mill masked over all surfaces. For the area to be bonded, the maskant was peeled from the surface and the part placed in the stripping tank where the sulfuric acid anodize was removed. The part was then transferred to the chromic acid tank and anodized for adhesive bonding. This newly-anodized area was then sprayed with the designated primer system. The panels were wrapped in Kraft paper and stored in a clean room until they were needed for the bonding process.

6.2 BORON-EPOXY PROCESSING

The composite reinforcing strips were laminated to the dimensions specified on the drawing with a 0° orientation and ply stacking as required. In the ends of the strips where fasteners were to be installed, titanium shims were included in the lay-up. These titanium details were predrilled to the template for the given assembly, processed for bonding and sprayed with primer. Just prior to lay-up, the adhesive was applied to the bonding surfaces of the titanium and punched out in the hole areas. The lay-up of the boron-epoxy was made by stacking the plies required between the titanium doublers and punching the boron to the hole template. Pins were placed in these holes after punching and the titanium shim positioned over the pins. This process was continued until the lay-up was completed. For laminates which included the slots in the ends, the slot was also made using the punching template and a punch designed to produce the required slot.

After the lay-up was completed, the flat bonding tool was covered with a Mylar film, one ply of 116 glass cloth bleeder and a layer of Teflon coated glass cloth. The laminate was then placed over the Teflon coated cloth and dams installed around the laminate. Figure 38 shows four of the 5.08 cm (2 in.) wide boron strips, partially laid up and dammed on the tool. Note that the two strips on the left have the dams positioned in the slots on the near ends.

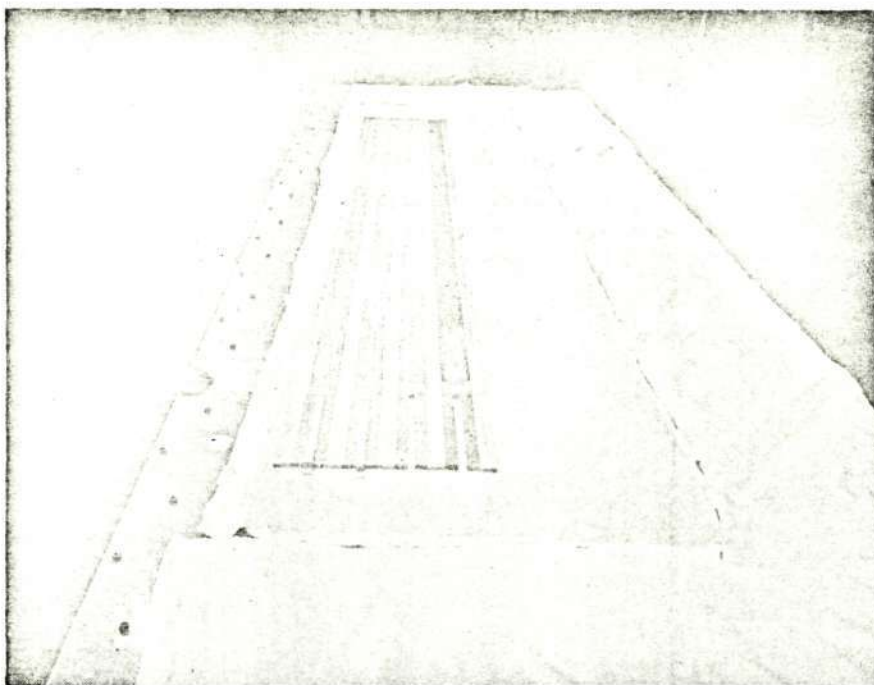


FIGURE 38. -BORON-EPOXY STRIPS ON TOOL PRIOR TO CURE

Undersize pins were placed in the holes. The laminates were then covered with one ply of Teflon-coated glass cloth and with the required number of plies of 116 glass cloth bleeder. The bleeder system was based on one ply of bleeder material for each six plies of boron. In areas over titanium shims, only the boron plies above the shim were counted in defining the required bleeder thickness. A rubber strip was placed over the bleeder system to serve as a pressure equalizer. A thin metal caul plate was placed on top of the rubber strips. Both the rubber strip and the metal caul plate were punched with holes and slots to match those in the laminates to assure the pressurization of the laminate in these areas during cure. A Mylar film was placed over the assembly and taped to isolate the resin bleeder system from the vacuum bag. A standard vacuum bag was placed over the assembly and checked for leaks.

The boron-epoxy laminate was then cured as defined in Section 4.2.1. A heatup rate of 3.89°K (7°F) per minute was used to bring the autoclave up to cure temperature. After cure, the laminates were cleaned by removing excess resin flash from the edges, and the holes were reamed to size using a diamond reamer. The side of the laminate to be bonded was lightly sanded and dry wiped with solvent just prior to bonding.

6.3 ASSEMBLY OF DETAILS

The bonding of the boron reinforcing strips to the aluminum skin planks and stringers was accomplished in a restrained condition of the steel tool. The first specimen fabricated, JE-1, was bonded on the steel tool with the aluminum skin and stringers restrained and the assembly bagged for autoclave cure. The cure cycle was 4 hours at 366°K (200°F) and $2.07 \times 10^5 \text{ N/m}^2$ (30 psig). Subsequent specimens were fabricated using the "cool tool" techniques as previously described. Specimen JE-4 was identical to JE-1 and was bonded in the "cool tool" as a check between the two bonding techniques. Figure 39 shows the specimen PF-2 skin, after bonding. Although some warpage is evident, this was straightened using conventional assembly techniques.

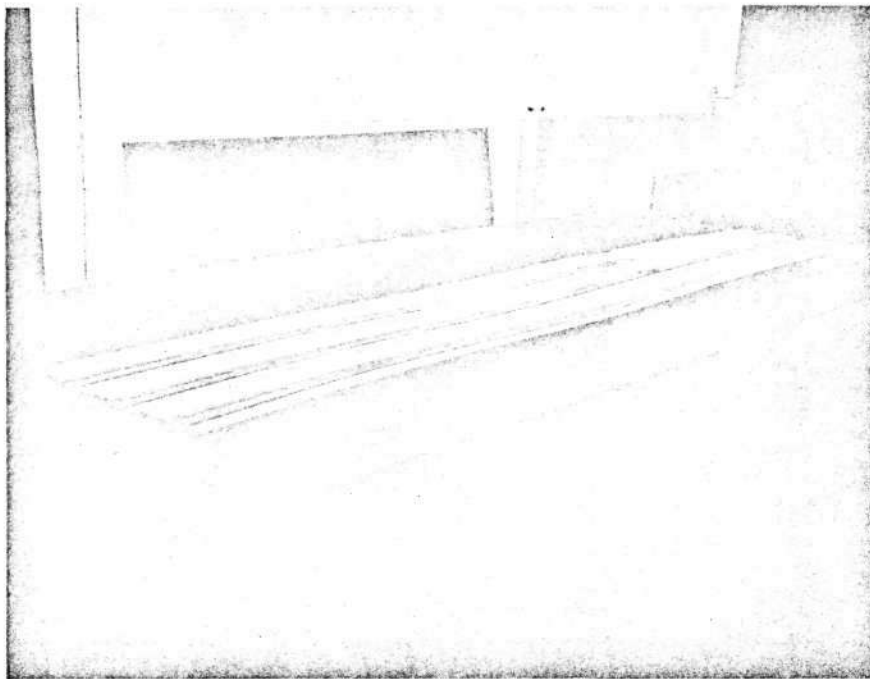


FIGURE 39.- SPECIMEN PF-2 SKIN AFTER BONDING

After bonding, the boron-reinforced skins and stringers were protected from atmospheric conditions. The boron strips were coated with sealant and oven cured. The entire assembly was then painted with clear epoxy primer and polyurethane paint. These coatings, described in Section 4.2.5, Sealing and Painting, were oven cured to minimize assembly time.

6.4 ASSEMBLY OF MAJOR COMPONENTS

Standard C-130 center wing box assembly procedures were used in the assembly of components for this program. Figure 40 shows the positioning of a stringer on the wing plank for specimen PF-1.

The stringer flanges were pilot drilled prior to installation and these holes were used to pilot drill the wing plank after positioning of the stringer. The holes were then back drilled and reamed for taper-lok fasteners as shown in Figure 41.

After the assembly had been drilled and reamed, fay surface sealant was applied to the stringer flanges and straps and the fasteners were wet installed. Torque-off collars were used on the high-lok fasteners.



FIGURE 40.- INSTALLATION OF STRINGER ON PF-1



FIGURE 41.- DRILLING AND REAMING PF-2 FOR TAPER-LOK FASTENERS

Certain metal reinforcing components were then installed. One such component was the reinforcing pad that is bolted around the access door. The installation of this pad on specimen PF-2 is shown in Figure 42. After the assembly had been completed, the protective finish was applied.

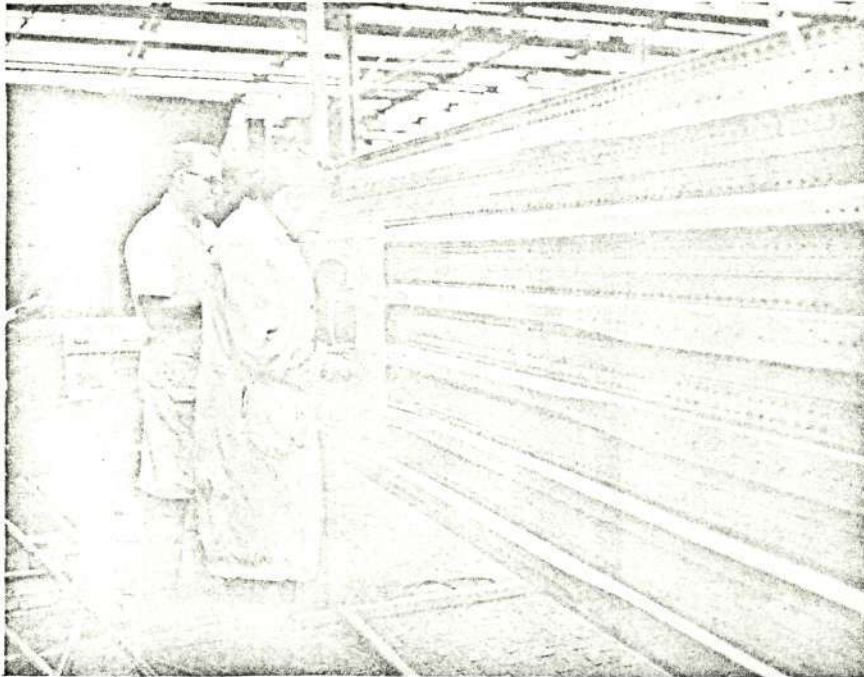


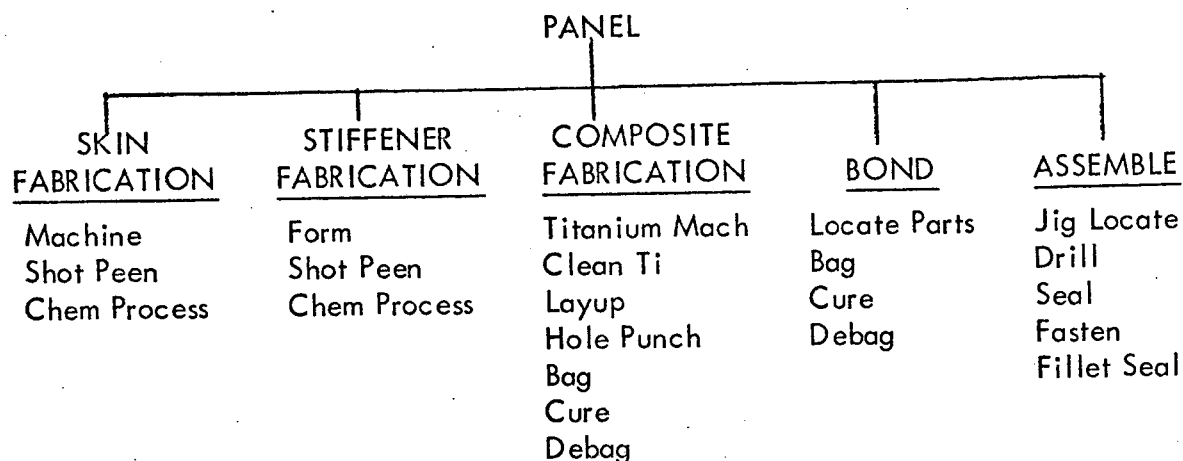
FIGURE 42.- INSTALLATION OF ACCESS DOOR PAD ON PF-2

7.0 COST/PRODUCIBILITY DEVELOPMENT

7.1 COST

Work in this area has been directed towards the development of a tentative cost model that will describe all elements of cost that are anticipated during the Phase II design effort and Phase III manufacturing program. This model is limited to that portion of the center wing box design and construction that is peculiar to boron-epoxy composite usage. The cost model shown below represents the design concept used in Phase I. Adjustments to this model during

Phase II will be made as necessary. This costing model will also be used in projecting the production cost of the center wing box constructed utilizing boron reinforcement.



7.2 PRODUCIBILITY

The overall producibility of the full-scale C-130 center wing box reinforced with boron-epoxy composite is anticipated to be good to excellent. The center wing box is a long-term production item with over one thousand units having been fabricated. Based on manufacturing developments and tests, most of the fabrication peculiar to boron composites will be within the surface panel assemblies and their detail parts. Wing panel skins and hat stiffeners after being reinforced with boron will be assembled into panel assemblies by conventional fabrication methods. Panel assemblies will be further assembled into the upper and lower wing surfaces. The remaining fabrication and assembly work will be basically conventional construction.

Tooling development, that has resulted in the "cool tool" concept, appears to have essentially resolved the fabrication problem of bonding materials of dissimilar thermal coefficients of expansion, although some details remain to be resolved for the full box tooling. Additional development in punching holes through the titanium reinforcing and uncured boron has improved the producibility of hole production for required fasteners.

The basic fabrication concepts developed during Phase I for use during the design and manufacturing phases will ensure good producibility by limiting the complexity of composite fabrication and assembly bonding to detail parts and subassemblies.

8.0 RELIABILITY AND QUALITY ASSURANCE

A reliability and quality assurance program was conducted in accordance with a NASA-approved program plan that complies with selected elements of NASA specifications NHB 5300.4(1A) and (1B). The plan defines the reliability and quality program policies and objectives for organization, implementation, and control for the C-130 composite wing box program.

8.1 RELIABILITY PROGRAM

The objective of the C-130 composite wing box program is to attain a high level of inherent reliability in system design; to assure that this level of reliability is not degraded throughout the production, test, and operational phases; and to provide NASA the assurance and visibility that specified reliability requirements are achieved. During Phase I, the approach was to promote an awareness of the reliability objectives, monitor program progress, and focus additional attention and resources as necessary on those tasks which are critical to reliability achievement. An initial briefing, and subsequent informal discussions with design, stress, materials and process, manufacturing, and test personnel; were used to communicate objectives and obtain specific task status information for reliability assessment.

In addition, weekly or biweekly program status meetings were held in which progress on each task was reviewed with the program manager. In these meetings problem areas were identified, action item responsibilities were assigned, and progress on problem solutions was reviewed and discussed. By maintaining good communications and an innovative environment, learning from each problem experience was maximized and significant reliability progress was permitted in this technology development phase.

8.1.1 Reliability Progress

The major thrust of the Phase I program was to develop and evaluate a process for producing boron-epoxy reinforced skin planks with minimum warpage and low residual stress at room temperature. Many steps were involved in the process and each has an impact on reliability potential. Several Phase I accomplishments are considered to have significantly enhanced achievement of reliability objectives.

The "cool tool" technique for controlling the relative strain in the aluminum and boron-epoxy during high-temperature bonding offers the following process advantages:

- o Close tolerance pins to physically restrain the boron and aluminum are eliminated.
- o The shorter bonding time permitted by a higher bonding temperature reduces the probability of process interruption due to equipment malfunction or other interference.

- o The use of a positive pressure during bonding minimizes adhesive porosity and assures good material contact.

The ability to control warpage with the "cool tool" concept has been demonstrated and the resulting low residual stress at room temperature directly extends fatigue endurance. Adhesive evaluation tests confirmed that the selected adhesive, AF 127-3, provides the desired shear and peel properties over the service temperature range. A corrosion-resistant bonding and finish system was developed with good strength properties. Static, fatigue and buckling tests have confirmed the understanding of the physical properties of materials and the accuracy of the analysis methods.

A preliminary draft of a design specification document for the composite reinforced C-130 center wing box was prepared. The specification defines the design, performance, test, and acceptance requirements for the complete wing box assembly. The specification will be finalized during Phase II design and submitted to NASA for approval.

A formal design review was conducted at the end of Phase I to provide a thorough evaluation of the technology development status by Lockheed management and NASA.

8.1.2 Reliability Assessment

Qualitative assessments were made of the confidence level for achievement of reliability objectives with the current state of technology in the areas of design, analysis, materials and processes, manufacturing, and testing. Each assessment was based on a detailed review of the many factors involved in each area. Consideration was given to the degree to which theoretical concepts are developed and proven; extent and type of experience data available; number of critical steps or sequences; number of relative unknowns; complexity of methodology; skill levels required; and schedule restraints. The consolidated assessment is that a good to high confidence level exists with current technology. In most areas the technology is well developed and is a continuation or direct extension of tried and proven techniques.

A high confidence level exists in the area of design. Changes to the existing aluminum wing box design are minimal. Boron-epoxy laminate design is straightforward with no problems anticipated in ply sizing, tapering run-outs, titanium shimming, or fastener location.

The confidence level is good in the stress and fatigue analysis area. Test results are confirming that the analysis methods are satisfactory. Thermal strain properties of the boron-epoxy coupled with the adhesive strength behavior during cure have produced a small degree of analytical uncertainty, but the relatively low residual stress at room temperature with the "cool tool" process has significantly reduced the thermal stress analysis problem.

In the materials and processes area the confidence level is also good. The boron-epoxy tape being used is fully qualified and in wide usage throughout the industry. Both suppliers are performing well, meeting schedule commitments with no quality problems. Experience with the qualified, though relatively new, AF 127-3 adhesive has been excellent. Based on aircraft experience with adhesives of similar composition, no problem is anticipated in aging. Corrosion prevention appears to be very adequate with the finish and sealer system being used.

The confidence level ranges from good to fair in the manufacturing area. No problems are expected in the aluminum fabrication or boron-epoxy tape lay-up. Techniques for producing fastener holes in the boron are developing well. Development of the cool tool concept progressed rapidly during Phase I. Each test panel revealed areas for further refinement. Some changes were incorporated; the press of schedule did not permit complete development of the tooling. Additional tooling development is recommended in Phase II prior to Phase III production tooling. Process controls need to be optimized for production use to ensure adequate control of physical tolerances as well as critical time, temperature, and pressure variables. Assembly methods appear to be adequate for production operations.

Wing box testing is a high confidence area because of the similarity to previous C-130 static and fatigue test programs. Test facilities and methods are proven. Additional complexities imposed by the presence of composite reinforcements are minimal.

8.2 QUALITY ASSURANCE PROGRAM

8.2.1 Procurement Controls

All material used in this program is subject to procurement controls. Standard metal parts and stock are controlled in the overall basic materials control program for stock supplies at the contractor's plant. Additional controls were generated or imposed for materials peculiar to this program and for those which might require extra attention. Such additional requirements are stipulated in applicable materials specifications - defined by Engineering and implemented by Quality Assurance.

Boron-epoxy pre-preg tape, adhesives, and primers were tested by the Quality Assurance Laboratory on receipt for conformance to requirements. The adhesive systems used, AF 127-3 and FM 123-7, are the same as those used on the C-130 production aircraft. The adhesive batch number was recorded on the shop order for each assembly bonded. Adhesives and primers were tested for volatile content, metal-to-metal peel strength and lap shear tests at the required temperature extremes.

Special attention was given to the boron-epoxy tape. It is shipped in a dry ice pack and its receipt was carefully coordinated so that refrigerated storage was provided immediately upon delivery. By preventing delivery of this material on a weekend, the chance of a substantial loss of work life was eliminated. Laboratory control numbers were issued for each shipment of boron pre-preg tape and each roll was identified with this number, to provide traceability to the vendor's records.

The Quality Assurance Laboratory evaluated incoming boron and adhesives to verify conformance. Specifically, the boron tape was tested for resin content, volatile content, resin flow, longitudinal flexure strength, and horizontal shear. The originally planned 90° flexure tests were cancelled, not being applicable nor practical, as all loading of boron fibers in this program is longitudinal compression or tension. Incoming material was not released for use until satisfactory test results were obtained. The range of test results for boron-epoxy tape is shown in Table X.

8.2.2 Fabrication Controls

Fabrication of all test details was conducted in two areas. Machine shop work was performed in the Engineering Structural Test Department; fabrication of the titanium shims, all mechanical assembly, and laminate lay-up and bonding was performed by the Manufacturing Research Department. Both of these areas are staffed with highly skilled personnel, which contributed to the high quality of product. Inspection activity in the manufacturing areas was only required on one shift, which simplified communications, and improved uniformity.

8.2.3 In-Process Controls

All work was performed in a sequence of activities defined on shop orders, which outline on paper each required step and inspection point. After completion of the part, the completed shop order becomes part of the permanent documentation. The control numbers for the materials used were entered on the shop order and verified by inspection. The mechanic stamped each callout on the order as he completed a planned segment of work. The inspector also stamped the order successively to identify inspection status. When any detail part or assembly was completed, the Shop Order and the part were stamped with the shop calendar date. The part was also stamped with the control number of the boron tape providing a double track for tracing controlled materials back to the vendor.

Any non-conforming items were withheld on Discrepancy Reports for disposition. During specimen fabrication the Audrey II dielectric constant measuring device was evaluated to see if it could provide in-process monitoring of proper adhesive cure by measuring the capacitance of the bond line. In these tests the instrument was damaged before firm conclusions could be reached. It is believed, however, that the system shows promise for future applications.

8.2.4 Destructive Tests

Test specimens were designed and built to evaluate the composite structure for all critical load conditions. Destructive test of these specimens was performed by the Structural Test Department. Inspection verified total conformance of the test specimens through in-process and close-out inspection before they were released for test.

TABLE X.-BORON-EPOXY ACCEPTANCE TEST SUMMARY

Control Number	Vendor	0° Flexure				Horizontal Shear				Resin Content %	Volatile Content %	Resin Flow %
		Minimum		Average		Minimum		Average				
		10^9 N/m^2 (ksi)	10^9 N/m^2 (ksi)	10^9 N/m^2 (ksi)	10^9 N/m^2 (ksi)	10^7 N/m^2 (ksi)	10^7 N/m^2 (ksi)	10^7 N/m^2 (ksi)	10^7 N/m^2 (ksi)			
Specification Requirement	-	1.55	(225)	1.65	(240)	7.58	(11)	8.96	(13)	Range 30-35	Max 2	Range 10-20
72651	AVCO	1.81	(263)	1.85	(268)	9.24	(13.4)	9.45	(13.7)	32.0	0.71	12.0
74092	AVCO	1.74	(252)	1.77	(256)	9.38	(13.6)	9.58	(13.9)	31.5	1.3	16.0
74359	AVCO	1.92	(279)	1.96	(284)	9.65	(14.0)	9.79	(14.2)	32.8	1.1	16.6
74297	3M	1.68	(243)	1.75	(254)	8.83	(12.8)	9.31	(13.5)	32.3	1.4	13.6
74648	3M	1.58	(229)	1.63	(237)	9.65	(14.0)	10.2	(14.8)	31.4	1.5	10.4
73316	3M	1.70	(247)	1.74	(253)	8.89	(12.9)	8.96	(13.0)	31.8	1.3	13.6
75551	3M	1.85	(269)	1.88	(273)	9.86	(14.3)	10.4	(15.1)	32.9	1.2	16.8
75323	AVCO	1.94	(282)	2.01	(291)	10.5	(15.3)	10.6	(15.4)	31.8	1.0	13.6

8.2.5 Non-Destructive Inspection

The primary NDI technique utilized in the investigation was ultrasonic. Evaluations were accomplished on the specimens during fabrication, testing, and after completion of structural tests. "Standards," with simulated defects, were built to represent good and void conditions in laminate to metal bonded specimens. Disbonds (delaminations) were simulated with 0.127 mm (0.005 inch) thick teflon inserts and voids were simulated with precured adhesive plugs. The "defects" were inserted in bondlines every five layers in the multi-layer specimens, based on previous experience with bonded composites and metal articles.

The standards were best suited for ultrasonic techniques which relied on sound transmission through a specimen to a receiver, or to an ultrasonic mirror then back through the specimen to a receiver. The thru-transmission technique was accomplished using two contact ultrasonic transducers with liquid acoustic couplant.

The composite parts were inspected with thru-transmission techniques with loss of sound transmission indicating void areas. The bondline between the hat section and the composite part was inspected using pulse echo ultrasonic techniques. This method detects voids by differentiating between high sound dampening areas (good bond) and no sound dampening (void). In the latter case, the sound energy continues to echo in the aluminum component and is indicated by a saturation signal on the flaw detector cathode ray tube.

The air-coupled 25 kHz ultrasonic Sondicator could not be efficiently utilized on this investigation for two reasons:

- o Specimen size - The effectiveness of the low frequency transducers were influenced by the edge of the parts. Since the composite strips were less than 5.08 cm (2 in.) wide, no meaningful inspection could be accomplished.
- o Standards - The Sondicator measures the phase change of sound transmitted through a specimen to a receiver as an indication of void, i.e., presence of a void changes the sound transit time, thus phase. The standards as previously discussed did not contain actual voids. The simulated defects suffice for high frequency ultrasonic testing (1 to 10 MHz) but actual voids must be present to calibrate the Sondicator.

8.2.6 Material Review Board Actions

Workmanship quality has been good. Only three rejections have been dispositioned scrap, and three have been dispositioned to repair. Two additional workmanship errors were dispositioned acceptable without repair. Approximately 500 parts and assemblies have been fabricated yielding a total in-plant defect rate of 1.6 percent.

Table XI presents a tabulation of these rejections and also the six rejections against vendor material.

TABLE XI. - MATERIAL REVIEW ACTIONS

Discrepancy Report Number	Part Number	Type of Failure	Disposition		
			Use "As Is"	Repair	Scrap
941533	130JE-1-3	Delaminated - separator sheet was not removed			x
941537	Boron Tape C/N 72651 AVCO	Transverse Flexure	x		
984469	130PF201-3	Machining error			x
984468	130PF201-7	Machining error			x
12253	130PF102-3	Machining error	x		
941541	Boron Tape C/N 74092 AVCO	0° flexure modulus low	x		
941540	Boron Tape C/N 74297 3M	Vendor test reports incomplete	x		
941539	Boron Tape C/N 73316 3M	0° flexure - modulus low	x		
941542	130PF301	Boron tape too long at room temperature	x		
941544	130PF301	Bonding temperature not held to specification limits	x		
19512	Boron Tape C/N 74648	Longitudinal flexure strength should be $1.65 \times 10^9 \text{ N/m}^2$ (240 ksi) avg., was $1.63 \times 10^9 \text{ N/m}^2$ (237 ksi)	x		
991403	130PF202-3	Disbonded area		x	
034241	130PF105-1	Disbonded area		x	
991404	130PF105-3	Disbonded area		x	

9.0 COMPONENT DESCRIPTION AND TEST DATA

In order to readily identify all test specimens and the associated tests in Phase I of this program, drawing numbers and titles were assigned to all specimens and test components. Specimen groupings were assigned on the basis of type of specimen and type of test. Specimen/test descriptions in this section follow the sequence listed below:

Drawing No.		
Fabrication Development	130-FD-1	Fabrication Development Specimen (Skin to Rainbow Fitting W.S. 220 Lower Surface)
	130-FD-2	Fabrication Development Specimen (Stiffener to Rainbow Fitting W.S. 220 Lower Surface)
Joints Evaluation	130-JE-1	Joint Evaluation Specimen W.S. 220 (-65°F) (Strain Survey and Low Temperature Fatigue)
	130-JE-2	Joint Evaluation Specimen (W.S. 220 Upper Surface) (Static Test)
	130-JE-3A	Boron Epoxy-to-Aluminum Transition Specimens
	130-JE-4	Joint Evaluation Specimen (W.S. 220 Lower Surface)
Panel Fatigue	130-PF-1	Fatigue Panel, Upper Surface with Access Door at A/C Centerline
	130-PF-2	Fatigue Panel, Upper Surface W.S. 220 Joint
	130-PF-3	Fatigue Panel, Lower Surface W.S. 220 Joint
Panel Buckling	130-PB-1	Panel Buckling Specimen (Upper Surface Single Plank)
	130-PB-2	Panel Buckling Specimen (Lower Surface Single Plank)
	130-PB-3	Panel Buckling Specimen (Upper Surface Double Plank)

9.1 FABRICATION DEVELOPMENT TESTS

Seven each of the 130-FD-1 and 130-FD-2 specimens were static tested and ten each were fatigue tested.

9.1.1 Fabrication Development Specimen Description

The 130-FD-1 specimen assembly was composed of a tapered aluminum skin and boron-epoxy laminate representing the manufacturing techniques and joint designs to be used in fabrication of the reinforced wing skins and rainbow fitting to skin joint. The laminate was step tapered toward the end of the laminate and incorporated interleaved titanium shims. The shims were sized and designed to supply the proper bearing area for the fasteners and to evenly distribute the induced loads into the laminate. Fasteners, installed through the aluminum skin and boron laminate, were used to facilitate bonding the laminate to the skin during the cure cycle, and also to serve as peel-stoppers. This specimen is shown in Figure 43.

The 130-FD-2 specimen assembly was composed of a simulated hat stiffener crown reinforced with a bonded boron-epoxy strip. As noted in describing the FD-1 specimen, the FD-2 specimen also contained titanium shims, but this reinforcement was not tapered, and the simulated rainbow fitting was bolted to the aluminum/boron-epoxy combination, as shown in Figure 44. In this specimen the load was transferred directly from the end fitting into the aluminum/boron-epoxy combination through bolt bearing.

These specimens, combined with the FD-1 specimens, not only provided a check for the anticipated rainbow fitting to wing plank design but also provided an evaluation for two different modes of load introduction.

9.1.2 Fabrication Development Specimens - Test & Evaluation

The 130-FD-1 and 130-FD-2 specimens represented structural element joints which would be restrained from rotation by surrounding structure in the airplane wing. Accordingly, lateral support was applied to prevent rotation during the static test by placing two aluminum alloy support bars on each side, bridging the bars on each side of the specimen and then attaching the bridges with mechanical fasteners. Lateral support bars were profiled to suit the specimen configuration and Teflon was used at the support bar-specimen interface to minimize friction. A specimen with the lateral supporting arrangement is shown in Figure 45.

A Missimers environmental chamber, shown in Figure 46, was used to cool and heat the specimen to the required low and elevated temperatures. Figure 47 shows a test specimen installed in the environmental chamber. Each specimen was instrumented with three thermocouples, one at each end of the test section and one at the center. Thermocouple outputs were displayed on a calibrated strip chart recorder. The required test temperature was stabilized for ten minutes prior to load application and was maintained within 2.80°K (5°F) during the test.

The room temperature and 218°K (-67°F) tests were conducted on a Tinius Olsen Universal Testing Machine. The 344°K (160°F) tests were conducted on a MTS Systems Corporation electrohydraulic servo controller test system. A loading rate of 3.56×10^4 newtons (8000 pounds) per minute was used.

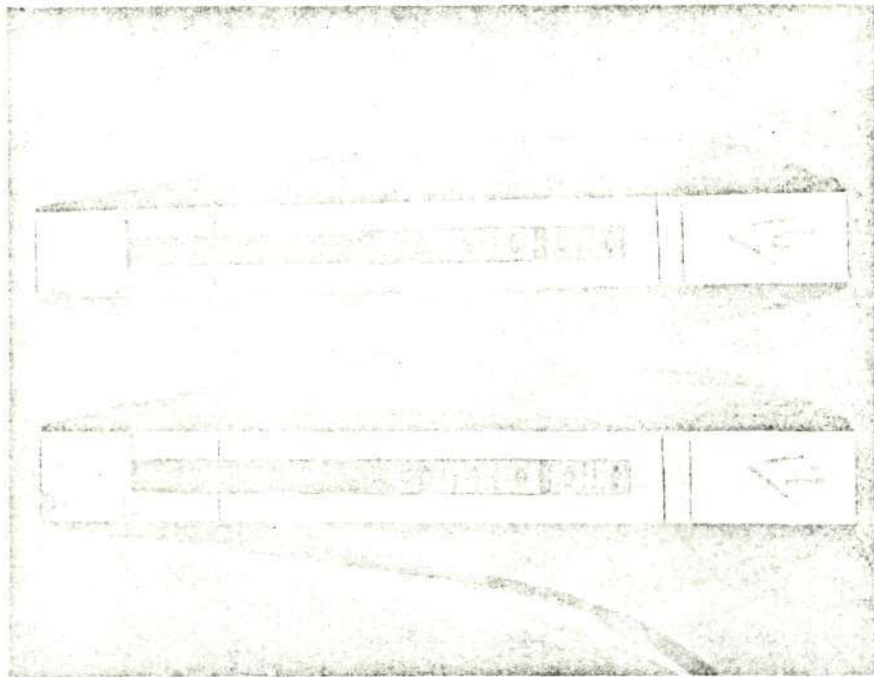


FIGURE 43.- FABRICATION DEVELOPMENT SPECIMEN (FD-1)
FROM BORON-EPOXY REINFORCEMENT SIDE

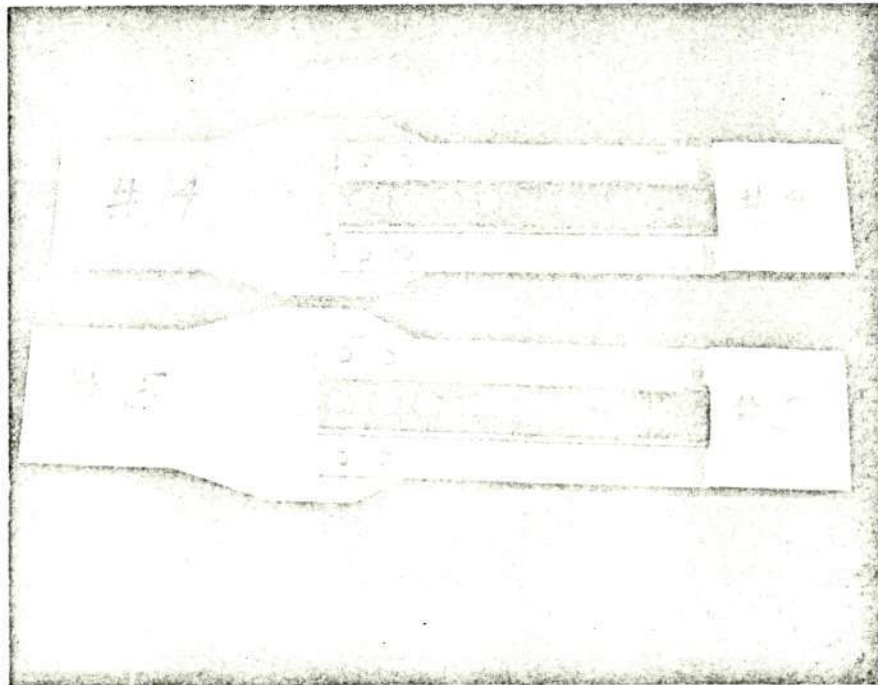
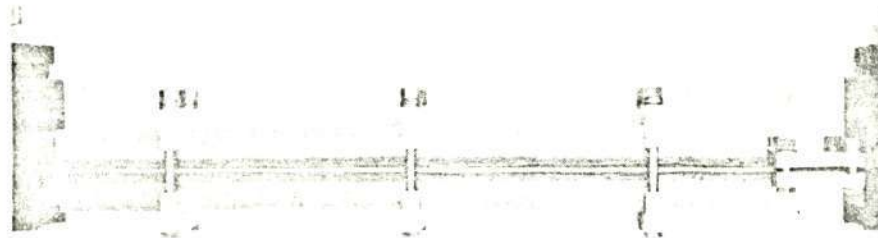
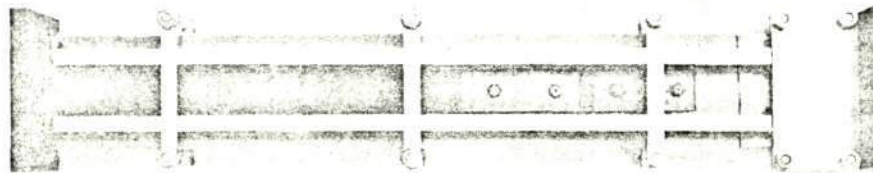


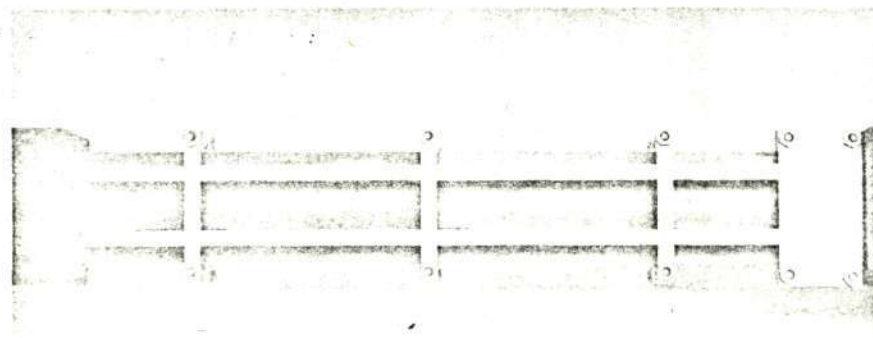
FIGURE 44.- FABRICATION DEVELOPMENT SPECIMEN (FD-2)
BORON-EPOXY REINFORCEMENT SIDE



Side View



Top View



Bottom View

FIGURE 45.- TYPICAL LATERAL SUPPORT ARRANGEMENT FOR 130-FD-1 SPECIMENS

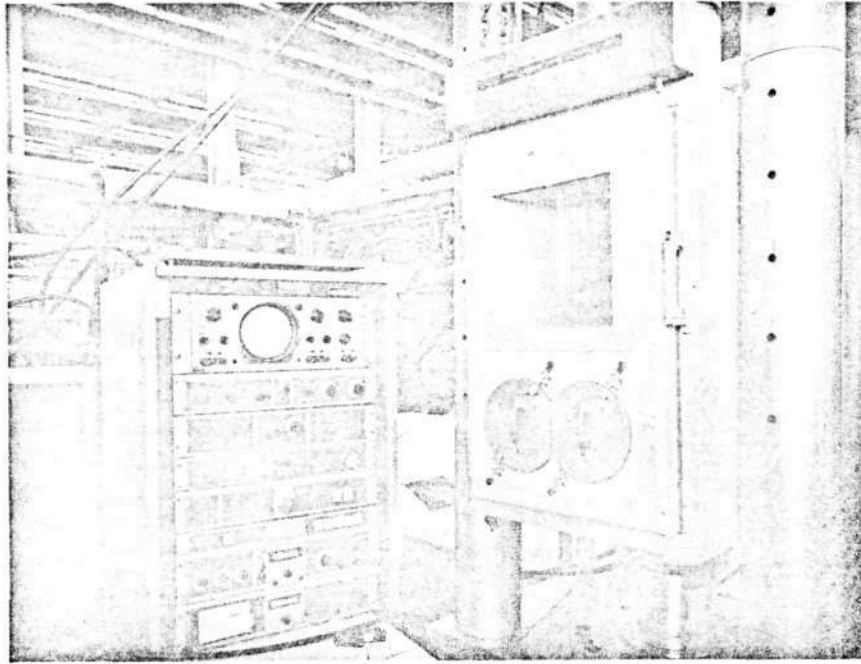


FIGURE 46.- MISSIMERS ENVIROMENTAL CHAMBER INSTALLED
IN THE TEST MACHINE

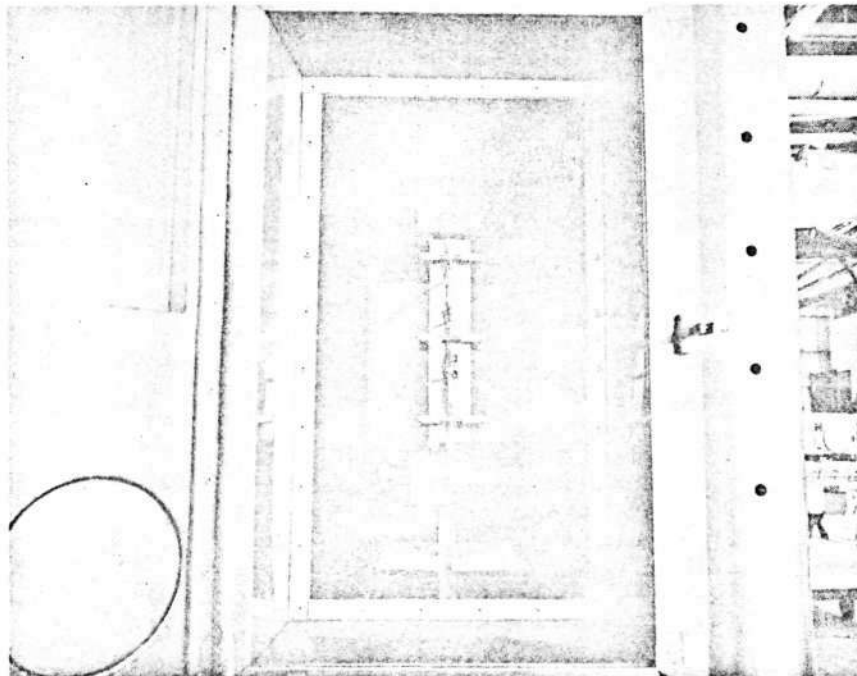


FIGURE 47.- FABRICATION DEVELOPMENT SPECIMEN INSTALLED
IN MISSIMERS ENVIROMENTAL CHAMBER

Static test results for the 130-FD-1 configuration are contained in Table XII, and the static test results for the 130-FD-2 configuration are shown in Table XIII. A typical static test failure of the 130-FD-1 specimen is shown in Figure 48. For the 130-FD-2 specimen, the primary failure mode for the room temperature and 344°K (160°F) tests was across the boron laminate at the first fastener as shown in Figure 49. Because of differences in moduli and strain capabilities between the boron laminate and aluminum, a considerable drop in load occurred upon failure of the boron without failure occurring in the aluminum. When this occurred for specimen number 2, loading was resumed until failure of the aluminum was obtained. This is noted in the Table XIII results, and the failure is shown in Figure 50.

TABLE XII. - STATIC TEST RESULTS FOR FABRICATION DEVELOPMENT SPECIMENS 130-FD-1

Test Specimen Number	Test Temperature		Ultimate Tensile Load		Aluminum Stress		Failure Mode
	°K	(°F)	10 ⁴ Newtons	(Lb) ¹	10 ² N/m ²	(KSI) ²	
130-FD-1-1	299	(78)	8.81	(19,800)	451	(65.3)	(A)
-2	295	(72)	8.94	(20,100)	458	(66.4)	(A)
-3	297	(75)	9.07	(20,400)	464	(67.3)	(A)
-4	218	(-67)	9.23	(20,750)	472	(68.4)	(A)
-5	218	(-67)	9.50	(21,350)	486	(70.5)	(A)
-6	344	(160)	8.54	(19,200)	436	(63.2)	(A)
-14	344	(160)	8.59	(19,300)	439	(63.6)	(A)


(A) Tension failure in aluminum across first fastener in boron runout.


¹ Required load 7.76×10^4 Newtons (17,450 lb.); laminate stress not computed since failure initiated in aluminum.

² Mean aluminum stresses are listed although maximum stresses may be greater due to slight misalignment of load axis.

The failure mode at low temperature was generally the same as that obtained at room temperature; however, some longitudinal splitting of the boron and partial failure of the bond between the boron-epoxy and titanium shims occurred at low temperatures. A typical low temperature failure is shown in Figure 51.

TABLE XIII.-STATIC TEST RESULTS FOR FABRICATION DEVELOPMENT
SPECIMENS 130-FD-2

Test Specimen Number	Test Temperature		Ultimate Tensile Load		Gross Laminate Stress		Failure Mode
	°K	(°F)	10 ⁵ Newtons	(lb) 	10 ⁹ N/m ²	(psi)	
130-FD-2-1	299.3	(79)	1.36	(30,600)	1.32	(191,000)	(A)
-2	298.7	(78)	1.35	(30,400)(28000)	1.31	(189,750)	(B)
-6	297.6	(76)	1.35	(30,400)	1.31	(189,750)	(A)
-4	218.15	(-67)	1.51	(33,900)	1.46	(211,650)	(C)
-17	218.15	(-67)	1.54	(34,700)	1.49	(216,500)	(C)
-10	344.26	(160)	1.34	(30,200)	1.30	(188,550)	(A)
-11	344.26	(160)	1.34	(30,200)	1.30	(188,550)	(A)

 Required load: 1.11×10^5 Newtons (24,960 lb)

- (A) Tensile failure in boron across first fastener common to rainbow fitting and simulated stringer.
- (B) Tensile failure in boron at location (A) at 1.35×10^5 Newtons (30,400 lb). Specimen reloaded and subsequently failed at same location in the aluminum at 1.25×10^5 Newtons (28,000 lb).
- (C) Tensile failure in boron at location (A) accompanied by longitudinal splitting of boron and partial failure of bond between boron and titanium shims.

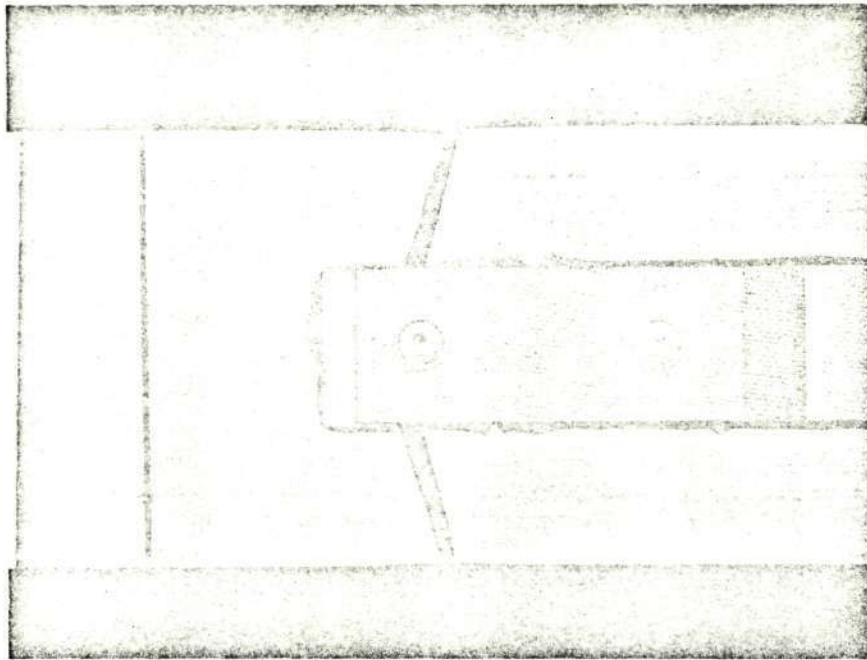


FIGURE 48.- TYPICAL STATIC TEST FAILURE OF 130-FD-1 SPECIMEN

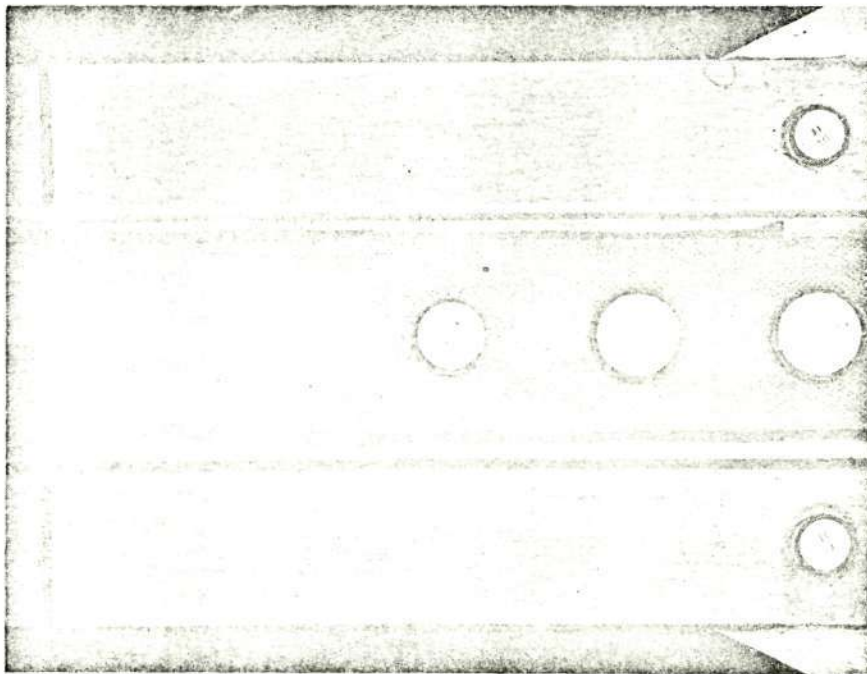


FIGURE 49.- TYPICAL ROOM TEMPERATURE STATIC TEST FAILURE FOR 130-FD-2 SPECIMEN

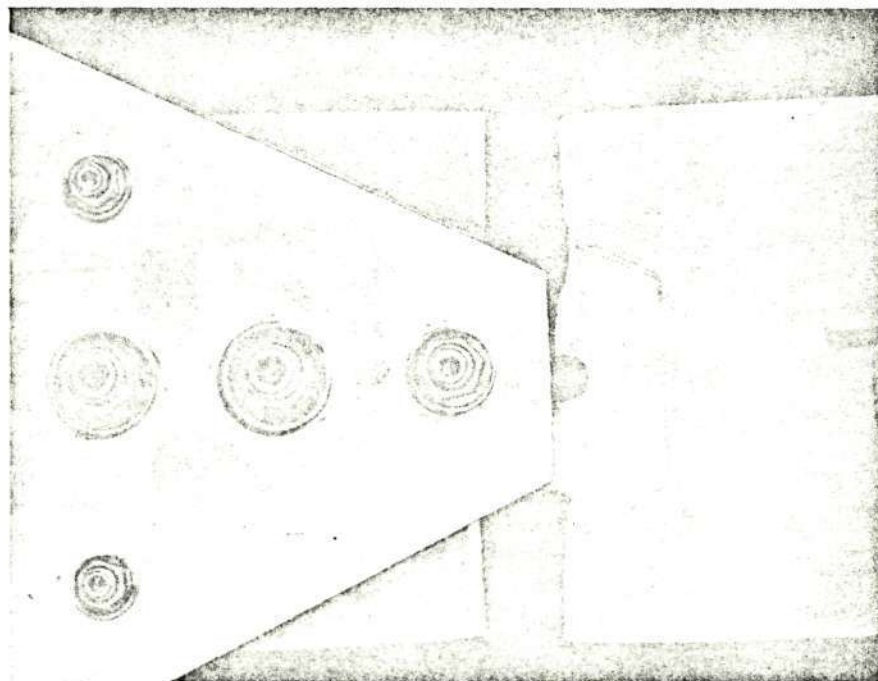
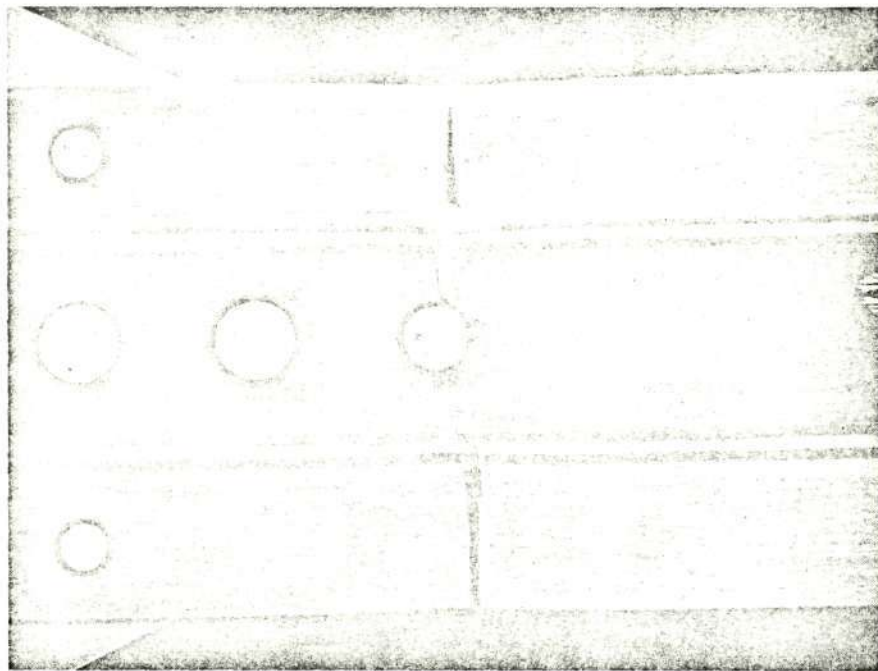


FIGURE 50.- STATIC TEST FAILURE SPECIMEN NUMBER 2
OF 130-FD-2

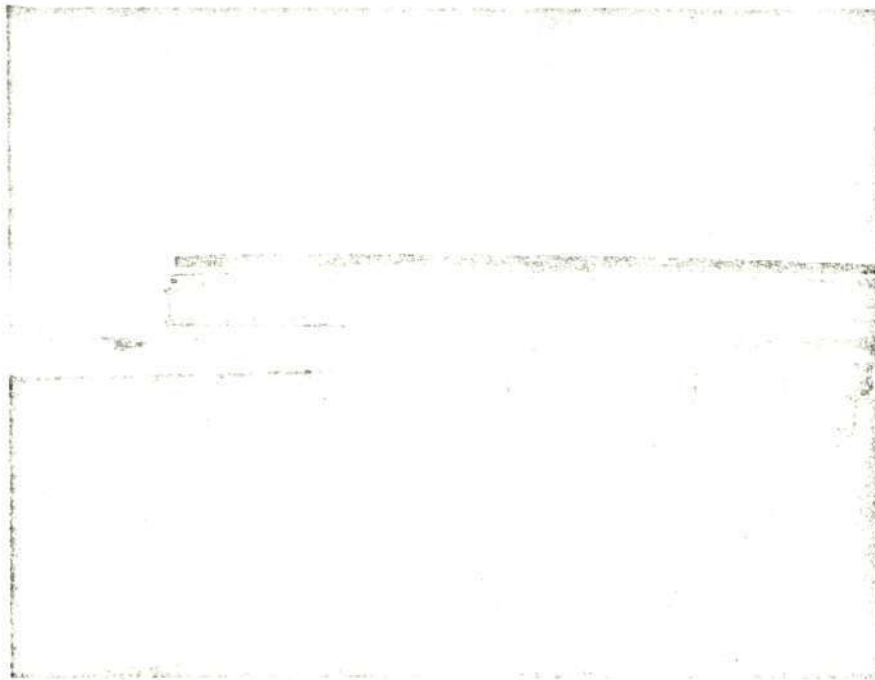
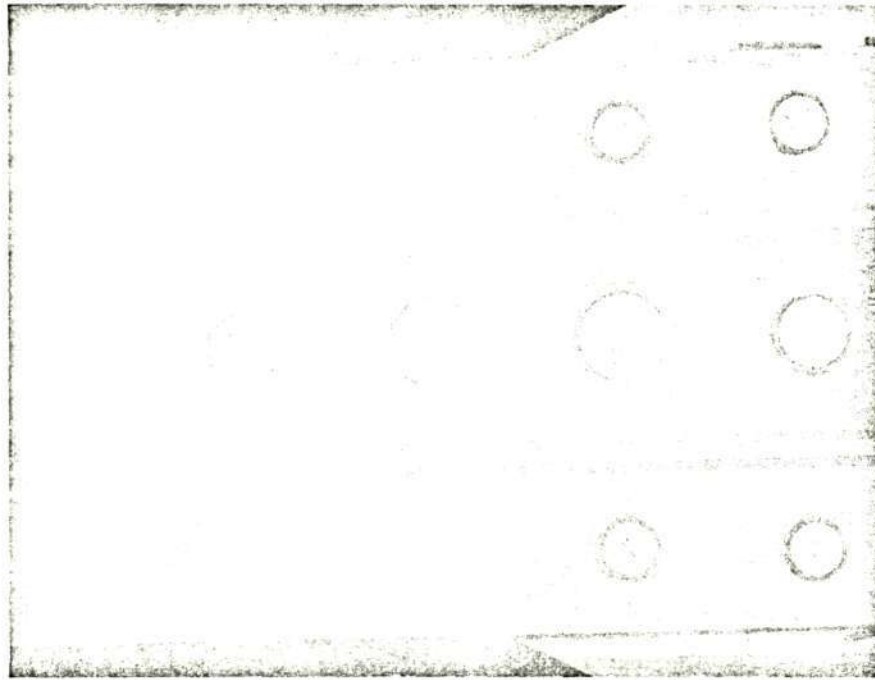


FIGURE 51.-TYPICAL -67°F STATIC TEST FAILURE FOR
130-FD-2 SPECIMEN

The ultimate tensile load of each fabrication development specimen 130-FD-1 exceeded the required ultimate load of C-130 B/E configuration of 7.76×10^4 N (17,450 lb), and each of the 130-FD-2 specimen exceeded the required ultimate load of C-130 B/E configuration of 1.11×10^5 N (24,960 lb). In each case the specimen tested at 218°K (-67°F) exhibited the highest ultimate load followed by the specimen tested at room temperature and 344°K (160°F), respectively.

All fatigue tests for 130-FD-1 and 130-FD-2 specimens were performed at a load ratio of +0.10 except that one test on each configuration was performed at 218°K (-67°F) and at a load ratio of +10.0.

Lateral support was applied to the fatigue specimens, in the manner previously described for the static tests, to prevent joint rotation and to prevent specimen buckling during the $R = +10.0$ fatigue test.

All 130-FD-1 fatigue tests were performed in a MTS System Corporation electrohydraulic servo-controlled test system. Hydraulically operated grips were used to attach the specimens to the testing machine loading heads. The load form was sinusoidal, and dynamic loads were controlled to within ± 1 percent of those desired. Cycling was accomplished within a rate range of five to eight cycles per second. The Missimers environmental chamber was used to provide required cooling and heating.

All 130-FD-2 fatigue tests were performed in Lockheed-designed resonance-operated fatigue machines. The specimens were loaded axially at a rate of approximately 30 cycles per second, and dynamic loads were controlled to within ± 1 percent of desired values. For the 218°K (-67°F) tests, cooled dry nitrogen gas flowed into a chamber surrounding the test specimen and provided cooling. The gas was cooled as it flowed through a copper coil submerged in liquid nitrogen. A chamber containing resistance heating elements was used for the 344°K (160°F) tests.

Results of the 130-FD-1 fatigue tests are contained in Table XIV. The specimens tested at $R = +.10$ and at a temperature of 218°K (-67°F) exhibited the greatest fatigue life, followed by the specimens tested at room temperature, and at 344°K (160°F), respectively. The relatively greater fatigue life of the low temperature specimens corresponds to the results of the static tests. The maximum test load (P_{max}) vs. cycles to failure is plotted in Figure 52.

Specimen FD-1-17 was tested at 218°K (-67°F) and $R = +10.0$. The maximum load, P_{max} , was -2.22×10^3 Newtons (-500 lb); P_{min} was -2.22×10^4 Newtons (-5000 lb). The specimen was cycled to 200,800 cycles with no failure. The quality level (K_t), based on the calculated thermal residual stress in the aluminum and the aluminum/boron-epoxy area ratio, was computed and is listed in Table XIV.

TABLE XIV. -FATIGUE TEST RESULTS OF FABRICATION DEVELOPMENT
SPECIMENS 130-FD-1

	Test Specimen Number	Test Temperature		Maximum Load		Cycles to Failure 10^3 Cycles	Quality Level (K_t)	Failure Mode
		$^{\circ}\text{K}$	$^{\circ}\text{F}$	10^4 N	(lb)			
$R = +0.10$	130-FD-1-7	RT	(RT)	6.09	(13,700)	7.5	3.39	(A)
	-8	RT	(RT)	4.98	(11,200)	33.31	3.16	(A)
	-9	RT	(RT)	3.65	(8,200)	164.	3.28	(A)
	-10	218	(-67)	6.09	(13,700)	37.26	1.97	(A)
	-17	218	(-67)	5.43	(12,200)	47.61	2.0	(B)
	-13	218	(-67)	4.98	(11,200)	99.68	1.96	(C)
	-11	344	(160)	6.09	(13,700)	6.38	3.90	(A)
	-15	344	(160)	4.45	(10,000)	24.33	3.93	(A)
	-12	344	(160)	5.43	(12,200)	10.43	3.98	(A)
$R = +10.0$	-17	218	(-67)	-.222	(-500)	Tested to 200,800 cycles		No Failure

(A) Failed in simulated aluminum skin across first fastener in laminate runout. This is the location where the static failures were experienced.

(B) Failed in aluminum skin adjacent to loading tab, accompanied by failure of laminate and bond.

(C) Type (B) failure with fatigue crack in aluminum skin beside the first fastener indicated in (A).

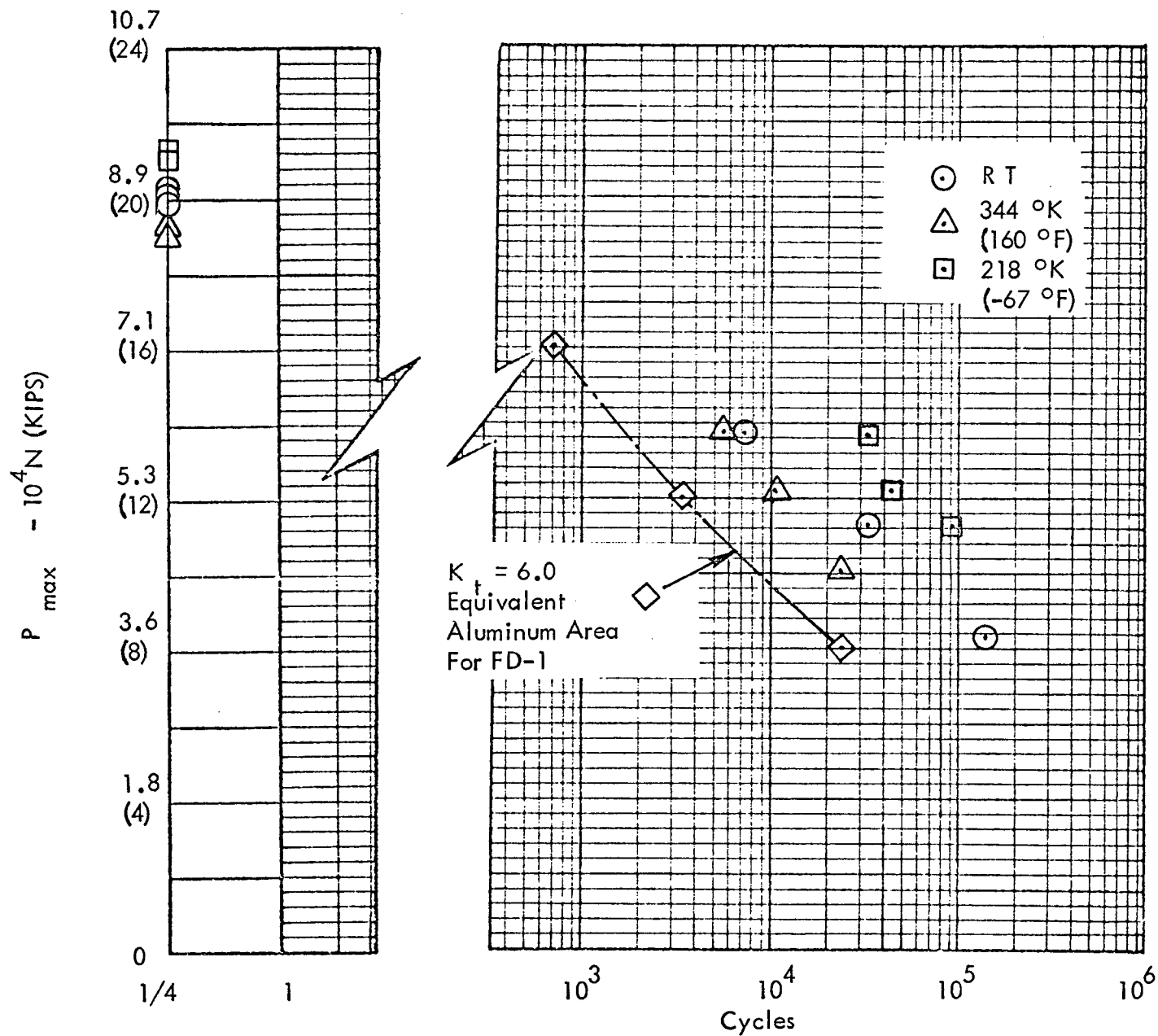


FIGURE 52.- STATIC & FATIGUE TESTS 130FD-1

Results for the 130-FD-2 fatigue tests are tabulated in Table XV. The fabrication development FD-2 specimens tested at $R = +.10$ (P_{min}/P_{max}) and at a temperature of 218°K (-67°F) exhibited the greatest fatigue life followed by the specimens tested at room temperature and 344°K (160°F), respectively. The relatively greater fatigue life of the low temperature specimens corresponds to the results of the static tests. The maximum test load (P_{max}) versus cycles to failure for each specimen tested at $R = +.10$ is plotted in Figure 53.

Specimen FD-2-15 was tested at 218°K (-67°F) and $R = +10.0$. The test load was varied from $-3.43 \times 10^3 \text{ N}$ (-770 lb) to $-3.43 \times 10^4 \text{ N}$ (-7700 lb). The specimen was cycled to 100,000 cycles with no failure. The quality level (K_t), based on the calculated thermal residual stress in the aluminum and the aluminum/boron-epoxy area ratio, was computed for each specimen and is listed in Table XV.

9.2 JOINT EVALUATION COMPONENTS

Structural elements representative of high load introduction areas in the composite reinforced metal structure were designed, fabricated and tested to verify design concepts from a static and fatigue standpoint. In addition, several detailed stress distributions were measured on specimens representative of boron-epoxy-to-aluminum transition areas.

9.2.1 130-JE-1 & 130-JE-4 Specimens

The 130-JE-1 and 130-JE-4 specimens are identical except for relatively minor changes in the laminate-to-aluminum bond cycle and in the laminate configuration. The 130-JE-4 was temperature cycled and fatigue cycled late in the Phase I program to determine the effect of these changes.

9.2.1.1 JE-1 and JE-4 Description

These specimens are two-stiffener sections of a lower surface wing plank to rainbow fitting transition joint. Overall dimensions are 0.315m (12.40 inches) wide and 1.04m (40.80 inches) long. The specimens, as designed, are symmetrical about their center span. Rainbow fittings are used on each end for use as test fixtures and to double the joint exposure in one test. Wing planks in the area of W.S. 220 fittings are the same thickness as on the Model C-130 B/E aircraft, and are tapered down to C-130E thicknesses in the center of the specimen. The stiffeners are also machined to the thinner cross section of the C-130E configuration. The laminates for both the wing planks and stiffeners are designed to taper out in the transition area of the C-130E skin to the C-130 B/E skin thickness at the rainbow fitting. This results in an all metallic joint in the rainbow fitting area and a composite reinforced structure in the net section area of the wing plank. With the specimen designed symmetrically about the spanwise centerline, the specimens represent a shortened wing plank with a W.S. 220.00 transition joint at each end. Typical joint design is illustrated in Figure 54.

TABLE XV. -FATIGUE TEST RESULTS OF FABRICATION DEVELOPMENT
SPECIMENS 130-FD-2

	Test Specimen Number	Test Temperature		Maximum Load		Cycles to Failure 10^3 Cycles	Quality Level (K _t)	Failure Mode
		°K	(°F)	10^4 N	(lb)			
R = +0.10	130-FD-2-7	RT	(RT)	5.89	(13,250)	22	4.21	(A)
	-5	RT	(RT)	4.94	(11,100)	38	4.67	(A)
	-3	RT	(RT)	2.60	(5,840)	506	6.79	(B)
	-9	218	(-67)	5.89	(13,250)	20	3.92	(C)
	-13	218	(-67)	4.94	(11,100)	42	3.96	(C)
	-8	218	(-67)	4.14	(9,300)	74	3.98	(C)
	-12	344	(160)	5.89	(13,250)	15	4.71	(C)
	-14	344	(160)	4.14	(9,300)	46	7.22	(C)
	-16	344	(160)	4.94	(11,100)	26	6.02	(C)
R = +10.0	-15	218	(-67)	0.343	(-770)	Tested to 100,000 Cycles		No Failure

(A) Failed in the aluminum skin across the first row of fasteners common to the rainbow fitting.

(B) Failed in the loading tab of the simulated rainbow fitting. The rainbow fitting had fatigue cracks at each outside fastener of the first row.

(C) Failed in the stringer adjacent to the loading tab.

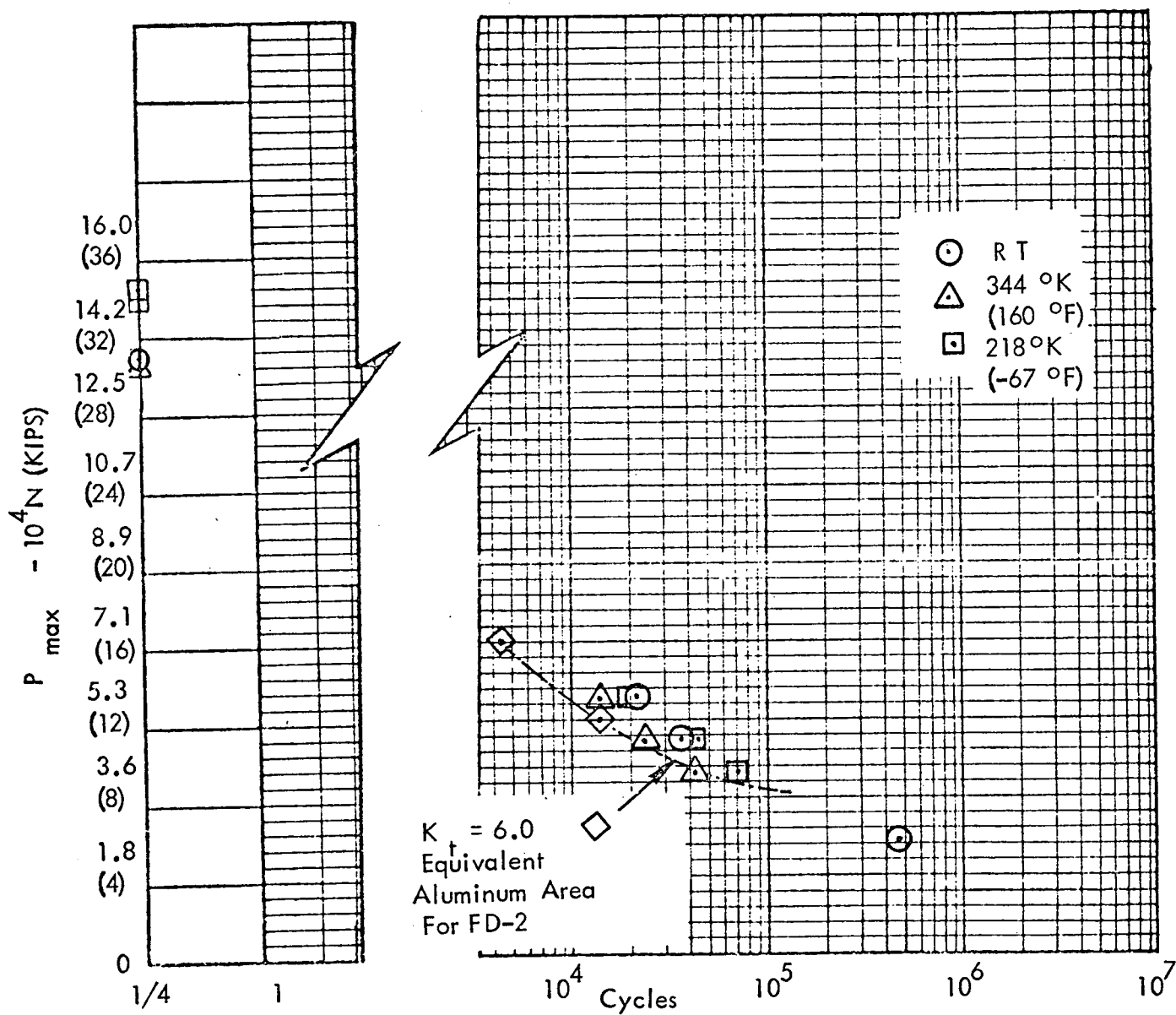


FIGURE 53.-STATIC & FATIGUE TESTS 130-FD-2

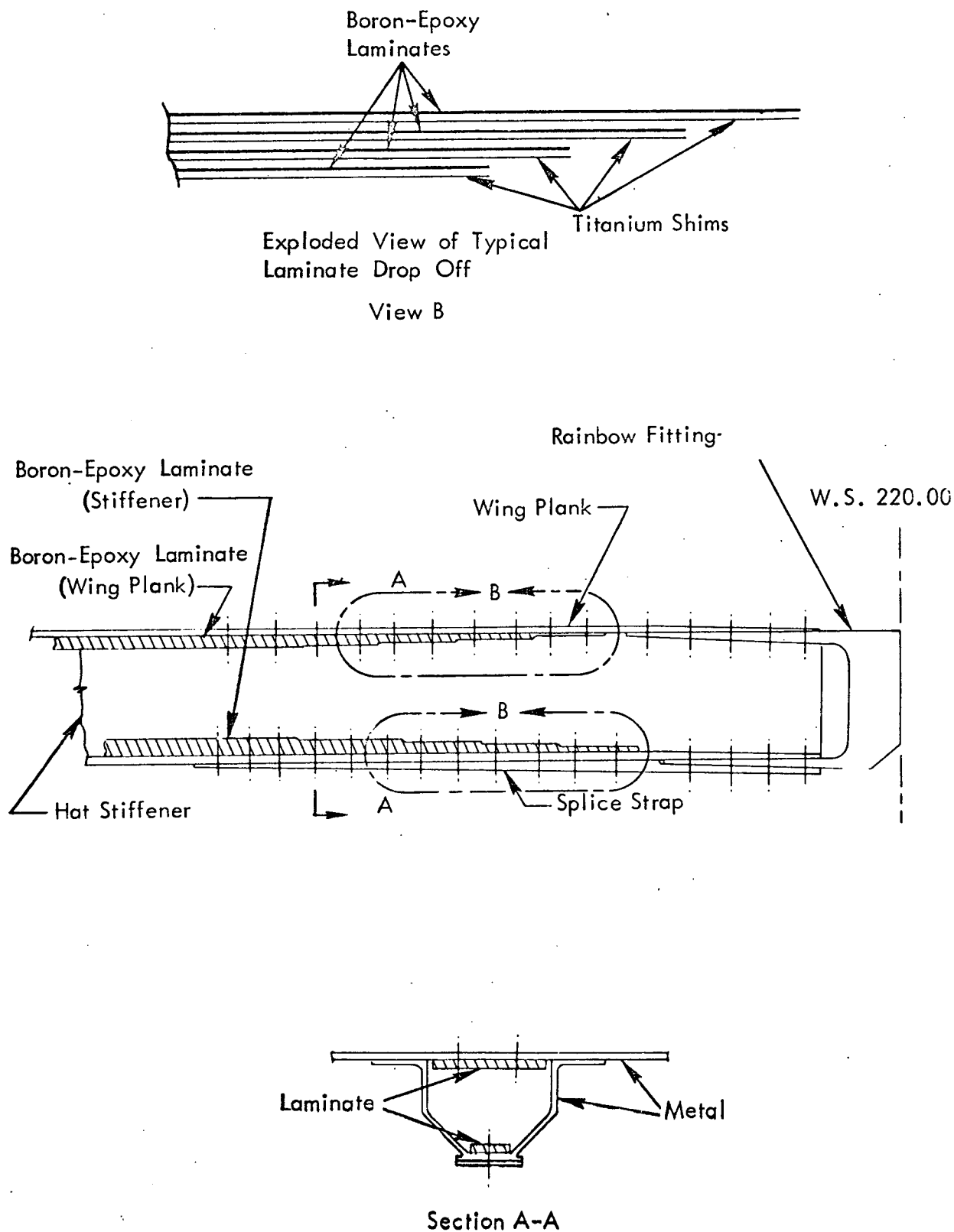


FIGURE 54.- TYPICAL WING STATION 220.00 JOINT DESIGN

9.2.1.2 130-JE-1 and 130-JE-4 Tests

The JE-1 and JE-4 specimens were instrumented with electrical resistance type strain gages and thermocouples required for strain data collection and temperature monitoring during subsequent testing. Ten axial strain gages were installed at the positions shown in Figure 55. Since gage positions 5 and 9 were inaccessible after specimen assembly, gages were installed at these two positions prior to assembly of the hat section stiffeners to the skin. Lead wires were then attached and routed spanwise in such a way as to allow their retrieval through the joint bolt access holes after specimen assembly. These two gages were applied to boron-epoxy laminates, and Baldwin Type FAE 25-12S6ET gages were used. The remaining eight gages were Baldwin Type FAE 12-12S13ET and were applied to aluminum alloy parts after specimen assembly was completed. The specimens were also instrumented with ten copper-constantan thermocouples. Five were located on each side of the specimens and positioned to determine chordwise and spanwise temperature distributions as shown in Figure 56.

The overall length of JE-1 and JE-4 was approximately equal to the C-130 airplane rib spacing; consequently, buckling under compressive loads contained in the fatigue spectrum was not expected to occur. This was verified by a conservative analysis; therefore, no lateral support was provided in the test arrangement. A fitting assembly was made for each end of the specimen to allow attachment to the testing machine and to provide representative loading at the specimen ends. Each assembly had an aluminum alloy part containing bolt and barrel nut holes which reasonably simulated the outer wing portion of the W.S. 220 joint on the C-130 airplane. One of these simulated outer wing parts was attached to each end of the specimen using production nuts, bolts and torque. Each of these parts was bolted to a steel fitting which was attached to the testing machine with a threaded adaptor. The specimen partially assembled in an MTS testing machine is shown in Figure 57.

Once the specimen was assembled in the testing machine, thermocouple leads were connected to a strip chart recorder and strain gage leads were connected to a B & F Model SY156, digital strain data acquisition system. An environmental chamber constructed of 5.08 cm (2 in) thick Styrofoam sheet was then assembled around the specimen. This chamber was ported at the top and bottom to a Missimers environmental chamber. The Missimers was baffled internally to allow hot or cold air to be circulated through the ports and around the test specimen. Air was heated by resistance heating elements in the Missimers, and liquid carbon dioxide was expanded to provide cold air. Set point temperature was automatically controlled by an Alnor Pyrotroller. Figure 58 shows the Styrofoam chamber assembled around the specimen and ported to the Missimers.

Prior to initiating the fatigue test, strain surveys were performed at room temperature, 344°K (160°F) and 218°K (-67°F). The room temperature surveys were performed under both tension and compression loads while those at high and low temperature were conducted under tensile loading only. Loads were applied in increments and each load was held constant long enough to record strains from the ten gages. The maximum loads applied during the strain surveys were the maximum tensile and compressive loads contained in the fatigue spectrum. Prior to initiating the high and low temperature strain surveys, the specimens were allowed to soak at test temperature for approximately 30 minutes. Specimen temperature at all ten thermocouple positions was within $\pm 5.56^\circ\text{K}$ (10°F) of that desired.

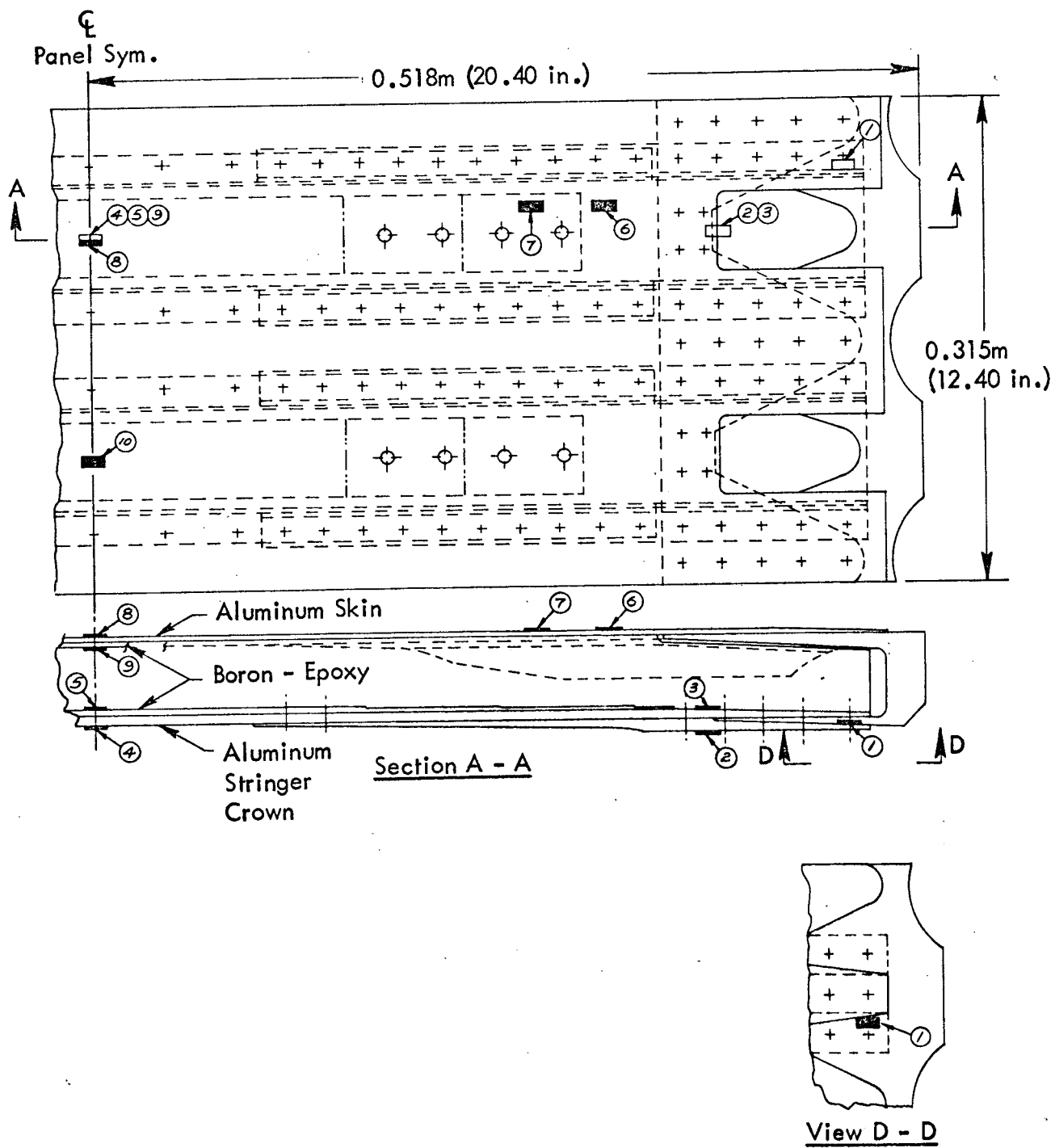


FIGURE 55.- STRAIN GAGE LOCATIONS FOR JE-1 AND JE-4 SPECIMENS

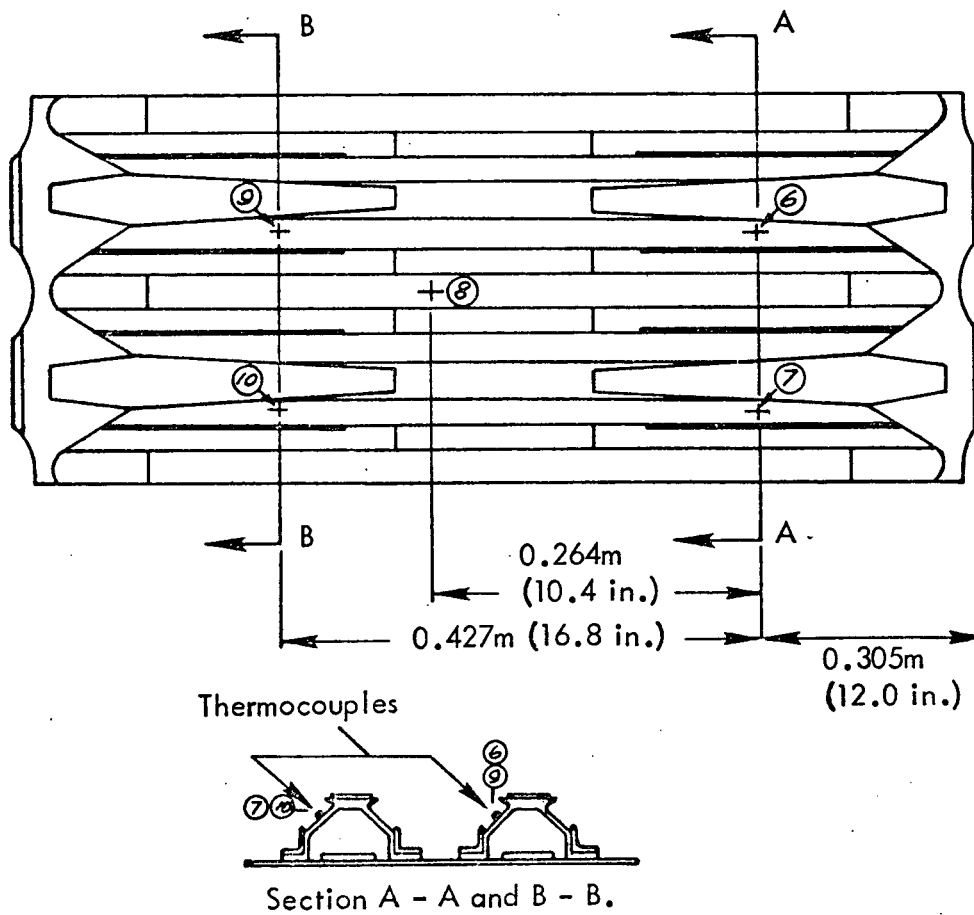
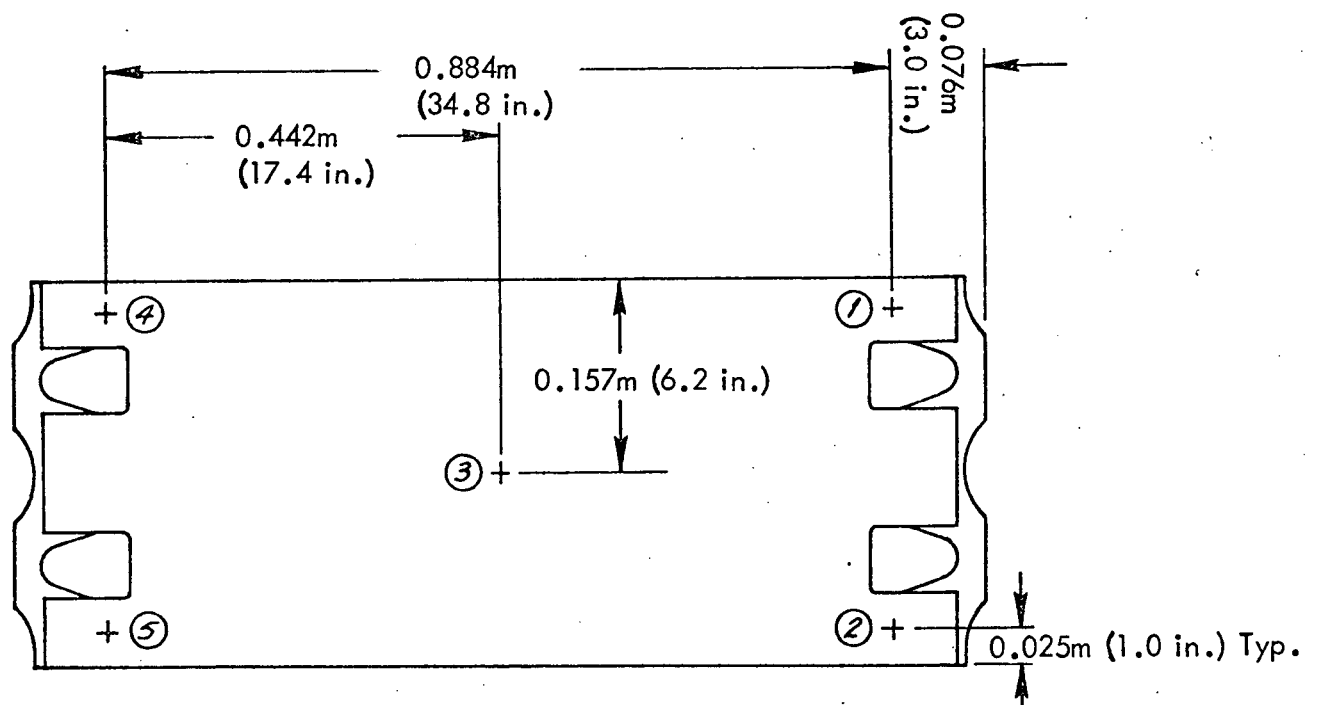


FIGURE 56. - THERMOCOUPLE LOCATIONS FOR JE-1 AND JE-4 SPECIMENS

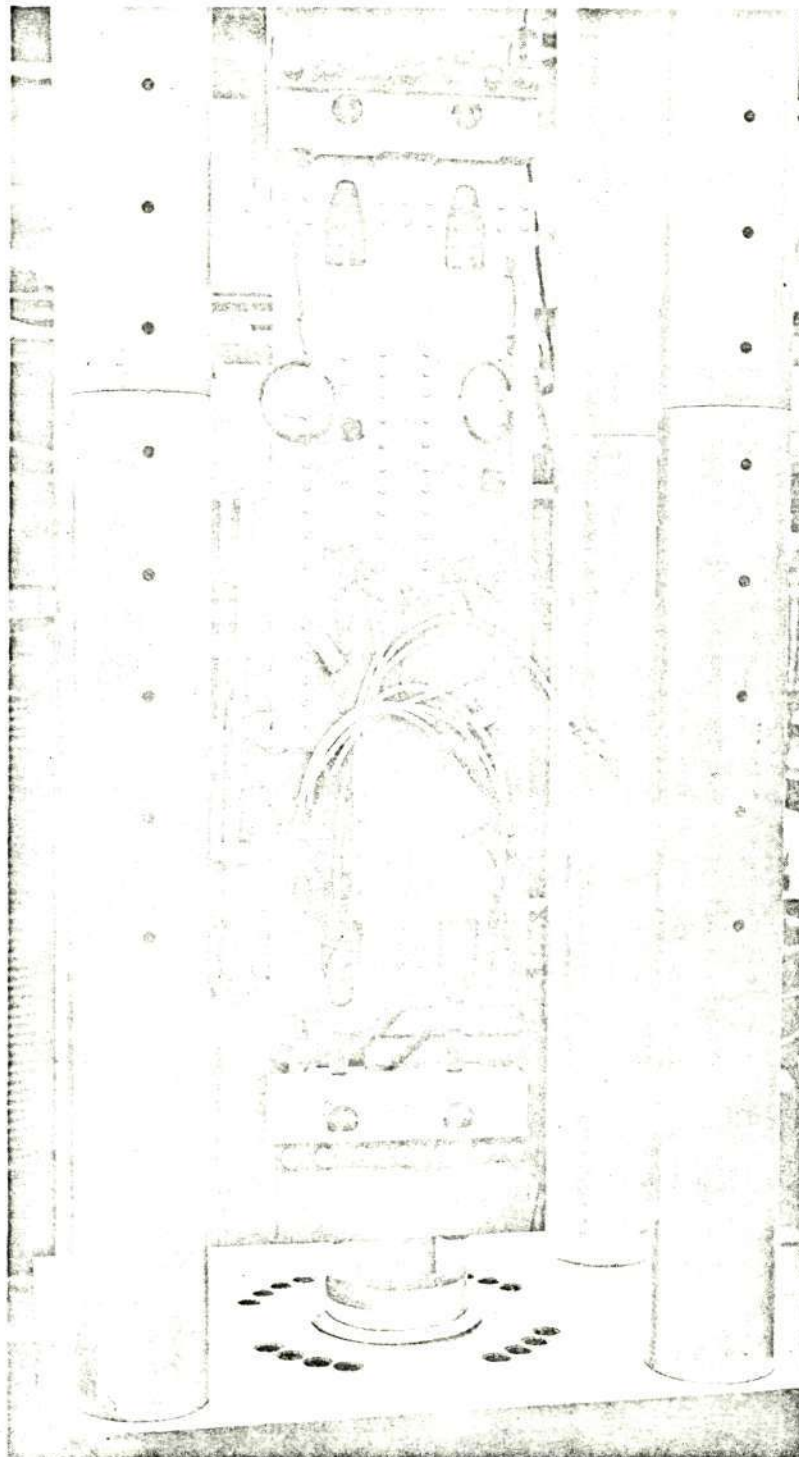


FIGURE 57.- JE-1 PARTIALLY ASSEMBLED IN MTS TESTING MACHINE

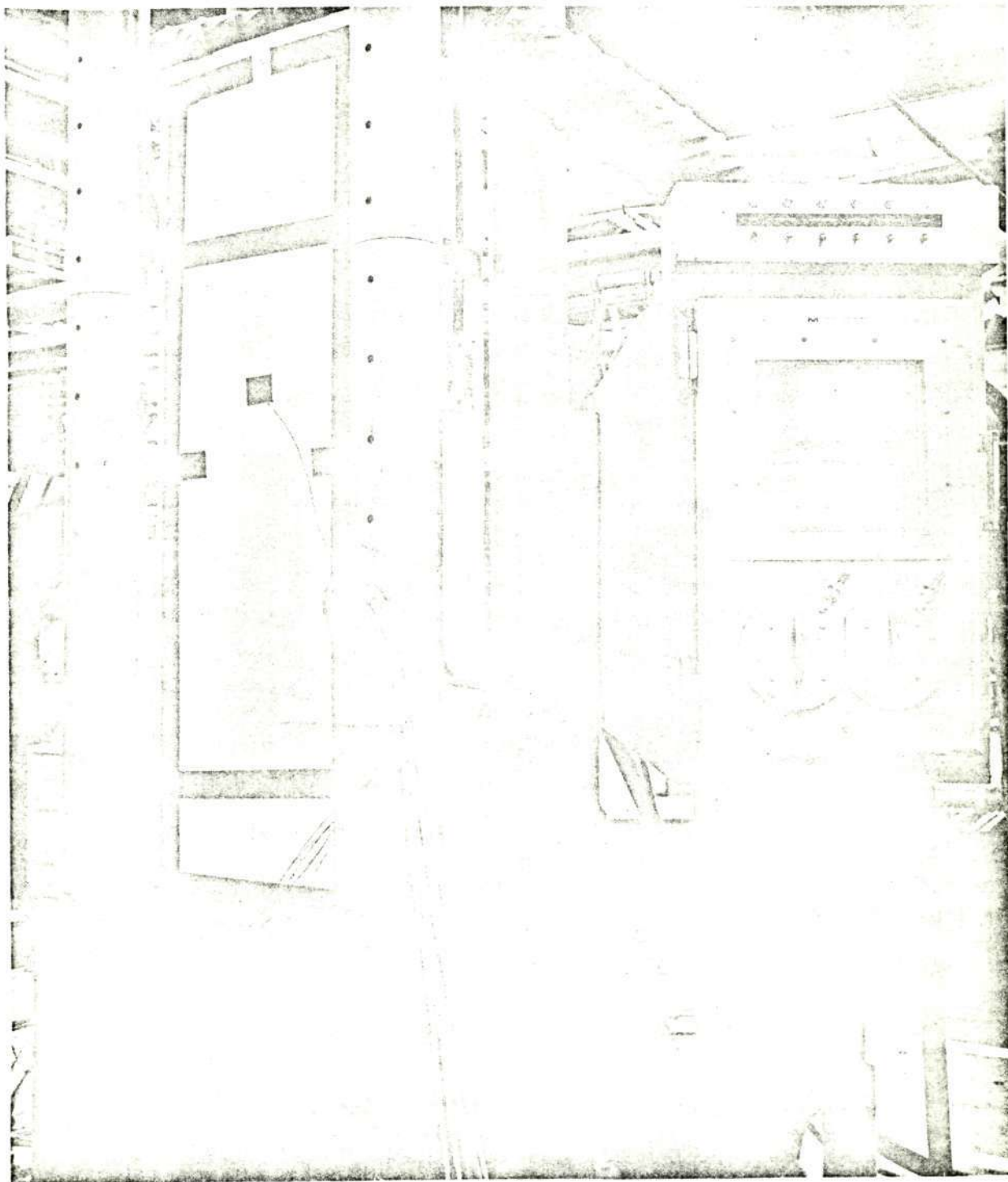


FIGURE 58.- ENVIRONMENTAL CONTROL ARRANGEMENT FOR JE-1
AND JE-4

Upon completion of the strain surveys, the fatigue test was initiated using the same testing machine and load range. An EMR, Model 1641P, profiler was used to provide commands necessary for precise application and sequencing of the spectrum loads. The complete test arrangement is shown in Figure 59. The C-130E fatigue spectrum was used and was applied in block format as shown in Table XVI. Fatigue and temperature cycling was initiated with the specimen at room temperature. Specimen temperature was cycled between 295°K (72°F) and 218°K (-67°F) for the duration of the fatigue test. Each temperature cycle had a period of approximately two hours and was controlled to produce an average specimen temperature of 250°K (-10°F). Dwell time at the temperature extremes was sufficient for all ten thermocouple positions to stabilize at 295°K (72°F) and 218°K (-67°F) within $\pm 5.56^\circ\text{K}$ (10°F). A typical temperature-time curve for one complete cycle is presented in Figure 60. Temperature was recorded throughout the test, and the beginning of each loading block was identified on the temperature recording. Examination of this record showed that the loading blocks were randomly distributed with respect to temperature. Accuracy of applied loads was within one percent of those desired.

The fatigue test was terminated after completion of 40 load spectrum passes which represents 80,000 C-130E flight hours. During application of the 40 passes, 11 temperature cycles were applied. At this time the previously described room temperature strain survey was repeated, and the specimen was then removed from the testing machine for detailed inspection.

Before disassembling the JE-1 specimen, an ultrasonic inspection was made to verify the use of ultrasonic inspection on full-size tested parts. The inspection revealed no void areas. The specimen was X-rayed to check for cracks in the laminate or aluminum around the fasteners, and no cracks were found. The X-ray for the specimen is shown in Figure 61. One of the strain gage leads is visible in the lower center of the X-ray.

The JE-1 specimen was then disassembled by removing the skin panel from the assembly. The Hi-loks were removed by unscrewing the nut and knocking out the Hi-lok fasteners. The Taper-lok fasteners were removed by drilling out the fasteners. The disassembled specimen is shown in Figure 62, with the skin panel with boron strips exposed and the stringers with boron strips exposed and rainbow fittings still installed.

Visual inspection revealed that the boron strips were intact with no damage evidenced. There were no bondline failures evidenced by coin tapping or visual inspection.

After these inspections, the JE-1 specimen was cleaned and reassembled for a residual strength test. The specimens were installed in the tension bay of a Baldwin universal testing machine, using end fitting assemblies previously described for the fatigue test. Figure 63 shows the test arrangement. An inspection of the strain gages revealed that only gage number 1 of the JE-1 specimen had been damaged during specimen inspection and reassembly; therefore, the remaining nine strain gages were connected to the B&F strain data acquisition system as before. Strain readings were recorded as tensile load was applied. Specimen failure for JE-1 occurred while stabilizing for strain readings at a tensile load of 8.90×10^5 newtons (200,000 pounds). Failure occurred at one of the joint attachments as shown in Figure 64, and was remote from the boron-epoxy laminates. The JE-4 specimen was fatigue tested to 5.8 lifetimes when a fatigue crack developed in a stringer crown. The failed specimen is shown in Figure 65.

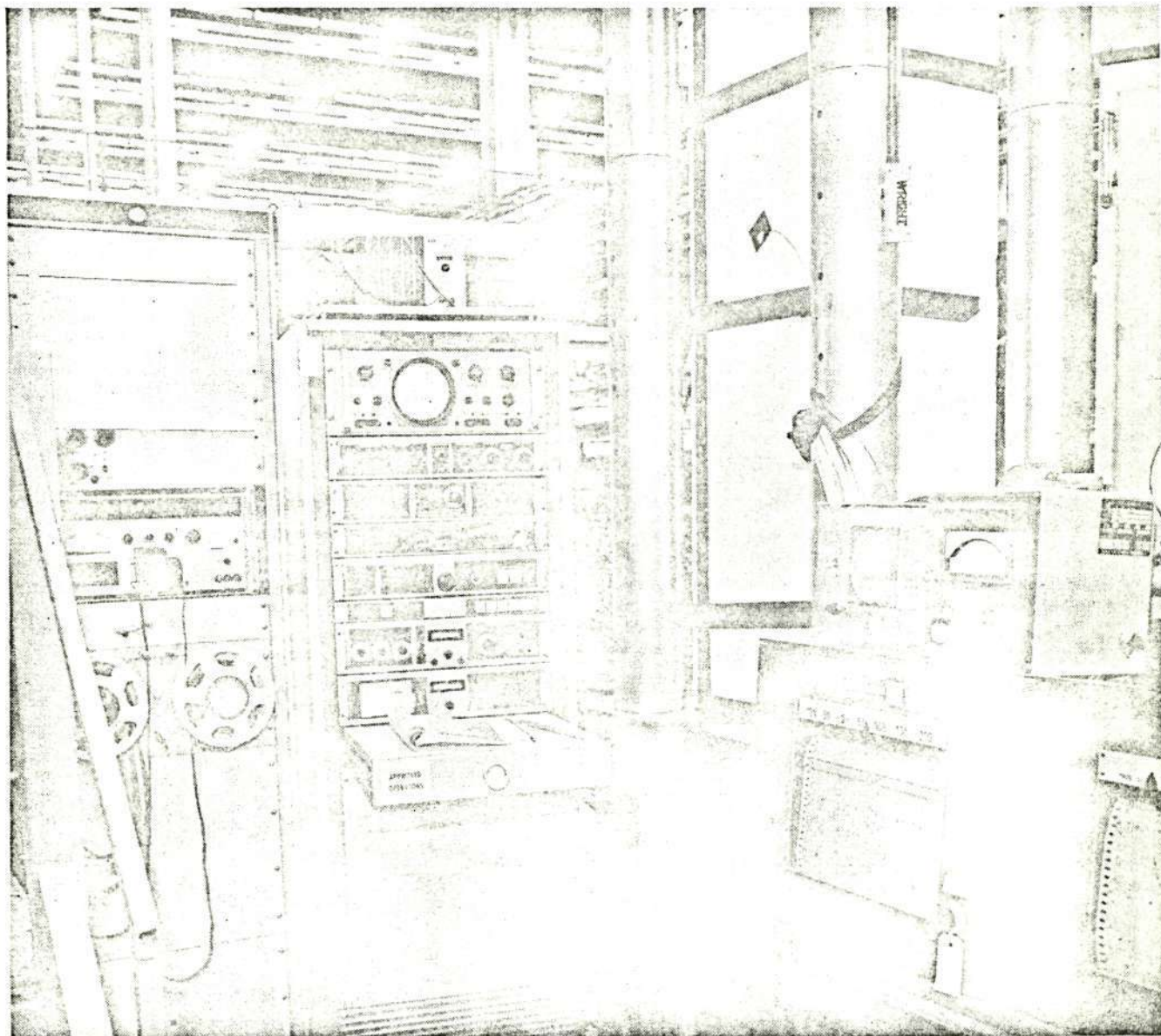


FIGURE 59.- FATIGUE TEST ARRANGEMENT FOR JE-1 AND JE-4 SPECIMENS

TABLE XVI.-BLOCK LOADING FATIGUE SPECTRUM FOR JE-1 AND JE-4 SPECIMENS

Type of Load	Load Level				Number of Cycles
	Mean		Alternating		
	10 ⁴ Newtons	Pounds	10 ⁴ Newtons	Pounds	
Gust A1	11.2	(25,200)	6.27	(14,100)	900
A2	11.2	(25,200)	7.78	(17,500)	356
Gust B1	11.7	(26,400)	6.09	(13,700)	2870
B2	11.7	(26,400)	7.56	(17,000)	875
B3	11.7	(26,400)	13.5	(30,300)	13
Gust C1	17.1	(38,400)	4.4	(9,900)	400
C2	17.1	(38,400)	5.65	(12,700)	341
GAG 1	-0.578	(-1,300)	11.4	(25,700)	151
2	0.489	(1,100)	9.16	(20,600)	409
3	1.73	(3,900)	1.09	(24,500)	42
3	1.73	(3,900)	1.09	(24,500)	42
2	0.489	(1,100)	9.16	(20,600)	409
1	-0.578	(-1,300)	11.4	(25,700)	151
Gust C2	17.1	(38,400)	5.65	(12,700)	341
C1	17.1	(38,400)	4.4	(9,900)	400
Gust B3	11.7	(26,400)	13.5	(30,300)	13
B2	11.7	(26,400)	7.56	(17,000)	875
B1	11.7	(26,400)	6.09	(13,700)	2870
Gust A2	11.2	(25,200)	7.78	(17,500)	356
A1	11.2	(25,200)	6.27	(14,100)	900

NOTE: 40 passes of the spectrum are equivalent to eight C-130E lifetimes or 80,000 simulated flight hours.

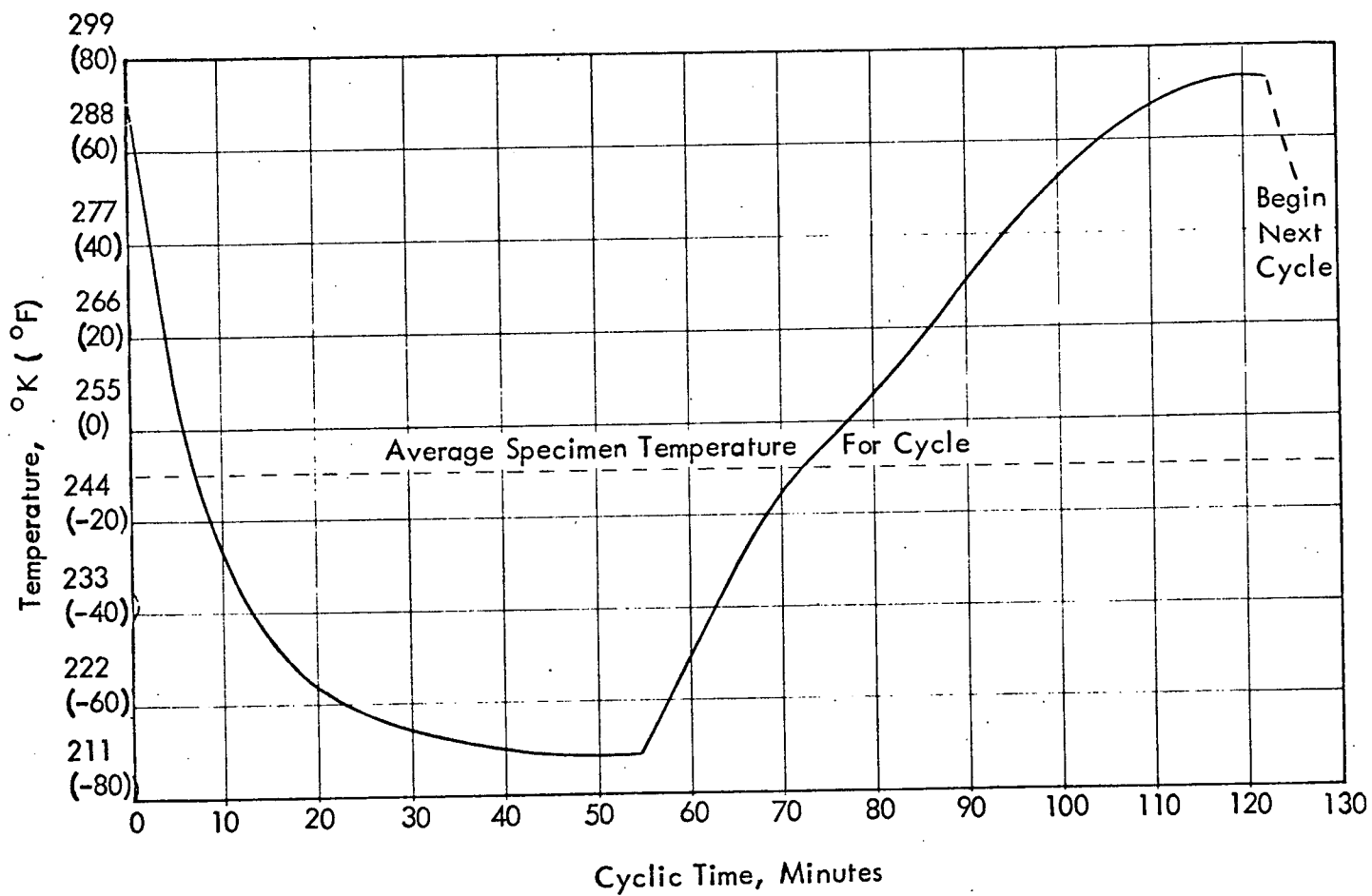


FIGURE 60. - TYPICAL TEMPERATURE VERSUS TIME CYCLE FOR JE-1 AND JE-4

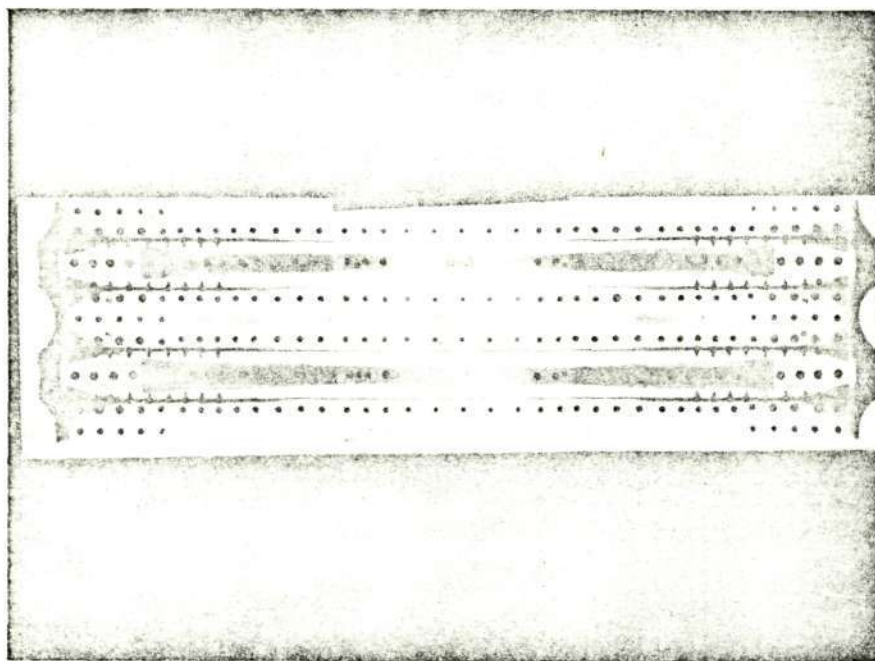


FIGURE 61.- X-RAY OF SPECIMEN JE-1 AFTER EIGHT LIFETIMES OF FATIGUE TESTING

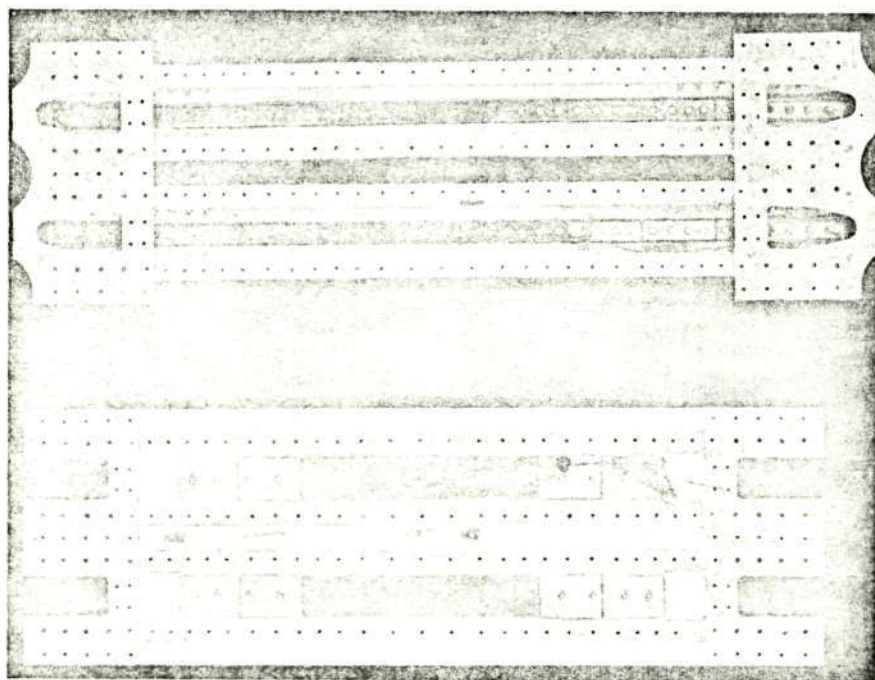


FIGURE 62.- SPECIMEN JE-1 DISASSEMBLED FOR INSPECTION

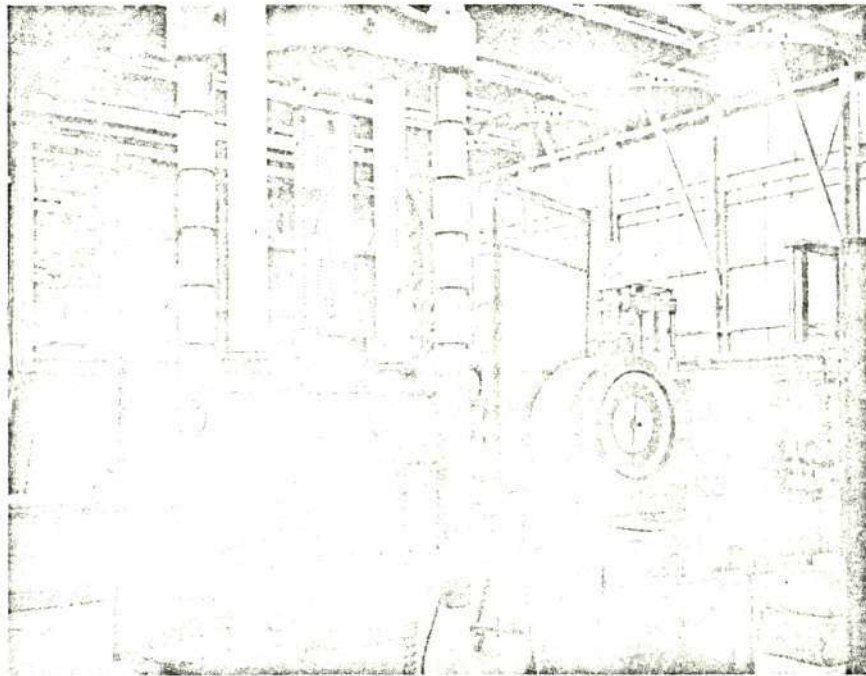


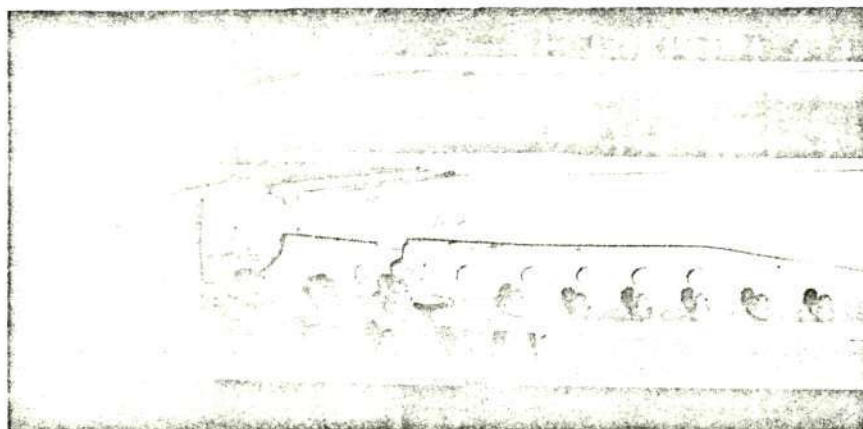
FIGURE 63.- STATIC RESIDUAL STRENGTH TEST ARRANGEMENT
FOR JE-1



Skin Side



Stringer Side



Side View

FIGURE 64.- STATIC RESIDUAL STRENGTH FAILURE FOR JE-1

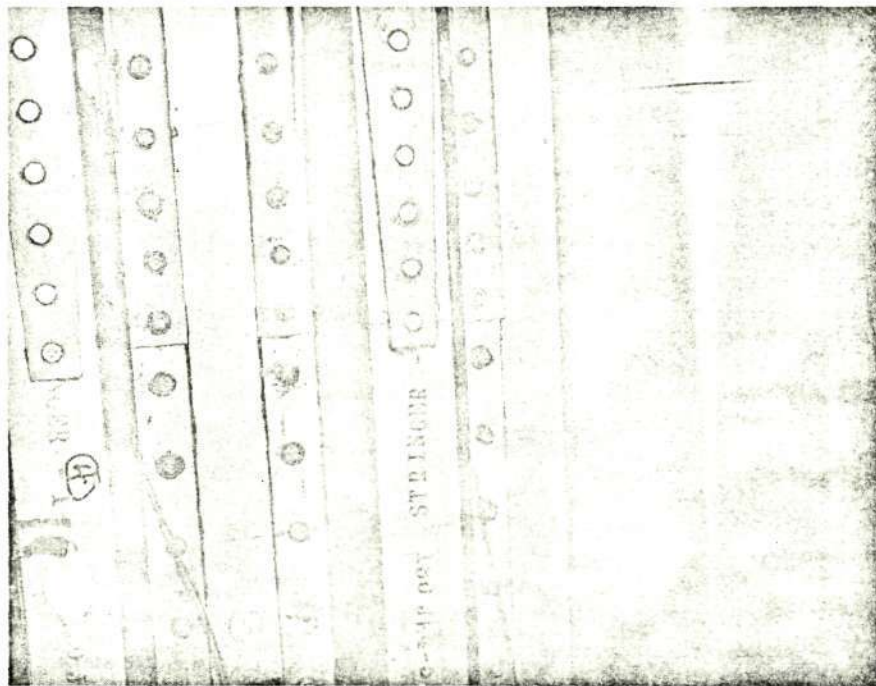


FIGURE 65.- JE-4 FAILURE

9.2.1.3 130-JE-1 and 130-JE-4 Test Evaluation

Component panel JE-1 was successfully tested to 80,000 simulated flight hours¹; the corresponding quality level (K_t) was computed to be 6.65. Specimen JE-4 was successfully tested to 58,000 simulated flight hours when a fatigue crack developed in a stringer crown; the corresponding quality level was computed to be 10.22.

An investigation of the failure in specimen JE-4 revealed the origin of the fatigue crack was in the fastener hole at the faying surface of the external strap. Subsequent examination of JE-1 revealed the beginning of an identical crack at the same location as in JE-4. The initiation of these cracks in JE-4 can be attributed to the lack of deburring of the fastener holes.

The completion of 80,000 simulated flight hours of fatigue testing on specimen JE-1 and 58,000 simulated flight hours on specimen JE-4 sufficiently exceeds the 10,000-hour single lifetime requirement to establish the design objectives as satisfactory.

The maximum strain recorded on specimens JE-1 and JE-4 occurred on the exterior aluminum surface of the stringer crown at the mid-section of the panel. The stress values derived from strain gages 4 and 5, located at the mid-section of the panel, on the aluminum and boron-epoxy surfaces, respectively, are in good agreement with the predicted values. Stress values derived from strain gages 4 and 5 are plotted in Figures 66 and 67, for JE-1 and JE-4 respectively. These values are based on strain due to applied loads and do not include thermally induced strain due to bonding.

In the residual strength test the JE-1 specimen sustained an ultimate load of 8.9×10^5 N (200,000 pounds), exceeding the design ultimate of 6.58×10^5 N (148,000 pounds). Figure 68 illustrates the predicted failing load of the most critical sections of the panel.

9.2.2 130-JE-2 Specimen

This specimen represented the upper surface structural configuration expected to be used for the C-130 composite reinforced center wing box at the wing station 220 joint.

9.2.2.1 JE-2 Description

The specimen was symmetrical about its center span and rainbow fittings were used on each end to simplify testing and to double the joint exposure in one test.

¹ Fatigue test requirements are discussed in detail in the section on Panel Fatigue Components

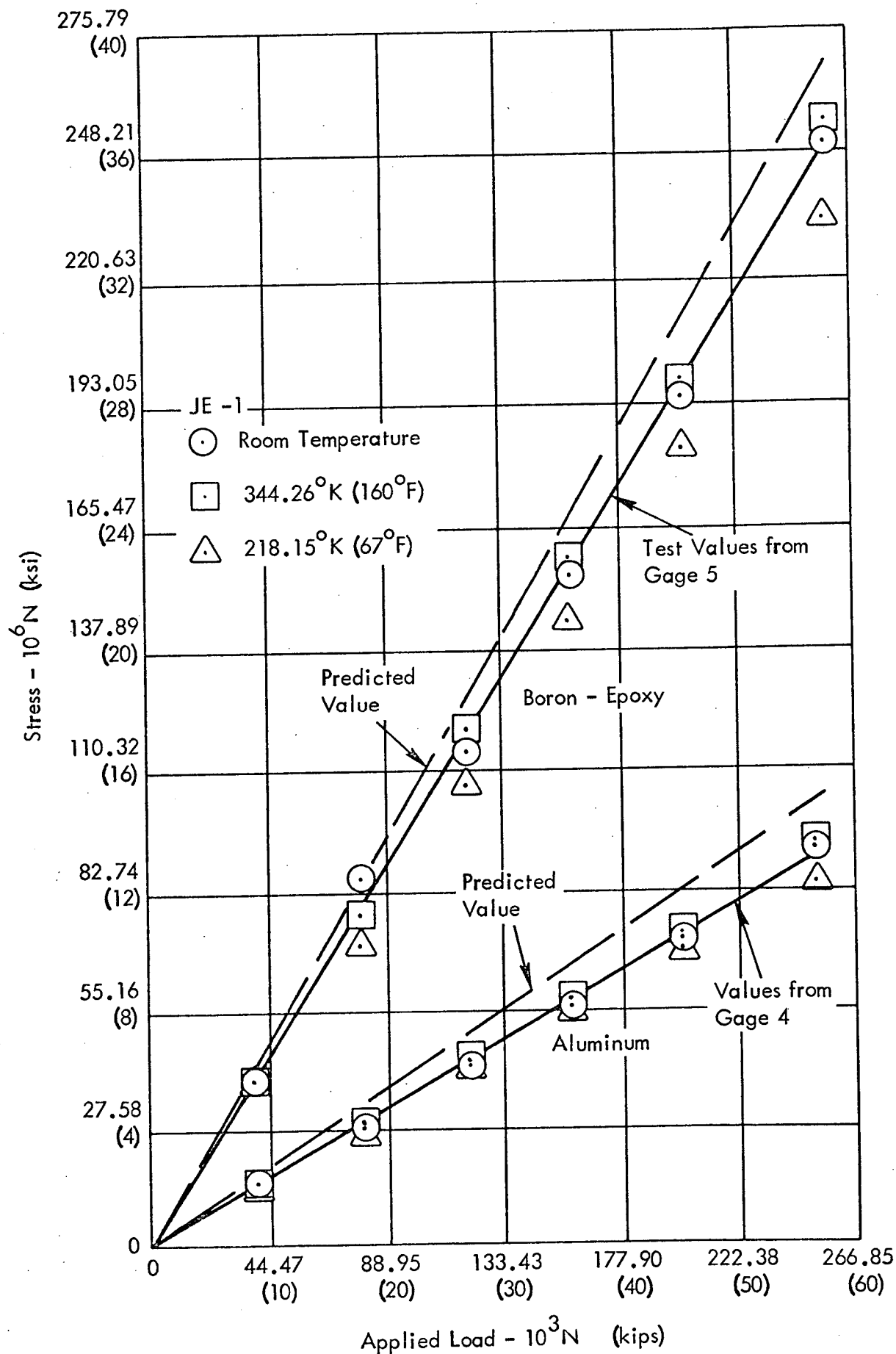


FIGURE 66. - ACTUAL STRESS VERSUS PREDICTED STRESS FOR JE-1

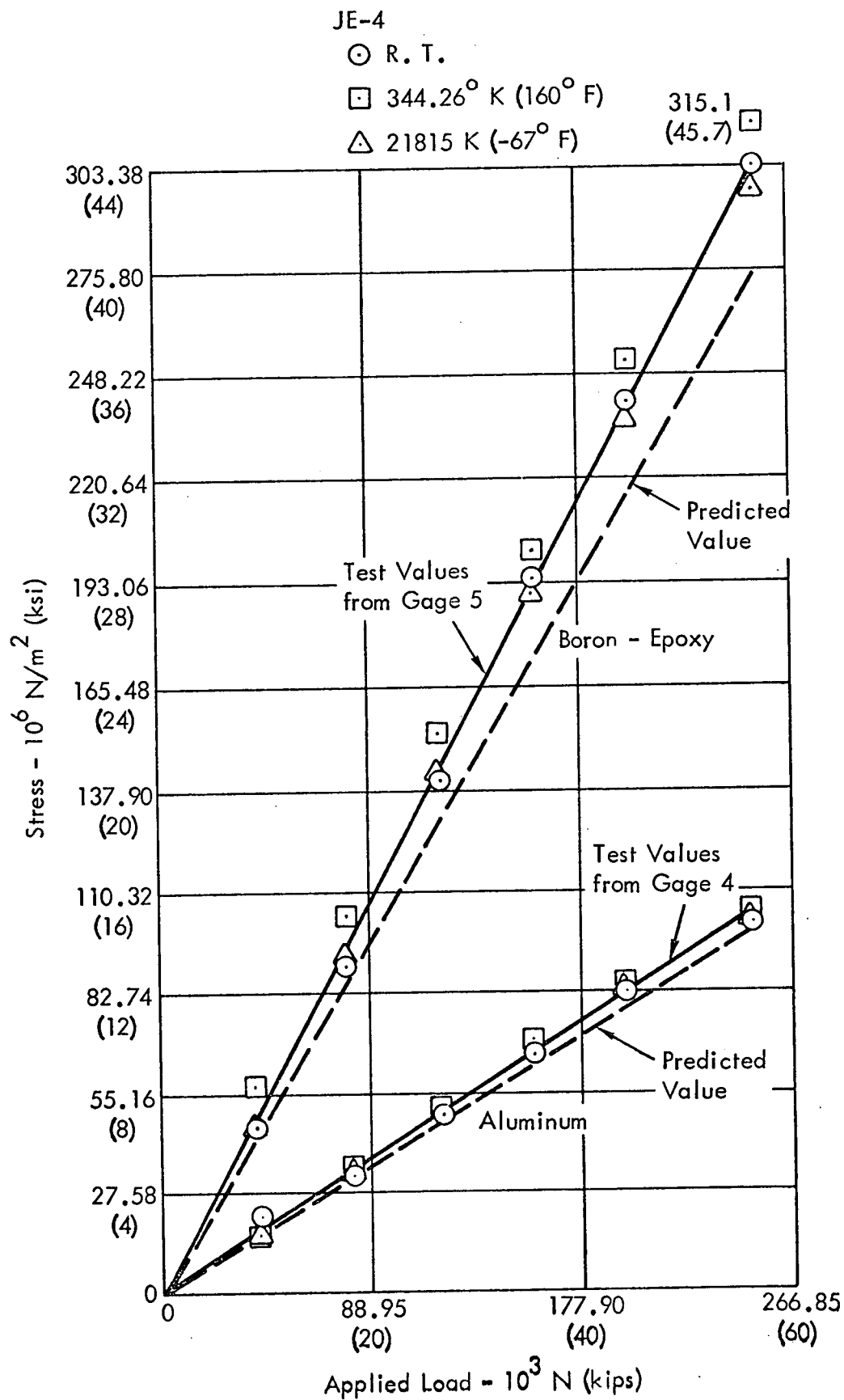


FIGURE 67.-ACTUAL STRESS VERSUS PREDICTED STRESS FOR JE-4

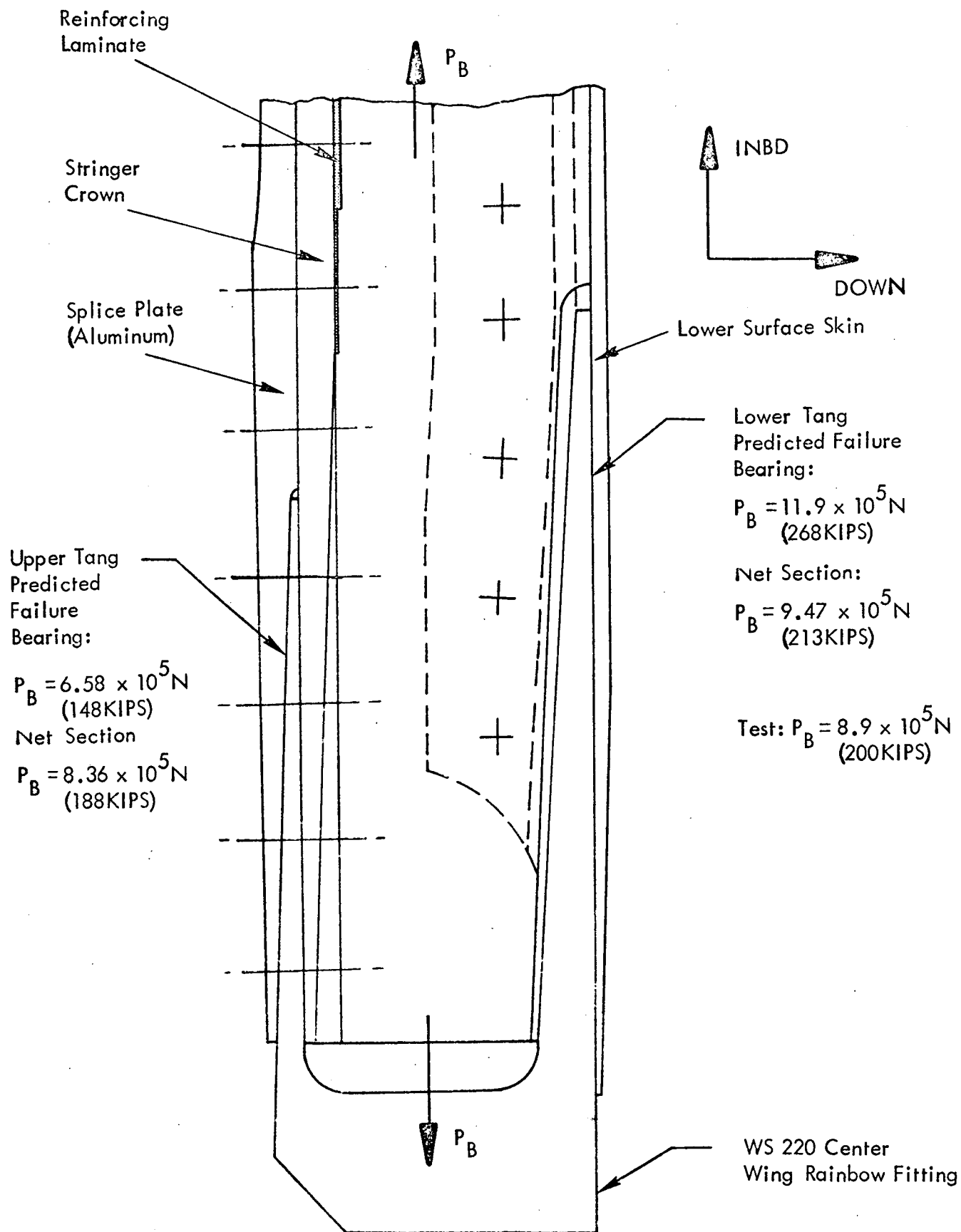


FIGURE 68. - PREDICTED FAILURE LOADS FOR STATIC TEST JE-1

The panel section had two integral stiffeners and was machined from an extrusion of 7075-T73511 aluminum alloy. Each skin laminate was two inches wide and contained 29 plies of unidirectional boron-epoxy oriented in the spanwise direction. The stringers were hat shaped and were machined from 7075-T6511 aluminum alloy extrusion. Each stringer laminate was 2.29 cm (0.9 inch) in width and contained 22 plies of unidirectional boron-epoxy material. Maximum deviation from flatness for the assembled specimen was 0.089 cm (0.035 inch). Finally, the specimen ends were machined flat and parallel. Measured length of the specimen was 121.7 cm (47.9 inches). A photograph of the specimen is shown in Figure 69.

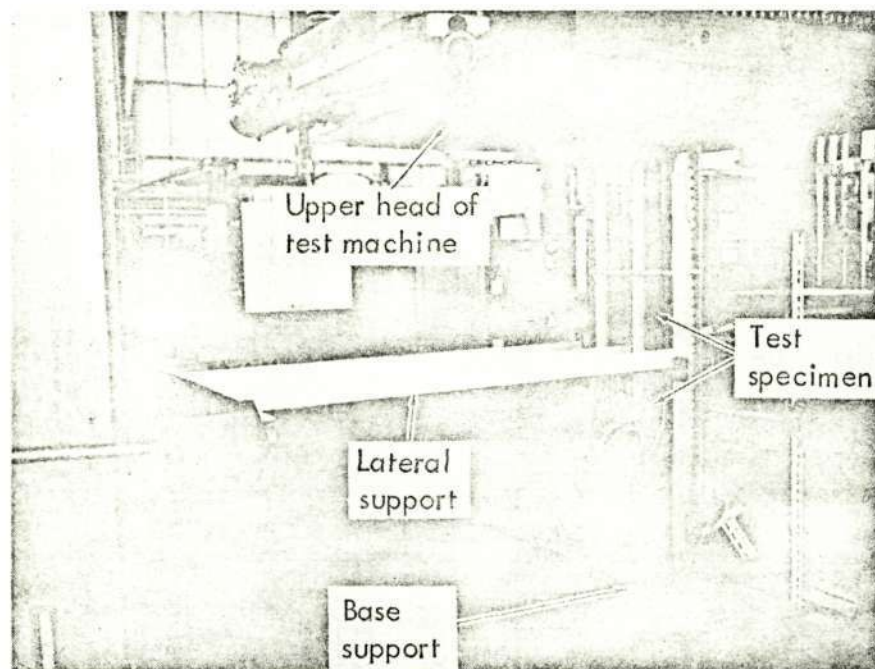


FIGURE 69.- 130-JE-2 SPECIMEN INSTALLED IN TEST MACHINE

9.2.2.2 JE-2 Tests

The 130-JE-2 specimen was instrumented with 38 electrical resistance-type strain gages to monitor specimen strain state during the test. Gages were located on the aluminum alloy elements as well as on the boron-epoxy laminates. Since the boron-epoxy laminates were inaccessible for gage installation after final assembly, gages located on the laminate surfaces were installed prior to completing the stringer to panel assemblies. Lead wires were attached to the gages and were then routed spanwise so that all leads extended from the same end. All gages were axial type and were aligned parallel to the spanwise direction.

This specimen was tested in the compression bay of a 5.34×10^6 N (1,200,000 pound) capacity Baldwin Universal Testing Machine. The general test arrangement was similar to that used for the panel buckling tests except that the specimen was laterally supported at the span center. To achieve this, two strips of aluminum 45.7 cm (18.0 in.) long by 2.54 cm (1.0 in.) wide by 0.64 cm (0.25 in.) thick, were positioned, one on each side of the specimen, such that the 2.54 cm (1.0 in.) wide surface was in contact with the specimen center and across its full width. Two pieces of "T" section steel 50.8 cm (20.0 in.) long by 6.35 cm (2.5 in.) flange by 0.64 cm (0.25 in.) thick, were placed on the aluminum strips with the flange of the "T" in contact with the other 2.54 cm (1.0 in.) wide surface of the strips. The pieces of steel were held in this position by four 0.79 cm (5/16 in.) diameter steel bolts, two located at each end as shown in Figure 70.

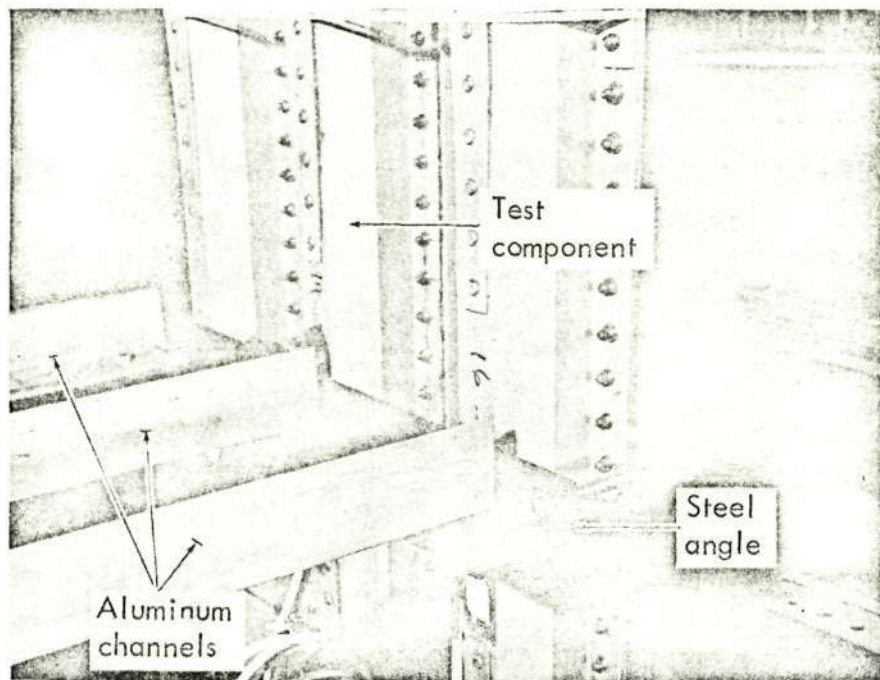


FIGURE 70.- 130-JE-2 TEST SUPPORT ARRANGEMENT

The ends of three aluminum angles, 121.9 cm (48.0 in.) long by 5.08 cm (2.0 in.) equal flanges by 0.54 cm (0.25 in.) thick, were then attached to the stem of the "T" on the stiffener side of the panel. The angles were spaced equally and each one was held in place by two, 0.54 cm (1/4 in.) diameter steel bolts. The other end of each angle was fastened to a rigid steel member on the column of the testing machine. The specimen was secured in the vertical position with the lateral supporting angles normal to the specimen length and width. Strain gage leads were connected to a B&F Model SY156 strain data acquisition system having 200 channel capacity and digital output at a print rate of up to 20 channels per second. Three dial gages were mounted on a portable frame and positioned to measure lateral deflection at the top, bottom, and center of the specimen. The test arrangement is shown in Figure 71.

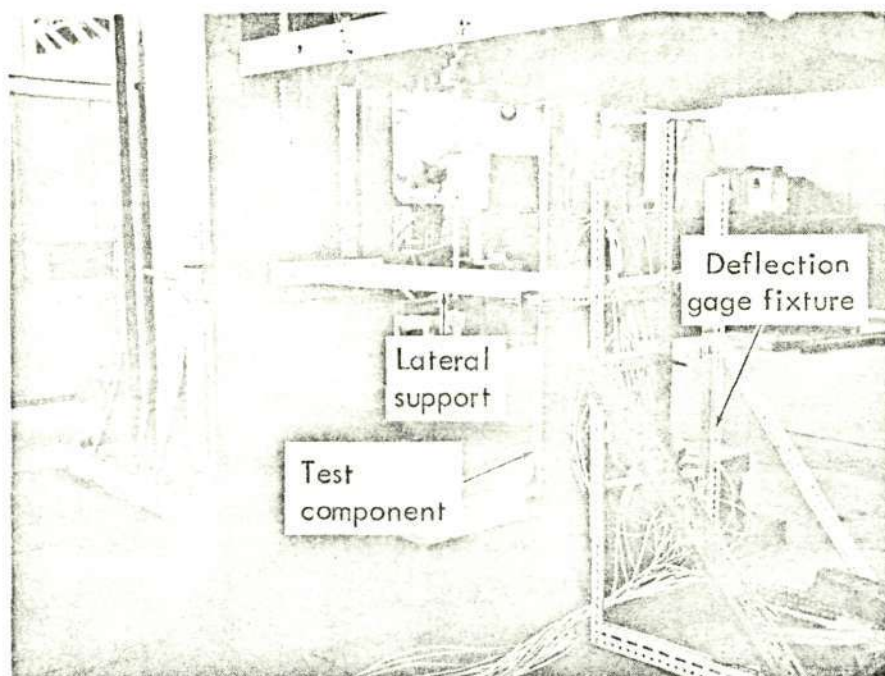


FIGURE 71.- 130-JE-2 TEST ARRANGEMENT

The 2.67×10^6 N (600,000 pound) load range was selected for this specimen. Initially, a small compressive load was applied and strain measurements were recorded. Based on these strains, alignment of loading was adjusted using the alignment mechanism which is an integral part of the testing machine compressive loading head. Strains were again measured and examined for uniformity. This process was repeated until acceptable uniformity in strain distribution was achieved. During this process, load magnitude was limited to approximately 30 percent of the predicted failing load. Dial gage readings were also recorded during the strain survey in order to assess the overall quality of the specimen supported arrangement. The lateral deflections were found to be within acceptable limits and therefore the dial gages were removed for the actual test. Load was applied to the specimen in 1.11×10^5 N (25,000 pound) increments up to 7.78×10^5 N (175,000 pounds) and each incremental load was held constant for a time sufficient to record strain data. The load was then reduced to 1.11×10^5 N (25,000 pounds) and strain data were again recorded. The load was subsequently increased to 6.67×10^5 N (150,000 pounds) and the strain data were compared with those obtained previously for the first application of this load level. Good correlation was obtained and the load was then increased in 1.11×10^5 N (25,000 pound) increments and strains recorded at each increment until failure occurred at 1.38×10^6 N (310,000 pounds). Failure was located in the skin adjacent to the edge of the rainbow fitting as shown in Figures 72, 73, and 74, and was in the all-metal section.

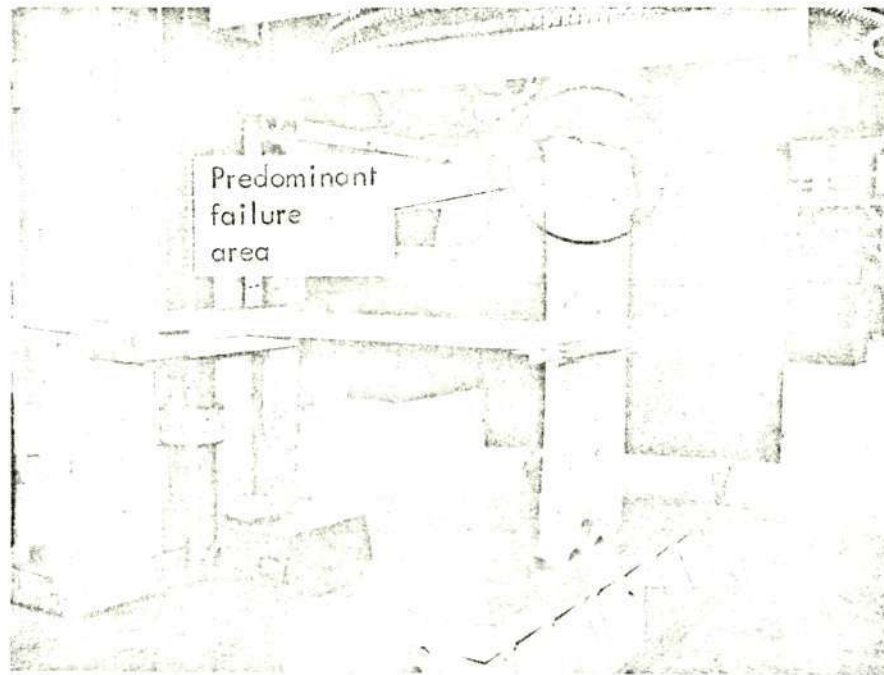


FIGURE 72.- COMPRESSIVE FAILURE OF 130-JE-2

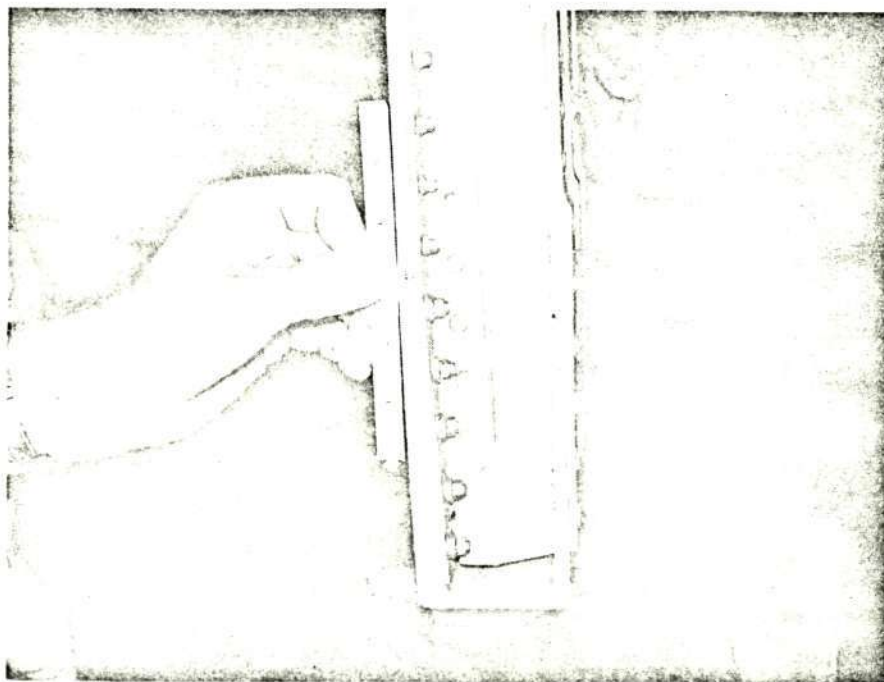


FIGURE 73.- FAILURE OF 130-JE-2 (OPPOSITE
PREDOMINANT END)

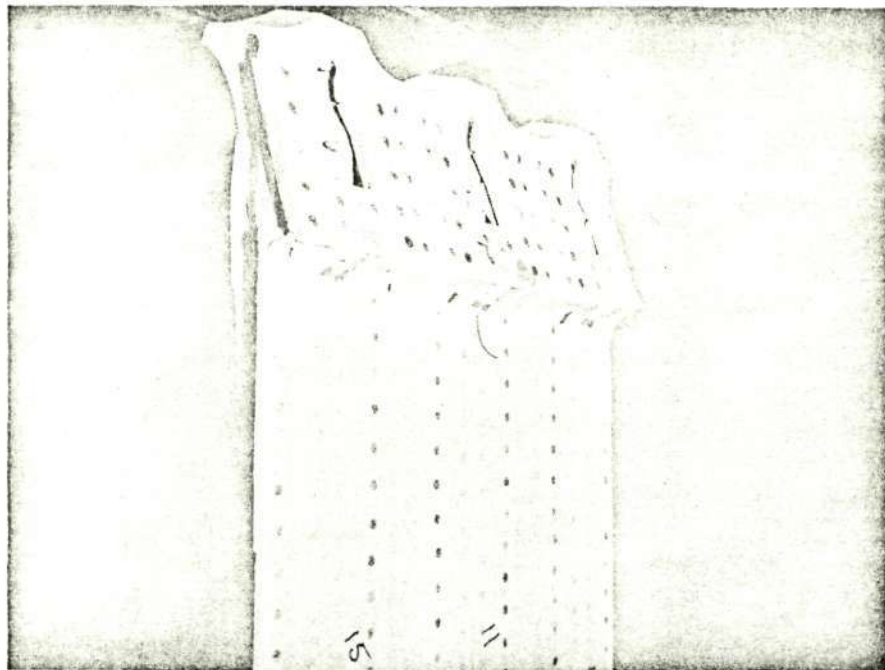


FIGURE 74.- FAILURE OF 130-JE-2 (PREDOMINANT END)

9.2.2.3 JE-2 Test Evaluation

This component failed in compression at a load of 1.38×10^6 N (310,000 lb.), exceeding both the aircraft ultimate load requirement of 1.10×10^6 N (247,000 lb.) and the predicted failure load of 1.19×10^6 N (267,000 lb.). Failure occurred in the skin element between the end of the Rainbow fitting and the beginning of the boron-epoxy laminate on the skin. The failure load corresponds to a calculated average cross-sectional strain of 4500 micro m/m (micro in./in.).

Non-linearity of measured strain readings occurred at approximately 51% of this value, and some permanent set was evident at limit load. Therefore, although aircraft ultimate load requirements were satisfied, a thicker skin may be required locally to eliminate yielding at limit load.

9.2.3 130-JE-3A Specimens

9.2.3.1 JE-3A Description

This is a set of four individual specimens for evaluating composite runouts. Each of the four specimens consists of a boron-epoxy laminate bonded to an aluminum plate 0.32 cm (0.125 in.) thick, 15.2 cm (6 in.) wide, and 10.2 cm (40 in.) long. The four laminates are attached to the aluminum plates differently. The (-1) and (-3) specimen laminates are 61 cm (24 in.) long, 5.08 cm (2 in.) wide and 24 plies thick, tapering at each end to four plies. The (-1) specimen laminate is bonded and fastened to the aluminum plate by 24 0.48 cm (3/16 in.) diameter Hi-lok fasteners at each end. Titanium shims are interleaved with the laminate at the ends to carry fastener loads. The (-3) specimen laminate is bonded to the aluminum plate and no fasteners or titanium shims are used. The (-5) is similar to the (-1) except that the shims are interleaved at different ply levels and the length of taper is reduced at each end from 22.5 cm (8.87 in.) to 13.6 cm (5.375 in.). The (-7) is similar to (-5) except that no fasteners or titanium shims are used. Figures 75 and 76 are views of the laminate and skin side of specimen (-1).

9.2.3.2 JE-3A Test and Evaluation

The static tensile test results of the JE-3A series of specimen tests are presented in Table XVII. These results show that early laminate disbond occurred in both specimens without fasteners and titanium shims. Laminate terminations which include both fasteners and titanium shims had disbond failures close to final failure loads and are therefore validated. These design concepts have been incorporated in the "JE" and "PF" series of component test specimens and are intended for incorporation into the Phase II structural design. Figures 77 and 78 show the (-5) specimen in the test machine.

The investigation of the boron-epoxy laminate and aluminum strain data obtained during the tests showed only minor differences in stress distribution between all specimens, indicating that, for the specimens tested, the transfer of load into the laminate was essentially independent of the number of laminate steps or the number of fasteners used. The photoelastic stress patterns obtained for each specimen showed the expected increase in stress concentration around the fastener holes and a similar increase at the beginning of each laminate assembly. Smaller increases were also evident at each laminate step. The fatigue component tests of the "JE" and "PF" series have shown, however, that these stress concentrations are not critical to the fatigue endurance requirements of the airplane. Figures 79 and 80 show the failure areas for each specimen.

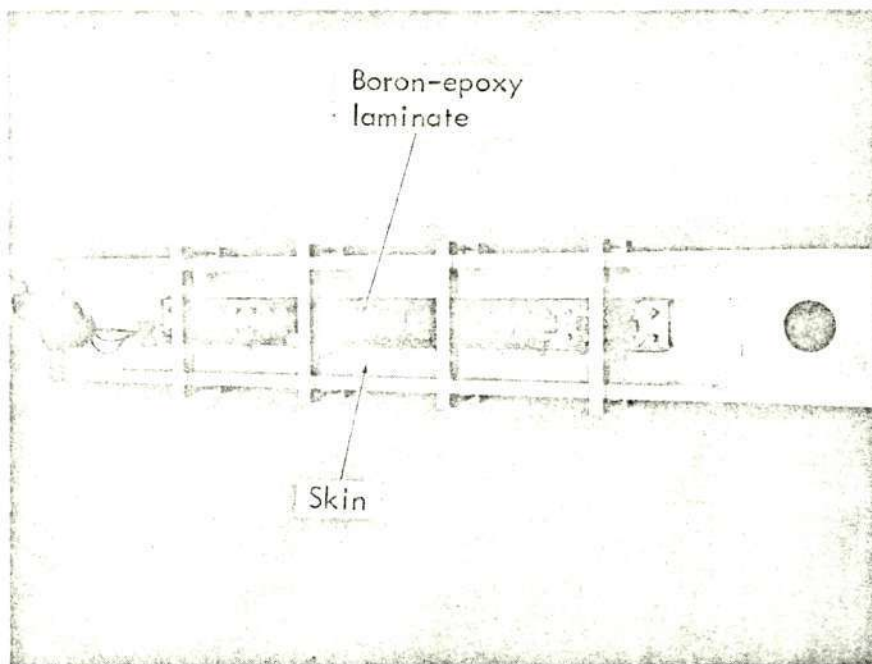


FIGURE 75.- LAMINATE SIDE OF JE 3A-1

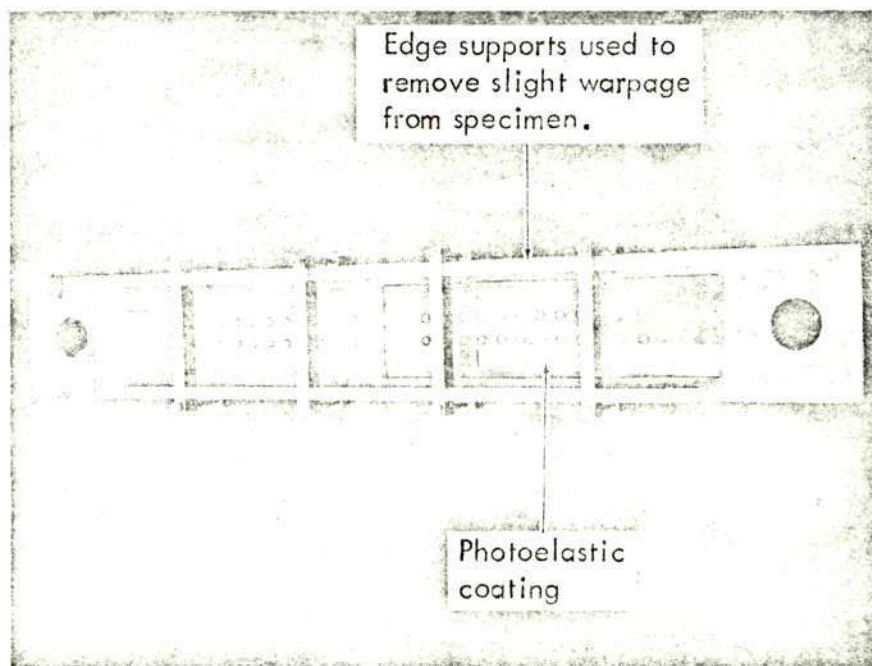



FIGURE 76.- SKIN SIDE OF JE 3A-1

TABLE XVII.-JE3A COMPONENT TEST SUMMARY

Component	Fasteners & Shims	Type Transition	Predicted  Failure Load		Failure Load		Disbond Load		Failure Description
			10 ⁵ N	(kips)	10 ⁵ N	(kips)	10 ⁵ N	(kips)	
JE3A-1	Yes	Long	2.49	(56.0)	2.40	(54.0)	2.31	(52.2)	Tension failure thru aluminum net section - delamination and failure of laminate at 3rd step.
JE3A-3	No	Long	2.67	(60.0)	2.74	(61.5)	1.74	(39.2)	Tension failure thru aluminum net section - delamination of laminate at 1st step.
JE3A-5	Yes	Short	2.49	(56.0)	2.45	(55.0)	2.45	(55.0)	Tension failure thru aluminum net section at end of laminate runout.
JE3A-7	No	Short	2.67	(60.0)	2.74	(61.7)	1.25	(28.0)	Tension failure thru aluminum net section - disbond and delamination of laminate at 1st step.

 Based on ultimate tensile stress and net section after disbond.

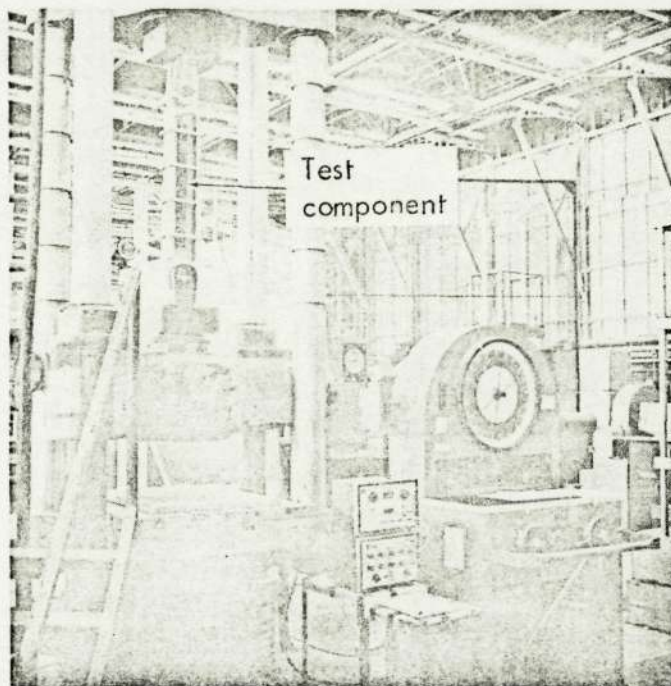


FIGURE 77.- SPECIMEN JE 3A-5 INSTALLED IN TEST MACHINE (OVERALL VIEW)

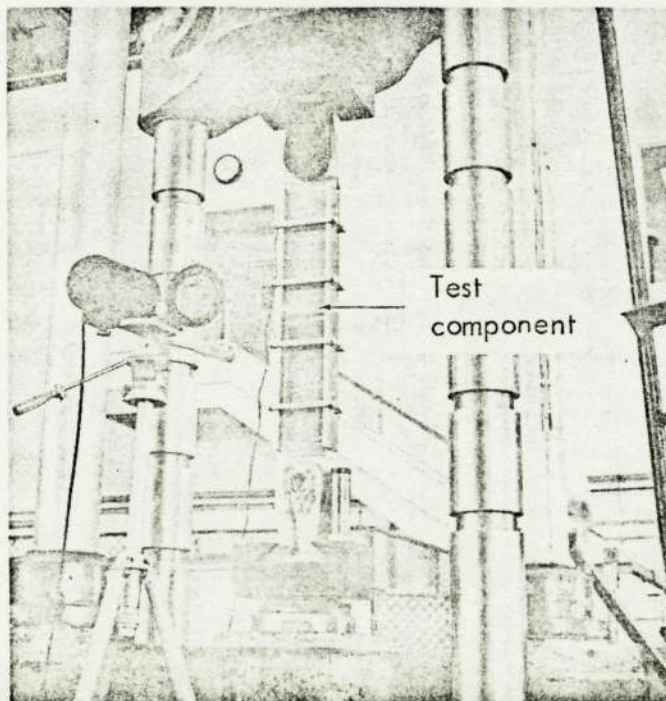
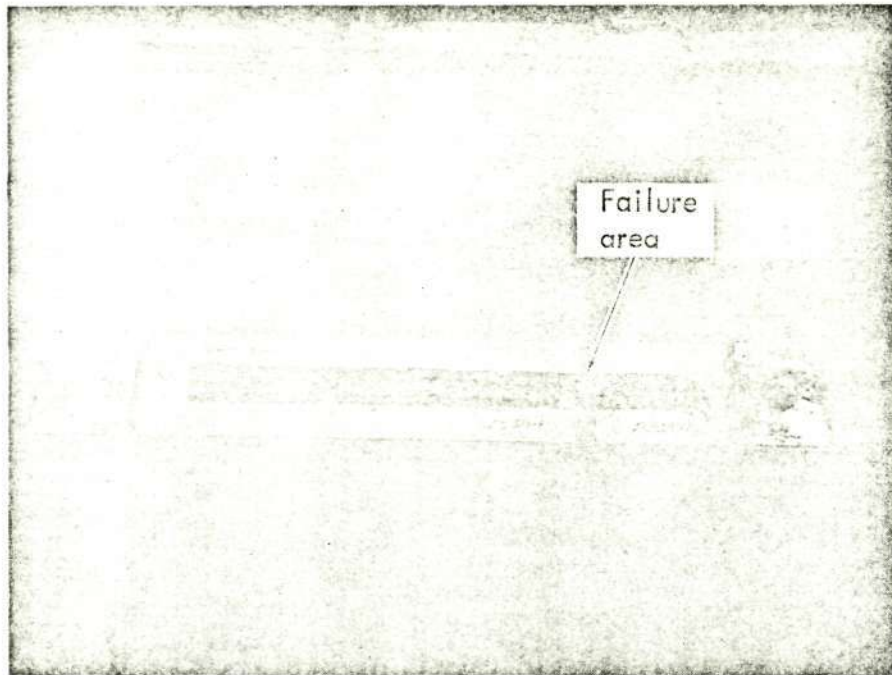
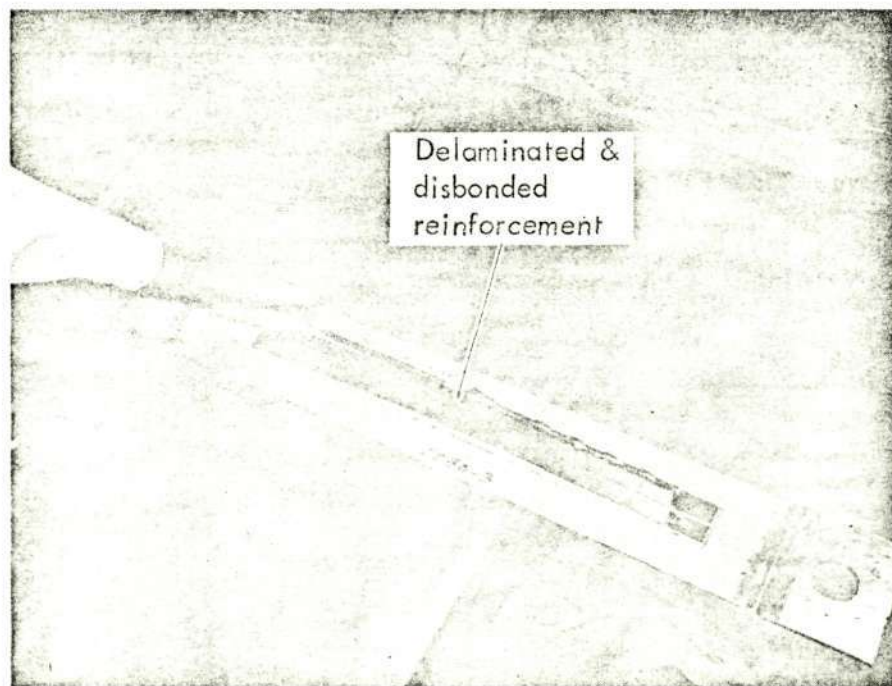


FIGURE 78.- SPECIMEN JE 3A-5 INSTALLED IN TEST MACHINE (CLOSE UP VIEW)



(a) Specimen JE 3A-1

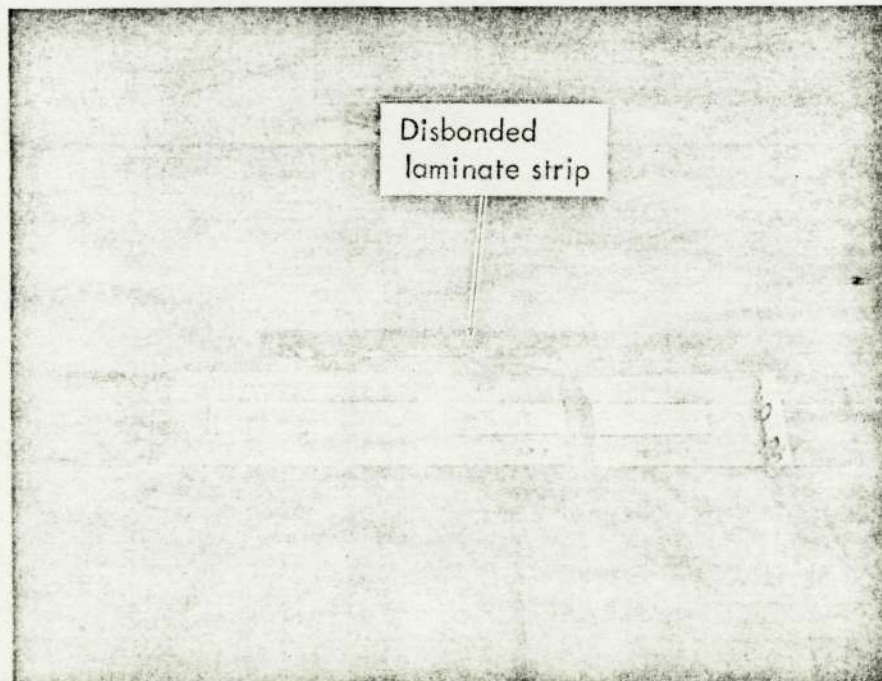


(b) Specimen JE 3A-3

FIGURE 79.- TEST SPECIMENS JE 3A-1 AND JE 3A-3
FAILURE



(a) Specimen JE 3A-5



(b) Specimen JE 3A-7

FIGURE 80.- TEST SPECIMEN JE 3A-5 AND JE 3A-7
FAILURE

9.3 PANEL FATIGUE COMPONENTS

Current military requirements for fatigue tests specify a scatter factor of four when a full-scale test is performed. When components of the full part are fatigue tested, an additional scatter factor is used to account for the inability to fully simulate the full-scale test set-up, the internal load distribution, and boundary conditions. The current C-130 B/E test spectrum is slightly more damaging for the lower surface than the "E-TAC"¹ spectrum employed in testing the boron-epoxy reinforced panels; damage for the upper surface remains the same. Because of this slight increase in fatigue damage, the lower surface panels were tested to eight lifetimes (80,000 simulated flight hours). Upper surface panels were tested to six lifetimes; the full-scale wing box will be tested to four lifetimes.

The 130-PF-1 test specimen was tested in the 6.67×10^6 N (1,500,000 pound) capacity, servo-controlled, fatigue test machine. Specimens PF-2 and PF-3 utilized the 1.78×10^6 N (400,000 pound) and 1.6×10^6 N (360,000 pound) capacity, servo-controlled, fatigue test machines, respectively. End fittings were bonded and bolted to the specimens to provide a smooth transition of load from the test machine to the specimen. To stabilize the test specimens under compressive loading, lateral support was provided by simulated rib structure located at rib stations on the specimen.

The loads applied to the three test specimens were identical to those applied to the specimens tested for the Model C-130 B/E aircraft, and corresponded to the "E-TAC" loading spectrum. Loads involving both ground and flight conditions with their respective mission configurations were grouped and subdivided with respect to mean and cyclic stresses.

Approximately forty electrical-resistance strain gages were installed on each specimen and connected to the calibrated millisec recording system, so that data printouts and scanning could be carried out. During the strain surveys calibrated strain indicators were used in conjunction with calibrated load cells to measure the applied load.

During the fatigue tests, load was applied to the specimens under the control of an AVCO load programmer, consisting of a "PDP" 8/L computer, function generator, amplifiers and a teletypewriter. A Beckman pen recorder was used to provide a near continuous record of the output of two specimen strain gages.

An inspector was present during the fatigue tests to monitor the nondestructive test equipment during the cycle and to conduct special tests at the end of each cycle corresponding to 1000 flight hours. Eddy current and zygo techniques were employed where confirmation of suspected damage was required. Ultrasonic inspections of the boron-epoxy laminate to aluminum bonds were conducted at intervals corresponding to approximately 1000 flight hours. Considerable care had to be taken when carrying out these ultrasonic checks since surface irregularities and machine marks can produce a signal similar to that produced from a disbond area.

¹ C-130E Tactical Air Command load spectrum 2; this spectrum was used for the C-130E fatigue test, and was applied to the C-130 B/E upper and lower surface component panels. In order to allow a direct comparison it was also applied to the NAS1-11100 component panels.

9.3.1 130-PF-1 Specimen

9.3.1.1 PF-1 Description

This specimen was symmetrical about its chordwise centerline and was two wing panels wide. Boron-epoxy composite laminates were bonded to the skins and stringers for their entire lengths. Fasteners were used at the ends of the bonded areas. The access door from a previous series of C-130 B/E tests was used with this specimen. The PF-1 specimen is shown in Figure 81.

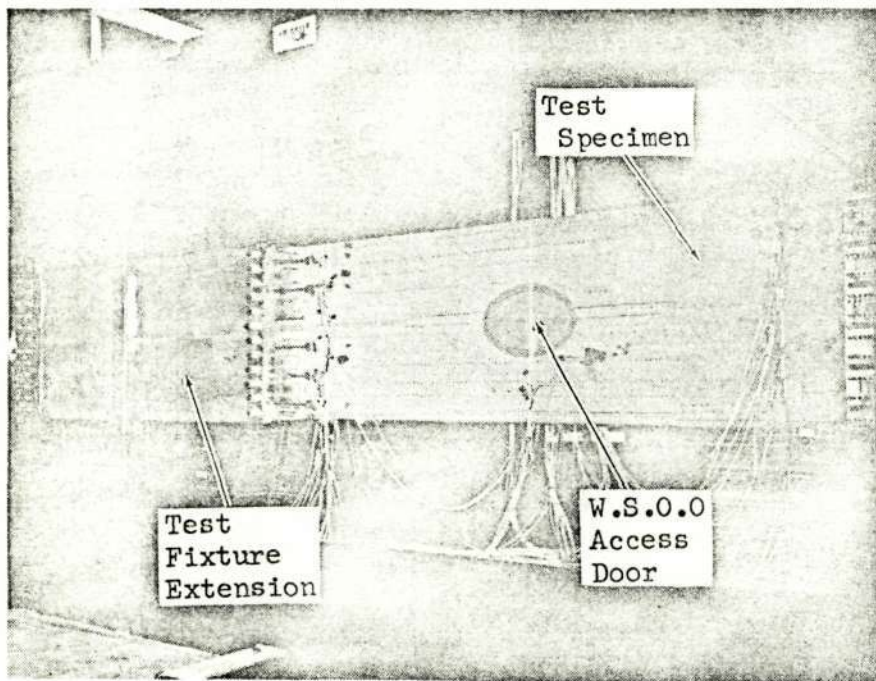
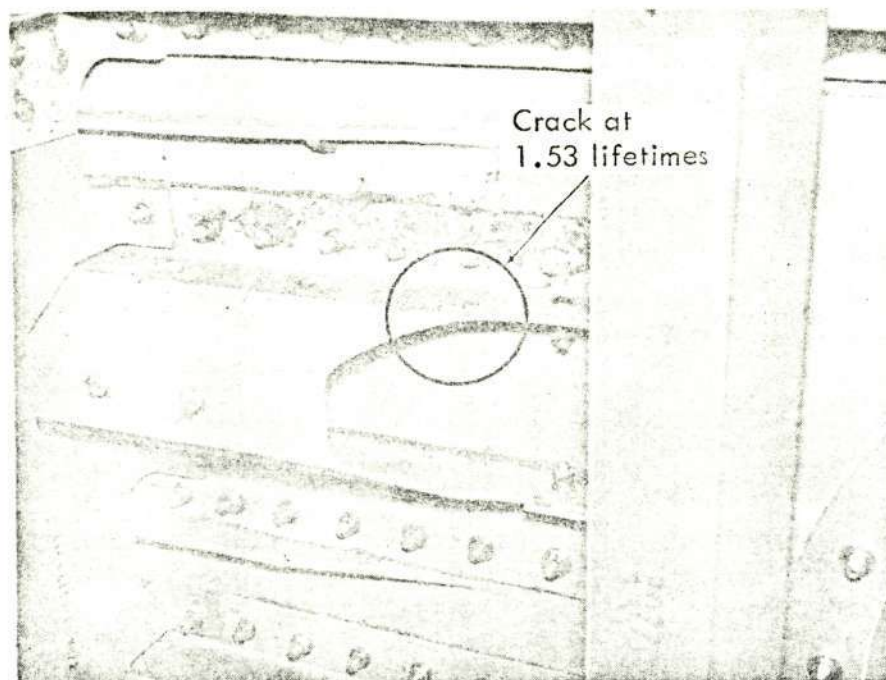


FIGURE 81.- PF-1 INSTALLED IN TEST MACHINE

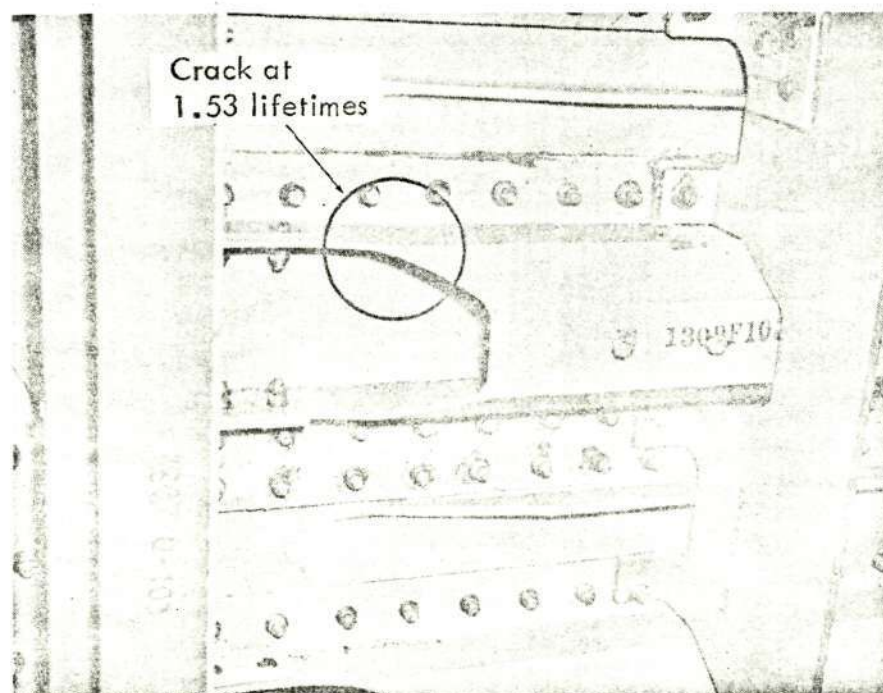
9.3.1.2 PF-1 Tests

When 1.53 simulated lifetimes were complete on the fatigue test specimen, two cracks were found on stringer No. 3. These were on opposite sides of the access door and are illustrated in Figure 82. The cracks were stop-drilled and a repair strap added at each position as shown in Figure 83. Testing was continued until 2.49 lifetimes were reached, when the crack on the left hand side extended past the stop-drilled hole and proceeded into the leg of the stringer. The original repair strap was removed and a repair angle incorporated.

With 5.60 lifetimes completed, further stop-drilling was required when the right hand side crack extended past the original hole. At 5.80 lifetimes a new crack from a fastener in the left hand side stringer runout repair was stop-drilled.

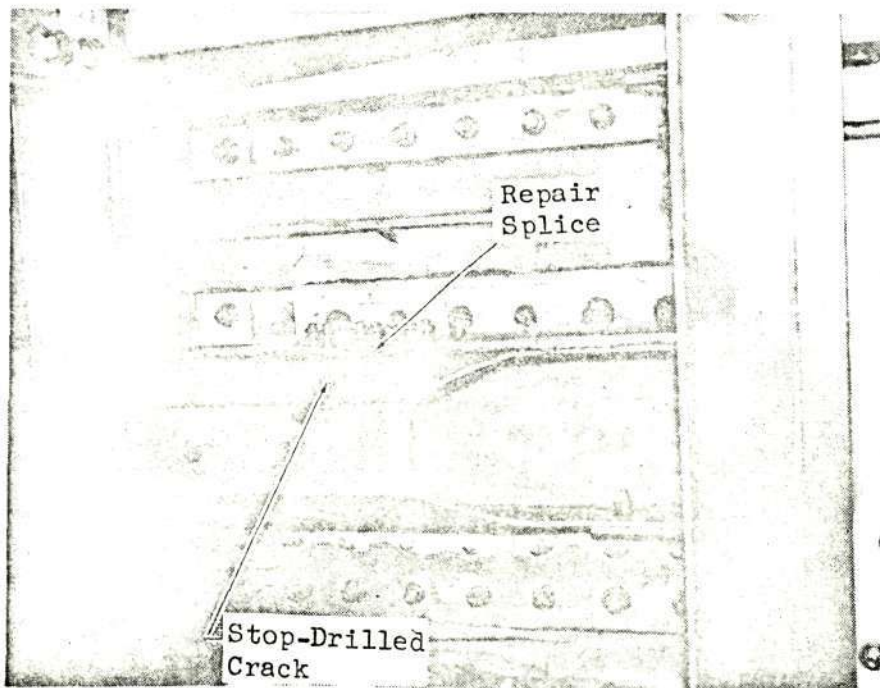


View of Damage at Stringer 3 Run-Out. Specimen 130-PF-1
(Left Side of Door)

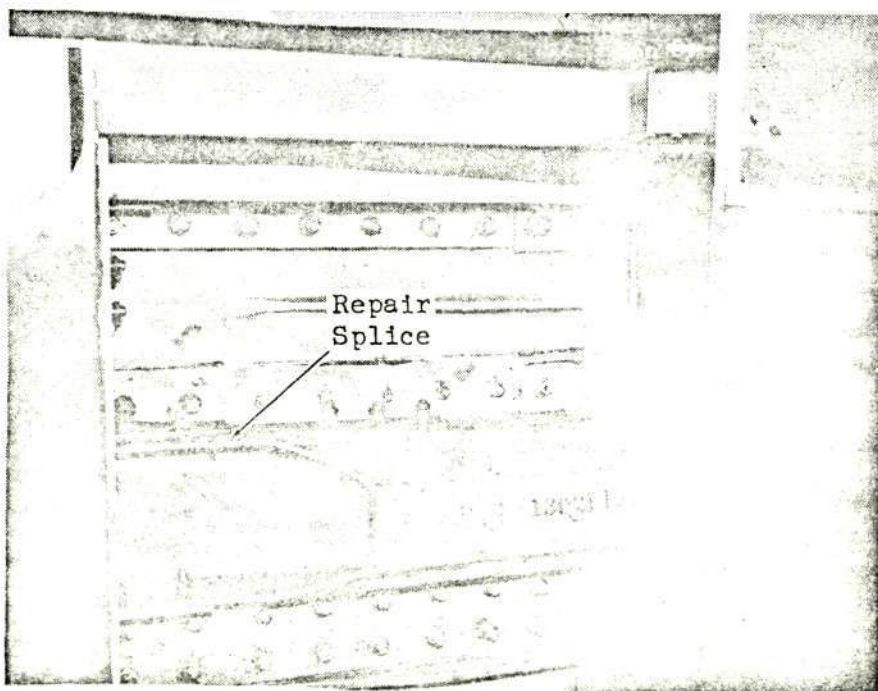


Damage at Stringer 3 Run-Out. Specimen 130-PF-1
(Right Side of Door)

FIGURE 82.- PF-1 FATIGUE DAMAGE



View of Final Repair at Stringer 3 Run-Out.
Specimen 130-PF-1 (Left Side of Door)



View of Repair at Stringer 3 Run-Out
Specimen 130-PF-1 (Right Side of Door)

FIGURE 83.- PF-1 FATIGUE DAMAGE REPAIR

Six lifetimes were completed with no further damage occurring and the specimen was then statically loaded in tension to $3.16 \times 10^6 \text{N}$ (710,000 pounds) with no further damage occurring. During this residual test, strain gages were monitored to ensure good alignment.

9.3.1.3 PF-1 Test Evaluation

Component panel PF-1 was fatigue tested to 60,000 simulated flight hours with no major failure. Fatigue cracks which occurred in the metal are categorized as "nuisance failures" and are considered minor. The quality level associated with the crack in the stringer 3 run-out was computed to be greater than 12.0.

The maximum strain recorded on specimen PF-1 during fatigue cycling occurred on the edge of the access hole (gage 41); the corresponding stress was $125 \times 10^6 \text{N/m}^2$ (18,200 psi) for an applied maximum tension load of $1.08 \times 10^6 \text{N}$ (243,700 lb.). The maximum stress calculated for the gross area was $69.6 \times 10^6 \text{N/m}^2$ (10,100 psi) for the same applied load. Strain gage 5, located on the skin, indicated a maximum gross area stress of $78.6 \times 10^6 \text{N/m}^2$ (11,400 psi). Similarly, at the same location but on the boron-epoxy laminate, strain gage 6 indicated a stress of $232 \times 10^6 \text{N/m}^2$ (33,600 psi). These values are based on strain due to applied loads and do not include thermally induced strains due to bonding.

After completion of fatigue testing to 60,000 simulated flight hours, component panel PF-1 was tested statically to determine its residual tensile strength. Design ultimate load for this panel was $2.94 \times 10^6 \text{N}$ (660 kips), and, unless unknown fatigue damage had occurred the residual strength would be at least this high. The panel was actually loaded to $3.16 \times 10^6 \text{N}$ (710 kips), which was the maximum load available from the test machine. Since no failures occurred and this was 162 percent of design limit load, the test was discontinued. Stresses derived from two of the strain gages are plotted in Figure 84, where good linearity may be seen.

9.3.2 130-PF-2 Specimen

9.3.2.1 PF-2 Description

This specimen consisted of two center wing panels and a representative outer wing panel and was symmetrical about its spanwise centerline. The boron-epoxy laminate was added in an identical manner to that used for the PF-1 specimen. Dihedral was omitted from the 220 joint for this specimen. The access door from an earlier C-130B/E specimen was used for this test.

Views of the skin and stringer sides of PF-2 are shown in Figure 85.

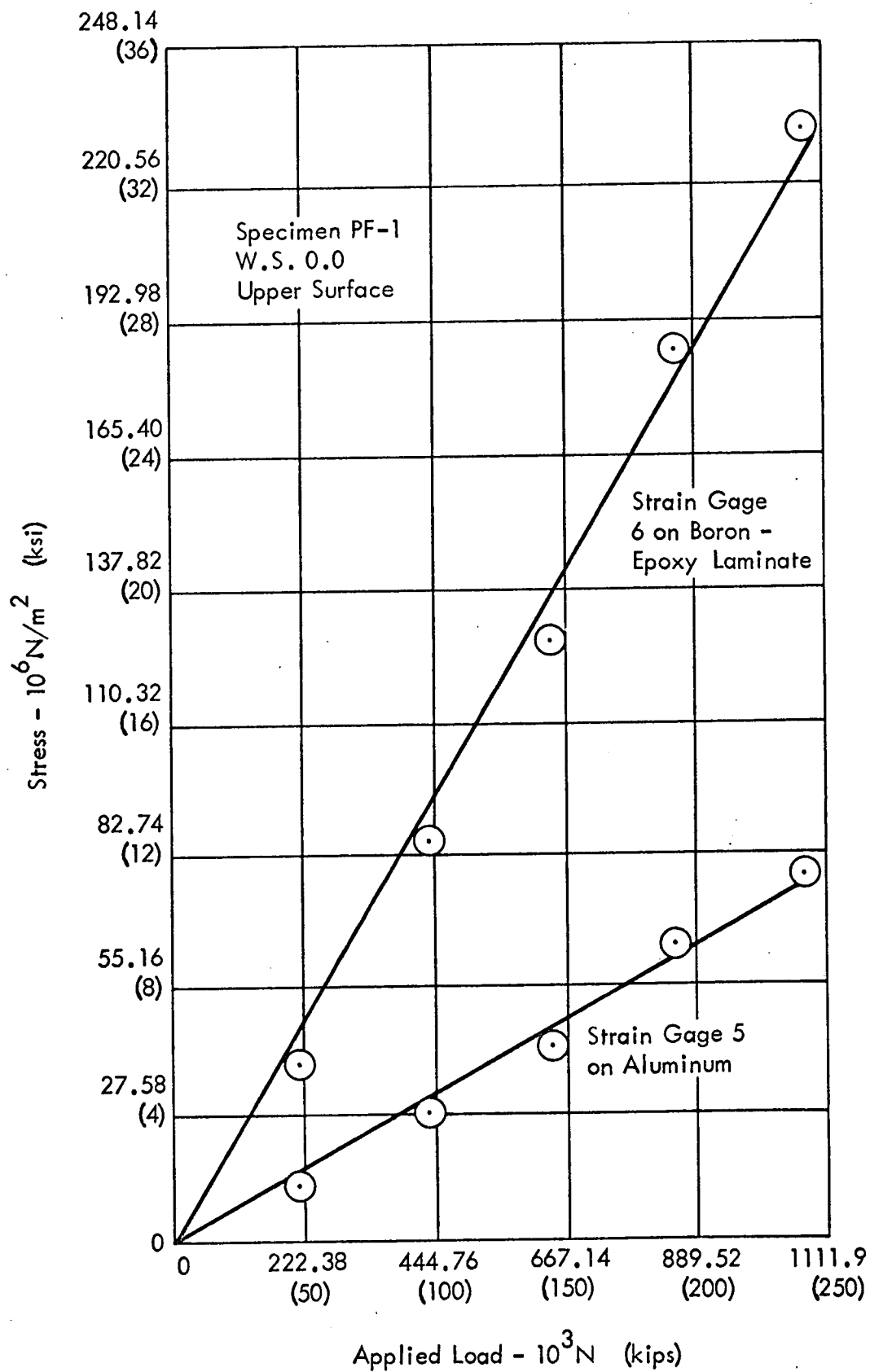
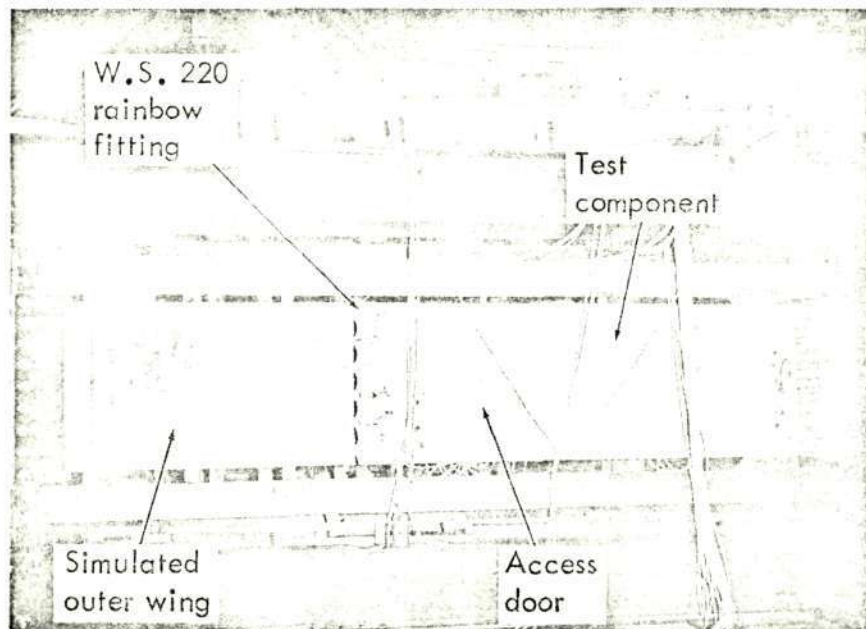
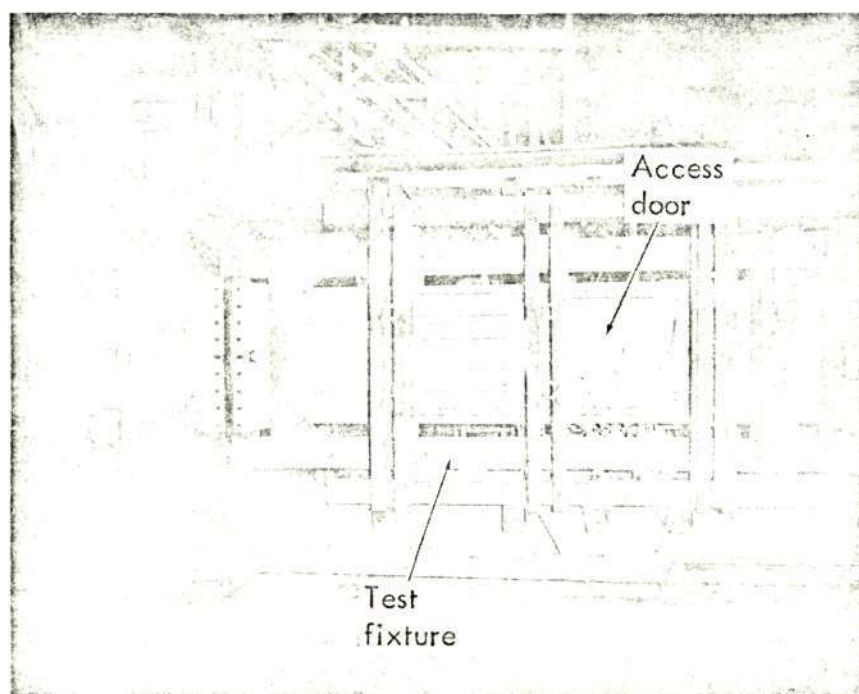


FIGURE 84. - STRESS VERSUS APPLIED LOAD FOR PF-1



Installation of Specimen 130-PF-2 in the 400K Test Machine



Reverse Side of Specimen 130-PF-2

FIGURE 85.- 130-PF-2 INSTALLED IN THE TEST MACHINE

9.3.2.2 PF-2 Tests

PF-2 was tested until 5.78 lifetimes were reached. At this point, stringer 6 at W.S. 210 was found to be cracked, as shown in Figure 86, and a repair was made (Figure 87). Eight strain gages were added around this region and outputs were recorded during a static application of limit tensile load, 9.16×10^5 N (206,000 lbs.), after which fatigue cycling was continued. With 6.11 lifetimes complete, the strap at stringer 6 position was found to be cracked. This was not considered important and cycling continued. Additional small local cracks were discovered at 6.76 lifetimes in the reinforcing structure at W.S. 212 at stringer 5, but cycling was continued until eight lifetimes were completed, at which time the test was discontinued.

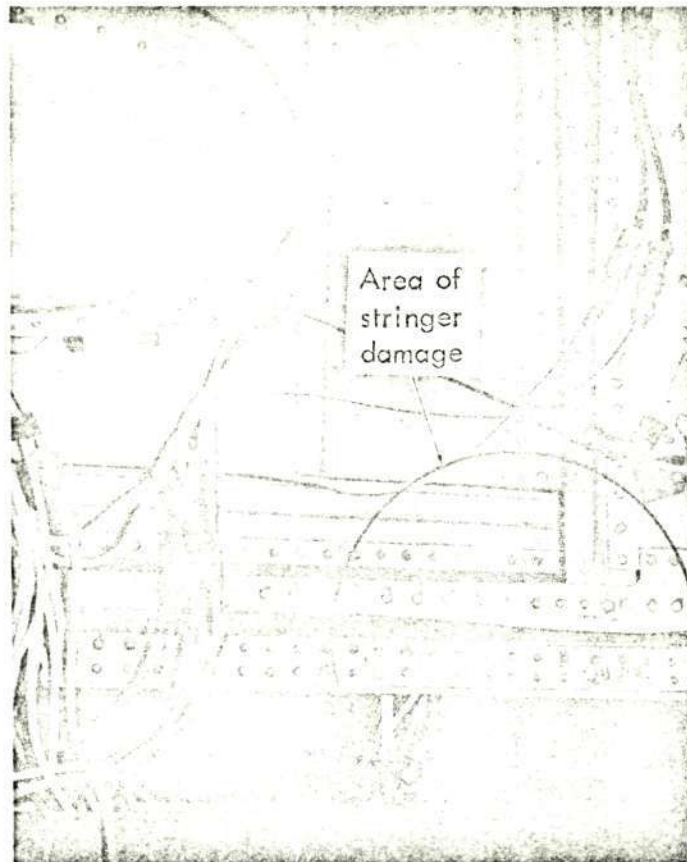
9.3.2.3 PF-2 Test Evaluation

Component panel PF-2 was fatigue tested to 58,000 simulated flight hours when stringer six failed at W.S. 209. The crack initiated at a fastener hole under the boron-epoxy laminate in the runout area. The adhesive bonding of the boron-epoxy to the aluminum in this area had been repaired during manufacture. The demonstrated quality level was computed to be greater than 12.0.

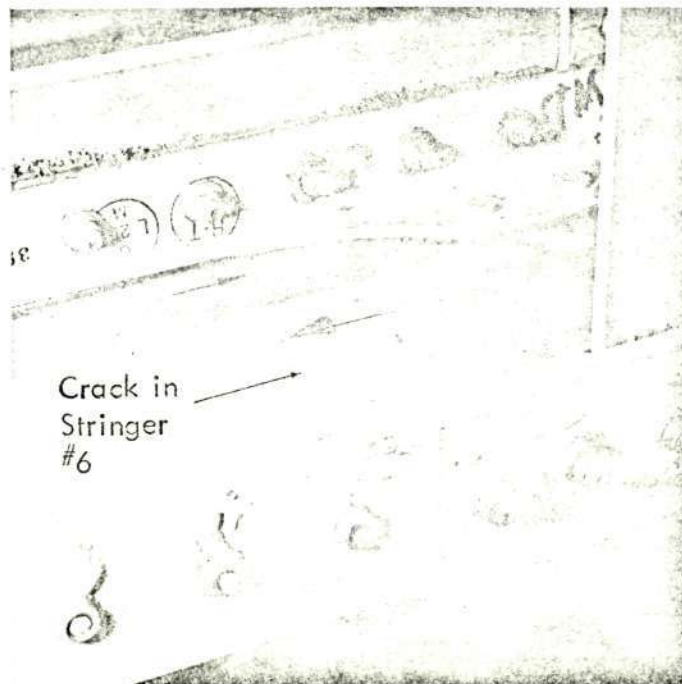
The maximum recorded stress for an applied load of 7.0×10^5 N (157,300 lb.) was 1.41×10^8 N/m² (20,400 psi), and occurred on the edge of the access hole. The maximum gross area stress occurred at gage 36 located on the skin, where the stress recorded for an applied load of 7.0×10^5 N (157,300 lbs.) was 6.18×10^7 N/m² (8,900 psi). The maximum calculated stress at this location was 6.1×10^7 N/m² (8,850 psi). Similarly, at the same location but on the boron-epoxy laminate the maximum recorded stress was 1.85×10^8 N/m² (26,820 psi). The calculated stress was 1.83×10^8 N/m² (26,600 psi). These experimentally derived stresses are plotted in Figure 88.

After additional strain gages were added to the skin and straps in the area around the cracked stringer the component panel was subjected to limit load. The panel sustained limit load without catastrophic failure and with no apparent extension of the crack in the stringer into the skin and straps attached to the stringer.

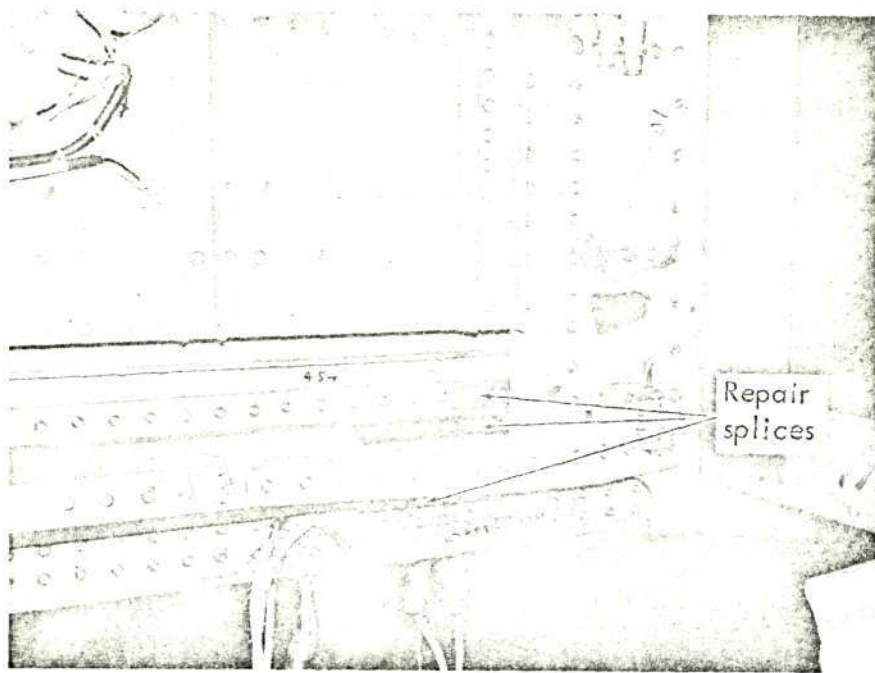
With the exception of two "nuisance" cracks on attaching strap and angle, the panel was successfully tested to 80,000 simulated flight hours. Since the component had been tested to limit load without failure and had subsequently successfully withstood two more lifetimes of fatigue cycling, the test was discontinued.



General View of Damage to Stringer 6



Detail View of Upper Crack in Stringer 6
FIGURE 86.- FATIGUE CRACK IN PF-2



Repair to PF-2

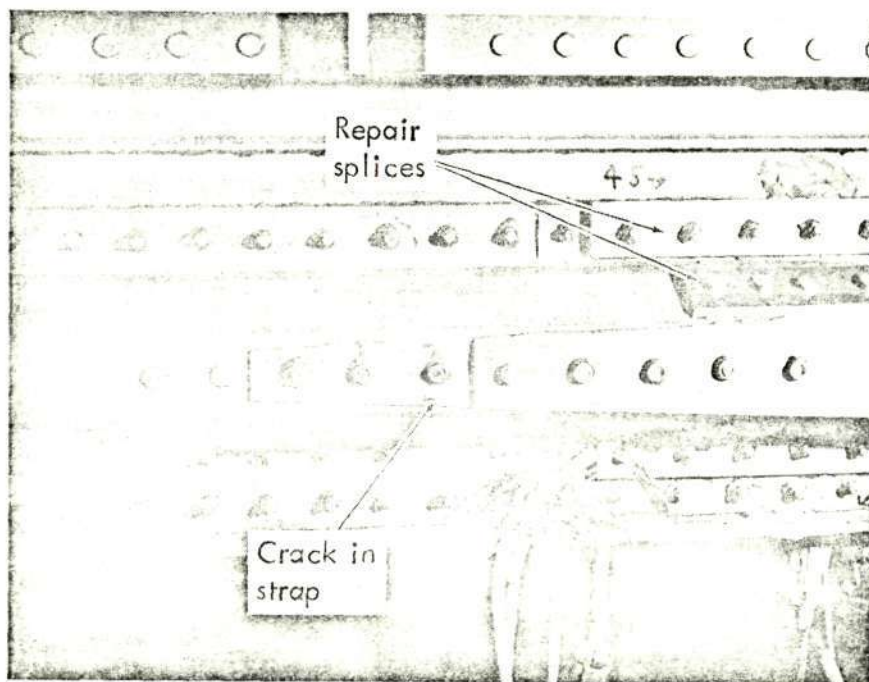


FIGURE 87.- DAMAGE TO PF-2 REPAIR STRAP AT 6.11 LIFETIMES

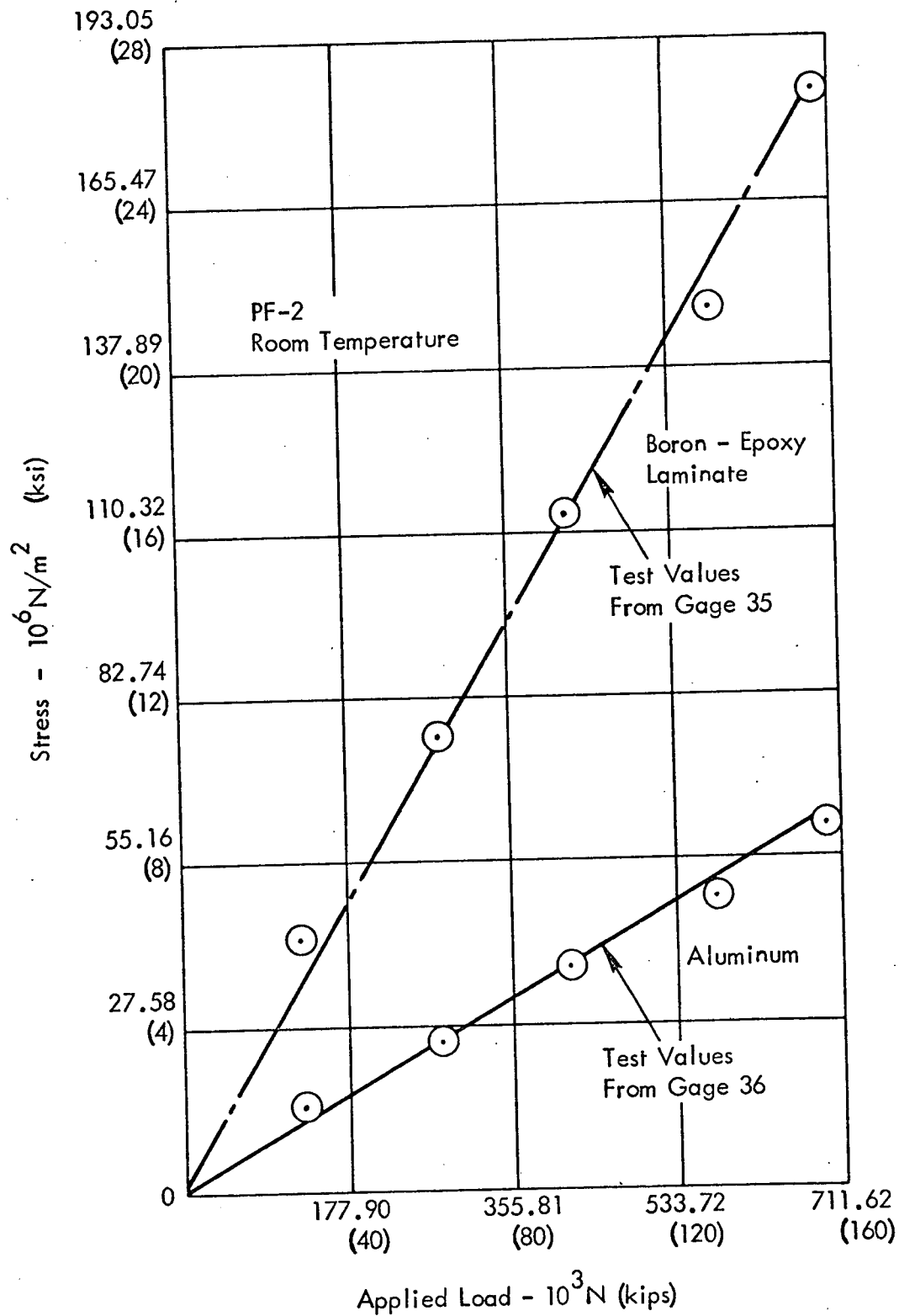


FIGURE 88. - APPLIED LOAD VERSUS STRESS VALUES FOR PF-2

9.3.3 130-PF-3 Specimen

9.3.3.1 PF-3 Description

This specimen consisted of a three-stiffener wide section of the lower surface. A representative outer wing section was attached at the W.S. 220 joint and was symmetrical about its spanwise centerline. Reinforcing boron-epoxy was added to this specimen in a similar manner to the previous two specimens described. Dihedral was omitted from the W.S. 220 joint region.

Two views of PF-3 installed in the test machine are shown in Figure 89.

9.3.3.2 PF-3 Tests

Eight simulated lifetimes of loading were applied with no fatigue damage being discovered. A tensile-test static load was then applied, failing the specimen in the Rainbow fitting as shown in Figure 90. The load at failure was 8.87×10^5 N (199,227 lbs.), 138 percent of design limit load.

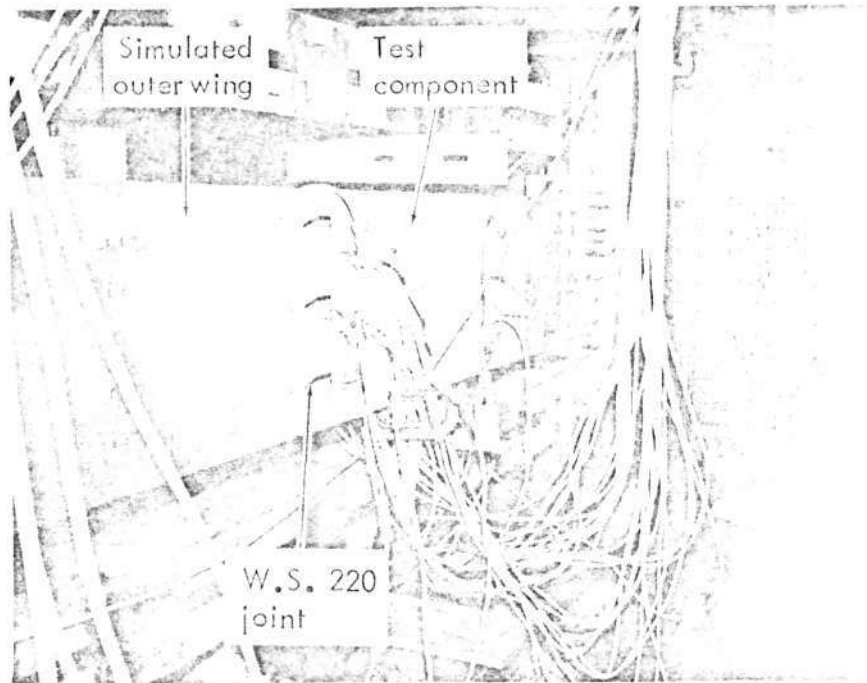
9.3.3.3 PF-3 Test Evaluation

Component panel PF-3 was successfully fatigue tested to 80,000 simulated flight hours. Preliminary inspection of the panel upon completion of fatigue testing revealed no apparent cracks. (However, in the subsequent residual strength test fatigue damage was detected in the fracture face of the rainbow fitting.) The corresponding quality level was computed to be 9.74. The fatigue performance of PF-3 compares favorably with the corresponding all-aluminum B/E component panel; it was also tested eight lives with no resultant visual cracks.

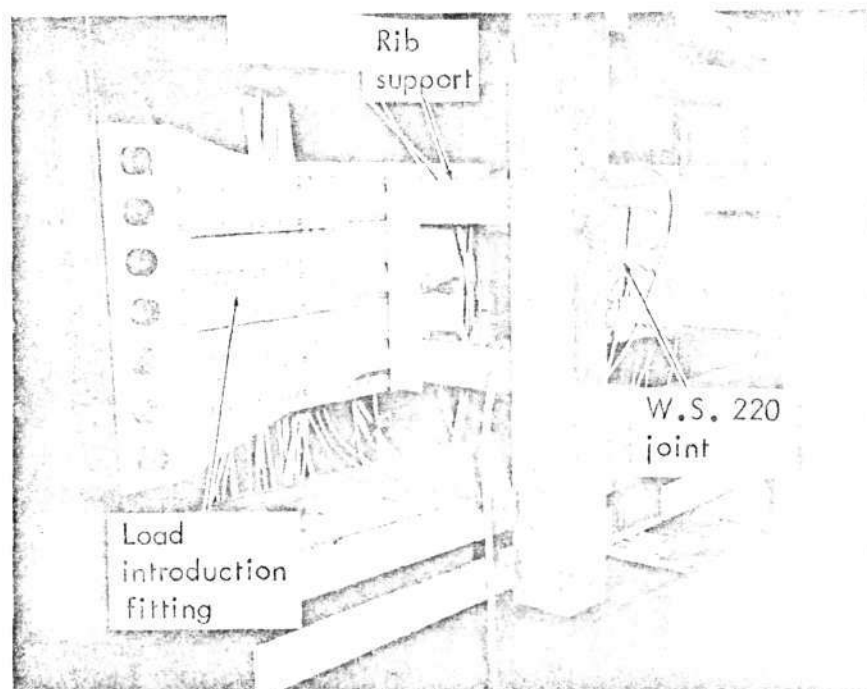
The maximum strain recorded on specimen PF-3, during the fatigue test, occurred on the exterior aluminum surface of a near-edge stringer at the mid-section of the panel (gage 14). The stress recorded for an applied load of 3.47×10^5 N (78,000 lbs.) was 9.27×10^7 N/m² (13,440 psi). The maximum calculated gross stress at this section for the same load is 10.6×10^7 N/m² (15,430 psi).

Similarly, at the same location (gage 13) but on the boron-epoxy laminate, the recorded stress was 2.67×10^8 N/m² (38,800 psi). The maximum calculated gross stress at this location for the boron is 2.60×10^8 N/m² (37,750 psi). These stress values were derived from strain gages 13 and 14 and are plotted in Figure 91. These values are based on strain due to applied loads and do not include thermally induced strains.

After successful completion of fatigue testing to 80,000 simulated flight hours, component panel PF-3 was tested statically to determine its residual tensile strength. Failure occurred in the metal in the rainbow fitting to stringer joint area at a load of 8.86×10^5 N (199,227 lbs.). This load is equivalent to 138 percent limit design load.

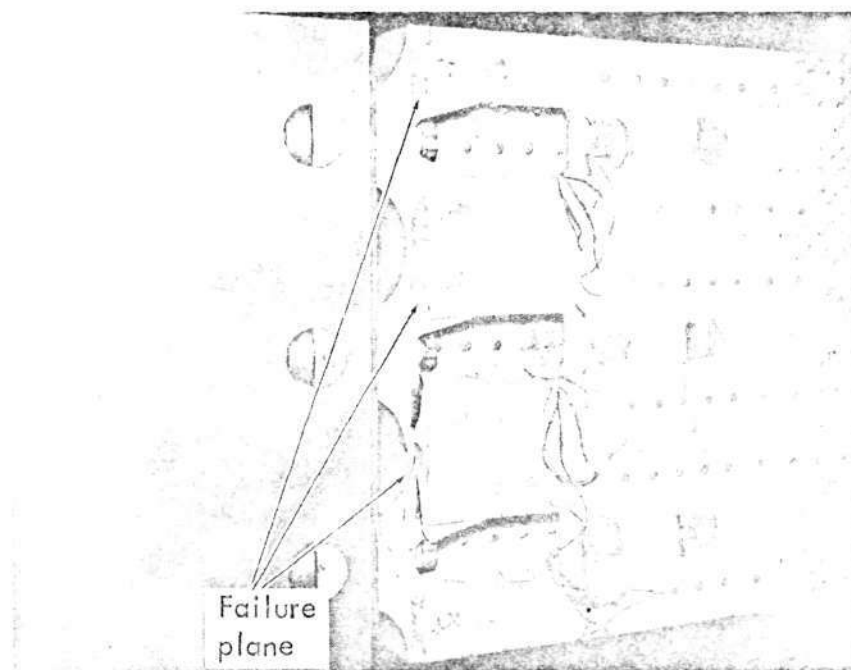


Installation of Specimen 130-PF-3 in the Test Machine

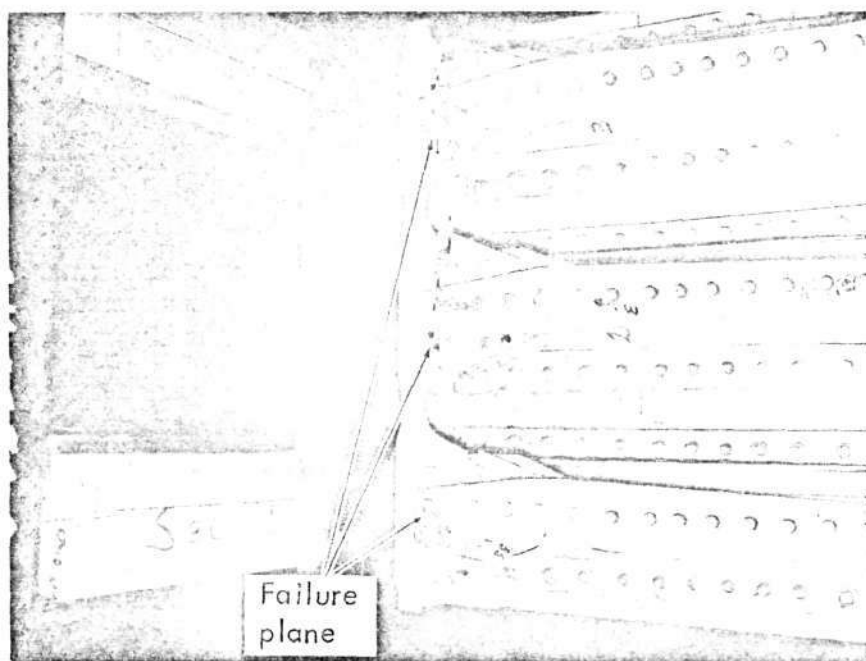


Stringer Side of Specimen 130-PF-3

FIGURE 89.- 130-PF-3 INSTALLED IN TEST MACHINE



View of Failure of 130-PF-3



Reverse Side of Failure to PF-3

FIGURE 90.- RESIDUAL STRENGTH FAILURE OF PF-3

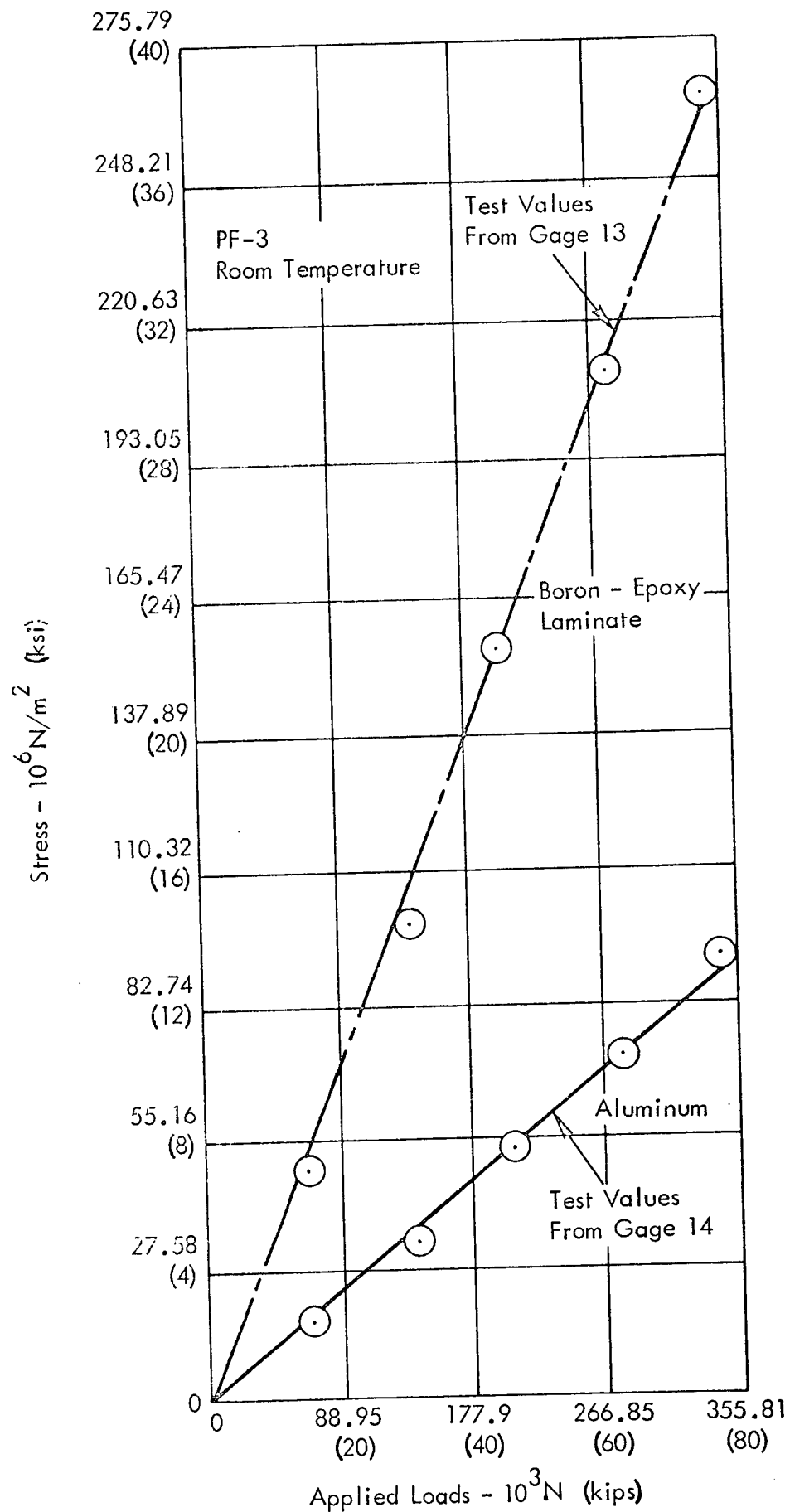


FIGURE 91. - APPLIED LOAD VERSUS TEST VALUES FOR PF-3

Preliminary visual inspection of the failure area revealed some evidence of fatigue damage in the fracture face of the rainbow fitting. Metallurgical examination confirmed the existence of fatigue damage. No fatigue damage was detected in the boron reinforcements or in the bondlines.

9.4 PANEL BUCKLING COMPONENTS

Each of the three specimens was instrumented with electrical resistance-type strain gages at locations where strain data were desired to guide specimen alignment prior to test as well as to monitor specimen strain state during test. Gages were located on the aluminum alloy elements as well as the boron-epoxy laminates. Since the boron-epoxy laminates were inaccessible for gage installation after final assembly of the specimens, gages desired on the laminate surfaces were installed prior to assembling the stringer assemblies to the panel assemblies. Lead wires were attached to the gages and were then routed spanwise such that all leads extend from the same end of each respective specimen. During final assembly of the specimen, a 0.48 cm (3/16 in.) diameter hole was drilled in one vertical leg of each of the stringer assemblies, and the lead wires were threaded through these holes to the outside. Otherwise, the leads would have been trapped inside the skin-stringer cavity after casting the specimen ends in Cerrobend. The holes were drilled 10.4 cm (4.5 in.) from the specimen ends on the approximate centroid of the skin-stringer element. Gages were applied to the aluminum alloy elements on the outside surfaces of the specimens. Baldwin type FAE-25-1256 gages were applied to the boron-epoxy surfaces, and Dentronics type 204 CL3 gages were applied to the aluminum alloy surfaces. All gages were axial type and were aligned parallel to the spanwise direction.

Specimen 130-PB-1 had 36 gages. Thirty-two gages were installed on specimen 130-PB-2, and specimen 130-PB-3 had 44 gages.

The instrumented specimens were tested in the compression bay of a 5.34×10^6 N (1,200,000 pound) capacity Baldwin Universal Testing Machine. A beam having ground faces was centered on the testing machine platen, and the specimens were placed on the beam. A ground plate was then sandwiched between the other ends of the specimen and the machine cross head. A frame was constructed on which dial indicators were attached to allow measurement of lateral deflections at various spanwise and chordwise positions on the specimens. The frame was portable and rested on the testing machine platen. The dial indicators used had a scale sensitivity of 0.0025 cm (0.001 in.). Strain gage leads were connected to a B&F Model SY156 data acquisition system having 200 channel capacity and digital output at a print rate of up to 20 channels per second.

The overall test arrangement for the three buckling specimens is shown in Figure 92. The 130-PB-1 specimen contained a small twist. The twist was eliminated in the test arrangement by applying a small torsional load to the specimen ends, and reacting the resulting loads through bolts and steel angles as shown in Figures 92 and 93. This was not necessary for specimen 130-PB-2. On specimen 130-PB-3-3, external clamping was applied to each end

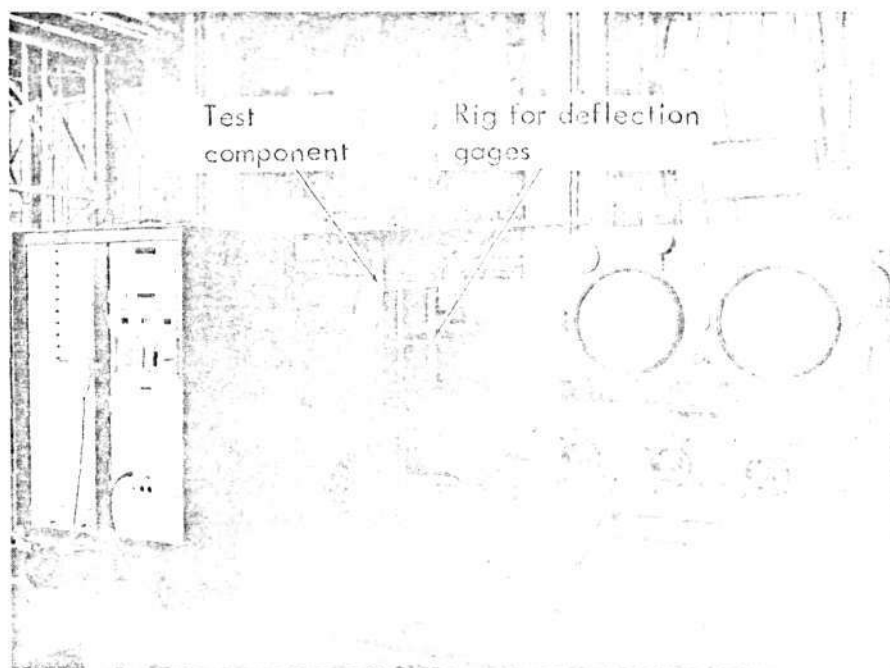


FIGURE 92.- TEST ARRANGEMENT FOR PANEL BUCKLING SPECIMENS

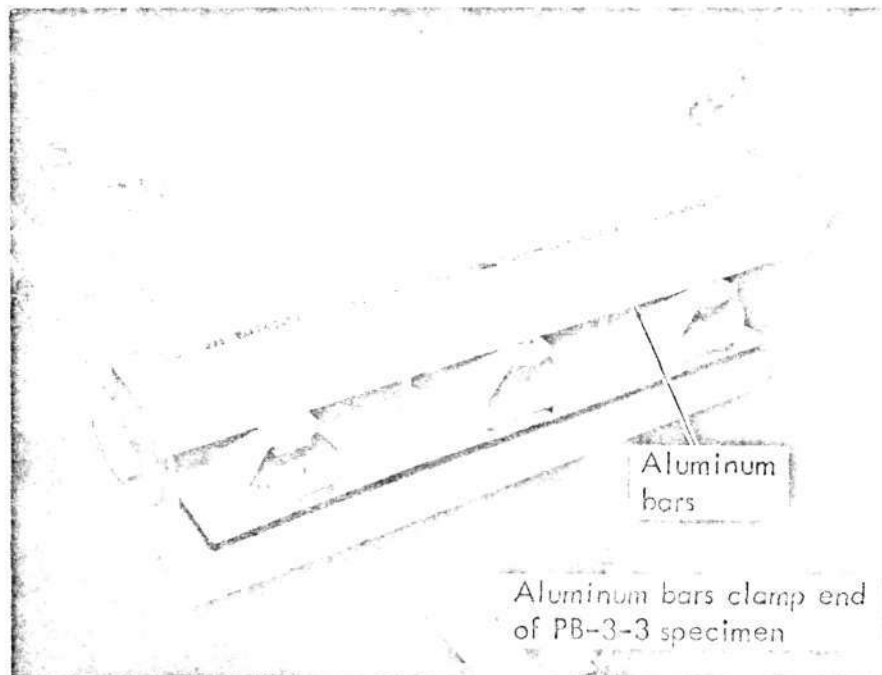


FIGURE 93.- TWISTING LOADS REACTION MECHANISM FOR PANEL BUCKLING SPECIMENS

of the specimen at the boron-epoxy laminate to titanium shim transition area to minimize effects of eccentricities which had been seen in the test on 130-PB-1. The clamping was accomplished by sandwiching the specimen between 7.6 cm (3 in.) by 2.5 cm (1 in.) aluminum bars. The bars at each end of the specimen were bolted together and additional clamping was provided by "C" clamps.

After the specimens were arranged in the testing machine, a small compressive load was applied and strain measurements were recorded. Based on these strains, alignment of loading was adjusted using the alignment mechanism which is an integral part of the testing machine compressive loading head. Strains were again measured and examined for uniformity. This alignment process was repeated until acceptable uniformity in strain distribution was achieved. During this process, load magnitude was limited to approximately 20 percent of the expected buckling load for the particular specimen.

9.4.1 130-PB-1 Specimen

9.4.1.1 PB-1 Description

This specimen was a single-plank upper surface specimen containing three hat section stiffeners. The specimen represented a spanwise test area between wing stations 20.00 and 61.60. The total length of the specimen was 191.8 cm (75.50 in.) which included the necessary end fittings and attachments required to interface with the test fixtures. The aluminum plank had a constant thickness of 0.254 cm (0.10 in.) and included two full-length integral stiffeners, located between the hat sections. These stiffeners were 1.68 cm (0.66 in.) in height. The typical hat section stiffeners used were machined to the cross-sectional configuration of the C-130E stiffeners.

The three skin-reinforcing laminates were 33 plies thick and 5.08 cm (2 in.) wide. The stringer laminates were 33 plies thick and 2.29 cm (0.9 in.) wide. Both the skin and stringer laminates had interleaved titanium shims at the ends to accommodate titanium fasteners. Figure 94 shows PB-1 installed in the test machine.

9.4.1.2 PB-1 Tests

The 2.67×10^6 N (600,000 lb.) load range was selected for this specimen. Load was applied to the specimen in 2.22×10^5 N (50,000 pound) increments up to 1.33×10^6 N (300,000 lb.), and each incremental load was held constant long enough to record strain and deflection data. The load was then reduced to 2.22×10^5 N (50,000 lb.) where strain and deflection data were again recorded. At this time the dial indicator support frame was moved away from the specimen to prevent damage upon specimen failure. Load was then increased to 1.33×10^6 N (300,000 lbs.) and held while strains were again recorded. Loading was then increased in 2.22×10^5 N (50,000 lb.) increments and strains were recorded at each increment. Failure of the specimen occurred at a compressive load of 1.71×10^6 N (385,000 lbs.). Primary failure was near the specimen ends where the boron-epoxy laminate terminated into

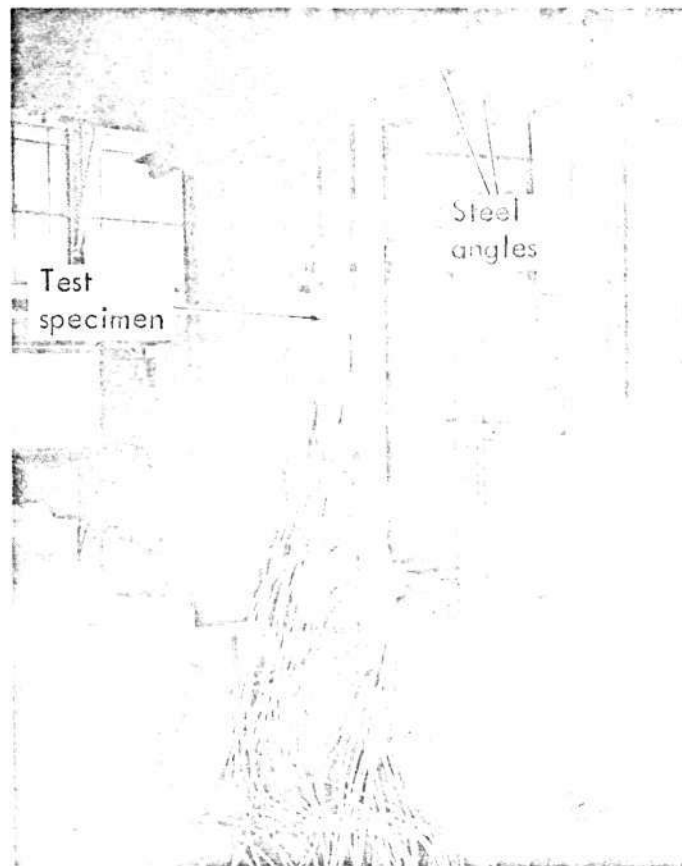


FIGURE 94.- 130-PB-1 INSTALLED IN TEST MACHINE

titanium end blocks. Both the skin and stiffeners failed on one end of the specimen, but only the skin failed at the other end. Figure 95 shows the failed specimen. In these photographs the circled fasteners designate those that failed in tension. The stringer assemblies were then removed from the panel assembly to allow visual inspection of the laminates. Visual examination of the laminates bonded to the stringers revealed no apparent damage. All three boron-epoxy laminates on the skin exhibited chordwise fractures through several plies. The assemblies were also failed over the entire span by a combination of interlaminar failure of the laminate and failure of the matrix between the scrim and first ply of the laminate on the adhesive-bonded side. The failed laminates are shown in Figure 96.

9.4.1.3 PB-1 Test Evaluation

The component failed in a local instability mode of the reinforced skin element at a load of 1.71×10^6 N (385,000 lbs.). This load was 13 percent lower than the predicted failure load of 1.86×10^6 N (440,000 lbs.). The failure was essentially symmetrical and occurred at both ends of the specimen adjacent to the termination of the titanium end blocks and reinforcing plates. Local eccentricities introduced by the end blocks and plates are thought to be the reasons for failure below predicted load. PB-3-3 tests were initiated to further investigate this phenomenon. The failure load corresponded to a calculated average cross-sectional strain of 4100 micro m/m. Non-linearity of measured strain readings occurred between 3500 and 4000 micro m/m. Failure finally occurred with substantial divergence of strains.

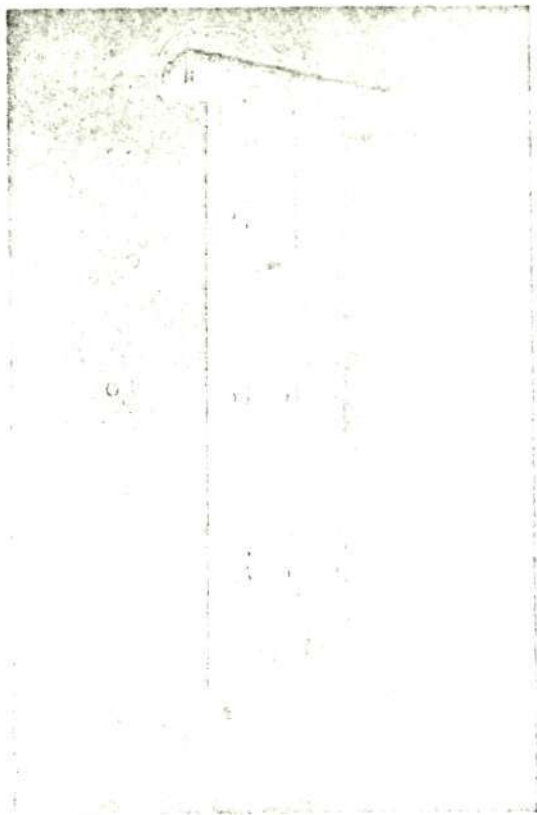
9.4.2 130-PB-2 Specimen

9.4.2.1 PB-2 Description

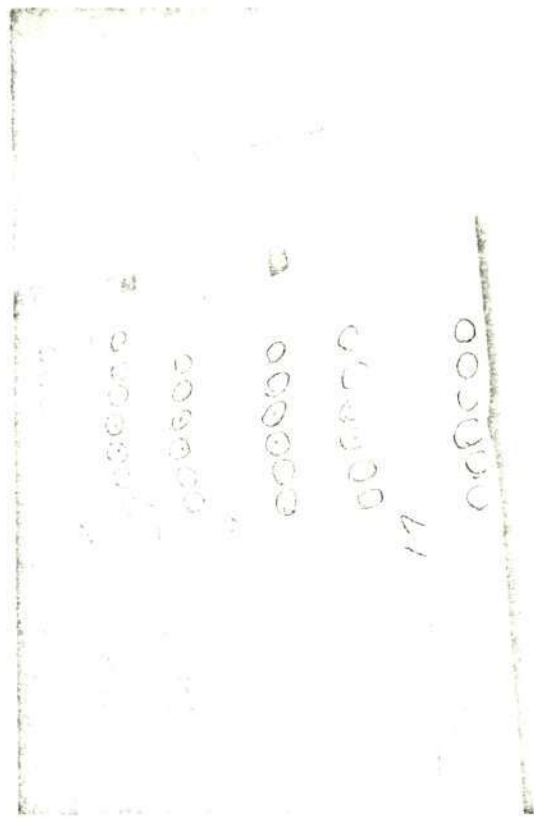
This panel was a lower surface single plank specimen containing four hat section stiffeners, and represented a spanwise test area between wing stations 20.00 and 61.60. The total length of the specimen was 191.8 cm (75.50 in.) which, as in PB-1, included the necessary test fittings and attachments. The aluminum plank had a constant thickness of 0.41 cm (0.160 in.). Hat sections were machined to the cross-sectional configuration of the C-130E. The four boron-epoxy skin laminates were 33 plies thick and 5.08 cm (2 in.) wide. The stringer laminates were 31 plies thick and 2.29 cm (0.9 in.) wide. Both the skin and stringer laminates had titanium interleaved shims at the ends to accommodate titanium fasteners. Two views of PB-2 installed in the test machine are shown in Figure 97.

9.4.2.2 PB-2 Tests

The 2.67×10^6 N (600,000 lb.) load range was selected for this specimen and the incremental loading and data collection procedures previously described for 130-PB-1 were used.



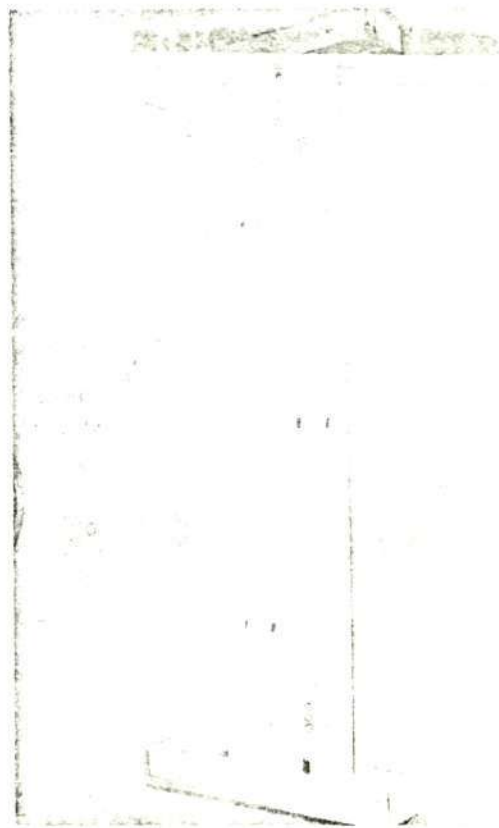
Overall View PB-1 Failure



Tension Failure of Fasteners PB-1



PB-1 Stringer Failure



PB-1 Skin Failure Both Ends

FIGURE 95.- VIEWS OF PB-1 FAILURE

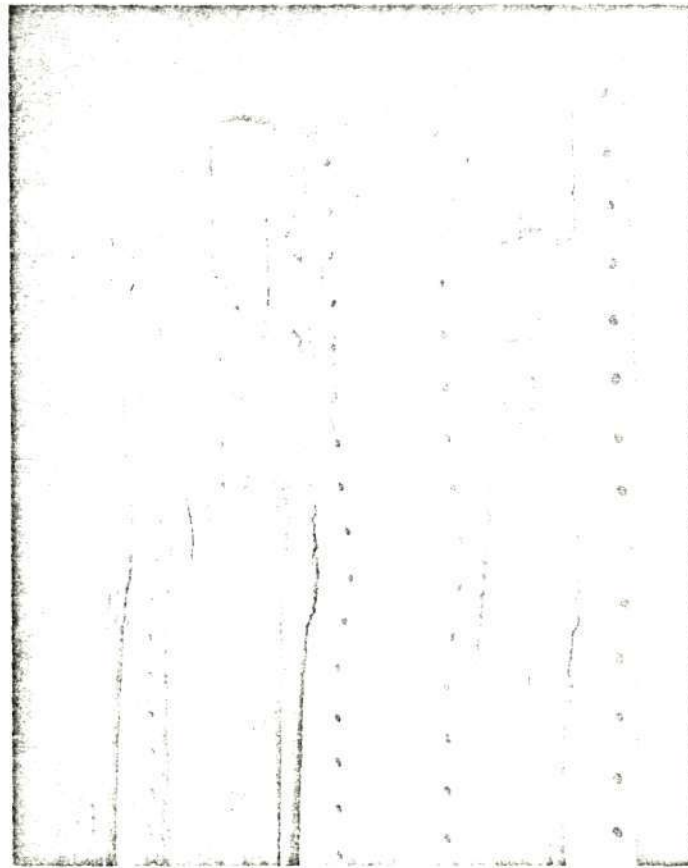
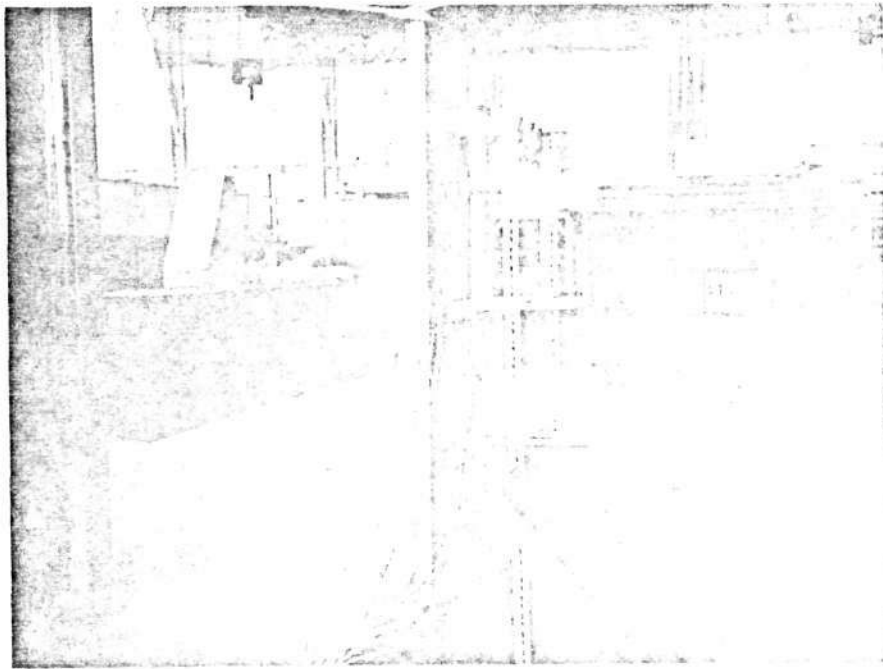


FIGURE 96.- PB-1 FAILED LAMINATES



PB-2 Overall View Installed in Test Machine



PB-2 Close-Up Installed in Test Machine

FIGURE 97.- PB-2 INSTALLED IN TEST MACHINE

Failure of the specimen occurred at a compressive load of 2.05×10^6 N (462,000 lbs.). The failed specimen is shown in Figure 98. After failure, the stringer assemblies were removed from the panel assembly to allow observation of the laminates. Inspection of the boron-epoxy assemblies in the stringers revealed no bond failures; however, fractures and splitting of the boron adjacent to the end terminations were observed for two of the stringers. The skin had four boron-epoxy reinforcements. One of these separated from the aluminum skin panel. Another exhibited an interlaminar failure of the laminate over about half the span. The other two had similar interlaminar failures along with failures of the laminate matrix between the surface scrim and first ply of boron-epoxy on the adhesive bonded side. One of these also had a chordwise fracture through several plies. Appearance of these fractures was generally the same as previously shown for specimen 130-PB-1.

The failure load for this specimen demonstrated a positive margin with respect to airplane requirements. However, the failure location suggests that there was some influence of boron terminations as previously described for 130-PB-1. Since the skin was considerably thicker on 130-PB-2, the influence of the termination was less dramatic.

9.4.2.3 PB-2 Test Evaluation

Failure in compression occurred at a load of 2.05×10^6 N (462,000 lbs.) due to local instability of the skin and stringer flange elements at a position approximately 50.8 cm (20 in.) from one end of the component. Stringer to skin fastener failures at the same location, in both shear and tension, were also evident. This load was 12 percent lower than the predicted column failure load of 2.32×10^6 N (522,000 lbs.) but exceeded aircraft ultimate load requirements. Failure was caused by beam column action due to initial eccentricities, combined with the effects of local eccentricities in the application of the load caused by the titanium end blocks and reinforcing plates located at both ends of the component. The failure load corresponds to a calculated average cross-sectional strain of 3400 micro m/m (micro in./in.). Non-linearity of measured strain readings occurred between 2200 and 3000 micro m/m (micro in./in.) depending upon location of strain gages. Failure finally occurred with wide divergence of strains.

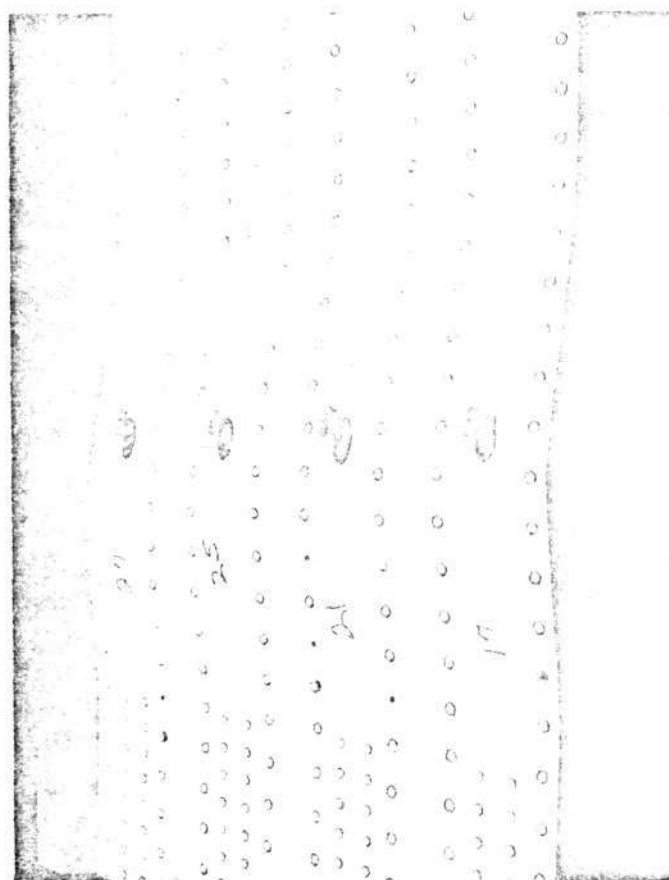
9.4.3 130-PB-3-3 Specimen

9.4.3.1 PB-3-3 Description

As originally constructed, this specimen was identical in design to the previously described 130-PB-1 except the specimen was two skin panels in width and, consequently, contained a spanwise splice. Nominally, length was 191.8 cm (75.5 in.), width was 95.8 cm (37.7 in.), and the specimen had two skin panels and six hat section stiffeners.



PB-2 Failure Stringer Side



PB-2 Failure Skin Side

FIGURE 98.- PB-2 FAILURE

Both panel sections contained integral stiffeners and were machined from an extrusion of 7075-T7351 aluminum alloy. The skin reinforcing laminates were 5.08 cm (2 in.) wide and contained 33 plies of boron-epoxy oriented in the longitudinal direction. The stiffener reinforcing laminates were 2.29 cm (0.9 in.) wide and contained 33 plies of boron-epoxy oriented in the 191.8 cm (75.5 in.) direction.

Results of the test on 130-PB-1 dictated the need for another test of the same general configuration. Consequently, the 130-PB-3 specimen was modified to produce that specimen which was designated as 130-PB-3-3. In producing the 130-PB-3-3, the 130-PB-3 specimen was disassembled at the spanwise splice which provided two panels, each having three stiffeners. The edge of the panel section having the spanwise-splice configuration was then machined flush with the base flange of the adjacent hat section stiffener. At this point the specimen was essentially identical to the 130-PB-1. Next, the aluminum rivets attaching the hat section stiffeners to the skin panel were replaced with steel alloy Hi-Loks at the first 18 locations on each end of the specimen. This was done to provide additional tension capability since the aluminum rivets failed in tension in this area during test of 130-PB-1.

In another modification, the titanium blocks terminating the laminate assemblies, were chamfered to reduce eccentricity produced by the laminate terminations. General configuration and essential elements of specimen 130-PB-3-3 are illustrated in Figure 99. Maximum deviation from flatness for the specimen was .076 cm (0.03 in.) in the spanwise direction and 0.128 cm (0.05 in.) across the chord.

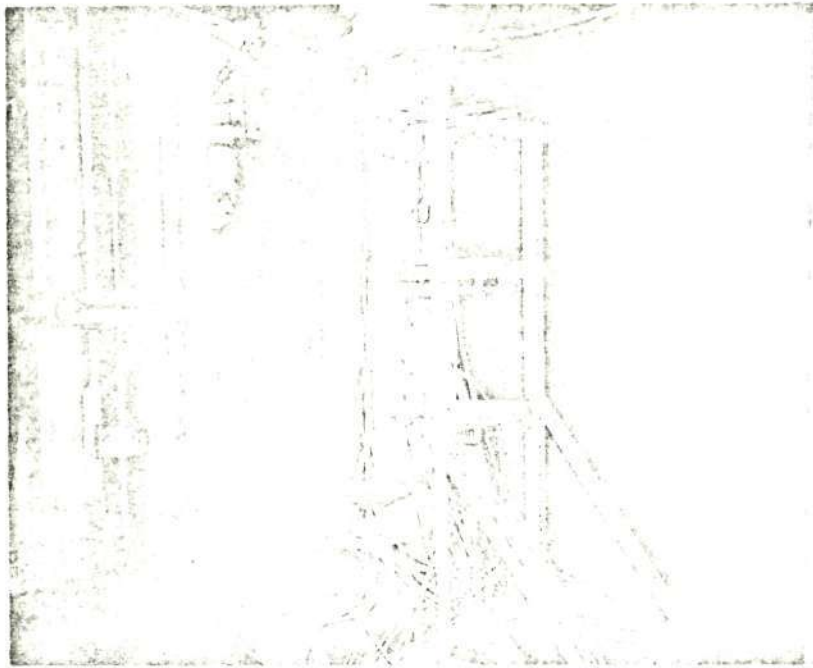
9.4.3.2 PB-3-3 Tests

The 2.67×10^6 N (600,000 lb.) load range was selected for this specimen, and the incremental loading and data collection procedures previously described for the other two specimens were employed. One exception, however, was that initial loading was carried to 1.11×10^6 N (250,000 lbs.) rather than 1.33×10^6 N (300,000 lbs.). Also, prior to specimen failure, strain gage data were collected by continuous scanning rather than at specific load increments. Specimen failure occurred at a compressive load of 1.89×10^6 N (425,000 lbs.). Each end of the panel failed adjacent to the previously described end clamps used on this specimen. Figure 100 shows one end of the failed specimen.

The end modification incorporated on this specimen provided considerable improvement over the 130-PB-1 specimen; however, the improvement was not sufficient to obtain a valid buckling load for the specimen.

9.4.3.3 PB-3-3 Test Evaluation

The component failed in a local instability mode of the boron-epoxy laminate reinforced skin element at a load of 1.89×10^6 N (425,000 lbs.). The mode of failure was similar to that of PB-1 except that fasteners holding the hat stringers to the skin remained intact. Local instability was combined with a tearing of the hat vertical legs. The failure load was 4 percent



View of Specimen From Skin Side



View of Specimen From Stringer Side

FIGURE 99.- PB-3-3 INSTALLED IN TEST MACHINE

lower than the predicted load of 1.96×10^6 N (440,000 lbs.). Local eccentricities introduced by the titanium blocks and reinforcing plates at both ends of the specimen were again thought to be the reasons for failure below predicted load. Strain gage readings, obtained during the test and presented on Figure 101, tend to confirm this theory. Further compression tests are planned during Phase II of this program in order to eliminate the effects of local "end effect" eccentricities and to obtain correlation of test results with analysis. The results of these tests may require further refinement of the compression allowables program to be used for Phase II design.

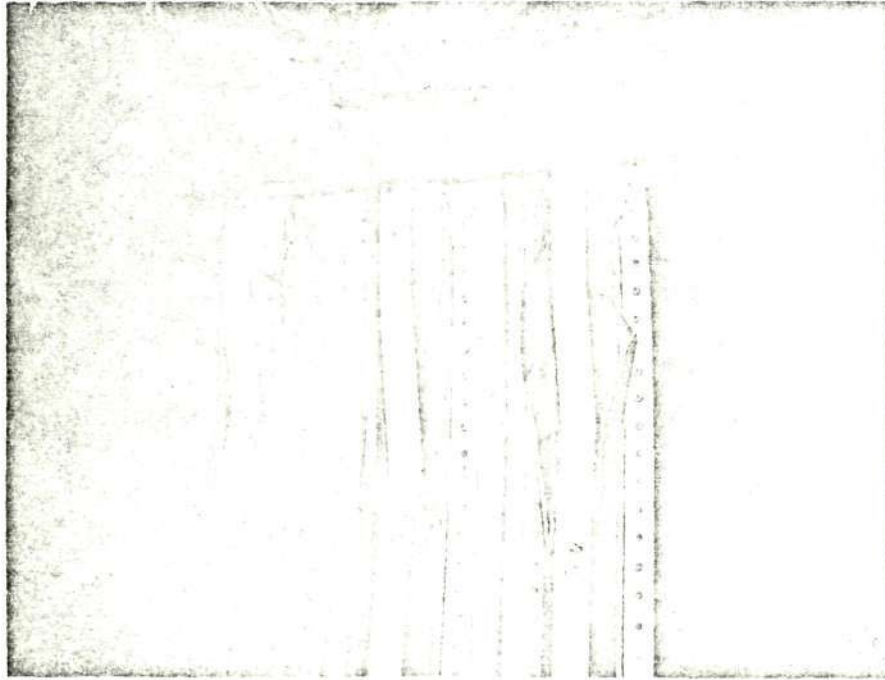


FIGURE 100.- PB-3-3 FAILURE



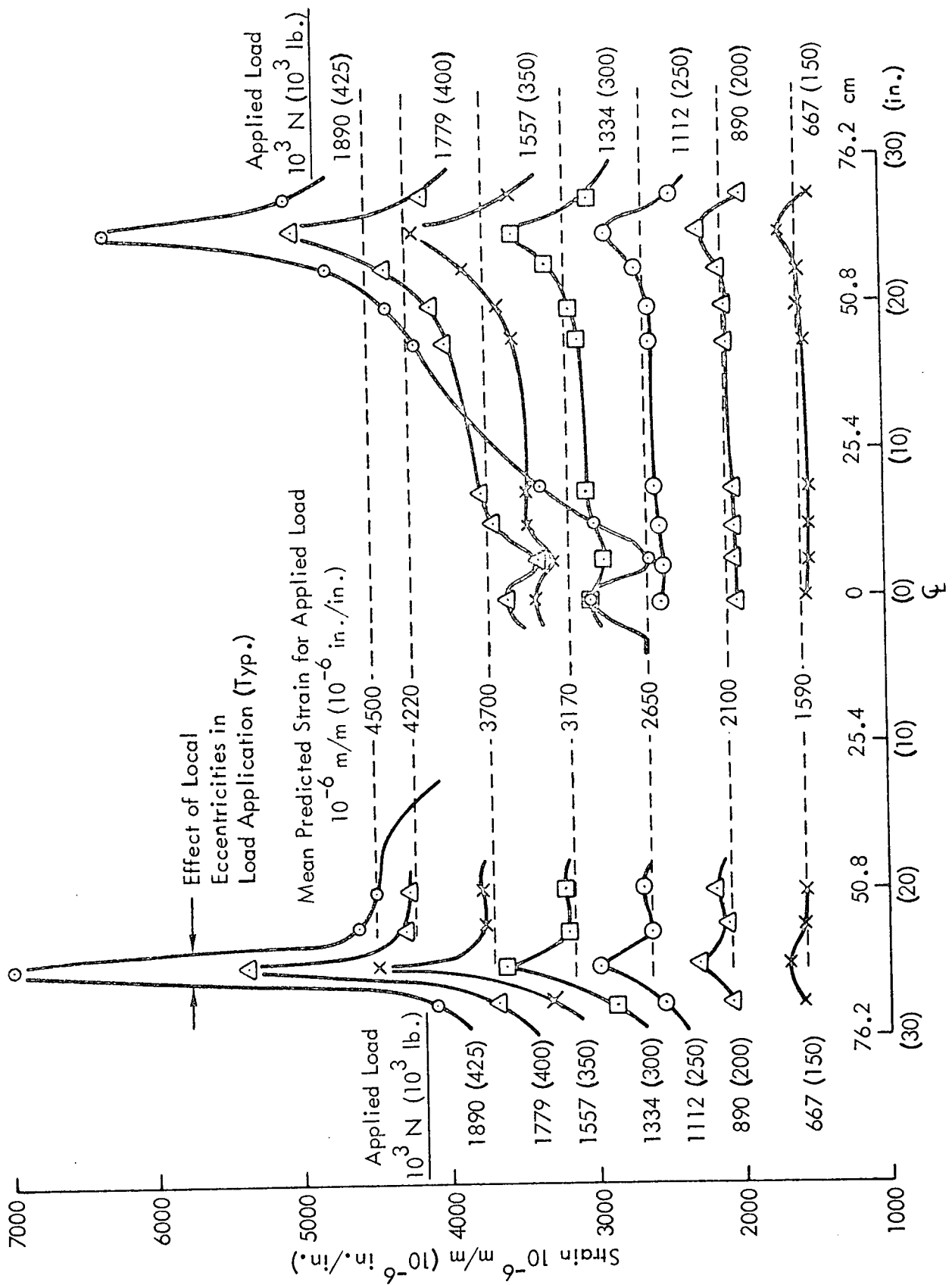


FIGURE 101.-PB 3-3 STRAIN DISTRIBUTION ALONG
CENTER STRINGER SKIN PANEL ELEMENT

PRECEDING PAGE BLANK NOT FILMED
APPENDIX A

RELATIONSHIP BETWEEN SI UNITS
AND U.S. CUSTOMARY UNITS

BASIC SI UNITS		
Physical Concept	Measurement	Abbreviation
Length	meter	m
Mass	kilogram	kg
Time	second	s
Force	Newton	N
Thermodynamic Temperature	degree Kelvin	$^{\circ}\text{K}$
Density	kilograms/meter ³	kg/m ³

PREFIXES		
Factor By Which Unit Is Multiplied	Prefix	Symbol
10^6	mega	M
10^3	kilo	k
10^2	hecto	h
10	deca	da
10^{-1}	deci	d
10^{-2}	centi	c
10^{-3}	milli	m
10^{-6}	micro	μ

Preceding page blank

CONVERSION FACTORS

To Convert From	To	Multiply By
Celsius (temp.)	kelvin	$t_K = t_c + 273.15$
Fahrenheit (temp.)	kelvin	$t_K = (5/9)(t_F + 459.67)$
foot	meter	3.048×10^{-1}
inch	meter	2.54×10^{-2}
pound mass (lbm avoirdupois)	kilogram	4.536×10^{-1}
pound mass force (lbf)	newton	4.44822
lbm/inch ³	kilogram/meter ³	2.768×10^4
psi	newton/meter ²	6.895×10^3

APPENDIX B

ANALYSIS METHODS TO ESTABLISH PRELIMINARY THERMAL RESIDUAL STRESSES AND STRESSES DUE TO APPLIED AIRPLANE LOADS

The residual thermal stresses used in the Phase I analysis were established by conventional methods and considered only the longitudinal physical and mechanical properties of the utilized materials. In addition it was assumed that the aluminum/boron-epoxy cross-sectional area ratios of the individual skin and hat section adherends during adhesive cure were identical to the area ratios of the finally assembled skin/hat composite. A more refined analysis was later developed to include the differences of area ratios and of bi-axial material properties and is presented in Appendix C.

Although symbols used in this appendix are consistent with those used in the body of the report, they are repeated here for clarity because of the widespread use of subscripts.

Symbols and Abbreviations Used in Appendix B

- σ_a = final stress in aluminum.
- σ_b = final stress in boron-epoxy laminate.
- σ_R = residual stress in aluminum resulting from restraint load P_R during elevated temperature cycle.
- σ_{Ra} = residual stress in aluminum resulting from removal of restraint load P_R , after adhesive cure and during cooling to room temperature.
- σ_{Rb} = residual stress in boron-epoxy resulting from removal of restraint load P_R , after adhesive cure and during cooling to room temperature.
- σ_{ca} = residual stress in aluminum caused by differences in coefficients of expansion during cooling cycle to operating temperature.
- σ_{cb} = residual stress in boron-epoxy caused by differences in coefficients of expansion during cooling cycle to operating temperature.
- σ_{oa} = stress in aluminum due to applied airplane loads.
- σ_{ob} = stress in boron-epoxy laminate due to applied airplane loads.
- P = applied airplane load.
- P_R = restraint load due to cool tool.

A_a = aluminum cross-sectional area.
 A_b = boron-epoxy cross-sectional area.
 A_s = steel tool cross-sectional area.
 E_a = aluminum modulus of elasticity.
 E_b = boron-epoxy modulus of elasticity.
 E_s = steel tool modulus of elasticity.
 α_a = aluminum coefficient of expansion.
 α_b = boron-epoxy coefficient of expansion.
 α_s = steel tool coefficient of expansion.
 T = adhesive cure temperature.
 T_s = steel tool temperature.
 T_{RT} = room temperature.
 L = length.
 δ = deflection.
 ϵ = strain.

Subscripts

a = subscript pertaining to aluminum.
 b = subscript pertaining to boron-epoxy laminate.
 s = subscript pertaining to steel.
 R = subscript pertaining to restraint load.
 c = subscript pertaining to cooling cycle.
 o = subscript pertaining to operating temperature.

Total Stresses

The total stress in the aluminum or boron-epoxy laminate element of a typical C-130 stringer is the sum of several stress components as follows:

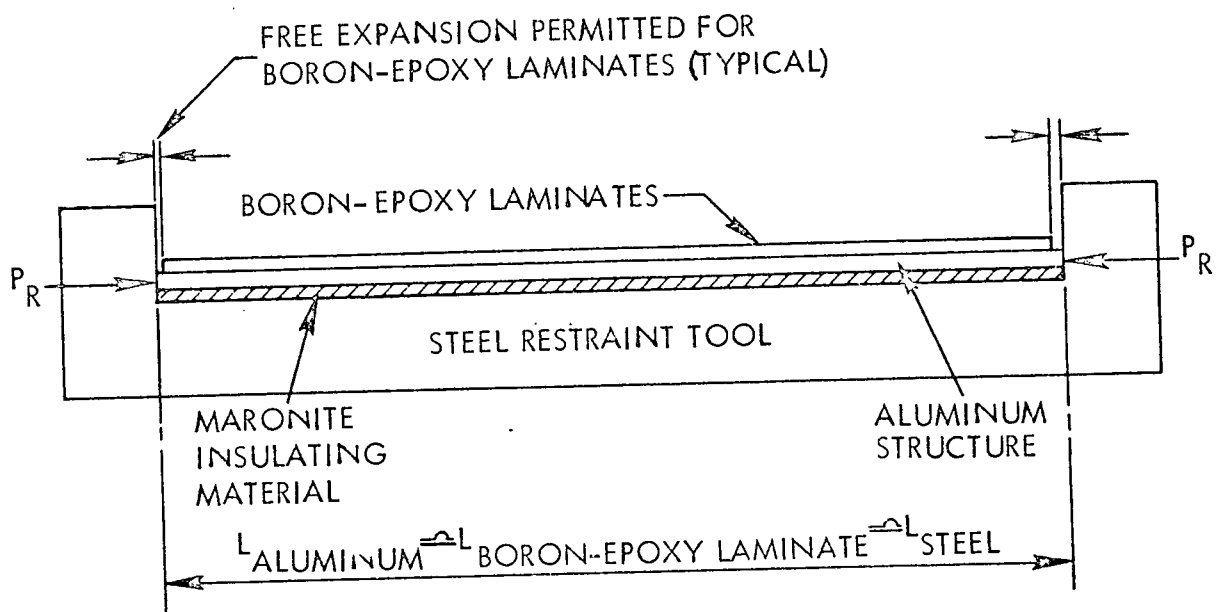
For aluminum:

$$\sigma_a = \sigma_R + \sigma_{R_a} + \sigma_{c_a} + \sigma_{o_a} \quad (1)$$

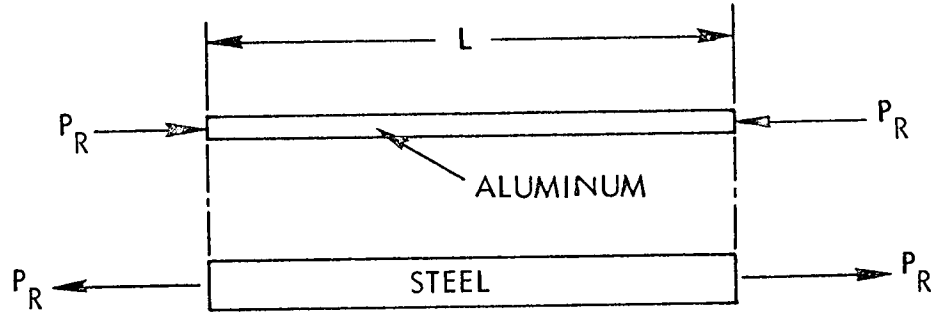
For boron-epoxy laminate:

$$\sigma_b = \sigma_{R_b} + \sigma_{c_b} + \sigma_{o_b} \quad (2)$$

Stresses Due to Steel Restraint Tool During Elevated Temperature Cycle



The steady state at elevated temperature prior to adhesive cure is as follows:



Aluminum Strain:

$$\epsilon_a = \alpha_a (T - T_{RT}) - \frac{P_R}{A_a E_a} \quad (3)$$

Steel Tool Strain:

$$\epsilon_s = \alpha_s (T_s - T_{RT}) + \frac{P_R}{A_s E_s} \quad (4)$$

Equating Strains:

$$\begin{aligned} \epsilon_a &= \epsilon_s \\ \therefore \alpha_a (T - T_{RT}) - \frac{P_R}{A_a E_a} &= \alpha_s (T_s - T_{RT}) + \frac{P_R}{A_s E_s} \end{aligned} \quad (5)$$

from which

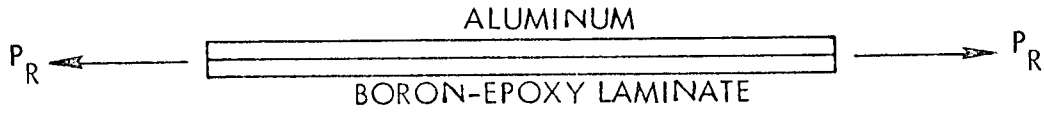
$$P_R = \frac{[\alpha_a (T - T_{RT}) - \alpha_s (T_s - T_{RT})] A_a E_a A_s E_s}{A_s E_s + A_a E_a} \quad (6)$$

but $\sigma_R = -\frac{P_R}{A_a}$ (compressive stresses are negative)

$$\therefore \sigma_R = \frac{-[\alpha_a (T - T_{RT}) - \alpha_s (T_s - T_{RT})] E_a E_s A_s}{A_s E_s + A_a E_a} \quad (7)$$

Stresses Due to Removal of Restraint Load During Cooling Cycle

The removal of the restraint load P_R during cooling to room temperature is analogous to applying a tensile load P_R to the composite. The tensile load is shared by the composite elements in proportion to their longitudinal stiffnesses.



Aluminum Stress:

$$\sigma_{R_a} = \frac{P_R}{A_a + A_b \frac{E_b}{E_a}} \quad (\text{where } P_R = -\sigma_R A_a)$$

$$\therefore \sigma_{R_a} = \frac{P_R \cdot E_a}{A_a E_a + A_b E_b} \quad (8)$$

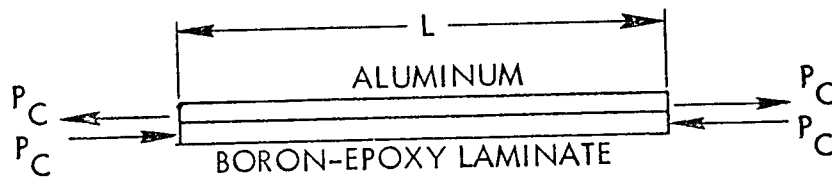
Similarly, Laminate Stress:

$$\sigma_{R_b} = \frac{P_R}{A_b + A_a \frac{E_a}{E_b}}$$

$$\therefore \sigma_{R_b} = \frac{P_R \cdot E_b}{A_a E_a + A_b E_b} \quad (9)$$

Stresses Due to Differences in Coefficients of Expansion During Cooling Cycle

At operating temperature T_o the residual forces in the adherends after adhesive cure are as shown:



The force P_C may be found by equating the change in length of individual adherends:

For the aluminum, the change in length is:

$$\delta_a = -\alpha_a L(T - T_o) + \frac{P_c L}{A_a E_a} \quad (10)$$

For the boron-epoxy laminate, the change in length is:

$$\delta_b = -\alpha_b L(T - T_o) - \frac{P_c L}{A_b E_b} \quad (11)$$

but $\delta_a = \delta_b$

\therefore Equating changes in length:

$$-\alpha_a (T - T_o) + \frac{P_c}{A_a E_a} = -\alpha_b (T - T_o) - \frac{P_c}{A_b E_b}$$

or

$$P_c = \frac{(\alpha_a - \alpha_b)(T - T_o) A_a E_a A_b E_b}{A_a E_a + A_b E_b} \quad (12)$$

\therefore Aluminum Stress:

$$\sigma_{c_a} = \frac{P_c}{A_a}$$

$$\therefore \sigma_{c_a} = \frac{(\alpha_a - \alpha_b)(T - T_o) E_a A_b E_b}{A_a E_a + A_b E_b} \quad (13)$$

Similarly, for the boron-epoxy laminate:

$$\sigma_{c_b} = \frac{-P_c}{A_b} \quad \begin{matrix} \text{(compressive stresses)} \\ \text{(are negative)} \end{matrix}$$

$$\therefore \sigma_{c_b} = \frac{-(\alpha_a - \alpha_b)(T - T_o) A_a E_a E_b}{A_a E_a + A_b E_b} \quad (14)$$

Stress Due to Applied Airplane Loads

Applied axial load P is distributed between the two materials in proportion to their longitudinal stiffnesses:

i.e., for aluminum

$$\sigma_{o_a} = \frac{P E_a}{A_a E_a + A_b E_b} \quad (15)$$

for boron-epoxy

$$\sigma_{o_b} = \frac{P E_b}{A_a E_a + A_b E_b} \quad (16)$$

Sample Calculation

- Adhesive cured at 235°F .
- Operating temperature of -67°F .
- No externally applied load.

Parameters

$$P = 0.0$$

$$\alpha_a = 12.9 \times 10^{-6} \text{ in./in./}^{\circ}\text{F}$$

$$\alpha_b = 2.4 \times 10^{-6} \text{ in./in./}^{\circ}\text{F}$$

$$\alpha_s = 6.8 \times 10^{-6} \text{ in./in./}^{\circ}\text{F}$$

$$A_a = 1.0 \text{ in.}^2$$

$$A_b = .25 \text{ in.}^2$$

$$A_s = 3.0 \text{ in.}^2$$

$$E_a = 10.4 \times 10^6 \text{ lb./in.}^2$$

$$E_b = 31.6 \times 10^6 \text{ lb./in.}^2$$

$$E_s = 29.0 \times 10^6 \text{ lb./in.}^2$$

$$\begin{aligned}
 T &= 235^{\circ}\text{F} \\
 T_{\text{R.T.}} &= 75^{\circ}\text{F} \\
 T_o &= -67^{\circ}\text{F} \\
 \eta &= 0.9 \text{ (thermal insulating efficiency factor)}
 \end{aligned}$$

Step 1:

Calculate T_s :

$$\begin{aligned}
 T_s &= T_{\text{R.T.}} + (1 - \eta)(T - T_{\text{R.T.}}) \\
 &= 75 + 0.1 (235 - 75) \\
 &= 91^{\circ}\text{F}
 \end{aligned} \tag{17}$$

Step 2:

Calculate σ_R from equation (7):

$$\begin{aligned}
 \sigma_R &= \frac{- [12.9 \times 10^{-6} \times 160 - 6.8 \times 10^{-6} \times 16] 10.4 \times 10^6 \times 29.0 \times 10^6 \times 3.0}{(3.0 \times 29.0 + 1.0 \times 10.4)} \\
 &= -18162 \text{ lb/in.}^2 \text{ (Point 'A', Figure B-1)}
 \end{aligned}$$

Step 3:

Calculate σ_{R_a} from equation (8):

$$\begin{aligned}
 \sigma_{R_a} &= \frac{18162 \times 10.4 \times 10^6}{(1.0 \times 10.4 + 0.25 \times 31.6) 10^6} \\
 &= +10321 \text{ lb/in.}^2
 \end{aligned}$$

Step 4:

Calculate σ_{c_a} from equation (13):

$$\begin{aligned}
 \sigma_{c_a} &= \frac{(12.9 - 2.4) 10^{-6} \cdot (235 + 67) 10.4 \times 10^6 \times 0.25 \times 31.6 \times 10^6}{(1.0 \times 10.4 + 0.25 \times 31.6) 10^6} \\
 &= +14236 \text{ lb/in.}^2
 \end{aligned}$$

Step 5:

Calculate σ_a from equation (1):

$$\begin{aligned}\sigma_a &= -18162 + 10321 + 14236 + 0.0 \\ &= + 6395 \text{ lb/in.}^2 \text{ (Point 'B', Figure B-1)}\end{aligned}$$

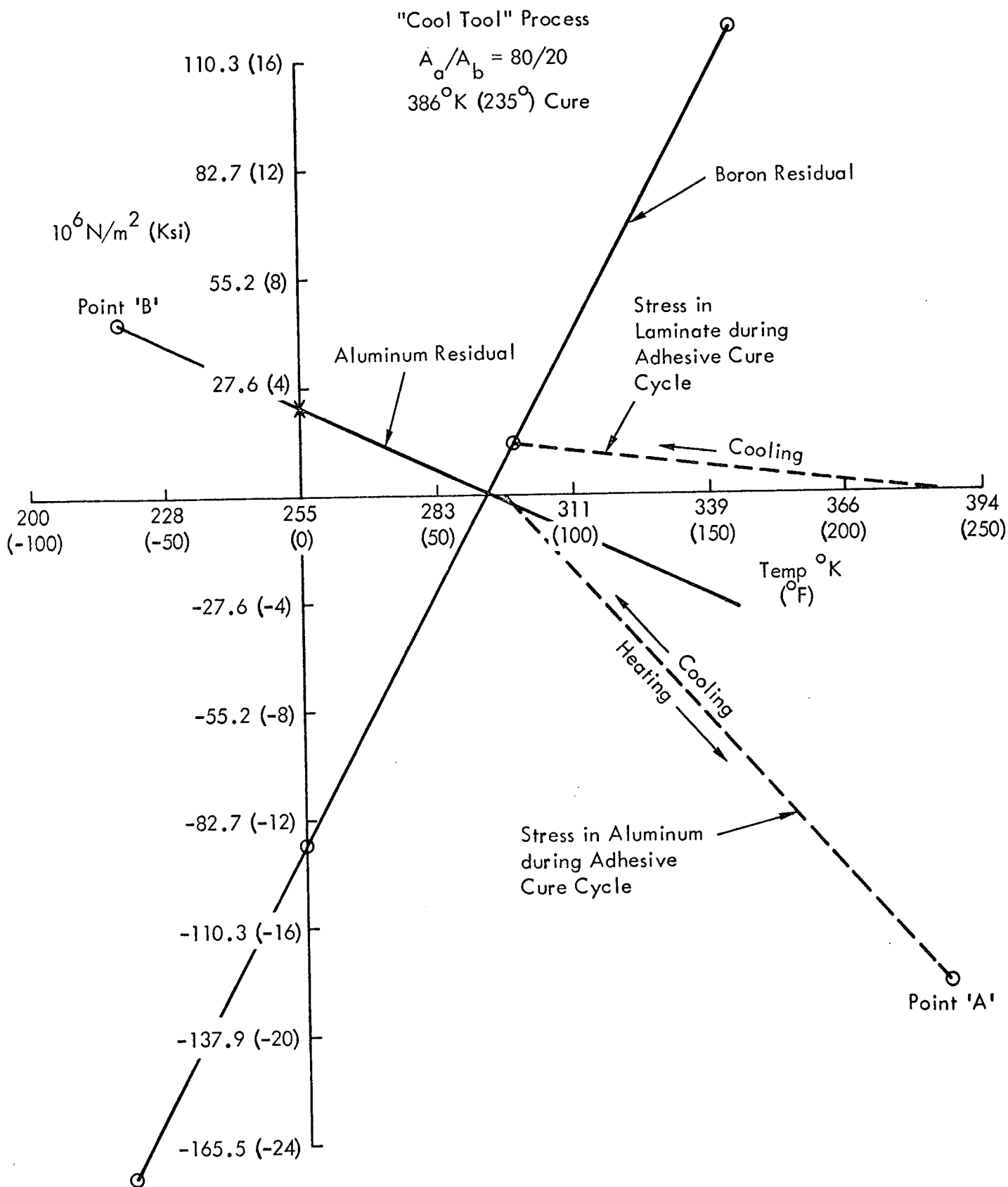


FIGURE B-1.-RESIDUAL STRESS VERSUS TEMPERATURE

APPENDIX C

ANALYSIS METHODS

A computer program for the analysis of the composite reinforced aluminum skin panels has been completed and checked out. Material properties of 7075-T73 aluminum and ply level properties of boron-epoxy are stored in the program as semi-permanent data. Numerical values are given in Table C-1.

TABLE C-1. -MATERIAL PROPERTIES

		Units	Boron-Epoxy	7075-T73 Aluminum
Modulus of Elasticity	E_1	10^{10} N/m^2	21.8 (31.6)	7.17 (10.4)
	E_2	(10^6 psi)	2.55 (3.7)	7.17 (10.4)
Shear Modulus	G_{12}	10^9 N/m^2 (10^5 psi)	5.52 (8.0)	26.9 (39.0)
Poissons Ratio	ν_{12}		0.36	0.33
	ν_{21}		0.042	0.33
Thermal Exp. Coefficients	α_1	$10^{-6} \text{ m/m/}^\circ\text{K}$	1.33 (2.40)	7.17 (12.9)
	α_2	$(10^{-6} \text{ in/in/}^\circ\text{F})$	6.67 (12.0)	7.17 (12.9)

Figure C-1 shows a cross-section of the stiffened skin panel which has been subdivided into 9 separate plate elements. After calculating the bending stiffness (EI) of the cross-section about its neutral axis, the wide column buckling load is obtained from the relation:

$$N_{x_{cr}} = \frac{\pi^2 EI}{b_1 L^2} \quad (1)$$

When two materials with different elastic moduli and/or thermal expansion coefficients are bonded together, shear stresses will be introduced in the bond-layer when the parts are loaded or cooled below the bonding temperature. These shear stresses peak near the free edges of the boron-epoxy laminate, but reduce rapidly and become insignificant at a relatively short distance from the edges. Therefore, for the purpose of this analysis, it was assumed that the principal strains ϵ_1 and ϵ_2 remain constant within the aluminum/laminate plate elements. This yields the following relations for the stresses:

Aluminum:

$$\begin{aligned}\sigma_{1A} &= kE_A \left[[E_A t_A (1 - \nu_{12}\nu_{21}) + E_{B2} t_B (1 - \nu_A \nu_{12})] \epsilon_1 - \left\{ \alpha_A E_A t_A (1 - \nu_{12}\nu_{21}) + \right. \right. \\ &\quad \left. \left. + E_{B2} t_B [\alpha_A + \nu_A (\alpha_A - \alpha_{B2}) - \nu_A \nu_{12} \alpha_{B1}] \right\} T \right] \\ \sigma_{2A} &= kE_A E_{B2} t_B \left\{ (\nu_A - \nu_{12}) \epsilon_1 + [\alpha_{B2} + \nu_{12} \alpha_{B1} - \alpha_A (1 + \nu_A)] T \right\}\end{aligned}\quad (2)$$

Boron-Epoxy:

$$\begin{aligned}\sigma_{1B} &= kE_{B1} \left[[E_A t_A (1 - \nu_A \nu_{21}) + E_{B2} t_B (1 - \nu_A^2)] \epsilon_1 - \left\{ \alpha_{B1} E_{B2} t_B (1 - \nu_A^2) + \right. \right. \\ &\quad \left. \left. + E_A t_A [\alpha_{B1} + \nu_{21} (\alpha_{B2} - \alpha_A) - \nu_A \nu_{21} \alpha_A] \right\} T \right] \\ \sigma_{2B} &= -kE_A E_{B2} t_A \left\{ (\nu_A - \nu_{12}) \epsilon_1 + [\alpha_{B2} + \nu_{12} \alpha_{B1} - \alpha_A (1 + \nu_A)] T \right\}\end{aligned}\quad (3)$$

$$\text{where } k = \frac{1}{E_A t_A (1 - \nu_{12}\nu_{21}) + E_{B2} t_B (1 - \nu_A^2)}$$

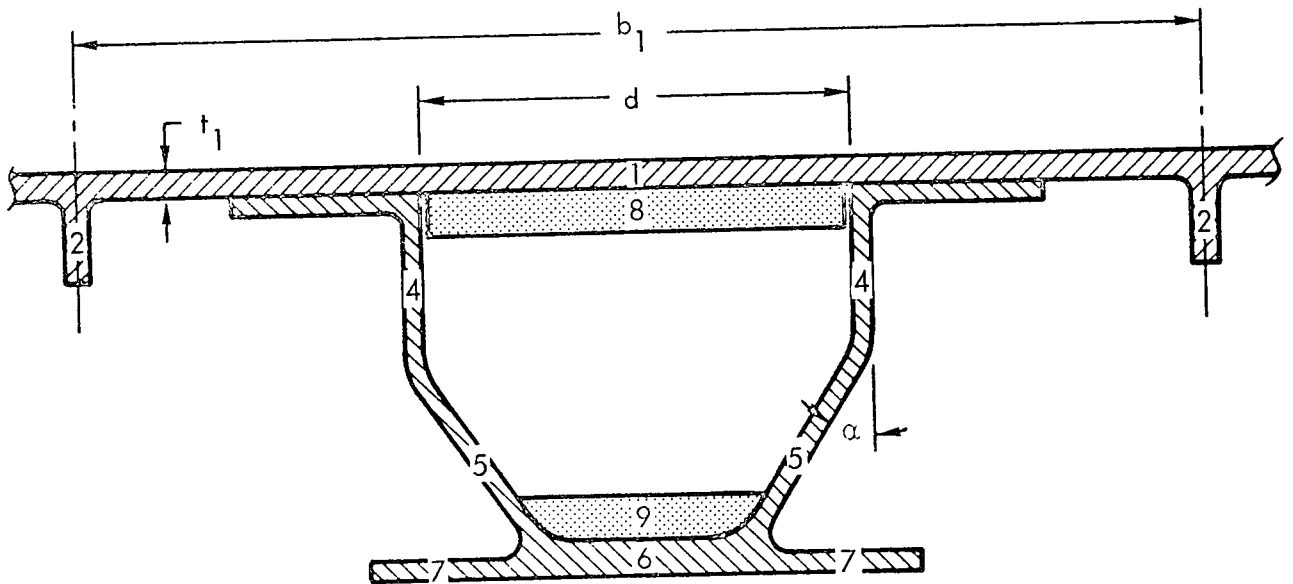


FIGURE C-1.-CROSS-SECTION OF STIFFENED PANEL

The stresses in the aluminum plate elements to which no boron-epoxy is attached are given by:

$$\begin{aligned}\sigma_{1A} &= E_A(\epsilon_1 - \alpha_A T) \\ \sigma_{2A} &= 0\end{aligned}\quad (4)$$

In general, the longitudinal stress in the i^{th} plate element is represented by:

$$\sigma_i = c_i \epsilon_1 + c_2^i T \quad (5)$$

The longitudinal load in each plate element is obtained by multiplying the stress given above by the area of the corresponding plate element. The strain, ϵ_1 , resulting from an applied load, N_x (lb/in), is found by summing the element loads and setting the temperature differential, T , equal to zero:

$$\epsilon_1 = \frac{N_x b_1}{\sum c_i A_i} \quad (6)$$

The stresses resulting from the applied load, N_x , may now be obtained by substituting the strain ϵ_1 into equations (2), (3), and (4).

The stresses in the elements caused by the shear N_{xy} are calculated by requiring compatible shear deformation of the skin and hat section. The shear flow, q' , in the hat section is determined from the relation:

$$q' = \frac{N_{xy}}{t_1} \frac{\eta_1}{\eta_1 + \eta_2} \quad (7)$$

$$\text{where: } \eta_1 = \frac{1}{t_1} \left(d + b_3 + t_4 - \frac{G_B b_8 t_8}{G_A t_1 + G_B t_8} \right)$$

$$\eta_2 = \frac{b_3}{t_3} + \frac{2b_4 + t_3}{t_4} + \frac{2b_5 + t_6/\cos\alpha}{t_5} + \frac{G_A [b_9 + t_5/\cos\alpha - (t_6 + t_9)\tan\alpha]}{G_A t_6 + G_B t_9}$$

Thermal stresses, induced in the structure as a result of the difference in thermal coefficients of the adherends, are calculated in two parts.

The first part computes the stresses caused by bonding at elevated temperature and subsequent cooling to the temperature at which the panels are assembled. Because of difference ratios of boron-epoxy to aluminum, stresses must be calculated separately in the skin and hat sections. The difference between the bonding temperature and the assembly temperature is denoted by ΔT ; then, since the resultant load on the section must be zero, the strain ϵ_1 may be calculated from

$$\epsilon_1 = - \frac{\sum c_2^i A^i}{\sum c_1^i A^i} \Delta T \quad (8)$$

where in one case the summation extends over all the elements in the hat section and in the second case over the elements in the skin assembly.

The second part determines the stresses due to an aircraft operating temperature above or below the assembly temperature. In this case, the stiffened skin assembly is assumed to expand or contract as a unit. Equation (8) may again be used to obtain the strain but ΔT in this case represents the difference between assembly and operating temperature and the summation is performed over all plate elements of the cross-section.

In order to reduce the residual thermal stresses in the composite-reinforced aluminum, plans have been made to restrain the aluminum in a steel fixture during the bonding process. The sequence of events from a stress standpoint is presented schematically in Figure C-2. At the bonding temperature the boron-epoxy is unstressed while the aluminum is under a compression load P_1 . Since the effective thermal expansion coefficient of the composite-reinforced aluminum combination is smaller than that of the aluminum alone, the steel will still be under a tension force when the temperature is reduced back to room temperature. After removal from the steel fixture, the aluminum will be in tension and the boron-epoxy in compression.

A further reduction in residual thermal stresses may be accomplished with the use of the "cool tool" concept. In this procedure the steel fixture is insulation and as a result the temperature rise is considerably less than that in the parts being bonded. The load and stresses at the bonding temperature are

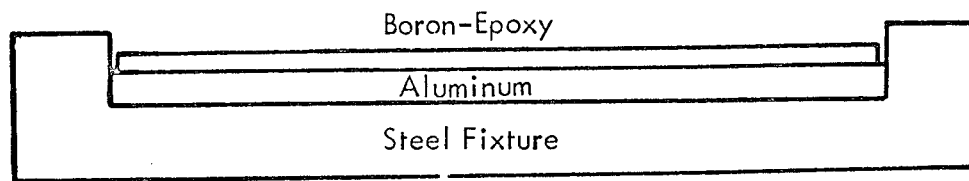
$$\sigma_{1A} = \frac{E_A (\alpha_{ST} \Delta T_{ST} - \alpha_A \Delta T_A)}{1 + \frac{E_A A_A}{E_{ST} A_{ST}}} \quad (9)$$

$$\sigma_{1B} = 0 \quad P_1 = \sigma_{1A} A_A$$

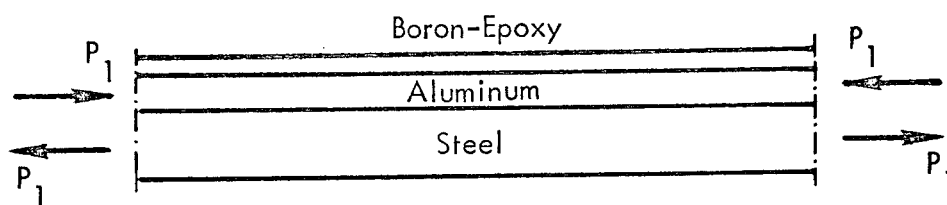
where α_{ST} and ΔT_{ST} are the thermal expansion coefficient and temperature rise of the steel fixture, respectively. The stresses due to bonding may be assumed to consist of three parts, or

$$\left(\begin{array}{c} \text{Stress Due} \\ \text{to Bonding} \end{array} \right) = \left(\begin{array}{c} \text{Stress at} \\ \text{Bonding} \\ \text{Temperature} \end{array} \right) - \left(\begin{array}{c} \text{Stress Due} \\ \text{to Temperature} \\ \text{Differential, } \Delta T \end{array} \right) - \left(\begin{array}{c} \text{Stress Due} \\ \text{to Applied} \\ \text{Load, } P_1 \end{array} \right) \quad (10)$$

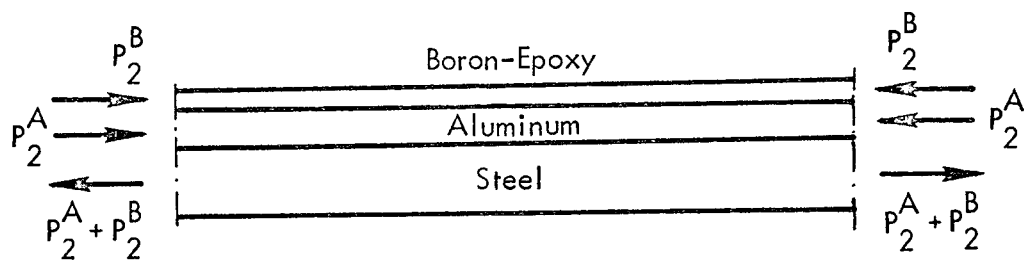
The stresses at the bonding temperature are given by equations (9). To determine the stresses due to the temperature differential, ΔT_A , and due to the applied load, P_1 , one must first



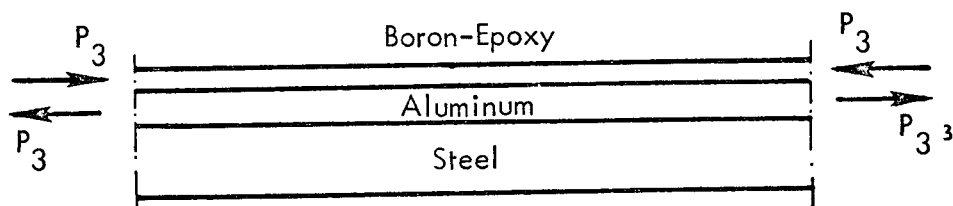
(a) Room Temperature Before Curing



(b) At Bonding Temperature



(c) Room Temperature After Curing



(d) Room Temperature After Removal from Fixture

FIGURE C-2.-STEEL FIXTURE RESTRAINT DURING BONDING

obtain the longitudinal strains from equations (8) and (6), respectively. The combined effect of these two causes yields for the longitudinal strain

$$\bar{\epsilon}_1 = - \frac{\Delta T_A \sum c_2^i A^i + P_1}{\sum c_1^i A^i}$$

By substituting the above strain for ϵ_1 and $-\Delta T_A$ for T in equations (2), (3), or (4) the corresponding stresses are obtained.

An addition to the program involves the calculation of bending stresses resulting from column eccentricity. Initial eccentricities are assumed in the form

$$w_o = w_{\max} \left\{ \cos \left[\frac{\pi}{2} \sqrt{c} \left(1 - \frac{2x}{L} \right) \right] - \cos \frac{\pi}{2} \sqrt{c} \right\} \quad (11)$$

where the column fixity factor, c , and the maximum deflection, w_{\max} , are specified input quantities. For a simple supported column ($c = 1.0$) this reduces to:

$$w_o = w_{\max} \sin \frac{\pi x}{L} \quad (12)$$

while for a column with fixed ends, the following relation is obtained:

$$w_o = w_{\max} \left(1 - \cos \frac{2\pi x}{L} \right) \quad (13)$$

The maximum moment now becomes

$$M_{\max} = \frac{P w_{\max}}{1 - \frac{P}{P_{cr}}} \quad (14)$$

where P_{cr} is the wide column buckling load.

Local Instability in Composite Reinforced Aluminum Skin

The general analysis computer program was expanded to include a more rigorous determination of the local buckling stresses of the skin elements under the hat section. The method of stationary potential energy was used to calculate the critical stresses of a simple supported plate, reinforced with an orthotropic strip as shown in Figure C-3. The strip extended over the entire length of the plate and had a specified width equal to or less than the plate width. The width of the plate was taken as the distance between the hat-to-skin fasteners. The composite reinforced aluminum may be subjected to compression (or tension) and shear.

Plate deflections were assumed in the form

$$w = \sum_{m=1}^M \sum_{n=1}^N a_{mn} \sin \frac{m\pi x}{a} \sin \frac{n\pi y}{b} \quad (15)$$

where M and N were taken as 10 and 6, respectively, for pure compression and as 16 and 6, respectively, in the presence of shear. The integrations representing the strain energy and the work done by the external forces were performed by parts along the width of the plate.

Figure C-3 shows the critical stresses versus strip width obtained with the program. The solid line represents the pure compression case while the dashed line gives the results for combined compression and shear in a ratio of approximately 2 to 1.

Composite to Aluminum Joints

The bonded joint analysis program BONJO I, which was developed under Air Force Contract F33615-70-C-1302, is available for use for all simple joint configurations. This program calculates the stresses in the bondline and in the adherends caused by applied loading as well as those resulting from thermal considerations. More complex joints will be analyzed using finite element methods.

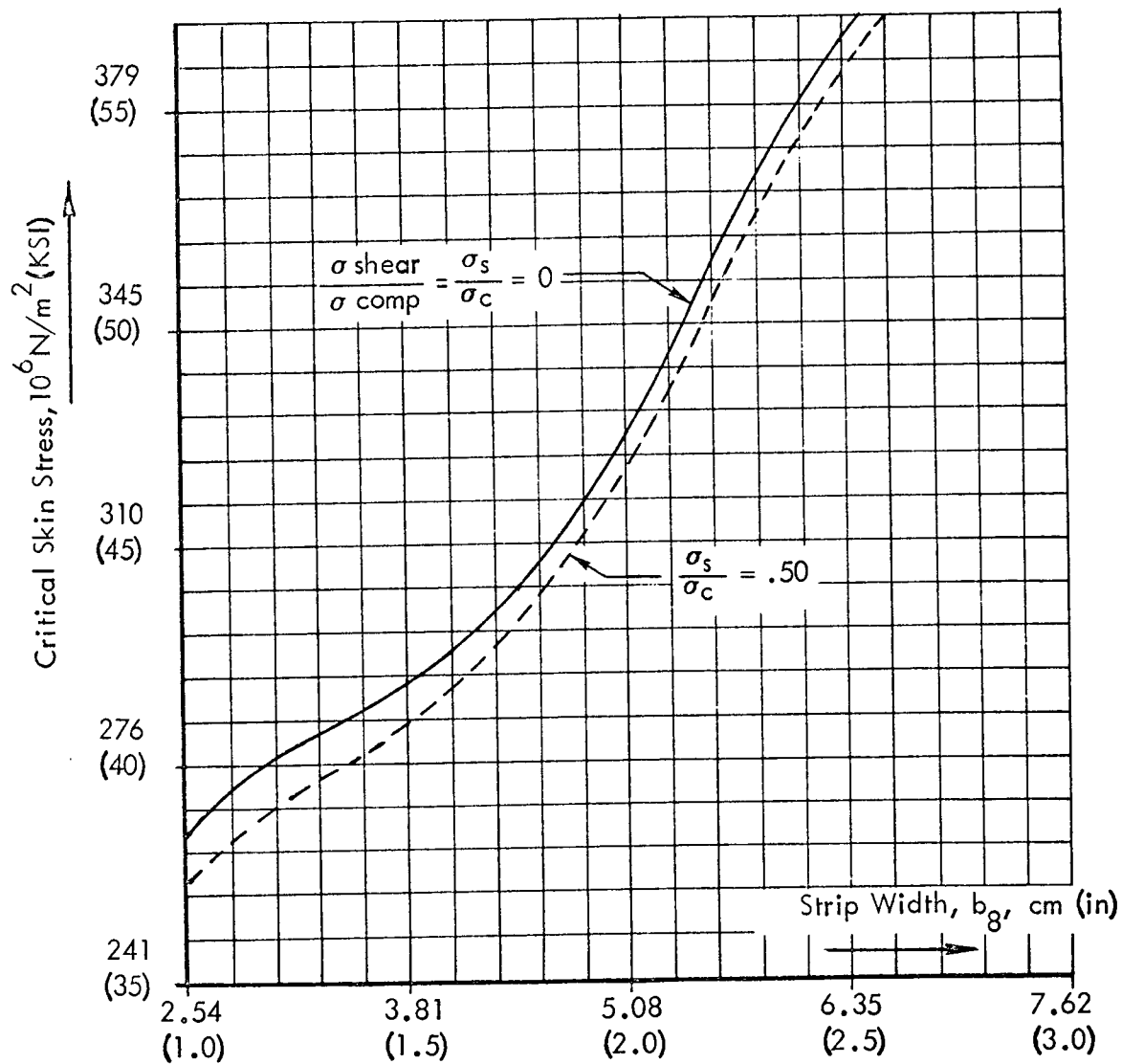
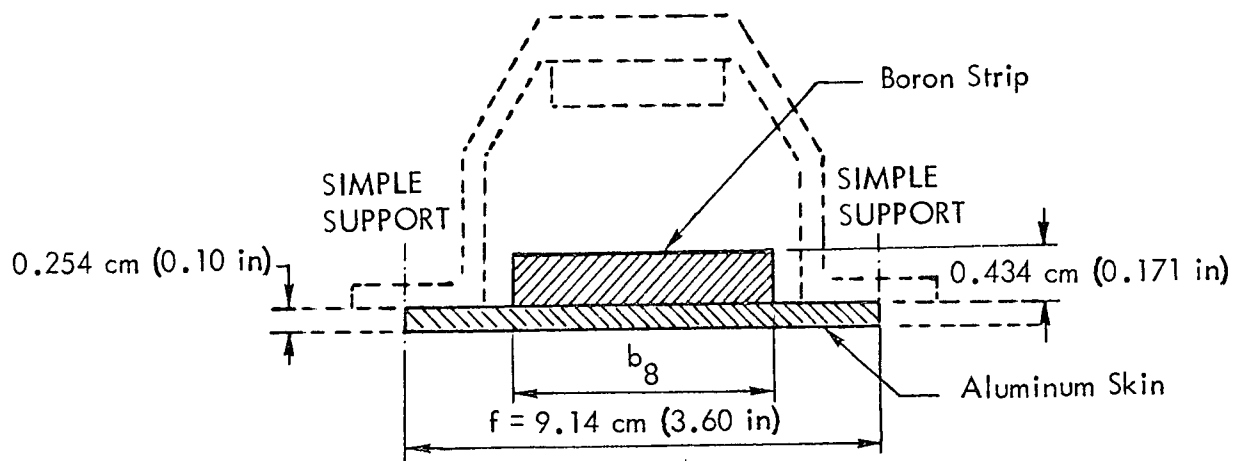


FIGURE C-3.- LOCAL INSTABILITY ALUMINUM/BORON SKIN

APPENDIX D

TABULAR TEST DATA FROM ADHESIVE EVALUATIONS

This appendix contains both summary and individual specimen test results of aluminum bonded to aluminum and boron-epoxy laminates bonded to aluminum using AF127-3 adhesive. These data provide the basis for summaries shown in the body of this report and include the results of tensile shear, Bell peel, creep, and environmental tests.

TABLE D-1.-SUMMARY OF TENSILE SHEAR TEST RESULTS

Adherends	Prior Exposure	Overlap cm (in)	Tensile Shear Failure Stress and Mode					
			218.2°K (-67°F) 10 ⁷ N/m ² (psi)	Failure Mode $\triangle 1$	RT 10 ⁷ N/m ² (psi)	Failure Mode $\triangle 1$	344.3°K (160°F) 10 ⁷ N/m ² (psi)	Failure Mode $\triangle 1$
Al to Al	-	1.27 (0.5)	2.48 (3600)	100 AP	3.72 (5400)	90 CA 10 AP	3.17 (4600)	100 CA
B to Al	-	1.27 (0.5)	3.59 (5200)	80 CBR 20 AM	3.93 (5700)	100 CBR	3.10 (4500)	100 CBR
B to Al	-	3.81 (1.5)	1.45 (2100)	100 CBR	2.78 (4035)	BF	2.60 (3770)	60BF 40 MF
B to Al	-	6.35 (2.5)	.65 (950)	100 CBR	1.67 (2420)	60 BF 40 BD	6.58 (2290)	100 BF
B to Al	JP-4, 7 days	1.27 (0.5)	-	-	3.86 (5600)	95 CBR 5 AP	-	-
B to Al	High Humidity 30 days	1.27 (0.5)	-	-	3.52 (5100)	90 CBR 10 CA	-	-
B to Al	5% Salt Spray	1.27 (0.5)	-	-	3.45 (5000)	100 CBR	-	-
B to Al	Temp-Hum. Cycling (30 Cycles)	1.27 (0.5)	-	-	3.38 (4900)	98 CBR 2 CA	-	-

$\triangle 1$ The number refers to the percent of the failure in the failure modes noted below.



- AP - Adhesive to primer
- CA - Cohesive in AF 127-3
- CBR - Cohesive in the boron laminate resin
- AM - Adhesive to metal
- BF - Boron laminate failure
- MF - Metal failure
- BD - Boron laminate delamination

TABLE D-2. - TENSILE SHEAR TEST RESULTS - INDIVIDUAL SPECIMENS

Adherends	Specimen Number $\triangle 1$			Overlap cm (inch)	Tensile Shear Failure Stress and Mode					
	218.2°K (-67°F)	RT	344.3°K (160°F)		218.2°K (-67°F) 10^7 N/m^2 (psi)	Failure Mode $\triangle 2$	RT 10^7 N/m^2 (psi)	Failure Mode $\triangle 2$	344.3°K (160°F) 10^7 N/m^2 (psi)	Failure Mode $\triangle 2$
Al to Al	1-2	4-2	1-4	1.27 (0.5)	3.24 (4700)	100 AP	3.72 (5400)	90 CA 10 AP	3.03 (4400)	100 CA
	2-2	5-2	1-5	1.27 (0.5)	2.62 (3800)	100 AP	3.86 (5600)	90 CA 10 AP	4.27 (6200)	100 CA
	3-4	4-3	2-5	1.27 (0.5)	2.34 (3400)	100 AP	3.72 (5400)	90 CA 10 AP	2.96 (4300)	100 CA
	2-4	5-3	3-2	1.27 (0.5)	2.00 (2900)	100 AP	3.59 (5200)	90 CA 10 AP	2.83 (4100)	100 CA
	4-1	4-4	5-1	1.27 (0.5)	2.21 (3200)	100 AP	3.59 (5200)	90 CA 10 AP	2.62 (3800)	100 CA
B to Al	1-8	1-4	1-14	1.27 (0.5)	3.72 (5400)	90 CBR 10 AM	3.93 (5700)	100 CBR	2.96 (4300)	100 CBR
	2-10	2-4	1-15	1.27 (0.5)	3.59 (5200)	100 CBR	4.90 (5800)	100 CBR	3.17 (4600)	100 CBR
	3-8	3-4	2-15	1.27 (0.5)	3.52 (5100)	20 CBR 80 AM	3.86 (5600)	100 CBR	3.24 (4700)	100 CBR
	1-10	1-16	3-10	1.27 (0.5)	3.24 (4700)	100 CBR	3.72 (5400)	100 CBR	3.10 (4500)	100 CBR
	2-14	2-8	3-14	1.27 (0.5)	3.72 (5400)	100 CBR	4.14 (6000)	100 CBR	3.03 (4400)	100 CBR
B to Al	4-6	4-3	4-11	3.81 (1.5)	1.44 (2090)	100 CBR	2.85 (4130)	100 BF	2.68 (3890)	100 BF
	4-7	4-4	4-12	3.81 (1.5)	1.38 (2000)	100 CBR	2.77 (4020)	100 BF	2.54 (3680)	100 BF
	4-8	4-5	4-13	3.81 (1.5)	1.45 (2110)	100 CBR	2.94 (4270)	100 BF	2.46 (3570)	100 MF
	4-9	4-16	4-14	3.81 (1.5)	1.43 (2080)	100 CBR	2.56 (3720)	100 BF	2.68 (3880)	100 BF
	4-10	-	4-15	3.81 (1.5)	1.54 (2240)	100 CBR	-	-	2.65 (3850)	100 MF
B to Al	5-2	5-1	5-3	6.35 (2.5)	.827 (1200)	100 CBR	1.96 (2840)	100 BF	1.62 (2350)	100 BF
	5-5	5-4	5-6	6.35 (2.5)	.552 (800)	100 CBR	1.63 (2360)	100 BD	1.69 (2450)	100 BF
	5-8	5-7	5-9	6.55 (2.5)	.552 (800)	100 CBR	1.48 (2150)	100 BF	1.59 (2300)	100BF
	5-11	5-10	5-12	6.35 (2.5)	.676 (980)	100 CBR	1.64 (2380)	100 BF	1.39 (2010)	100 BF
	5-14	5-13	5-15	6.35 (2.5)	.683 (990)	100 CBR	1.63 (2370)	100 BD	1.61 (2340)	100 BF

Notes and Symbols are defined on Page 171.

TABLE D-2.-TENSILE SHEAR TEST RESULTS - INDIVIDUAL SPECIMENS (CONTINUED)

Adherends	Specimen Number 	Prior Exposure	Overlap cm (inch)	Tensile Shear Failure Stress and Mode	
				RT 10 ⁷ N/m ² (psi)	Failure Mode 
B to Al	1-1	JP-4, 7 days	1.27 (0.5)	4.27 (6200)	100 CBR
	1-13		1.27 (0.5)	4.07 (5900)	100 CBR
	2-1		1.27 (0.5)	3.10 (4500)	80 CBR 20 AP
	2-13		1.27 (0.5)	3.93 (5700)	90 CBR 10 AP
	3-5		1.27 (0.5)	4.00 (5800)	95 CBR 5 AP
B to Al	1-3	High Humidity 30 days	1.27 (0.5)	3.59 (5200)	90 CBR 10 CA
	1-7		1.27 (0.5)	3.52 (5100)	90 CBR 10 CA
	2-3		1.27 (0.5)	3.65 (5300)	90 CBR 10 CA
	2-7		1.27 (0.5)	3.59 (5200)	90 CBR 10 CA
	3-7		1.27 (0.5)	3.17 (4600)	90 CBR 10 CA
B to Al	1-11	5% Salt Spray	1.27 (0.5)	3.59 (5200)	100 CBR
	2-11		1.27 (0.5)	3.52 (5100)	100 CBR
	3-1		1.27 (0.5)	3.45 (5000)	100 CBR
	3-3		1.27 (0.5)	3.31 (4800)	100 CBR
	3-9		1.27 (0.5)	3.38 (4900)	100 CBR
B to Al	1-5	Temp. - Humidity Cycling (30 Cycles)	1.27 (0.5)	3.45 (5000)	100 CBR
	1-9		1.27 (0.5)	3.45 (5000)	100 CBR
	2-5		1.27 (0.5)	3.38 (4900)	100 CBR
	2-9		1.27 (0.5)	3.52 (5100)	100 CBR
	3-11		1.27 (0.5)	3.03 (4400)	90 CBR 10 CA



The first number refers to the panel number; the second number refers to the specimen location within the panel.



The number refers to the percent of the failure which occurred in the noted modes:

AP - Adhesive to primer

CA - Cohesive in AF 127-3

CBR - Cohesive in the boron laminate resin

AM - Adhesive to metal

BF - Boron laminate failure

TABLE D-3. -SUMMARY OF BELL PEEL TEST RESULTS

Adherends	218°K (-67°F) N/mw ³ (piw) ²	Failure Mode ¹	RT N/mw (piw)	Failure Mode ¹	344°K (160°F) N/mw (piw)	Failure Mode ¹
A1 to A1	1769 (10.1)	10 CA 90 AP	8424 (48.1)	80 CA 20 AP	7828 (44.7)	100 CA
B to A1	3432 (19.6)	20 CA 80 CBR	3100 (17.7)	100 ScBL	4291 (24.5)	100 ScBL



The number refers to the percent of the specimen failure which occurred in the noted modes:

CA - Cohesive in AF127-3
 AP - Adhesive to primer
 CBR- Cohesive in boron laminates
 ScBL - Scrim pulled from boron laminates



(piw) - pounds per inch of width at failure



N/mw - Newtons per meter width at failure.

TABLE D-4.-BELL PEEL TEST RESULTS - INDIVIDUAL SPECIMENS

Adherends	Specimen Number ¹			218°K (-67°F)	Failure Mode ²	RT	Failure Mode ²	344°K (160°F)	Failure Mode ²
	218°K (-67°F)	RT	344°K (160°F)	N/mw (piw) ³		N/mw (piw) ³		N/mw (piw) ³	
Al to Al	1-2	1-1	1-3	2312 (13.2)	20 CA 80 AP	7671 (43.9)	100 CA	7758 (44.3)	100 CA
	1-5	1-4	1-6	1051 (6.0)	5 CA 95 AP	9002 (51.4)	75 CA 25 AP	7565 (43.2)	100 CA
	1-8	1-7	1-9	1121 (6.4)	100 AP	8651 (49.4)	80 CA 20 AP	7565 (43.2)	100 CA
	1-11	1-10	1-12	1664 (9.5)	100 AP	8336 (47.6)	80 CA 20 AP	8826 (50.4)	100 CA
	1-14	1-13	1-15	2662 (15.2)	20 CA 80 AP	8441 (48.2)	75 CA 25 AP	7110 (40.6)	100CA
B to Al	2-2	2-1	2-3	1961 (11.2)	10 CA 90 CBR	2557 (14.6)	100 ScBL	3538 (20.2)	100 ScBL
	2-5	2-4	2-6	4658 (26.6)	20 CA 80 CBR	3468 (19.8)	100 ScBL	3643 (20.8)	100 ScBL
	2-8	2-7	2-9	3222 (18.4)	20 CA 80 CBR	2767 (15.8)	100 ScBL	4869 (27.8)	100 ScBL
	2-11	2-10	2-12	3888 (22.2)	25 CA 75 CBR	3538 (20.2)	100 ScBL	5239 (30.2)	100 ScBL
	2-14	2-13	2-15	3397 (19.4)	20 CA 80 CBR	3187 (18.2)	100 ScBL	4098 (23.4)	100 ScBL



The first number refers to the panel number; the second number refers to the specimen location within the panel.



The number refers to the percent of the specimen failures which occurred in the noted modes:

CA - Cohesive in AF127-3
AP - Adhesive to primer
CBR - Cohesive in Boron Laminate
ScBL- Scrim pulled from Boron Laminate



(piw) - Pounds per inch of width at failure.



N/mwC - Newton per meter width at failure.

TABLE D-4.- BELL PEEL TEST RESULTS - INDIVIDUAL SPECIMENS

TABLE D-5.-ALUMINUM-TO-ALUMINUM CREEP DEFLECTION

	Specimen No.	Hours at Load	Creep Deflection 10^{-5}_m (in.)	
Room Temperature Exposure	4-5	256.7	1.52	(0.0006)
	4-6	256.1	1.77	(0.0007)
	5-4	208.6	-	None
	5-5	196.9	1.01	(0.0004)
	5-6	196.5	1.52	(0.0006)
	Avg.	223.0	1.27	(0.0005)
344.3°K (160°F) Exposure	2-6	260.5	1.77	(0.0007)
	3-1	209.5	2.54	(0.0010)
	3-3	212.0	2.54	(0.0010)
	3-5	404.6	5.03	(0.0020)
	3-6	284.6	0.254	(0.0001)
	Avg.	274.2	2.54	(0.0010)

TABLE D-6.-BORON-EPOXY-TO-ALUMINUM CREEP DEFLECTION

	Specimen No.	Hours at Load	Creep Deflection 10^{-5}_m (in.)	
Room Temperature Exposure	1-2	209.5	2.54	(0.0010)
	2-2	407.1	3.81	(0.0015)
	2-12	197.1	2.54	(0.0010)
	3-2	208.8	1.77	(0.0007)
	3-6	196.8	2.03	(0.0008)
	Avg.	243.9	2.54	(0.0010)
344.3°K (160°F) Exposure	1-12	209.4	2.54	(0.0010)
	3-15	209.3	2.03	(0.0008)
	3-12	255.9	2.54	(0.0010)
	1-6	192.5	2.79	(0.0011)
	2-6	192.1	3.3	(0.0013)
	Avg.	211.8	2.54	(0.0010)

APPENDIX E

PREPARATION OF ALUMINUM SURFACES

All aluminum surfaces were sulfuric acid anodized. In areas where laminates were to be bonded to the aluminum, the sulfuric acid anodic film was stripped and replaced with a reduced chromic acid anodic film. The chromic acid anodized surfaces were then covered with a primer to prolong shelf life and improve corrosion resistance. The following processes were used:

E.1 SULFURIC ACID ANODIZE

The sulfuric acid process used was a standard process as outlined below:

<u>Step</u>	<u>Process</u>	<u>Time, Minutes</u>
1	Vapor degrease	Approximately 3
2	Alkaline clean	10 to 15
3	Spray rinse	At least 1
4	Immersion rinse	At least 1
5	Deoxidize	5 to 7
6	Spray rinse	At least 1
7	Immersion rinse	At least 1
8	Alkaline etch	3 to 3-1/2
9	Spray rinse	At least 1
10	Immersion rinse	At least 1
11	Hot deoxidize	5 to 7
12	Spray rinse	At least 1
13	Immersion rinse	At least 1
14	Sulfuric acid anodize	29 to 31
15	Spray rinse	At least 1
16	Immersion rinse	At least 1

<u>Step</u>	<u>Process</u>	<u>Time, Minutes</u>
17	Neutralizing rinse	5 to 7
18	Spray rinse	At least 1
19	Immersion rinse	At least 1
20	Hot dichromate seal	12 to 15
21	Spray rinse	At least 1
22	Immersion rinse	At least 1
23	Hot water rinse	1 to 3
24	Hot air dry	Until dry

E.2 CHROMIC ACID ANODIZE

Processes for stripping the sulfuric acid anodize and replacing with chromic acid anodize are outlined below:

<u>Step</u>	<u>Process</u>	<u>Time, Minutes</u>
1	Alkaline clean	10 to 15
2	Spray rinse	At least 1
3	Immersion rinse	At least 1
4	Deoxidize	5 to 7
5	Spray rinse	At least 1
6	Immersion rinse	At least 1
7	Alkaline etch	3 to 3-1/2
8	Spray rinse	At least 1
9	Immersion rinse	At least 1
10	Hot deoxidize	5 to 7
11	Spray rinse	At least 1
12	Immersion rinse	At least 1
13	Chromic acid anodize	33 to 35
14	Spray rinse	At least 1
15	Immersion rinse	At least 1
16	Hot air dry	Until dry

E.3 PRIMING

Priming the anodized areas to be bonded is accomplished in the following sequence:

1. Accomplish priming within sixteen (16) hours after chromic acid anodizing.
2. Brush or spray apply primer, in cross-coat pattern, to bond area in a thickness range of 2.54 to 7.62 microns (0.1 to 0.3 mil).
3. Air-dry primer for 2 hours minimum at room temperature.
4. Remove the chem mill maskant.
5. Cover primed details with clean paper to prevent contamination during storage.